AD NUMBER

ADB006930

NEW LIMITATION CHANGE

TO

Approved for public release, distribution unlimited

FROM

Distribution authorized to U.S. Gov't. agencies only; Test and Evaluation; 11 MAR 1975. Other requests shall be referred to Air Force Materials Laboratory, Attn: Manufacturing Tech. Division, Wright-Patterson AFB, OH 45433.

AUTHORITY

AFML ltr, 26 Oct 1978

EFFECT OF BEARING DEFECTS

MPB Corporation
Keene, New Hampshire

TECHNICAL REPORT AFML-TR-75-6
December 1974

FINAL REPORT FOR PERIOD NOVEMBER 1971-NOVEMBER 1974

Air Force Materials Laboratory
Air Force Systems Command
Wright-Patterson Air Force Base, Ohio

NOTICE

When Government drawings, specifications, or other data are used for any purpose other than in connection with a definitely related Government procurement operation, the United States Government thereby incurs no responsibility for any obligation whatsoever; and the fact that the Government may have formulated, furnished, or in any way supplied the said drawings, specifications, or other data, is not be regarded by implication or otherwise as in any manner licensing the holder or any other person or corporation, or conveying any rights or permission to manufacture, use, or sell any patented invention that may in any way be related thereto.

Copies of this report should not be returned unless return is required by security considerations, contractual obligations, or notice on a specific document.

This final report was submitted by MPB Corporation, Keene, New Hampshire, under Contract F33615-72-C-1243, Manufacturing Methods Project 743-1, "Effects of Bearing Defects." Mr. William A. Harris, AFML/LTM, was the laboratory monitor.

This technical report has been reviewed and is approved for publication.

William C. Harris

WILLIAM A. HARRIS
Project Monitor

FOR THE DIRECTOR

H. A. Johnson

H. A. JOHNSON
Chief, Metals Branch
Manufacturing Technology Division

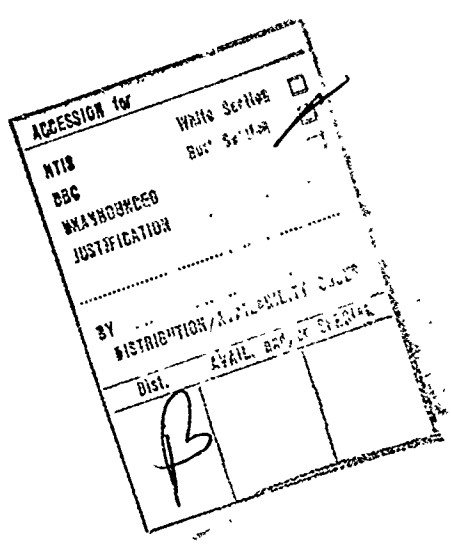

UNCLASSIFIED

SECURITY CLASSIFICATION OF THIS PAGE *(When Data Entered)*

REPORT DOCUMENTATION PAGE	READ INSTRUCTIONS BEFORE COMPLETING FORM
1. REPORT NUMBER: AFML-TR-75-6	2. GOVT ACCESSION NO. / 3. RECIPIENT'S CATALOG NUMBER
4. TITLE *(and Subtitle)*: EFFECT OF BEARING DEFECTS.	5. TYPE OF REPORT & PERIOD COVERED: Technical Report, Nov 1971 - Nov 1974
	6. PERFORMING ORG. REPORT NUMBER: RX-002
7. AUTHOR(s): Colby G. Beecher	8. CONTRACT OR GRANT NUMBER(s): F33615-72-C-1243
9. PERFORMING ORGANIZATION NAME AND ADDRESS: MPB Corporation, Precision Park, Keene, New Hampshire	10. PROGRAM ELEMENT, PROJECT, TASK AREA & WORK UNIT NUMBERS: AF-743-1
11. CONTROLLING OFFICE NAME AND ADDRESS	12. REPORT DATE: December 1974
	13. NUMBER OF PAGES: 221 (12) 229 p.
14. MONITORING AGENCY NAME & ADDRESS *(if different from Controlling Office)*	15. SECURITY CLASS. *(of this report)*: Unclassified
	15a. DECLASSIFICATION/DOWNGRADING SCHEDULE

16. DISTRIBUTION STATEMENT *(of this Report)*

Distribution limited to U. S. Government agencies only; Test and Evaluation Data: 11 March 1975. Other requests for this document must be referred to the Manufacturing Technology Division, Air Force Materials Laboratory, Wright-Patterson Air Force Base, Ohio 45433.

17. DISTRIBUTION STATEMENT *(of the abstract entered in Block 20, if different from Report)*

18. SUPPLEMENTARY NOTES

19. KEY WORDS *(Continue on reverse side if necessary and identify by block number)*

Bearing
Miniature Bearing Performance
Miniature Bearing Life
Bearing Race Defects

20. ABSTRACT *(Continue on reverse side if necessary and identify by block number)*

This program determined the relationship between selected raceway surface defects and performance and life of miniature ball bearings.

The first phase of this two phase program developed the test plan for utilization in the second phase test and evaluation effort.

DD FORM 1 JAN 73 1473 EDITION OF 1 NOV 65 IS OBSOLETE

UNCLASSIFIED

SECURITY CLASSIFICATION OF THIS PAGE *(When Data Entered)*

390 482

20. ABSTRACT (continued)

Nine (9) defect types were tested at various levels: Comet-Tail, Dig-Nick, Dirt Brinell, Grind-Skip Lines, Impingement, Orange Peel, Pit, Scratch and "Liney" Finish.

Bearing selected was 5/16 OD x 1/8 ID (MPB P/N S516MCK) in tolerance grades ABEC 1, ABEC 3, and ABEC 7P.

Performance tests included starting torque, low speed running torque and vibration.

Life tests utilized air driven turbine test rigs operating at 16,000 rpm with 2 lbs. axial load. Bearings were lubricated with KG-80 oil (MIL-L-83176).

Conclusions are that performance characteristics were influenced to a greater degree than were bearing life times.

A specification for defect limitation is presented based on performance and life test evaluation.

PREFACE

This Final Technical Report covers work performed under Contract F33615-72-C-1243, Project and Task number 743-1, from November 1971-November 1974, and submitted in December 1974. It is published for information only and does not necessarily represent the recommendations, conclusions, or approval of the United States Air Force.

This project is being performed as a part of the USAF Manufacturing Methods Program, the primary objective of which is to establish manufacturing processes, techniques, and equipment for use in economical production of USAF materials and components.

This contract is being implemented by MPB Corporation, Keene, New Hampshire, under the technical direction of William Harris, Manufacturing Technology Division, AFML/LTF, Wright-Patterson Air Force Base, Ohio 45433

Suggestions concerning additional manufacturing methods development required on this, or other subjects, will be appreciated.

SUMMARY

Specifications controlling race surface defects in instrument ball bearings are either left to the individual bearing manufacturer or determined arbitrarily by the bearing user. Presently there is no industry standard for such defects.

It is known by manufacturer and user alike, that certain defects occurring on race surfaces affect bearing performance in terms of frictional torque and smoothness of operation. It has been supposed that where such performance anomalies exist bearing operating life will be reduced.

Since the term "defect" means imperfection or blemish it suggests an uncontrolled characteristic of a manufacturing process applied to the raceway surface. This in turn suggests that specific defect definition must relate directly to the process or manufacturing method in which it originates.

This investigation, the results of which reported herein, was proposed to (a) select and categorize miniature ball bearing raceway defects typically resulting from conventional manufacturing processes and (b) to test the effect of these defects on both performance and operational life.

Nine defect types were identified and related to three miniature bearing tolerances, classes (ABEC 1, ABEC 3, ABEC 7P) according to conventional manufacturing methods, resulting in a total of 18 individual test groupings. Three levels of defect were categorized within each test grouping.

Performance tests consisting of running torque, starting torque, and noise measurements were conducted on each group and compared statistically with base line measurements determined from defect-free bearings in each tolerance class.

Life tests were conducted and similarly compared utilizing air-driven turbine test banks designed and built by MPB Corporation as part of this program.

Started in November 1972, this completed investigation has resulted in validating statistically the effect on performance and operating life of miniature ball bearing raceway defects and yielded a recommended defect limit specification for application in Military or Industry Standards.

TABLE OF CONTENTS

LIST OF ILLUSTRATIONS

CONCLUSIONS & RECOMMENDATIONS

In general performance characteristics were influenced to a greater degree than were bearing life times. Although the effect of defects on bearing performance was expected based on industry experience in meeting critical instrument application requirements for low frictional torque and noise levels, it was somewhat surprising to note the generally slight effect on bearing life of what are normally considered gross defect levels.

This insensitivity of life to defect level is undoubtedly explained by the presence of an elastohydrodynamic (EHD) oil film within the rotating bearing, which under the test conditions imposed, separated the rolling elements from the raceway surfaces precluding the incidence of metal-to-metal contact sufficient to significantly shorten bearing life times in comparison to defect-free base line bearings. Obviously some lower value of EHD film thickness due to lower viscosity lubricants, higher temperature, or lower speeds would become significant. Care should be exercised in applying the defect level to life relationship determined in this investigation to applications with inherently lower EHD film characteristics.

Performance relationships to defect types and levels are shown graphically in Figure 1. The selection of defect levels made in this investigation were successful in bracketing performance effects with the exception of Test #14 (pits, ABEC 7P), Test

EFFECT OF DEFECTS ON PERFORMANCE

Test Groups			Running Torque Test Data Analysis														Starting Torque Test Data Analysis						Noise Analysis			
			ART			PRT			AHW			PHW			SPIKE			AST			PST			VANT			
ABEC Class	Test Number	Description	Large	Medium	Small	Large	Medium	Small	Large	Medium	Small	Large	Medium	Small	Large	Medium	Small	Large	Medium	Small	Large	Medium	Small	Large	Medium	Small	Conclusion
7P	1	Scratch			●	●	●	●	●	●	●	●	●		●	●	●	●	●	▥	●	●		●	●		"Small" level effectively reduces performance.
	3	Dig-Nick	●		●	●			●			●			●			●			●			●			"Large" level effectively reduces performance.
	5	Dirt Brinnel	●	▥	◑	●			●			●			●		●	●	▥		●			●			"Large" level effectively reduces performance. "Small" level effective for critical performance requirements
	6	Orange Peel		▥	●	●		●			●			●	●	●	●							●	●	●	"Small" level effectively reduces performance
	9	Comet Tail	●			●	●	●	●	●	●	●		●	●	●	●			●							"Small" level effectively reduces performance.
	11	Grind-Skip Lines		●	●	●	●	●	●	●	●	●	●	●	●	●	●	●	●	●	●	●	●	●	●	●	"Small" level effectively reduces performance.
	14	Pits																●	●	●	●	●	●				Inconclusive. Suggests "Small" level effects static but not dynamic performance.
	17	Liney Finish	●		●	●	●	●	●	●	●	●	●	●	●	●	●	●		●	●		●	●	●	●	"Small" level effectively reduces performance.
3	2	Scratch				●	●				▥	●	●		●	●			●		●	●			●		"Medium" level effectively reduces performance.
	4	Dig-Nick				●	●					●	●		●	●	●	●			●	●		●		▥	"Medium" level effectively reduces performance.
	12	Grind-Skip Lines																			●	●	●				Although "Small" affects PST, non-significance of other categories suggest "Large" is acceptable
	15	Pits	▥	▥		▥	▥	●	▥		●	▥	▥	●			●	●	●								"Small" level effectively reduces performance.
1	7	Dig-Nick	▥		▥	●			◕			●	●	●	●	●	●	●			●	●		●			"Large" level effectively reduces performance. PHW and SPIKE not important for ABEC 1 application
	8	Impingement				●		●	●	●	●	●		●	●			●			●						"Large" level effectively reduces performance. PRT, AHW and PHW not important for ABEC 1 application.
	10	Comet Tail			●	●	●	●	●	●		●	●	●	●	●		●				●		●			"Medium" level effectively reduces performance.
	13	Grind-Skip Lines				●	◑	●	●	●	●							●	●	●	●	●	●	●	●	●	"Small" level effectively reduces performance
	16	Pits																									"Large" level does not reduce performance.
	18	Liney Finish				●	●	●				●		●				●	●	●	●	●	●	●	●	●	"Small" level effectively reduces performance.

● = Significant difference — baseline value smaller

▥ = Significant difference — baseline value larger

FIG. 1

#16 (pits, ABEC 1), and Test #12 (grind-skip lines, ABEC 3). In these three categories even the largest defect chosen had little to no effect on the performance criteria. It is felt that the allowance of even larger defects in these categories, although possible without decreasing performance, is not practical in terms of cost savings since the steel cleanliness and manufacturing processes used are easily controlled within the limits chosen and tested.

Life test results are given in Figure 2 "Weibull Life Ratio Analysis." Of the 18 defect groupings only the "large" category of Test #2 (scratch, ABEC 3) showed significance in both mean life and B10 life at the 99% confidence level. The B10 life significance for "small" category is not explainable. Test #3 (dig-nick, ABEC 7P) showed mean life significance for the "large" category.

All other test groupings showed insignificant defect effects on both mean and B10 lives.

Both performance and life considerations made from the results of this investigation have been combined to obtain the defect limitation specification described in Figure 3. This specification has been divided into three parts, each dealing with a specific Annular Bearing Engineering Committee (ABEC) tolerance grade (i.e., ABEC 7P, ABEC 3, ABEC 1). The recommended defect level limit is based primarily on performance test results since they were more

WEIBULL LIFE RATIO ANALYSIS

TEST NO.	DEFECT	ABEC CLASS	DEFECT LEVEL	NUMBER TESTED	WEIBULL SLOPE	CORRELATION COEFFICIENT	MEAN LIFE (HRS)	MEAN LIFE RATIO	* DECISION (99% CONFIDENCE)	B10 LIFE	B10 LIFE RATIO	** DECISION (99% CONFIDENCE)
					σ_1	r	L_M	MLR		L_{10}	L_{10R}	
	BASE LINE	7P	--	40	1.0	0.98	1300	-	--	140	--	
	BASE LINE	3	--	40	1.5	0.98	1300	-	--	310	--	
	BASE LINE	1	--	40	1.1	0.97	1550	-	--	210	--	
1	SCRATCH	7P	SMALL	40	1.5	0.96	1050	1.24	NO SIGNIFICANCE	260	+1.86	NO SIGNIFICANCE
			MEDIUM	41	1.0	0.99	1350	1.04	" "	130	-1.08	" "
			LARGE	46	0.9	0.99	1600	1.23	" "	122	-1.15	" "
2	SCRATCH	3	SMALL	46	1.0	0.95	1000	1.30	" "	100	-3.10	SIGNIFICANT
			MEDIUM	49	1.2	0.99	1000	1.30	" "	165	-1.88	NO SIGNIFICANCE
			LARGE	48	1.0	0.99	800	1.63	SIGNIFICANT	90	-3.44	SIGNIFICANT
3	DIG-NICK	7P	SMALL	28	1.0	0.99	1400	1.08	NO SIGNIFICANCE	130	-1.08	NO SIGNIFICANCE
			MEDIUM	45	0.9	0.99	1500	1.15	" "	120	-1.17	" "
			LARGE	46	1.1	0.99	700	1.86	SIGNIFICANT	95	-1.47	" "
4	DIG-NICK	3	SMALL	7	0.7	0.87	1200	1.08	NO SIGNIFICANCE	53	-5.85	" "
			MEDIUM	29	1.1	0.98	1200	1.08	" "	190	-1.63	" "
			LARGE	48	1.1	0.97	1150	1.13	" "	160	-1.94	" "
5	DIRT BRINELL	7P	SMALL	7	0.6	0.99	1750	1.35	" "	30	-4.67	" "
			MEDIUM	18	0.7	0.98	2400	1.85	" "	76	-1.84	" "
			LARGE	47	1.2	0.99	1600	1.23	" "	225	+1.61	" "
6	ORANGE PEEL	7P	LARGE	47	1.2	0.95	1000	1.30	" "	150	+1.01	" "
7	DIG-NICK	1	LARGE	49	1.1	0.98	1950	1.26	" "	260	+1.28	" "
8	IMPINGEMENT	1	LARGE	36	1.1	0.99	2450	1.58	" "	310	+1.48	" "
9	COMET TAIL	7P	LARGE	19	1.2	0.98	1700	1.31	" "	270	+1.93	" "
10	COMET TAIL	1	LARGE	20	1.1	0.97	1750	1.13	" "	230	+1.10	" "
11	GRIND SKIP LINES	7P	LARGE	20	1.15	0.99	2100	1.62	" "	320	+1.29	" "
12	GRIND SKIP LINES	3	LARGE	20	1.2	0.97	1150	1.13	" "	250	-1.24	" "
13	GRIND SKIP LINES	1	LARGE	19	1.2	0.98	2650	1.71	" "	450	+2.14	" "
14	PITS	7P	LARGE	20	1.0	0.97	1850	1.42	" "	400	+2.96	" "
15	PITS	3	LARGE	20	1.0	0.98	1800	1.38	" "	800	+2.58	" "
16	PITS	1	LARGE	20	1.0	0.96	1400	1.11	" "	95	-2.21	" "
17	LINEY FINISH	7P	LARGE	20	1.3	0.96	1300	1.00	" "	260	+1.86	" "
18	LINEY FINISH	1	LARGE	20	1.2	0.93	1150	1.35	" "	180	-1.17	" "

* REFERENCE LIPSON & SHETH, TABLE A-22 "TEST FOR SIGNIFICANT DIFFERENCE IN MEAN LIVES (WEIBULL DISTRIBUTION)

** REFERENCE LIPSON & SHETH, TABLE A-25 "TEST FOR SIGNIFICANT DIFFERENCES IN B_{10} LIVES (WEIBULL DISTRIBUTION)

FIGURE 2

Precision Instrument Ball Bearings - ABEC 7P

Defect	Description	Limitation
Scratch	A removal or upsetting of metal with length much greater than width. (Angle of incidence 20° to ℄ of raceway)	<.0005" width
Dig-Nick	A removal or upsetting of metal with length approximately equal to width.	<.003" max. dim.
Dirt Brinell	Shallow irregular indentation of surface.	<.0015 max. dim. (<.0008)*
Orange Peel	Pebbly appearance of raceway surface.	Small **
Comet Tail	Pit followed by circumferential scratch.	<5 per raceway
Grind-Skip Line	Discontinuous closely spaced circumferential lines.	<Small **
Pits	Irregular surface discontinuity caused by steel inclusion or corrosion.	<.0005"max. dim.
Liney Finish	Continuous, closely spaced circumferential lines.	<Small **

Semi-Precision Instrument Ball Bearings ABEC 3

Scratch	As above	<.001" width
Dig-Nick	As above	<.001" max. dim.
Grind-Skip Line	As above	<Large **
Pits	As above	<.0005"max. dim.

Industrial Ball Bearings ABEC 1

Dig-Nick	As above	<.003" max. dim.
Impingement	Irregular raceway surface indentation caused by contact with other parts.	<.007" max. dim.
Comet Tail	As above	<10 per raceway
Grind-Skip Line	As above	<Small **
Pits	As above	<.003" max.dim.
Liney Finish	As above	<Small **

Figure 3

Defect Specification - Miniature Ball Bearings

*Limit for critical application
**Subjective determination. See Appendix F for visual comparison

significant than life test data. General application requirements of each tolerance grade also were considered in arriving at the recommended defect levels.

PROGRAM DESCRIPTION & DISCUSSION

1. Phase I - Selection of Bearing, Critical Defects and Inspection Methods

1.1 Bearing Selection

The bearing size and configuration chosen for use in this investigation is represented by MPB P/N S518MCK (Figure 4). This bearing conforms to the definition of "miniature" bearing since its outside diameter is less than 9 mm.

Produced in high volume in ABEC 7P and ABEC 3 tolerance grades, the S518MCK is representative of established manufacturing processes. The internal geometry and ball size is similar to the ABEC 1 SR2C bearing, also produced in high volume (although not meeting the "miniature" definition).

Applications of this bearing size are well established. ABEC 7P S518 size bearings are used extensively in synchro and servo motors as well as in gyro gimbals, precision gear heads and other instrumentation used by the Military.

ABEC 3, S518 bearings are used in synchros and cooling fans as well as in other Military end-use equipment.

ABEC 1 bearings of this size are used in precision potentiometers.

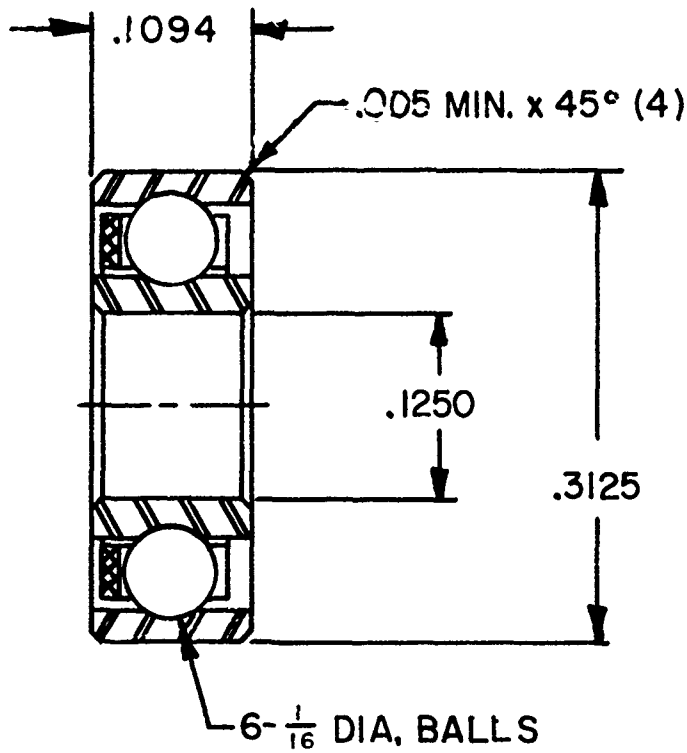

MPB P/N: S518MCK P35 LY185

Material: Rings and Balls – AISI 440C
Retainer — MINAPAR II

Radial Play: .0003 to .0005

Lubrication: KG 80, MIL-L-83176

FIGURE 4
TEST BEARING SPECIFICATIONS

MPB Corporation's manufacturing processes, although proprietary, differ in race finishing technique between each ABEC tolerance class of bearing. Thus the testing of all three tolerance grades is representative of processes unique to each.

The nonmetallic ball retainer configuration chosen is of a design and material unique to the MPB Corporation. It has been shown compatible with both high speed operation and low, uniform frictional torque performance.

The 440C stainless steel ring and ball material is chosen as being representative of instrument ball bearings manufactured in the United States.

1.2 Selection of Ball Track Defects

1.2.1 Inspect Production Rings

A total of 47 lots of production rings have been sampled and visually inspected for surface defects. These lots totaled 263,475 parts and involved the actual inspection of 6,770 individual rings.

Thirty-five (35) lots (207,411 parts) were ABEC 7P, grade, eleven (11) were ABEC 3 (51,419 parts) and one (1) was ABEC 1 (4,645 parts).

All lots thus inspected were finished components processed in the manner typical for each tolerance grade. Surface defects noted in these inspections are not necessarily considered to be rejectable

but rather point up the occurrence of the specific defect type in standard production parts. Results of these inspections are tabulated in Figure 5. Note that the ranking of defects in the ABEC 7P category was accomplished by multiplying the number of lots by the number of defects in each category. This allows consideration of both factors in establishing the ranking number. This method of ranking was not necessary in the ABEC 3 and ABEC 1 categories in order to discern significant differences.

1.2.2 Preliminary Performance Test

Performance tests utilizing MPB Corporation's MARK III Running Torque Tester, the Bendix starting torque tester and MPB Corporation's Vibration and Noise Tester (VANT), were run on typical defect-containing bearings assembled from the above inspected rings. (See Appendix for description of test equipment) Defects represented were scratch; dig-nick; impingement; grind-skip lines; and orange peel. The data obtained indicated that these defects in most cases, affected bearing performance in at least one of the performance parameters but not necessarily all three. (Fig. 6)

1.2.3 Defect Selection

Through analysis of the inspection data, performance data and past experience the defects for study were selected. Results are tabulated in Figure 7.

Considerations leading to the choice of each item in Figure 7 are discussed below.

Defect	ABEC 7P			ABEC 3		ABEC 1
	Lots (35)	Parts (3,295)	Rank (Lots x Parts)	Lots (11)	Parts (1,970)	Parts (1,500)
Abrade	3	4	12	1	1	
Chatter						4
Comet Tail	16	29	464			80
Dig-Nick	9	17	153	1	1	29
Liney Finish	20	98	1960			571
Impingement						516
Orange Peel	2	12	24			
Pit	2	10	20	1	1	
Scant	1	1	1			
Scratch	5	6	30			1
Grind-Skip Lines	6	14	84	9	246	94

Figure 5

Ranking of Defect Types

Defect	Size	No.	Running Torque	Starting Torque	Vibration (VANT)
Scratch	.001" wide	2	Periodic Spiking	No indication	No indication
Scratch	.001" wide	3	Periodic Spiking	No indication	No indication
Dig-Nick	.001" wide	2	No indication	No indication	No indication
Dig-Nick	.0016 x .015	1	Spiking	Hang-up	No indication
Impingement	.005" wide	2	Periodic Spiking	Hang-up	High vibration level
Impingement	.005" wide	1	Periodic Spiking	No indication	High vibration level
Grind-Skip Lines	.001" wide	4	No indication	No indication	High vibration level
Orange Peel	---	-	Slight hash	No indication	Moderately high vibration level

Figure 6

Preliminary Performance Tests

Defect	ABFC 7P	ABEC 3	ABEC 1
Comet Tail	X		X
Dig-Nick	X	X	X
Dirt Brinell	X		
Grind-Skip Lines	X	X	X
Impingement			X
Orange Peel	X		
Pit	X	X	X
Scratch	X	X	
Liney Finish	X		X

Figure 7

Selected Defects by Tolerance Grade

Comet Tail - This defect, characterized by a pit followed by a circumferential scratch is peculiar to a raceway honing or polish process which accounts for its significant occurrence in the ABEC 7P and ABEC 1 bearing ring lots. (ABEC 3 parts are not finished in this manner.)

Dig-Nick or Gouge - An upsetting or removal of metal, usually likened to marking with a sharp tool, this defect can exhibit raised metal with demonstrated effect on performance and presumably life.

Although not as significant in occurrence on the ABEC 3 parts inspected it is our opinion that all three ABEC grades should include this defect since its acceptance may vary with tolerance grade and its occurrence is no more controllable in one than the other.

Dirt Brinell - This defect is caused by the ball train in an assembled bearing running over dirt or other foreign matter during operations under load.

Dirt brinells were not evident in the parts inspected since inspection was done prior to bearing assembly. However, ABEC 7P bearings are typically performance tested under load as assemblies and because of the common occurrence of dirt brinells under these conditions it is concluded that inclusion of this defect is warranted.

Grind-Skip Lines - Characteristic of any ground surface, this defect is generally acceptable to various degrees according to the tolerance grade and the finishing method used.

Its occurrence in significant numbers of all three ABEC grade inspection samples justify its choice.

Impingement - Found only on inspected parts from the ABEC 1 category, this defect is related to bulk handling of hardened components which is typical of this bearing class.

Its investigation is limited to the ABEC 1 category.

Orange Peel - This pebbly appearance (as seen under magnification) of highly finished race surfaces occurring on ABEC 7P tolerance rings, is normally cause for rejection.

Its effect on performance is typically minimal but its effect on life was unknown.

The investigation of this defect type in terms of its characteristics and its effects was considered of potential significance in increasing production yields of Class 7P rings.

Pit - This defect, usually the result of steel inclusions or corrosion damage, was seen in ABEC 7P and to a lesser extent, ABEC 3 parts.

Since ABEC 1 bearings are typically made from air melt steel with a higher incidence of inclusions, it is deemed appropriate to include all three ABEC classes in investigation of this defect type.

Scratch - This defect is usually caused by gaging or other handling, much of which is done after the point at which these parts were inspected. Since raised metal may well result from this damage it is potentially effective on reduction of performance and life. Since minimal raceway gaging and handling is done with ABEC 1 bearing components, scratch investigation is included only on ABEC 7P and ABEC 3 components.

Liney Finish - This condition is not necessarily a defect although its presence in ABEC 7P rings is usually considered undesirable. A function of the final race finishing process, the lines referred to are not rough or "torn" as are grind lines but rather exhibit a smooth, uniform appearance. Some indications in past experience suggest an improvement in bearing performance due to a liney finish. The effect on life is not known. ABEC 1 bearing race surfaces typically contain a degree of "liney" finish characteristics since shorter finish operation cycles are utilized.

Our inspection sample did not show this condition in ABEC 7P bearing components because the race finishing processes were controlled to preclude its generation. Because of the possible

improvement in performance, on ABEC 7P bearings, and its existence in ABEC 1 bearings, we included this feature in both ABEC grades.

1.3 Selection of Inspection Techniques

1.3.1 Optical Inspection Methods

Optical inspection techniques were reviewed in relation to determining the existence, the location, and the size of race surface defects.

It was decided that initial selection of test parts for Phase II testing would be made by use of an American Optical Cycloptic Stereoscopic Microscope at 20X magnification with fluorescent light.

Parts selected above would then be examined under a Leitz-Gaertner toolmaker's microscope under 30X magnification. The micrometer adjustable table in conjunction with an eyepiece reticle allows measurement of defect characteristics to .0001". Location of defect is accomplished by measuring the length of chord from raceway shoulder to the defect center and through a simple proportion thereby relating it to a bearing contact angle.

In order to determine necessary accuracy of the location measurement to assure that the defect would indeed be in the ball race contact area of the assembled bearing, the following tests and analyses were undertaken.

First, 12 - S518C bearings were assembled with radial play values documented. These bearings were rotated under a 2 pound thrust load with a small quantity of aluminum oxide abrasive placed in each bearing. The resulting wear track on the inner raceway was measured by the above optical method to obtain both width of wear track and the contact angle from raceway center to the wear track center. The data obtained was then compared with the calculated contact angle and wear track width. (See Figure 8).

Good correlation exists between measured and calculated contact location. Although the measured wear band is wider than that calculated, presumably due to the dimension of the abrasive used, the apparent symmetry of the generated band allowed accurate determination of contact area center.

It should be noted that the calculated "footprint" of the ball-race contact area for the test bearing with a .0003 to .0005 radial play represents an approximate contact angle range of 16° (5.5° to 21.5°). Thus a raceway defect lying within this 16° range will be in the contact area under test thrust loading and its effect demonstrated.

It was concluded that this method of optically locating and determining size of defect would suffice and assure that the effect of raceway defects would be picked up on subsequent bearing assembly testing.

Radial Play Inches	Contact Angle (Measured)	Contact Angle (Calculated)	Wear Band Width (Measured)	Wear Band Width (Calculated)
.0005	14.4°	14.8°	.0097	.0074
.0008	17.2°	18.8°	.010	.0068

Figure 8

Actual versus Calculated Contact Bands
(Average of Six Bearings)
Two Pound Thrust Load

1.3.2 Defect Characterization

For characterization of raceway defects, both Interference Microscopy and Scanning Electron Microscopy (SEM) have been investigated.

A search of literature concerned with the principle and use of the Zeiss Interference Microscope indicated that although depths of extremely small defects (less than 0.54 microns) can be accurately measured, defects one or two orders of magnitude larger present definition problems. The fringe pattern seen through an interference microscope is not unlike elevation lines on a contour map which, although helping to visualize a dimension of depth on a two dimensional plane, are inferior to a good aerial photograph for characterizing surface topography.

The Scanning Electron Microscope (SEM) on the other hand, due to its large depth of field and wide range of magnification, is ideal for our purpose of categorizing specific defect types by their unique topographical qualities regardless of defect size. For these reasons, the SEM was selected for use in this investigation.

1.4 Test Program Development

To assist in design of the specific test program the consulting services of The Center For Industrial & Institutional Development (CIID), University of New Hampshire, were retained

The CIID involvement was primarily related to the determination of optimum statistical evaluation techniques for both performance and life testing. Preliminary test data obtained during the Phase I effort were utilized to determine the best fitting statistical distributions in the various test categories.

1.4.1 Performance Tests

Two sets of "defect-free" bearings were tested on the MARK III torque tester, the Bendix starting torque tester, and VANT. Detailed statistical analyses of these test results were conducted. A number of significant correlations between measurements were discovered. It was found that "set up" of the MARK III torque tester on different days had a large influence on the results for average hash width. It was shown that, for most of the measurements, the scatter of results is approximately described by a normal distribution.

Sample sizes necessary to detect differences in the average levels of each of the test measurements at specified probability levels were calculated. It was found that the number of bearings required in each group varied with the tests. In general, adequate sensitivity at a 99% probability level could be achieved with between 10 and 40 bearings.

Appendix D details the analysis of these data and the basis for the above conclusions.

1.4.2 Life Tests

1.4.2.1 Life Test Design

Life testing of bearings for this investigation was based on (a) choice of speeds and loads compatible with typical miniature bearing application, and (b) utilization of the basic air-driven test turbine design previously proven by MPB Corporation and capable of economically testing large numbers of test bearings.

Since typical instrument bearing failures are characterized by lubricant breakdown and occur long before theoretical fatigue life is reached, it is assumed that bearing life is dependent on maintaining an elastohydrodynamic (EHD) oil film between rolling element contacts. This EHD film thickness is primarily dependent on oil viscosity and bearing speed. A design parameter found to be valid through application experience, is known as "Lambda", an EHD film thickness to contact surface finish ratio.(1) It is generally accepted that a $\Lambda \geq 4$ is conservative in assuring contact separation and optimizing life. As Λ decreases to less than 2 the bearing operating life decreased rapidly due to the high incidence of metal-to-metal contact.

(1) Ref: "Life Adjustment Factors for Ball & Roller Bearings" ASME pp 12-13

In determining test conditions for this investigation a $\Lambda \simeq 3$ was chosen. This value is at the "top of the cliff" giving marginally acceptable theoretical EHD separation. It was thought that defects on the contact surfaces would provide their maximum effect on bearing life as they broke through the marginal EHD film, pushing life expectancy "over the edge" toward rapid bearing failure. The use of KG-80 oil, 2 lb. thrust load, 135° to 140°F temperatures, and 16,000 rpm provide $\Lambda = 3.4$ and were chosen as test conditions.

1.4.2.2 Test Turbine Design

As part of the Phase I effort MPB Corporation designed and built a prototype air turbine test bank for evaluation of bearing operating life. Patterned after test bank units previously designed and utilized by MPB Corporation, this test bank incorporated improvements in temperature control and speed-sensing devices. A description of this test unit is provided in Appendix E.

1.4.2.3 Test Turbine Evaluation

Ten prototype test turbines were run utilizing defect-free bearings. The resulting failures were influenced by outer race slippage in the housing block. Three more test groups were run with the test bearing outer races fixed to the housing block with Loctite(R) sealant. (Subsequently turbine blocks were re-made to allow closer fitting of the test bearing outer race precluding further use of Loctite(R).)

At this point it was decided to establish an accelerated life test of defect-free bearings by reducing oil viscosity so that a $\Lambda \simeq 1$ was obtained. A substitution of MIL-L-6085A oil in defect-free bearings produced the required Λ value and this "accelerated life test" procedure was utilized on subsequent turbine banks as a means for qualification (i.e., to assure that failures produced from each turbine bank were comparable and not significantly affected differences in individual turbines).

1.4.2.4 Statistical Method of Life Test Analysis

The accelerated life test data obtained from the prototype test turbine bank was analyzed by the Center For Industrial & Institutional Development (CIID) University of New Hampshire. Figure 9 shows the actual test data.

The data were first plotted on linear coordinate paper in the form of a frequency histogram using time groupings of 50 hours (Figure 10). The general shape of this distribution is strongly indicative of a "log-normal" distribution. Consequently a log-normal distribution plot was made plotting frequency versus log of time to failure in hours (Figure 11). It is clear that this is not an ideal normal distribution; and, yet, it is also clear that it has the general properties of a Gaussian-type distribution.

Turbine Bank #1
Time to Failure in Hours

Turbine	#1	#2	#3	#4	#5	#6	#7	#8	#9	#10
Run #1	110	116	670	530	260	190	116	254	150	99
Run #2	600	1130	525	242	336	414	300	213	769	140
Run #3	350	90	1100*	194	112	78	558	1616*	1243*	308
Run #4	280	123		108	330	930	320			41
Run #5	96				690		925			92
Run #6	122									

*Tests are still going

Figure 9

Initial Bearing Life Tests

FREQUENCY HISTOGRAM FOR TIME TO FAILURE—LINEAR COORDINATES

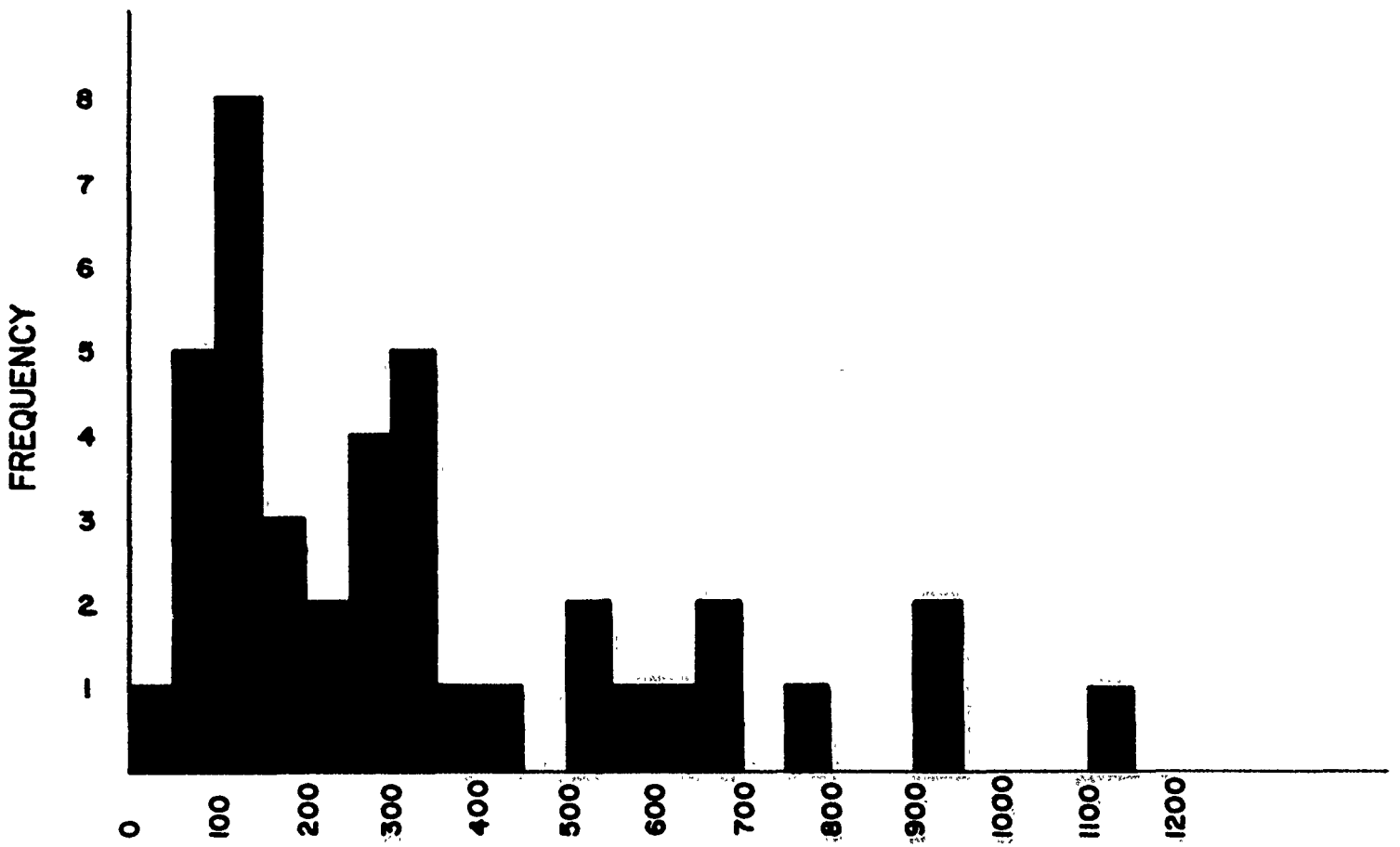

FIGURE 10

FREQUENCY HISTOGRAM FOR TIME TO FAILURE
TIME EXPRESSED ON LOG SCALE

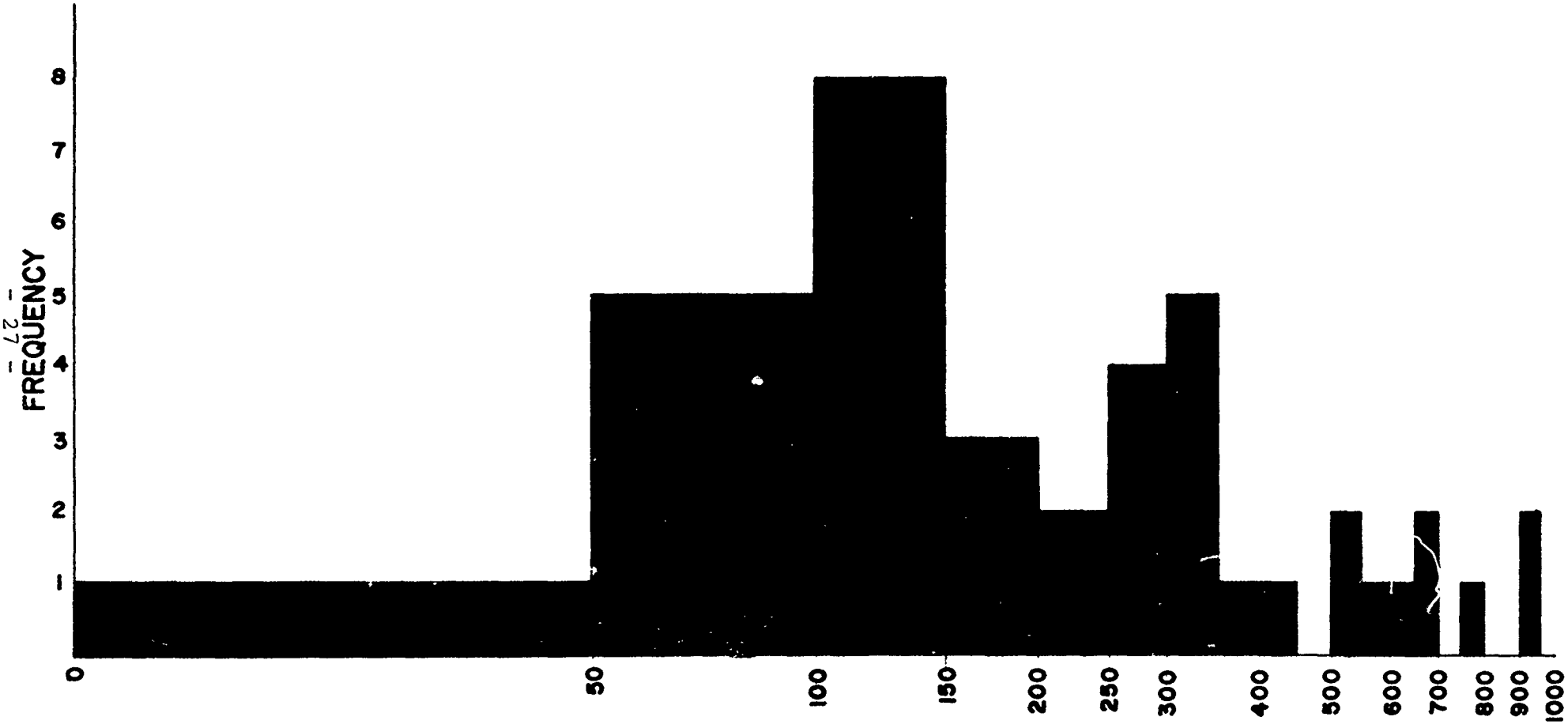

FIGURE 11

Several types of probability plotting paper are available for treating failure data. Curves were plotted on regular normal probability paper (Figure 12) in which the time to failure is plotted on a linear scale and the percent cumulative frequency is plotted on a probability scale. Since this curve is obviously not a straight line, it indicates that this is not the correct model and agrees with our conclusion from examination of the frequency histogram (Figure 10).

Next was plotted the probability curve using log of time to failure in hours versus the percent relative cumulative frequency (Figure 13), and this produced an excellent fit to a straight line with a correlation coefficient of 0.987. This would agree with our deduction from observation of the general shape of the frequency histogram in Figure 11.

Before deciding that the log-normal distribution was the correct fit for this data, we felt the need to plot the two parameter Weibull distribution which is frequently employed to describe failure data. This plot is shown in Figure 14, and it is clear that the data do not follow a straight line at least for the failure times below approximately 200 hours.

At this point in the program the log-normal distribution was chosen the most suitable for future analysis and qualification of all test turbines was based on log-normal distribution analysis. (Later in the program the three parameter Weibull

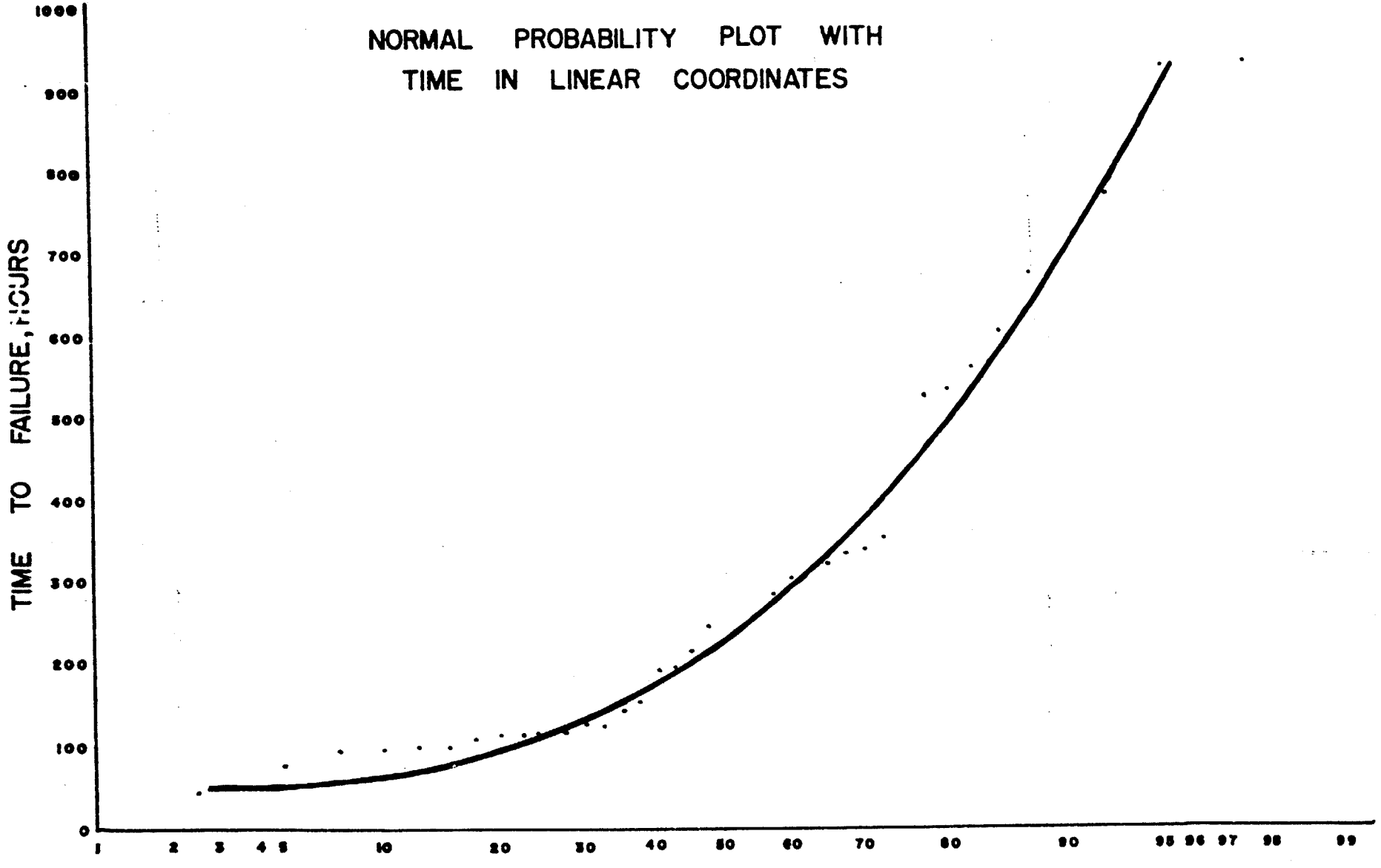
NORMAL PROBABILITY PLOT WITH
TIME IN LINEAR COORDINATES
TIME TO FAILURE, HOURS
1000
900
800
700
600
500
400
300
200
100
0
1
2
3
4
5
10
20
30
40
50
60
70
80
90
95
96
97
98
99
PERCENT RELATIVE CUMULATIVE FREQUENCY

FIGURE 12

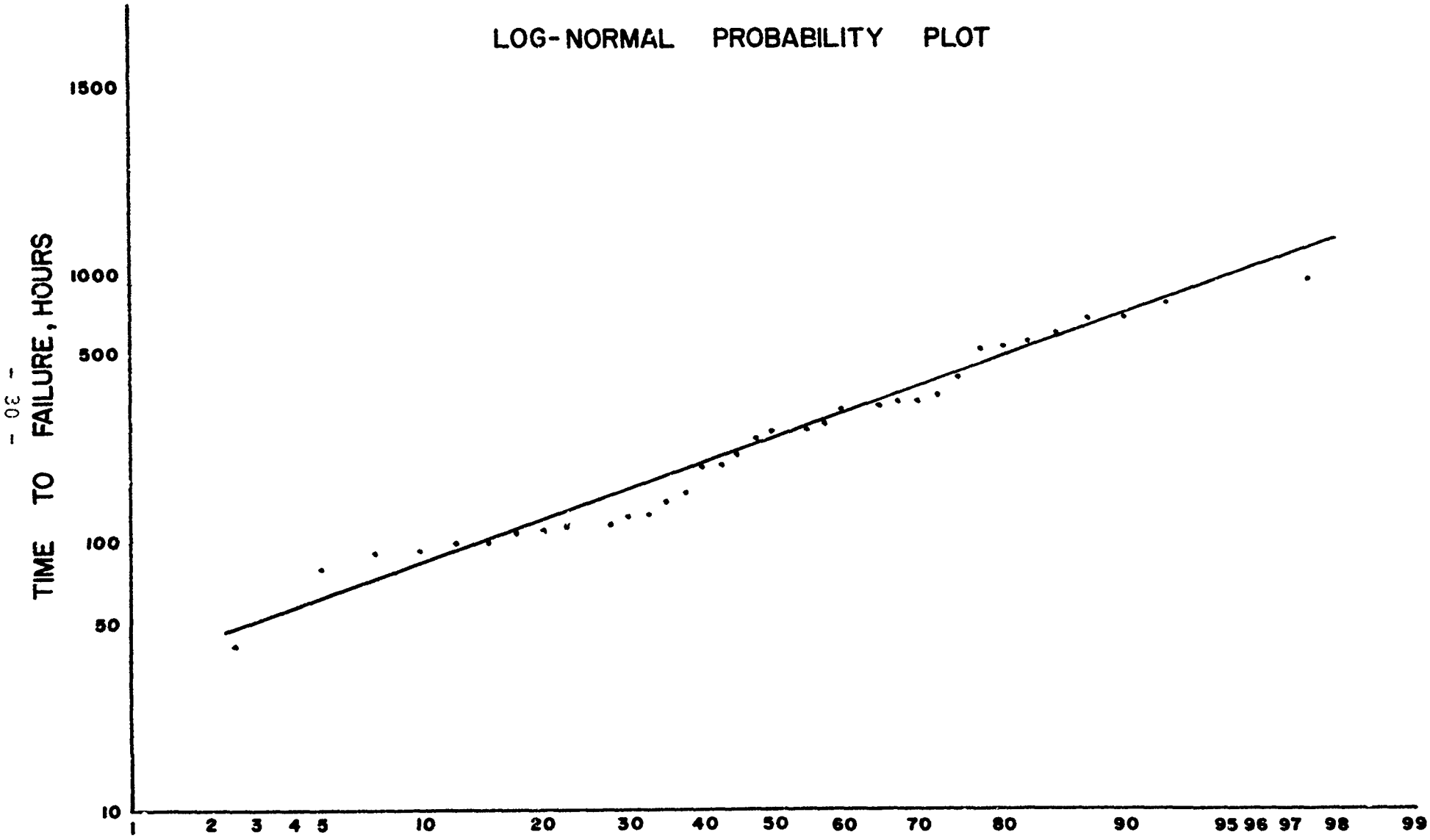
LOG-NORMAL PROBABILITY PLOT
TIME TO FAILURE, HOURS
1500
1000
500
100
50
10
1
2
3
4
5
10
20
30
40
50
60
70
80
90
95
96
97
98
99
PERCENT RELATIVE CUMULATIVE FREQUENCY

FIGURE 13

TWO PARAMETER PROBABILITY PLOT
WEIBULL

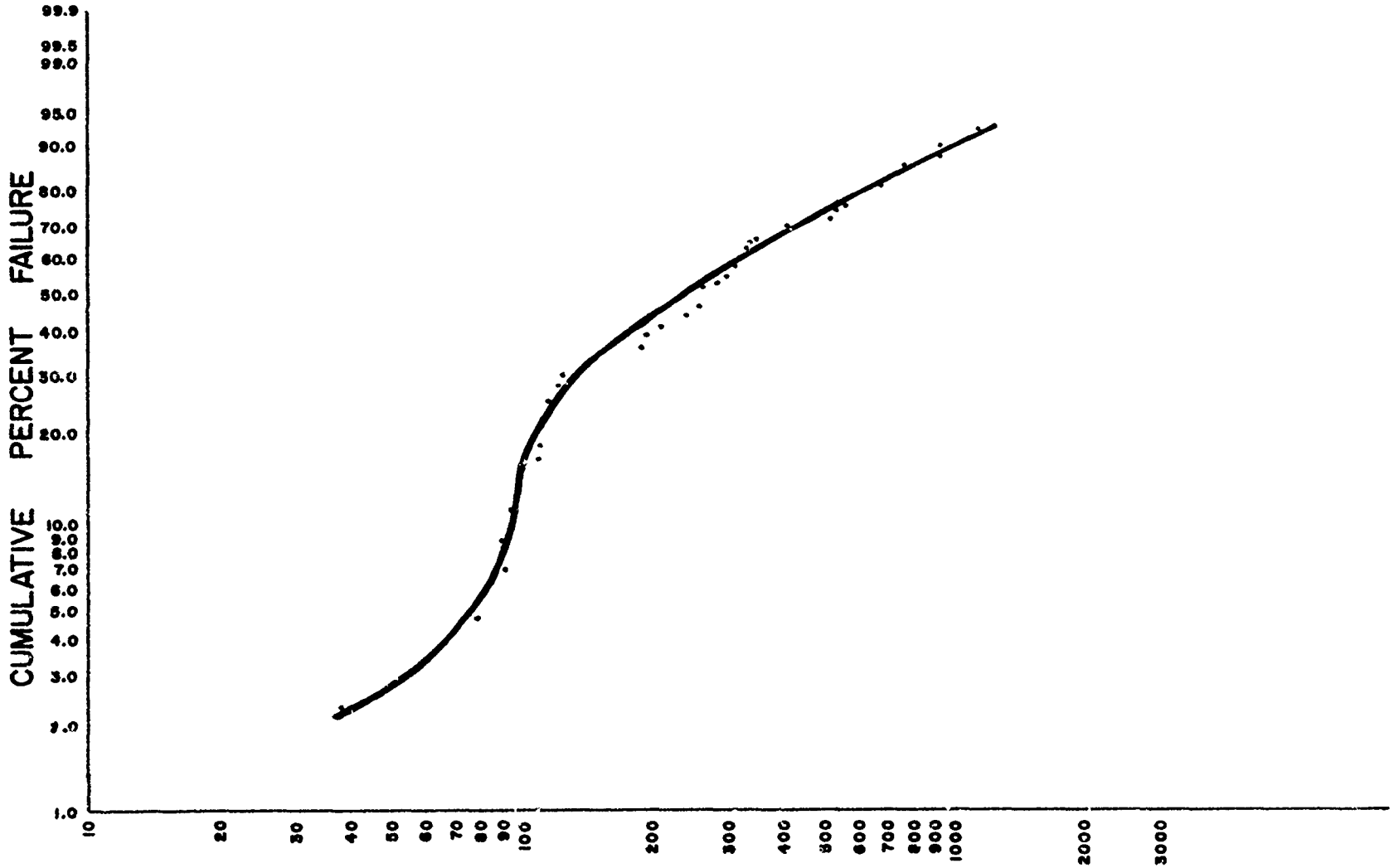

FIGURE 14

THREE PARAMETER
WEIBULL PROBABILITY PLOT
$X_o = 72$ HOURS

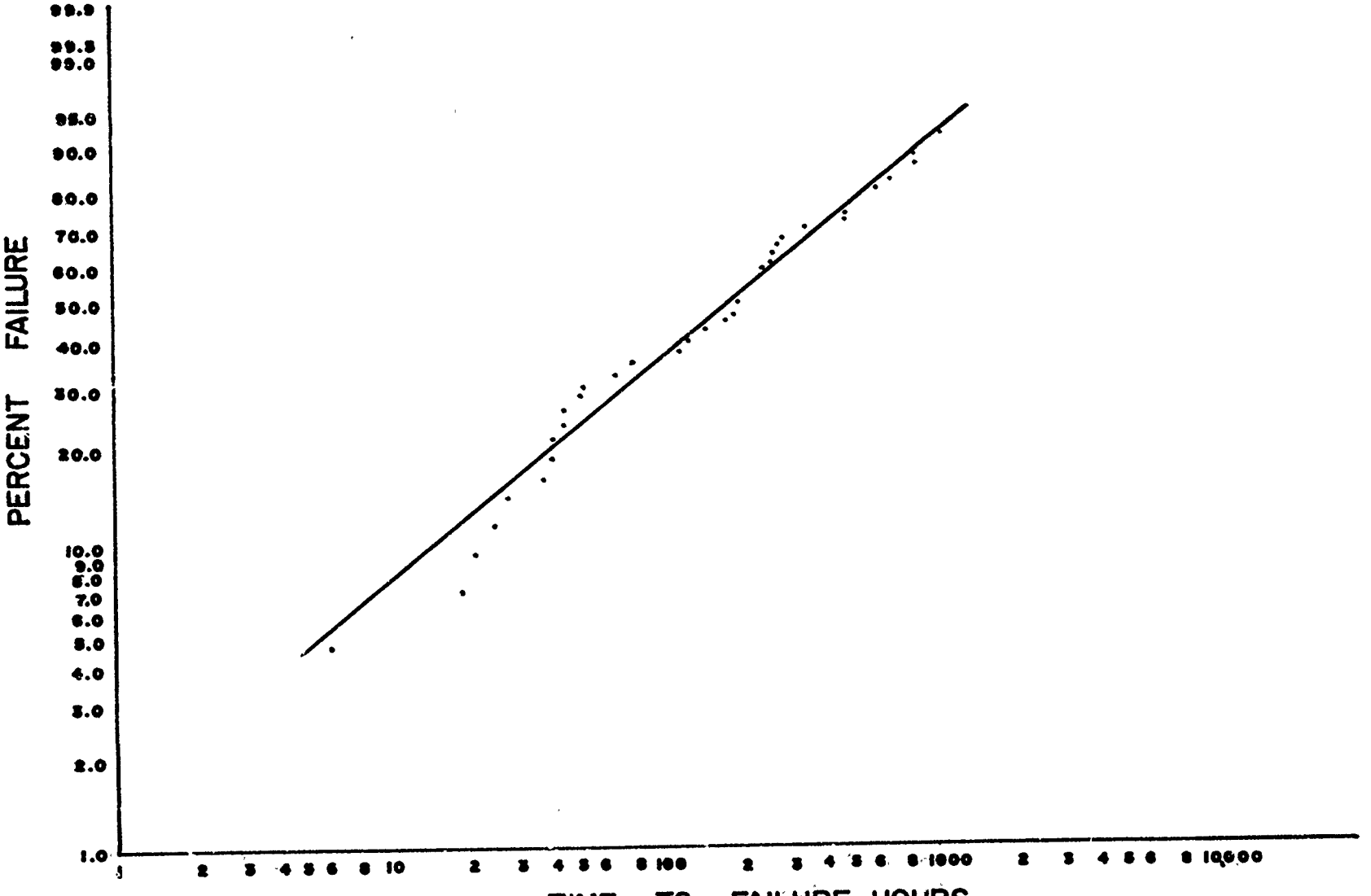

FIGURE 15

distribution was found to be equally applicable as shown in Figure 15, with a correlation coefficient of 0.987.[2] The lower boundry of life was established at 72 hours since this time period was utilized as a turbine stabilization period and failures occurring within this time period were not included as valid test data.

1.4.3 Test Plan for Phase II Testing

The following test program was established and applied to the Phase II test effort.

1.4.3.1 Ring Fabrication

Inner and outer rings for bearing MPB P/N S518MCK to be fabricated in sufficient quantity to obtain the anticipated 6,000 test bearings. Outer rings will be selected from lots produced by standard production methods, in each of the ABEC 1, ABEC 3, and ABEC 7P tolerance categories, to obtain defect-free ball tracks. Inner rings to be produced in sufficient quantity to yield the desired number of sample rings in each defect type-defect level,ABEC class category. (A minimum of 57 categories are anticipated including baseline, defect-free bearings in each ABEC tolerance grade.

(2) "Statistical Design & Analysis of Engineering Experiments" Lipson & Sheth, pp 42

A maximum of 50 defect-containing rings are anticipated for each of the categories.

Ten categories of defects related to dig-nick, dirt brinell, impingement, pit, and scratch type defects may be produced by inducing the defect on rings that have already been produced by standard methods.

Nine categories related to comet tail, grind-skip lines, orange peel, and liney finish will be produced by controlling processes to accentuate the generation of the specific defects desired.

1.4.3.2 Ring Inspection

Initial defect determination will be made on inner ring ball tracks by optical microscopy utilizing standard inspection techniques and inspection personnel.

Representative samples of each defect type will be examined by Scanning Electron Microscopy to characterize defect features.

Outer ring raceways will be microscopically examined to select defect-free surfaces for test bearings.

Specific defect levels of size and location will be determined by Toolmaker's Microscope and test rings documented.

Test rings will be selected from these documented parts to the levels desired for each test.

1.4.3.3 Bearing Assembly

Test bearings to be assembled, utilizing the inspected and documented rings, in each of the categories to be tested (Figure 7)

1.4.3.4 Test

The test bearings to be submitted to the following tests: It is planned to first test the two extremes and one intermediate level in each of the defect type-ABEC class groupings (18), then, based on results, test in intermediate levels as necessary to establish significance. A minimum of three defect levels in each defect type-ABEC class anticipated for a total of 54 test categories (18 x 3).

1.4.3.5 Bendix Starting Torque Test

Each test bearing will be tested with thrust load of 75 gm, MIL-L-6085A lubrication, and a total of 10 starts per bearing.

The torque value for each start will be recorded, average starting torque and peak starting torque (highest reading per bearing) will be evaluated for each test group. Anticipated lot size for each of the defect type-ABEC class-defect level categories will be a minimum of 10 bearings.

1.4.3.6 MPB MARK III Running Torque Test

Test loads and lubrication as utilized in 1.4.3.5 test bearing will be rotated one revolution in both clockwise and counter clockwise directions and the instantaneous frictional torque recorded on a strip chart. From chart interpretations, values for average

running torque, average hash width, significant "spikes," and "spike" number will be recorded for each test bearing.

Lot size for each test bearing group will vary between 10 and 50 depending on severity of defect and standard deviation of each test group.

1.4.3.7 MPB Vibration & Noise Test (VANT)

Test loads and lubrication as utilized in 1.4.3.5 test bearing will be rotated at 600 rpm and the noise level recorded as microns per second, as the bearing coasts to 300 rpm.

Lot size for each test group is estimated to be 14 bearings minimum.

1.4.3.8 Life Test

Fourteen (14) MPB designed and built ten-turbine test beds will be utilized for life testing. Test bearings utilized in performance tests will be used in life testing.

Operating conditions will be as follows:

Speed: 16,000 rpm nominal

Load: 2 lbs. thrust

Temperature: 135°F to 140°F ambient

Lubrication: KG-80 oil as manufactured by Kendall Oil Company

Each test turbine will contain one test bearing mounted in the front position. One defect-free bearing will be mounted in the rear position.

Bearing failure will consist of speed drop below 10,000 rpm after initial turbine stabilization at 16,000 rpm (72 hours max.). One restart attempt will be allowable. Defect-free bearings will be tested in each turbine bank to obtain comparative baseline data. This baseline bearing test data will be obtained concurrently with defect-containing bearing data to include any variations of test method or test equipment.

Lot size is conservatively estimated at 50 bearings in each test grouping. (Later reduced to 20 bearings.)

2. Phase II - Fabrication, Inspection & Testing

2.1 Test Ring Fabrication

Test rings were manufactured in ABEC 7P, ABEC 3 and ABEC 1 tolerance levels. Defects to be evaluated were produced on inner ring raceways only, the outer raceways being defect-free.

Defects in the following categories were induced on finished inner raceway surfaces: Scratch, Dig-Nick, Dirt Brinell, Orange Peel, and Impingement. Manufacturing processes were controlled to achieve desired surface condition for categories: Comet Tail, Grind-Skip Line, and Liney Finish. An attempt was made to obtain various defect levels in the "Pit" category through selection of "dirty" steel. However, this approach was successful only in the "small" level and the larger defect levels were induced.

The specific methods utilized for defect-containing ring fabrication and photomicrography of typical defects are included in Appendix F.

2.2 Test Ring Inspection & Selection

Inspection sequence for baseline bearings and induced defect test bearings was as follows:

a. Visual Inspection - Inner & Outer Rings - No defects accepted.

b. Assemble

c. Radial play check (all bearings)

d. Running Torque Test (sample)

e. Starting Torque Test (sample)

f. Vibration & Noise Test (sample)

Further inspection of induced defect test bearings, as defined in 2.1 was as follows:

g. Disassemble bearings selected from above

h. Induce defect desired on inner rings

i. Visually locate and classify defects on inner rings

j. Select inner rings for scanning electron microscopy (SEM) examination

k. Reassemble test bearings

Inspection sequence for process controlled defect types, as defined in 2.1, was as follows:

a. Visual inspection of outer rings - no defects accepted

b. Visually locate and classify defects on inner rings

c. Select inner rings for SEM examination

d. Assemble test bearings

e. Radial play check test bearings

In most defect categories 50 test bearings were selected in each of three defect levels. No fewer than 46 test bearings were available in any one defect level test group.

Sample rings representative of each defect type were subjected to scanning electron microscopy (SEM) to provide a characterization of the raceway surface topography, which was not possible with optical microscopy techniques. A comparison of these SEM photomicrographs with those taken with conventional optics is detailed in Appendix G.

No basic inconsistencies are apparent between these SEM photomicrographs and the supposed defect characteristics outlined previously in 1.2.3.

2.3 Life Test Turbines

A total of 14, ten station turbine banks were fabricated at MPB utilizing the design concept evolving from the Phase I phototype turbine bank development. Prior to placing a completed turbine bank "on line" for testing of defect-containing bearings, a qualification was performed. This qualification consisted of running baseline bearings with MIL-L-6085A oil as explained previously (para. 1.4.2.4) until at least two failures occurred for each test station.

Data from the first seven turbine banks were submitted to CIID for more rigorous statistical testing. The results are described in Appendix H and show that the data fit a log-normal distribution and are from the same population.

Subsequently Bartlett's test of variances was applied to all 14 test turbine bank data showing homogeneity of variances (Figure 16).

On this basis all 14 test turbine banks were considered acceptable for testing of defect-containing bearings.

2.4 Bearing Test

2.4.1 Performance Testing

All defect-containing bearings selected previously were subjected to the torque and noise tests described in the test program (para. 1.4.3.5 through 1.4.3.7).

2.4.2 Life Testing

Life tests were executed utilizing test program (para. 1.4.3.8).

Initially it was planned to test 150 bearings in each defect category (50 bearings in each of 3 levels) and, in fact, testing was completed in this manner on test groups 1 and 2 and partially completed on groups 3, 4, and 5 (Ref: Figure 2).

It became apparent as these tests progressed that even the larger defect categories were producing mean lives of about double those attained on the turbine bank qualification runs. At this rate it would be impossible to complete testing of all defect categories within the calendar time limitation of this program.

As a result the test program was modified to test only the largest defect level in each category.

Turbine #	Variance of Log Time-To-Failure
A	0.0896
B	0.1610
C	0.1833
D	0.2000
E	0.1140
F	0.1900
G	0.1600
H	0.1295
I	0.1140
J	0.1860
K	0.2040
L	0.1750
M	0.1666
N	0.1736

Results of Bartlett's Test of Variances

$$X^2/C = 6.87$$

Tabular Value at 95% Probability = 22.36

(Ref: "Applied Statistics for Engineers" by William Volk)

Figure 16

Turbine Bank Qualification Analysis

Also further information leading to use of the Weibull distribution rather than log-normal allowed a reduction of sample size from 50 to 20 test bearings.

Visual examination of failed bearing components was made to validate test bearing degradation. As expected, failure typically was associated with lubricant thickening or breakdown (Figure 17).

2.5 Evaluation of Test Results

2.5.1 Performance Test Data Analysis

The basic approach to test data analysis applied one way analysis of variance to each defect level and baseline bearing group to detect groups in which significant differences existed. The application of the Tukey Wholly Significant Difference Test [3] then allowed determination of which sub-groups within a group were significantly different. Twenty-five (25) piece samples were utilized in each defect category and level and compared with a 25 piece baseline sample from the appropriate ABEC tolerance class. Significant differences at the 95% confidence level were noted.

A visual presentation of the conclusions reached for each performance feature evaluated is made in Figure 1.

(3) "Applied Statistics for Engineers" by W. Volk, pp 178-181

Inner Raceway - 100X
Grind-Skip Lines - ABEC 1
9,965 Hours Operation

As removed from test

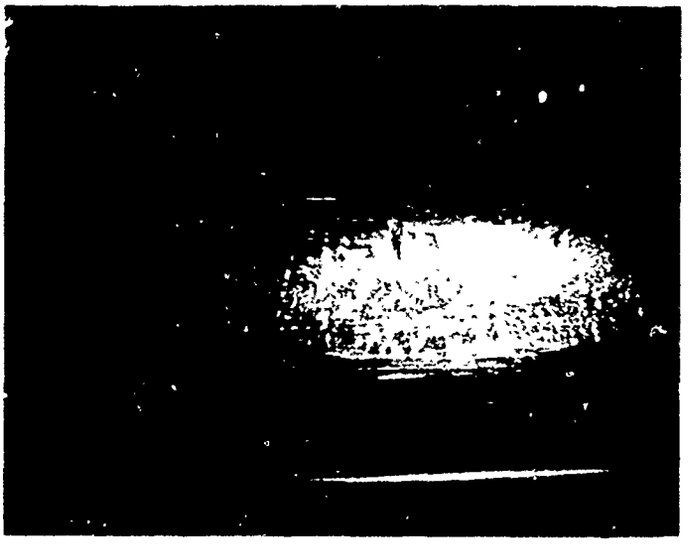

After Cleaning

Typical Test Bearing Failures

Figure 17

2.5.2 Life Test Data Analysis

Several statistical distributions were examined which adequately describe bearing life data. Of these, the three parameter Weibull distribution best satisfies the requirements of this program.

Of three statistical methods studied, the mean life ratio test was most effective in analyzing the bearing life data. By using this method, 20 bearings of a given group run to failure will, in most cases, provide nearly as much discrimination between groups as would 50 test bearings.

Excerpts from the CTID final report are reproduced in Appendix I and detail the considerations leading to the above conclusions. Also included in this report are analyses of actual test data.

A further refinement of the three parameter Weibull fit was made by equating X_o to 72 hours, this being the run-in period on each bearing life test during which failures would be excluded from test data.

Figure 2 details the results of this analysis. The correlation coefficients listed against each test group confirm the close relationship of this data to the classic Weibull distribution.

Both mean life ratio and B10 life ratio analyses were performed and presented.

APPENDIX A

EXCERPTS FROM MANUAL FOR THE MARK III RUNNING TORQUE TESTER

SECTION I

I. Introduction

A. Bearing Running Torque

The running torque of a ball bearing is the sum of couples and moments caused by friction during rotation among the various components of the bearing. Bearing torque is a very complex variable affected by such factors as operating conditions, basic characteristics of the bearing material, factors introduced by the design of the bearing, the resulting internal geometry of the bearing, lubricant, and contamination.

The running torque level when adequately recorded and analyzed reflects the degree of perfection of all the bearing characteristics mentioned above.

B. MPB Mark III Running Torque Tester

1. Features

The MPB Mark III Running Torque Tester, Fig. 1, meets all but two and exceeds several of the requirements put forth in MIL-Standard 206, specifically written to cover Running Torque Testing.

The two deviations from MIL-Standard 206 are the speed of rotation and the absence of a "go or no go" indicator.

The Mark III Torque Tester's normal operating speed is 2 rpm. MIL-Standard 206 calls out a bearing test speed of ½ rpm. The differences in torque measurements at ½ and 2 rpm are insignificant. The 2 rpm speed for the Mark III was chosen for economical use of test time without sacrifice of resolution or accuracy. Approximately 40 bearings can be tested per hour on the Mark III. ½ rpm test speed is available on the Mark III if required.

The Mark III was designed as a true bearing quality analyzer, reading out maximum torques as only a small part of the total information on a particular bearing. Bearings can then be accepted or rejected on this basis of complete evaluation rather than on a high torque reading only. For this reason the Mark III does not register a pass or fail verdict as required by MIL-STD 206 since this information is contained in the torque trace.

The Mark III is supplied with a standard 2 rpm drive system. Through the use of different diameter drive wheels other speeds can be obtained.

The initial test thrust load of 75 grams is a dead weight load. Additional thrust loading up to 400 grams total load is applied through an air cell without any effects on sensitivity or response of the instrument.

For ready interpretation of the torque traces five paper speeds are available on the Sanborn 151 recorder.

The test cycle is fully automatic and infinitely variable, with the exception of loading and un-loading the bearing. Manual control is supplied for extended clockwise or counterclockwise rotation.

The most important advantage of the Mark III over other testers is its extreme sensitivity. The standard sensitivities of the Mark III can be selected over five ranges from X1 to X20 which represent 50 to 1000 milligram millimeters per minor division. Standard full chart width would equal 2500 to 50,000 mg mm. For special circumstances the range can be moved higher or lower by adjustment of the loop gain and calibration controls.

The Mark III has a maximum sensitivity of 10 milligram millimeters per minor division with an overall accuracy of ±1% of full scale deflection. The normal operating range for the Mark III tester on standard instrument bearings is 100 milligram millimeters per minor division.

2. Theory of Operation

Fig. 1 shows the complete Mark III Running Torque Tester. Left to right is the electronic section, the mechanical section and the strip chart recorder. Fig. 2 is a closeup of the mechanical section of the Mark III Running Torque Tester. Fig. 3 is an exploded view of the mechanical section.

The block diagram of the Mark III Running Torque Tester is shown in Fig. 4. Figs. 3 and 4 illustrate the shaft which is suspended vertically from the inner race of the test bearing. A guide jewel at the bottom holds the shaft in alignment while the outer ring of the bearing is supported in a massive housing which turns at the required test speed

The inner ring tends to rotate the shaft in the direction of rotation of the outer ring, due to the friction transmitted from the outer through the balls to the inner ring. The signal generator and torque motor rotors, which are microsyns, are attached to the shaft. As the inner ring and shaft are displaced in angular position due to the transmitted torque, the signal generator produces an electrical signal proportional to the angular displacement of the shaft. This signal is fed to the amplifier and out to the recorder. The amplifier, through a servo loop, provides power to the torque motor which restores the shaft to its null position. An air loading cell to which external air pressure is applied for additional thrust loads is also attached to the shaft.

3. Torque Trace

A typical torque trace is shown in Fig. 5. It is a graph of instantaneous values of torque obtained for 2 revolutions of the outer race, one clockwise and one counterclockwise, with a 75 gram axial load applied to the inner race. Normal rotational speed is 2 rpm. Reading from the bottom to the top of

the trace shown in Fig. 5, there is a 360 degree revolution of the outer race in a clockwise direction, then a dwell when the bearing is stationary, followed by a 360 degree revolution of the outer race in a counterclockwise direction.

Each small mark at the right of the chart represents 90 degrees of rotation. This marking is used to determine when 360 degrees of outer ring rotation has occurred and to aid in the interpretation of the torque trace.

Each minor division of the chart can equal any value from 50 to 1000 milligram millimeters, depending upon the attenuator setting and the loop gain calibration. A value of 100 milligram millimeters per minor division is standard.

The trace can be analyzed for the following quantitative measures: (1) Average running torque. (2) Peak running torque. (3) Average peak running torque. (4) Average hash width. (5) Maximum hash width. (6) Ring wander due to geometrical imperfections. (7) Torque variations due to retainer action.

SECTION II

II. Interpretation of Results

Average running torque is the average of all torque values throughout the test cycle (Fig. 6). Lines representing the average value of the trace on each side of the dwell position are drawn on the chart. Halfway between these two lines is the zero torque line of the chart for any particular bearing. The determination of these average lines can be accomplished by two means. First, by use of a Polar Planimeter, whereby the entire graph is traced and the average line calculated from the area of a rectangle being equal to its base times its height. An easier method is by the use of a transparent rule laid over the trace for determination by eye of the average value of the trace. Both methods have been used and the latter method has proven to be much faster and quite accurate.

One-half the number of chart divisions between the two average lines, times the value of each minor division in mg mm, is the average running torque value.

Peak running torque is the maximum instantaneous value of torque occurring in the test cycle (Fig. 7). Having found the zero point of the chart, as above, the peak running torque is the number of divisions from the zero line to the maximum peak value obtained in the cycle times the value of each division in mg mm.

Average peak running torque is the average of the instantaneous peak values of torque occurring in the test cycle (Fig. 8). The tedious but most accurate method of determining this property is by calculating the value of each instantaneous peak in the trace and finding the average. A faster and more efficient method is to draw a line passing through all the instantaneous peaks and estimating, with a transparent rule, the average peak line for each revolution. The average peak running torque is one-half the number of divisions between the two average peak lines, times the value of each minor division in mg mm.

Average hash width is that value of torque which is the average of all the instantaneous torque values in a test cycle. This can be visualized as a band of torque through the trace (Fig. 9). The exact method of determining the average hash width is to find the numerical average of all the instantaneous torque values. However, this is a long and tedious process and it is more practical to estimate the average by a study of the torque trace.

Maximum hash width is that band of torque which would include all instantaneous torque values occurring in the torque trace. This is equal to the width of the largest spike (Fig. 10).

The "wander" due to geometrical imperfections is the amount of waviness of the torque trace in a test cycle. The maximum geometrical wander can be calculated by drawing a line through the trace representing the low frequency torque deviation and then measuring the largest deviation from a straight line (Fig. 11).

Retainer hangup is the amount of "drift" of the torque trace due to retainer action. The amount of torque drift beyond a bearing's normal peak is a quantitative measure of hangup. (See Retainer Analysis Section.)

Having described the Mark III Running Torque Tester and the interpretation of torque charts, we can now discuss the use of this and supporting instrumentation in the determination and correlation of fundamental bearing parameters

A. Geometry Analysis

The waviness of the torque trace is a function of bearing geometry. Ball groove roundness, ball groove to I. D. or O. D. concentricity of inner and outer race, groove to face run-out, and groove curvature all contribute to the bearing's ultimate torque performance. The degree to which each of these geometrical variables affects torque is currently being investigated.

Fig. 12 is a trace of a bearing with good geometrical properties. The average running torque of this bearing is 200 mg mm and the peak running torque 700 mg mm, with a maximum geometrical wander of 150 mg mm. Also shown in Fig. 12 are Talyrond charts of the outer and inner ball grooves of

this bearing. These charts show the radial deviations of the ball grooves from a true circle, magnified 10,000 times with an accuracy of .000003". Each minor division on the graph equals .000010" when the magnification is 10,000X and 000025" when it is 4,000X. The filter setting of 1-15 indicates that all radial deviations occurring 15 times or less in one circumference will be sensed and recorded. The outer and inner ball grooves in Fig 12 are 000017" and .000010" two point out-of-round respectively

Fig. 13 is an example of a bearing with poor geometrical characteristics, namely an .000083" out-of-round outer ball groove The average and peak running torques of this bearing are 250 mg mm and 950 mg mm respectively, with a maximum geometrical wander of 900 mg. mm.

Fig. 14 is another torque trace of a bearing with poor geometrical characteristics. In this case both the inner and outer ball grooves are badly out-of-round. The inner is .000275" two point out-of-round and the outer .000310" three point 60 out-of-round. The peak running torque is 1750 mg mm with a maximum geometrical wander of 2,300 mg mm.

Bearing geometry characteristics are easily discernible qualitatively, without the aid of any of the measures described above. A visual examination of the torque trace gives a clear, comparative picture of the degree of a bearing's geometrical perfection

B. Retainer Analysis

Retainer hangup, and its affect on torque performance, can also be determined but is often not easily distinguishable from geometry "wander". However, the majority of the time it can be recognized because it is a randomly occurring defect, whereas, geometrical "wander" is more or less sinusoidally repetitive.

Figs. 15 and 16 are illustrations of typical retainer hangups. In Fig. 15 the hangup occurs in only one clockwise revolution. If this were a geometrical defect it would be seen also in the counterclockwise revolution and would occur more than once in each direction. The bearing whose trace appears in Fig. 15 has an average running torque of 200 mg mm and a peak running torque of 1650 mg mm. The retainer hangup contributes 650 mg mm of the 1650 mg mm peak

Fig. 16 is an illustration of retainer hangup which occurred in both revolutions. This bearing has an average torque of 450 mg mm and a peak of at least 2500 mg mm. The exact amount of the peak cannot be ascertained because it is off the scale of the paper. The scale of the chart could have been adjusted so that this peak would have stayed on the chart but for illustrative purposes it is left as is. At least 1500 mg mm of the peak running torque in this example is due to retainer hangup.

C. Surface Finish Analysis

The torque trace provides excellent qualitative surface finish analysis of the combined surface finish characteristics of ball grooves, balls, and separators as well as randomly occurring defects. Before presenting examples of surface finish analysis, other instrumentation and terminology must be more clearly defined as follows·

1. Wavometer — an instrument for the measurement of ball groove waviness. A low band meter indicates the rms height of irregularities occurring 3.5 to 17 times in one circumference and a high band meter shows the rms height of irregularities occurring 17 to 300 times per circumference.
2. VANT — a vibration and noise tester. This instrument measures the axial vibration velocity in microns per second of the inner ring with the outer ring rotating at various speeds. The rotational speed used for all data in this paper is 600 rpm.
3. Ball Surface Quality — this is measured with a comparator type instrument which gives a qualitative measure of ball surface finish quality in terms of torque. Grade L is representative of the best quality ball surface finish and is equal to .25 micro-inches rms.

The four torque traces in Figs. 17 and 18 illustrate examples of surface finish analysis and the correlation of the torque data with that obtained from the supporting instrumentation. The four charts and the corresponding data demonstrate the following:

1. Effect on torque of overall excellent surface finish. (Left, Fig. 17.)
2. Effect of poor outer groove finish. (Right, Fig. 17.)
3. Effect of poor inner groove finish. (Left, Fig. 18.)
4. Effect of poor ball finish. (Right, Fig. 18.)

Beneath each trace is Wavometer and Ball Gage data showing the changes in the surface finish. Also listed is the VANT level of performance in microns per second. These four examples are typical and were selected from a large amount of data collected during this program.

Random defects, such as pits, scratches, comet tails, and brinell marks occur as random spikes on the torque trace. The left trace in Fig. 19 is af a bearing with a large comet tail in the ball path on the inner groove. There are three major peaks per revolution, each of a different magnitude.

The trace on the right of Fig. 19 represents a bearing with several scratches across the ball grooves. Accurrence of the peaks is haphazard and each is of different magnitude. The values of the surface finish parameters as measured

by the Wavometer and Ball Gage are given as well as the VANT levels of performance. Note that the Wavometer readings and VANT levels of these random defect bearings are similar to those with overall poor surface finish whereas the torque traces are distinctly different.

Brinell defects are seen as fairly regularly occurring spikes of greater width than most random defects (Fig. 20). They are also distinguishable by the occurrence of 2 or 3 spikes within 30 rotation, repeating a number of times in a 360 revolution depending upon the number of balls in the bearing. Also in Fig. 20 are Talyrond traces of the inner and outer ball grooves showing six brinell marks per groove. The running torque trace indicates that the balls roll over these marks four times per revolution of the outer race. This type of analysis is used to evaluate the relationship of defects of known magnitude and configuration with torque.

The normal chart speed is 2.5 mm per second. By increasing this speed, the torque trace may be spread for a more detailed picture of the individual torque spikes. Fig 21 shows a trace of a bearing with good surface finish on the left and then a portion of the same trace on the right with the paper speed increased to 12.5 mm per second. Fig. 22 is the same except that the bearing has poor surface finish.

The average and maximum hash widths on the trace do not need to be determined for the instrument to be of value. A visual examination of the trace will show the quality of a bearing's surface finish without resorting to any calculations once experience has been gained. The tester can distinguish between overall poor surface finish and random defects whereas the Wavometer and the VANT, as seen in the above examples, cannot. This is because the Mark III Tester is a peaking device and presents a qualitative picture of bearing defects as well as a quantitative one.

D. Dirt Analysis

The evaluation of bearing cleanliness and cleaning procedures is a simple matter. Figs. 23 and 24 show a dirt-contaminated bearing on the left and, on the right, the same bearing after washing. In Fig. 23 the maximum hash width was reduced from 4000 to 1600 mg mm by washing. In Fig. 24 the maximum hash width was reduced from 3500 to 600 mg mm as a result of washing.

Peak torque due to dirt can usually be distinguished from random surface finish defects by the thin "spikes" which they make on the torque traces. However, this is not always the case as a larger piece of dirt may very well contribute to a wide instantaneous value of torque. In order to accurately determine dirt contamination a bearing must be thoroughly cleaned and then re-tested.

E. Lubrication Analysis

A lubricant's contribution to bearing torque can be evaluated. Standard bearing lubricants will usually cause a large torque shift, increasing the average and peak torque values by an amount dependent on the lubricant's viscosity and the rotational speed of the bearing

Fig. 25 is an example of a bearing before and after lubrication with a standard instrument bearing lubricant. The larger torque value after lubrication is easily discernible. The average running torque increased by 250 mg mm and the peak running torque by 300 mg mm.

Lubrication cleanliness can also be evaluated This evaluation would be identical to that discussed in the previous section of contaminated vs. clean bearings. A lubricated bearing when torque tested may show dirt spikes on the trace. If, after washing the bearing, the dirt spikes disappear, then the lubricant was contaminated as indicated by the torque trace spikes.

SECTION III

III. Operating and Calibrating Instructions

A. General

1. Always insure cleanliness of the instrument's mechanical unit by observing the following items:
   a. Always keep the top of the mechanical unit enclosed with the dust cover when it is not in operation.
   b. Be sure that the mechanical unit of the instrument is level.
   c. Never touch the following adjustments on the instrument panel during normal operation:
      1. Time set at
      2. Sensitivity
      3. Resistance balance.
      4. Capacitance balance.
   d. The function lever on the mechanical unit controls the test weight on the bearing and also controls the recorder signal circuit.

e. Check the following controls shown in Fig. 26 before turning the master switch on:

Attenuator	– X2 position
Switch #2	– "on" position
Switch #3	- "auto" position
Switch #4	– Full bridge position
Switch #5	– Operate position
Switch #6	– "out" position
Switch #7	- "off" position
Switch #8	– "on" position
Switch #9	– Middle position
Recorder speed	– 2.5 mm per sec.
Function lever	– down or lock position

f. The entire tester is turned "on and off" with the master switch #1 on the recorder. When the master switch is in the "on position, the pilot lights "A", "B", and "C" will be lighted.

g. Warm-up time for the tester is 30-45 minutes.

B. Calibration

At the start of each day the tester should be calibrated, as well as at any other time when experience indicates that the tester is not functioning properly. For calibration there is a calibrating arm (with chuck key), one torsion wire (O. D. .006", length 3.530", k = 100 mgmm/degree), one master bearing, and one screwdriver.

The following procedure is used to calibrate the tester:

1. Disengage the function level (locked-down position).
2. Locate the calibrating arm into position on pickup base which is located left of the pickup as shown in Fig. 26. Level the unit.
3. Place torsion wire into calibrating arm "Jacobs" chuck. Take care not to bend wire, particularly near the chucks. To prevent bending, keep calibrating arm head high, so when wire is in place, there will be clearance between the tester and wire.
4. Place the cap, provided for this purpose with threaded hole in the knob, on end of the calibrating wire.
5. Mount a clean master bearing in the adapter.
6. Adjust recorder pen to middle of the chart by Potentiometer I.
7. Lower the wire with cap, by lowering the calibrating arm head, and put cap into the bearing. Leave a slight slack in the calibrating wire for locating the cap.

8. Seat the cap firmly on the inner face of the bearing but do push down.

9. Hold the cap knob and rotate cap body counterclockwise until cap is holding tight on pickup shaft. (This method prevents the calibrating wire from twisting.)

10. Take most of the slack out of the calibrating wire, by raising the calibrating arm head, but do not put strain on the wire.

11. Release the function lever. When doing this the recorder pen makes a move to right or left of the chart. The pen will return to the middle of the chart approximately to the same place where it was located when shaft was in a locked position. Tap the base of the mechanical unit to release any residual torque in the bearing. If the recorder pen does not return, the difficulty might be as follows:

    a. A twist in the calibrating wire.

    b. Improper cap location to the bearing or wire.

    c. Bearing not properly seated because of dirt present in the bearing.

    If this occurs, repeat steps 5 - 11.

12. Turn switch #3 to "manual". The recorder will start running.

13. Calibrate such that each minor division equals 100 mg mm at an attenuation of X2, i. e., eight minor divisions should equal 4000 mg mm.

14. Use 8 major divisions rather than the full 10 for calibration. Do not use the outside divisions during calibration. Twisting the wire 40 degrees will bring the recorder through 8 major divisions.

15. Make at least three different sweeps across 8 major divisions and determine the average calibration. Loosen the cap and change bearing orientation between sweeps. This average must be 4000 mgmm $\pm$50 mg mm. The calibration spread in 3 sweeps must not exceed 200 mgmm. If it exceeds 200 mg mm, this indicates trouble with the cap or bearing or possibly the instrument itself.

16. If it has been determined that the calibration is too high or too low, adjust the calibration control (Potentiometer II) in the main unit with a screwdriver to bring it to the desired point. Continue to recheck at least three different positions of the test bearing to obtain the correct average.

17. Having X2 = 100 mg mm per minor division calibrate at X5, X10, and X20 to insure attentuation linearity.
18. Turn switch #3 to "auto". This will stop the recorder.
19. Disengage the function lever.
20. Release the cap from pickup shaft by holding the cap knob and rotating cap body clockwise (one-half turn).
21. Raise the calibrating arm head until the cap clears the pickup shaft.
22. Remove the bearing and place it into a Petri dish.
23. Remove the cap from the calibrating wire.
24. Remove the wire from the calibrating arm "Jacobs" chuck and place it into a plastic tube with cap.
25. Remove the calibrating arm from pickup base.
26. Position and adjust pickup base into a level condition.

C. Operation

1. Disengage the function lever shown in Fig. 26.
2. Mount the proper housing in the tester and place the test bearing in the housing. See Fig. 27. Maintain cleanliness at this step.
3. Place the proper cap into the bore of the bearing and tighten it onto the tester shaft with a minimum of downward and twisting pressure. Too much pressure may tilt the cap, thereby resulting in hangups during the test run.
4. Position the recorder pen to the center of the recorder paper (if the recorder pen is not in this position) with Potentiometer I on the main control panel.
5. Release the function lever. If the cap and bearing are truly lined to the pickup shaft, the recorder pen will move off the recorder paper (right or left) and return near the position where it was set in step #4. Tap the base of the mechanical unit to release any residual torque in the bearing. If the recorder pen does not return near this position then the cap and/ or bearing must be relocated as in 2 and 3 above.
6. Automatic Operation
   a. With switch #3 on "auto", push start switch #10. The trace will be automatically completed.
   b. Pilot light "E" will be on constantly, and "F" will be blinking.

7. Manual Operation

   a. Turn switch #3 to "manual". The recorder will start running.

   b. Turn switch #7 to "counterclockwise" or "clockwise" as desired and tester will start to rotate.

   c. To stop the tester, turn switch #7 to "off", and turn switch #3 to "auto".

   d. When switch #3 is on "manual", pilot light "E" must be on.

   e. After manual operation, pilot light "F" might remain on but it can and should be turned "off" by gently turning the rotor by hand.

8. All possible operations should be done at an attenuation of X2 or 100 mg mm per minor division. If the trace exceeds the limit of the chart, switch to attenuation of X5 and run another trace. If it again exceeds the limit, switch to X10, etc.

9. If a load above 75 gms is desired, a conversion chart of pressure (or load) gage reading vs. actual load on the bearing is provided with the tester, Fig. 28. Operation of the tester under test loads greater than 75 grams load is identical to operation outlined above.

10 If an odd bearing trace occurs, i. e., one which appears to "hang" or drift too much, do not hesitate to stop the cycle, replace cap on bearing and start tester all over again. It is possible for the operator to twist or cock the bearing when the cap is applied.

11. When the test run is complete, place any clean bearing onto the tester to support the tester shaft, put housing cover on, and cover the mechanical unit with the dust cover.

SECTION IV

IV. Special Operating Instructions

A. High Thrust Loads in Excess of 75 Grams

The Mark III Running Torque Tester has provision for the selection of thrust loads from 75 to 400 grams which are infinitely variable and add no inertia to the system, hence do not change its dynamic characteristics. These axial loads are applied by air pressure acting upon a cup which is attached to the tester spindle. The diametral clearances of this cup in the test body are very small so that if air is fed in rapidly enough a positive pressure can be bulit up within the cup which forces the spindle down and loads it without causing any increase in inertia.

To operate with a higher than normal load (i. e., above 75 grams) the bearing is installed as usual and the air regulator knob (adjacent to the start button) is turned until the pressure gage reads a pressure corresponding to the desired load (see the Load vs. Pressure chart, Fig 28). The test is now run as before. It will usually be found at this point that the tester will not trace correctly since the torque will be too high for the pen to stay on the paper at the X2 position. Therefore, the attenuator will need to be turned to a somewhat less sensitive calibration such as X5 or X10. (See Section III C, paragraph 8.)

B. Duplex Bearings

The Mark III Running Torque Tester can be adapted to torque test duplexed pairs (in conjunction with a master bearing). The fixturing for a DF preloaded pair is illustrated in Figs. 29, 30, 31. Its principle operation is as follows:

A master bearing is installed on the tester in the normal fashion with a special cap having a reduced and ground O. D. This is shown in Fig. 29. A spindle which takes the inner races of the test pair of bearings, is installed over this cap and a cartridge carrying the test bearings themselves with provision for locking the outers together to obtain a DF preload is fitted in turn over the spindle. (See Fig. 30.) This cartridge has two arms which contact a drive pin mounted in the torque tester rotor as shown in Fig. 31.

In operation the unit is assembled to the torque tester with the exception of the drive pin. Note that the housing and spindle should be assembled prior to placing them on the cap to avoid the possibility of side loading the tester shaft.

The tester is run through one cycle to determine the average and peak running torques of the master bearing with the additional load and inertia of the duplex fixturing. Then the drive pin is screwed into place on the torque tester main rotor and one revolution in each direction is run manually. The torque readout will be the torque of the preloaded bearings plus the master bearing. The master bearing torque, determined from the first trace, can be subtracted. Note that the unit should be run with the manual controls when testing preloaded pairs as the 180° lag in rotation of the test bearings, upon reversal, will cause a short trace in one direction when using the automatic controls. If the torque is too high to stay on the trace at X2, then a somewhat higher attenuator setting such as X5 or X10 will have to be resorted to. (See Section III C for instructions on calibration at higher attenuator settings.)

SECTION V

V. Maintenance and Adjustments

A. Checking the Electrical Part of the Mark III

In the event that electrical difficulties are suspected in the Mark III Torque Tester, the circuit monitor device will determine if and where such difficulties exist. This circuit monitor device is furnished as part of the equipment and the AC vacuum tube voltmeter can be used as a general test instrument. The voltage measurements need not be made often while the tester is performing well. The tests made with this device are simple, fast and effective, and adjustments will not be necessary. Operation of the torque tester may be resumed in a matter of seconds after the testing is completed.

B. Circuit Monitor Device

This wiring harness is made especially to make certain critical voltage measurements easy on the Mark III Running Torque Tester. The harness is provided for use with an AC vacuum tube voltmeter with neither input terminal common to the chassis. (Do not use the AC section of a DC voltmeter.)

The voltage measurements serve a dual purpose: 1) To indicate the loop gain setting of the torque tester. 2) To give a check on the source of electronic difficulties.

The two test voltages, when measured and found to be .054 and 18.0 volts respectively indicate that:

1. the primary excitation of the microsyns is o. k.;
2. there are no broken or shorted wires;
3. the Sanborn Pre-Amp oscillator is functioning properly;
4. the tubes in the torque motor amplifier are good;
5. the torque motor amplifier is functioning properly;
6. the loop gain setting has not been changed.

C. Accomplishment of the Voltage Test Wiring Harness at Installation

The small box contains a 1 ohm resistor which is connected in series with the primary excitation of .054 amps (54 milliamps). The 54 milliamps thru 1 ohm gives 54 millivolts which is one of the test voltages. This test voltage is applied to the input of the torque motor amplifier. The output of the torque motor amplifier goes into a 500 ohm resistor in the small box. The second test voltage is the voltage across this resistor which is 18.0 volts. (±2 volts.)

D. Procedure for Installing the Wiring Harness for Testing

1. Facing the back of the Mark III mechanical unit, remove the 4-prong black Jones plug.
2. Insert the 4-prong plug in the socket on the small box.
3. Insert the 4-prong plug on the end of the cable from the small box into the socket on the mechanical unit.
4. Remove the phono plug and the 2-prong Jones plug from the torque motor amplifier chassis. Insert in their place the phono plug and 2-prong Jones plug from the wiring harness.
5. Plug the AC vacuum tube voltmeter into a 110V 60 cycle line.
6. Plug the two banana plugs from the wiring harness into the AC voltmeter.
7. A slide switch on the small box selects either test voltage.
8. It will be necessary to change the selector switch on the AC-VTVM to go from .054 volts to 18.0 volts. It is not necessary to have a bearing on the tester to make these measurements.
9. The voltage measurements should be recorded periodically.

E. Notes on Controls and Test Voltages

The control normally used in calibration is the sensitivity control in the Sanborn Pre-Amp. This can be adjusted with a jeweler's screwdriver. Do not confuse this control with the knob marked "sensitivity" which is turned counterclockwise and kept locked. The loop gain control is the torque motor amplifier gain control and is mounted vertically on the chassis.

If required, the loop gain control can be adjusted, however, it should remain within ±5% for extended periods of time. This loop gain controls the value of the second test voltage of 18.0 volts AC.

The first test voltage of .054 volts indicates that both microsyns are being excited properly. Possible sources of difficulty which could change this voltage would be a failure in the Sanborn power supply and/or a failure of V1107 (the 2400 cycle oscillator) in the carrier Pre-Amp.

The voltage is developed by 54 milliamps thru 1 ohm. If a wire should become broken in one of the microsyn primaries, the voltage would drop to 27 millivolts or ½ the normal value.

F. Mark III Null Adjustment by the Oscilloscope Method

The null position of the torque tester is reached by moving the torque motor stator with the null adjusting screw in the slot as shown in Fig. 32. This adjustment should be made when the torque tester is assembled and ready to run.

The oscilloscope method is very convenient for the first general location of the null position. For the final adjustments of the null position, a more precise method is also given.

1. Connect the ground terminal of the vertical input of the oscilloscope to any metal part of the mechanical unit
2. Select a test lead with an alligator clip on one end. Connect the other end to the vertical input of the scope.
3. Clamp the alligator clip on the insulation on the insulated wire going to the center Jones plug on the mechanical unit (the red Jones plug). The capacitance between the clip and the wire will gain sufficient coupling.
4. Place a bearing in the test position after the torque tester has warmed up. The eject lever should be up. The damping cylinder and cup should not be in place.
5. Adjust the oscilloscope gain and sweep controls. This will give a whole number of cycles and a pattern that is stationary.
6. At first the pattern will be characterized by square corners and sharp points. Move the null adjusting screw slowly back and forth in the slot. As the null position is approached, the square corners and sharp points on the trace will disappear and a sine wave will be observed. As the torque tester becomes nulled, the sine wave will degenerate to a straight line and the recorder pen will move to the center of the chart (use attenuator setting X200).
7. The recorder pen will be very sensitive and the slightest stimulation will cause it to break into a high frequency resonance.
8. To overcome the oscillation, install the damping fluid as outlined in the instructions in Section V - G.
9. The straight line on the oscilloscope may have appreciable width. This is due to 60 cycle line pickup in the leads to the scope. The 2400 cycle voltage is easily distinguished from the 60 cycle pattern.
10. The straight line will be present over an arc of several degrees of the torque motor stator. Select a point as near the center of this arc as possible for the position of the torque motor stator. The recorder pen should be near the center of the chart with the attenuator on X20.
11. Tap the base of the torque tester lightly and note the excursions of the pen; these should be as much as one or two major divisions but will damp out quickly.

12. Place the forefinger lightly against the side of the cap and rotate the shaft to the mechanical stop. Release and note how rapidly the pen returns to the null position. Repeat this step for the other side. The pen should return as quickly from one side as it does the other. If the return of the pen, one side to the other, is not consistent, move the null adjustment slightly, first in one direction then in the other. A point will be found where the pen returns equally well from either direction.

G. Removal and Installation of Damping Fluid

To Remove

1. Remove test bearing and cap. Also outer race housing.
2. Loosen the setscrew in the damping cylinder with a short .050" Allen wrench. (Fig. 33.)
3. Slide the damping cylinder up off the shaft. Damping fluid will drip from the cylinder so place it in a Petri dish or on absorbent material.
4. Lift out the donut-shaped damping cup.
5. Clean the silicone oil out of the damping cup and cylinder with lens tissue or wash them in a suitable solvent.

To Install

1. Draw 2 cc's of 2000 centistoke silicone fluid into a hypodermic syringe (without needle). Put this fluid into the damping cup taking care not to drop the fluid on the side of the cup.
2. Drop the damping cup back into the torque tester body.
3. Slide the damping cylinder back on the shaft taking care that the mechanical stop fits in its slot.
4. The eject lever should be in the "up" or "test" position.
5. With the thumb and index finger grip the shaft just above the damping cylinder and turn the shaft a few degrees in each direction. The recorder pen should go back and forth across the chart very rapidly.
6. Check the mechanical stop (see Item 3) and move it to the center of the slot and hold it with the index finger of the left hand. Turn the shaft back and forth with the right hand and stop when the pen comes onto the chart.
7. Tighten the Allen screw with the .050" wrench while still holding onto the damping cylinder with the left index finger.

8. Replace the outer race housing, test bearing and cap. The tester is now ready for operation.
9. Note the direction of torque shift when the rotor reverses direction. This should be to the left on the chart. If it is to the right, go back and repeat step 6, only turn the shaft 30 in either direction. This will use the next mechanical null position and will reverse the direction of torque shift. There are twelve nulls, only 6 shift according to our convention.

FIGURE 1

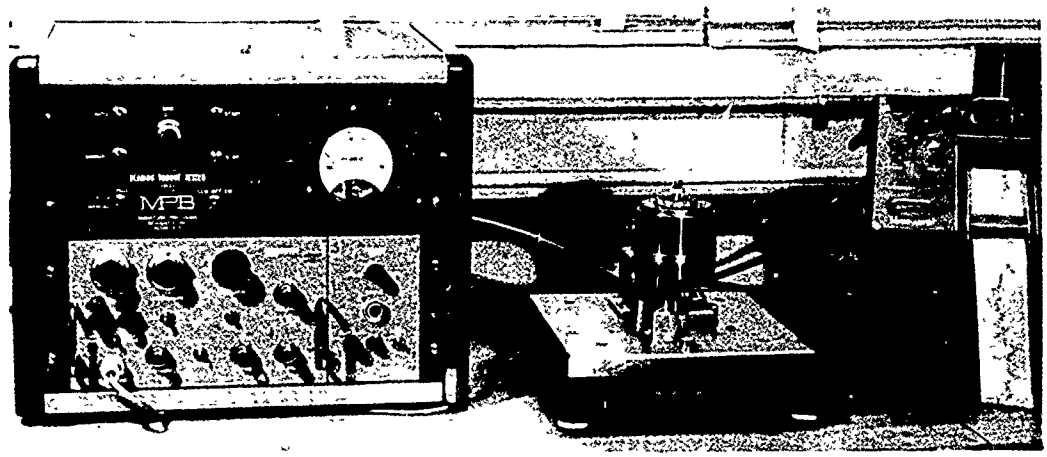

Complete Mark III Running Torque Tester

FIGURE 2

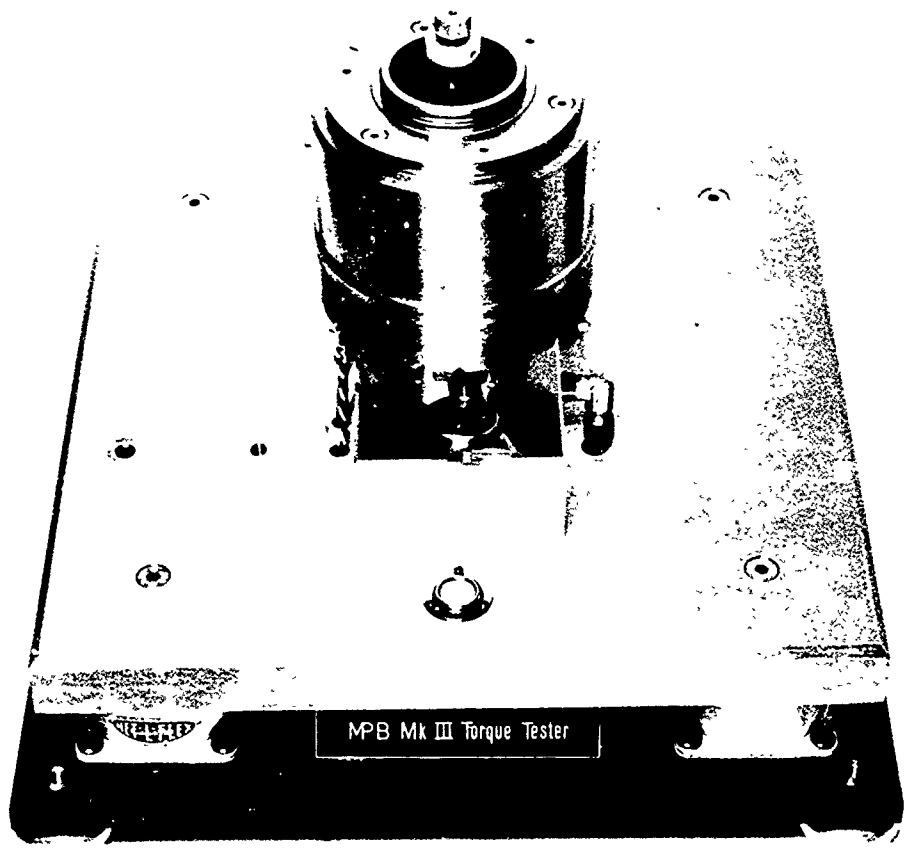

Assembled Mechanical Unit

FIGURE 3

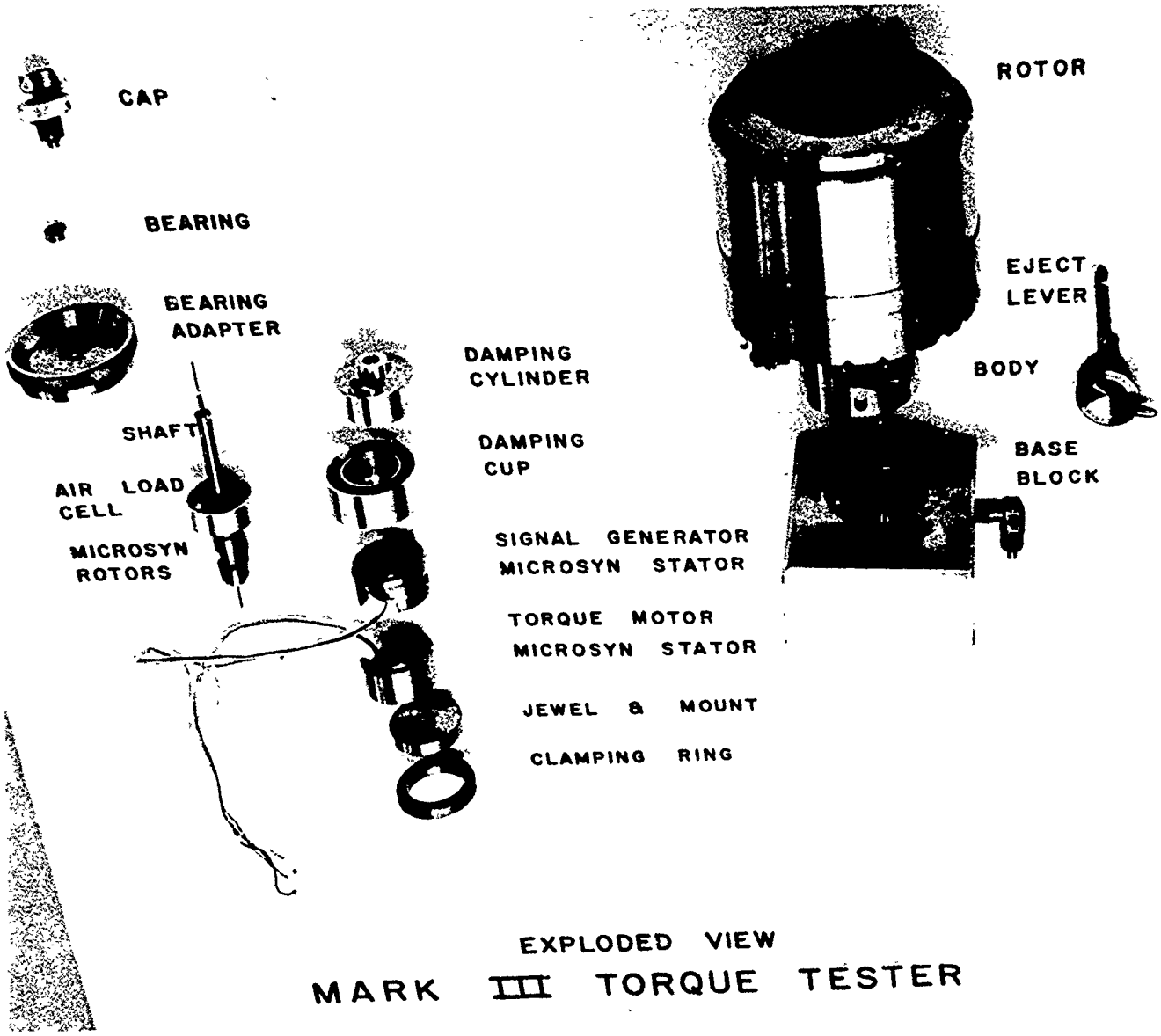

EXPLODED VIEW

MARK III TORQUE TESTER

Mechanical Section

FIGURE 4

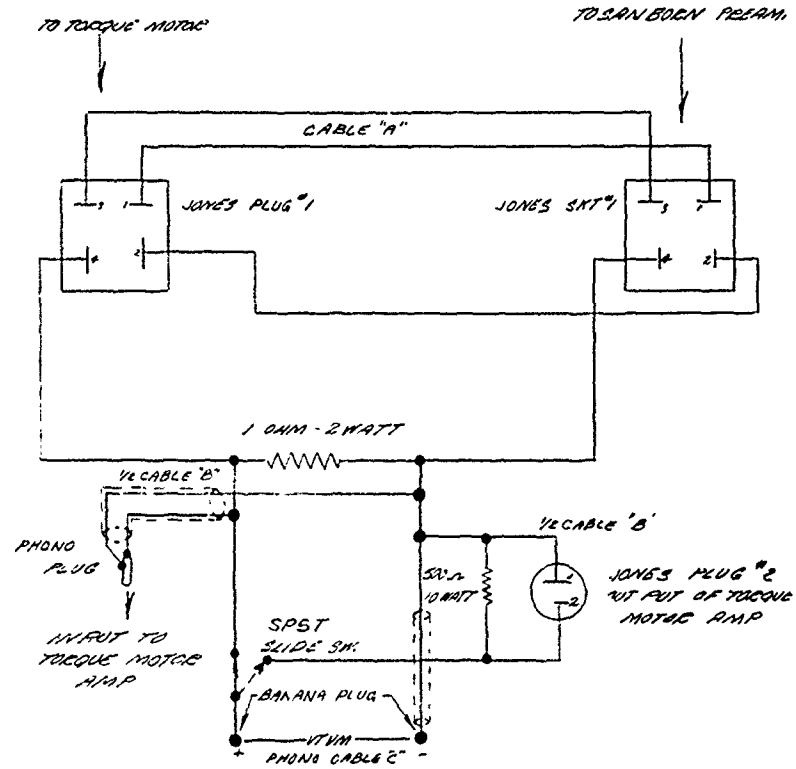

CABLE "A" - (4) CONDUCTORS
2 FT. (2) SHIELDED
CABLE "B" - (4) CONDUCTORS
4 FT. (2) SHIELDED
CABLE "C" - SHIELDED
4 FT. PHONO CABLE

HEATH MODEL AV-3
AC-VTVM

Circuit Monitoring Device for Mark III

FIGURE 5

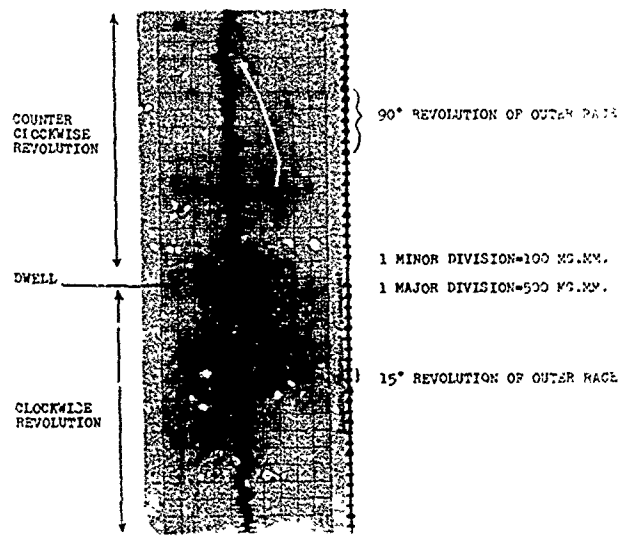

TYPICAL TORQUE TRACE

FIGURE 6

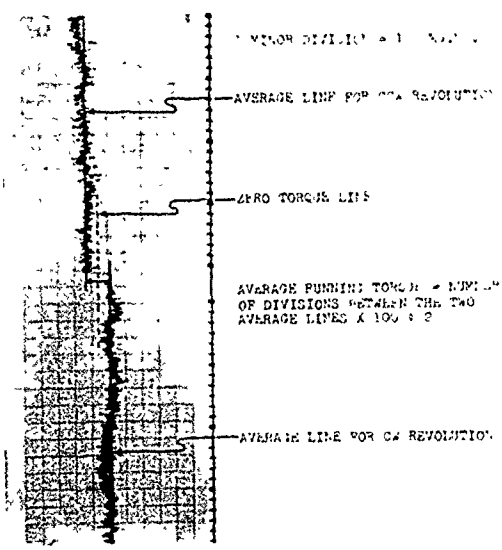

CALCULATION OF AVERAGE RUNNING TORQUE

FIGURE 7

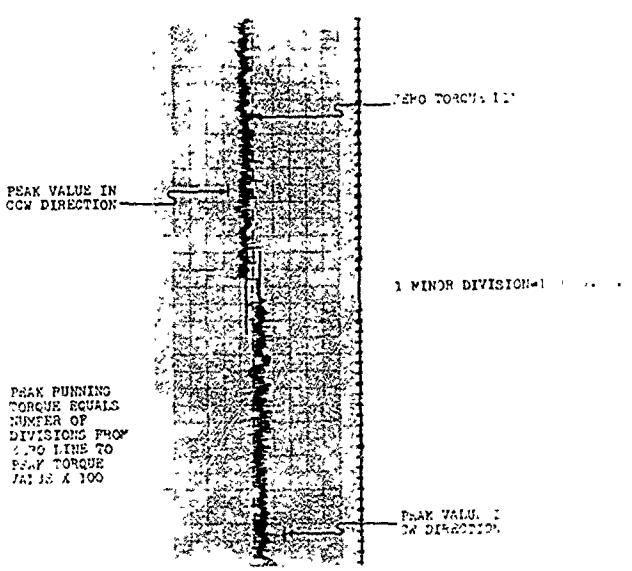

CALCULATION OF PEAK RUNNING TORQUE

FIGURE 8

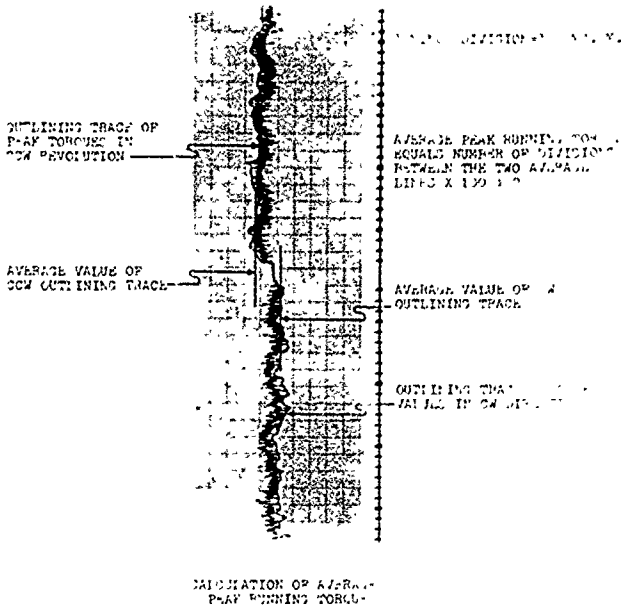

FIGURE 9

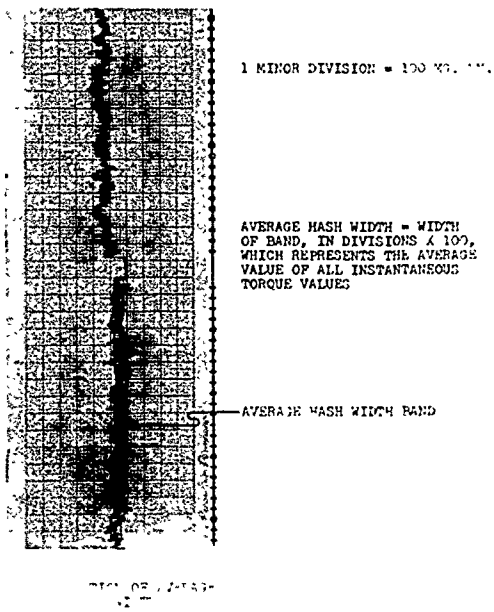

FIGURE 10

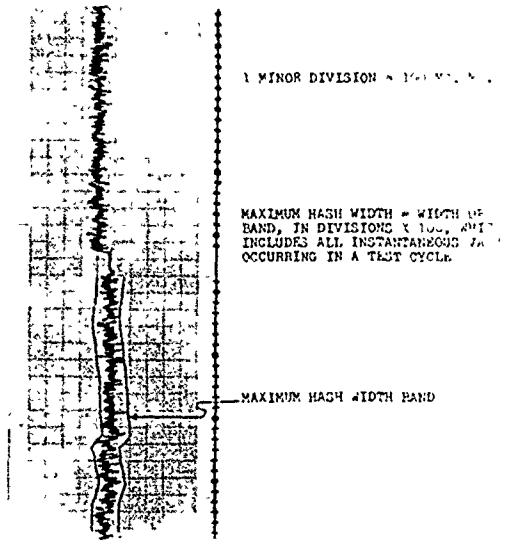

CALCULATION OF MAXIMUM HASH WIDTH

FIGURE 11

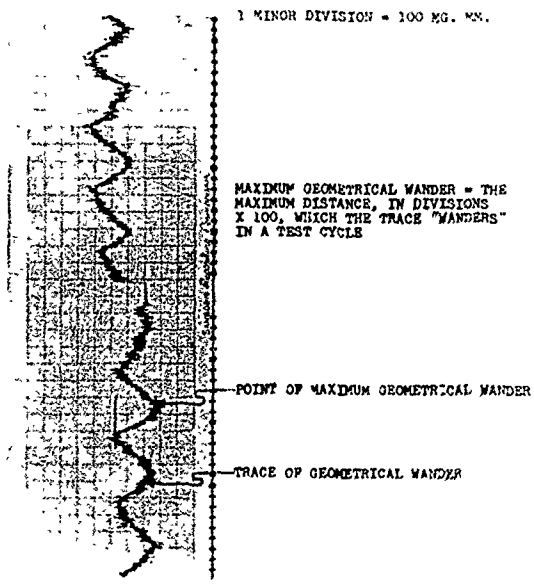

CALCULATION OF MAXIMUM GEOMETRICAL WANDER

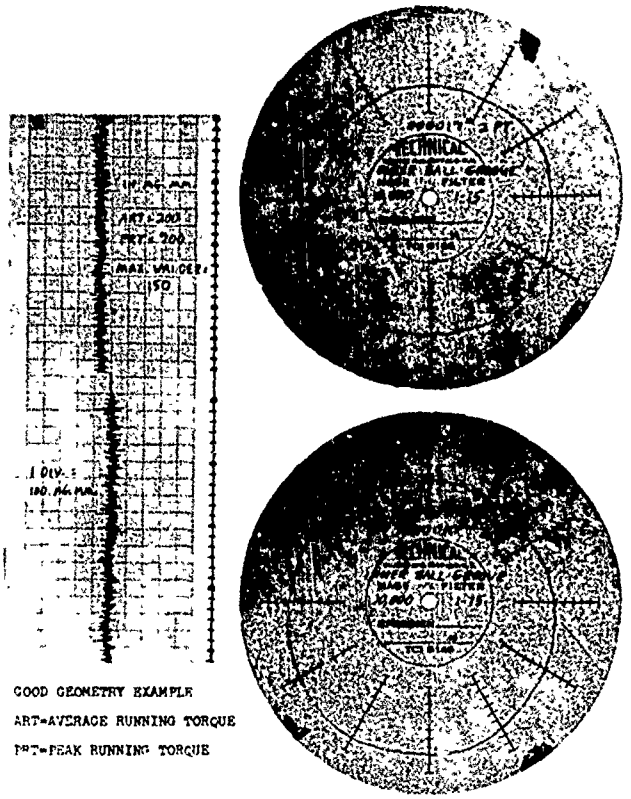

GOOD GEOMETRY EXAMPLE

ART=AVERAGE RUNNING TORQUE

PRT=PEAK RUNNING TORQUE

FIGURE 12

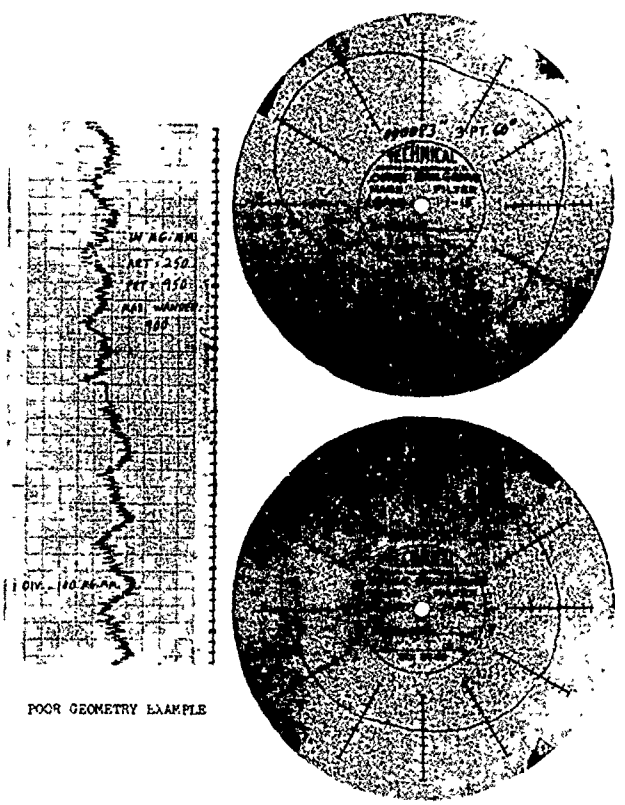

POOR GEOMETRY EXAMPLE

FIGURE 13

FIGURE 14

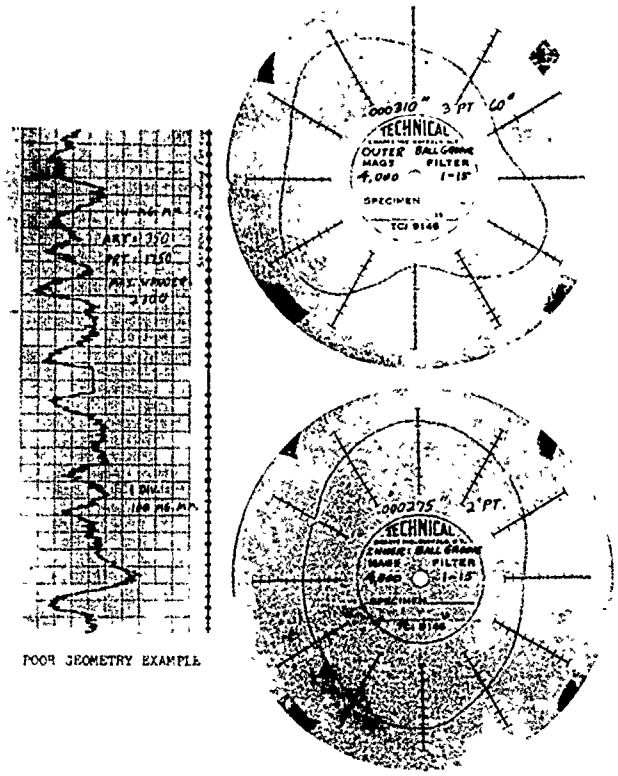

POOR GEOMETRY EXAMPLE

FIGURE 15

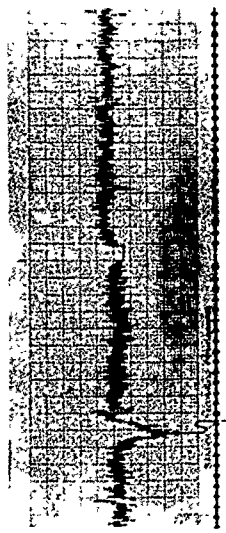

1 MINOR DIVISION = 100 MG.MM.

AVERAGE RUNNING TORQUE = 200 MG.MM.

PEAK RUNNING TORQUE = 1650 MG. MM.

RETAINER HANGUP

RETAINER HANGUP EXAMPLE

FIGURE 16

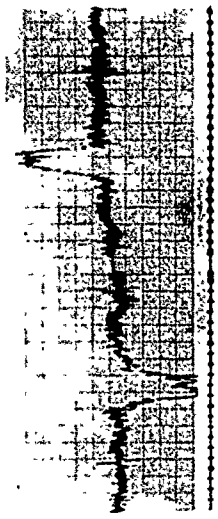

1 MINOR DIVISION = 10 [illegible].

AVERAGE RUNNING TORQUE = 450 [illegible].

PEAK RUNNING TORQUE ≯ 7500 MG.MT.

[illegible] RUNOUT EXAMPLE

FIGURE 17

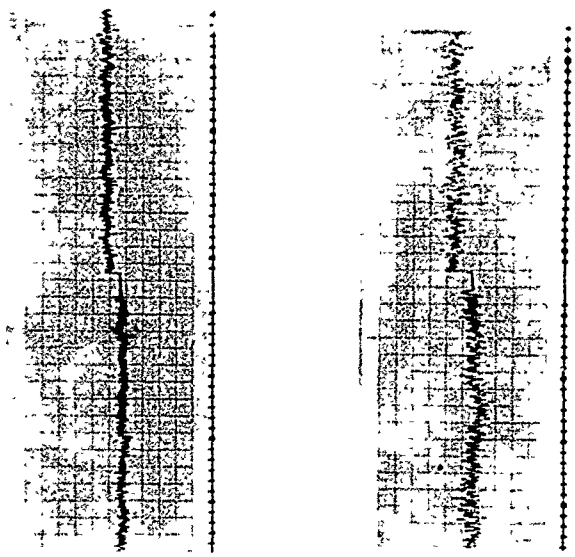

[illegible]	AVERAGE HASH WIDTH	550 [illegible]
[illegible]	MAXIMUM HASH WIDTH	1050 [illegible]
[illegible]	WAVEMETER HIGH BAND-INNER	[illegible]" r.m.s.
[illegible]	WAVEMETER HIGH BAND-OUTER	1.0[illegible]r.m.s.
[illegible]	[illegible] SURFACE QUALITY	Grade 1
[illegible]	[illegible] LEVEL	3%

[illegible] SPECTRUM ANALYSIS

FIGURE 18

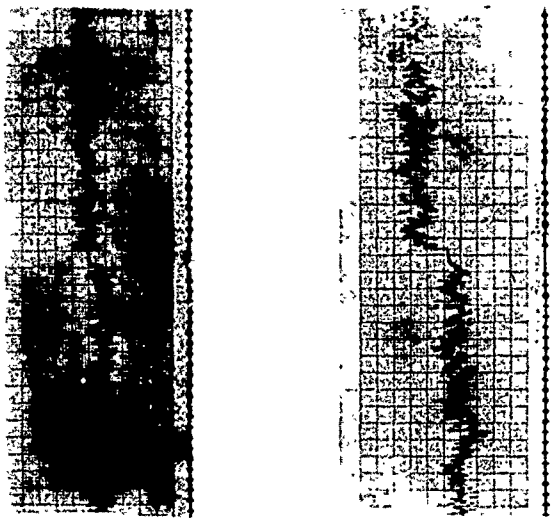

450 mg.mm.	AVERAGE HASH WIDTH	500 mg.mm.
1900 mg.mm.	MAXIMUM HASH WIDTH	1550 mg.mm.
1.2μ" r.m.s.	WAVOMETER HIGH BAND-INNER	.6μ" r.m.s.
.6μ" r.m.s.	WAVOMETER HIGH BAND-OUTER	.6μ" r.m.s.
Grade I.	BALL SURFACE QUALITY	4 times Grade I.
0	VANT LEVEL	45

SURFACE FINISH ANALYSIS

FIGURE 19

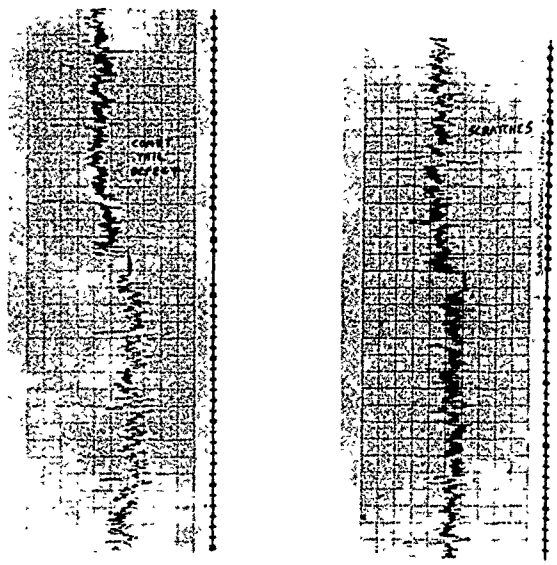

450 mg.mm.	AVERAGE HASH WIDTH	450 mg.mm.
2350 mg.mm.	MAXIMUM HASH WIDTH	2350 mg.mm.
.7μ" r.m.s.	WAVOMETER HIGH BAND-INNER	.7μ" r.m.s.
.7μ" r.m.s.	WAVOMETER HIGH BAND-OUTER	.7μ" r.m.s.
Grade I.	BALL SURFACE QUALITY	Grade I
	VANT LEVEL	45

SURFACE DEFECT ANALYSIS

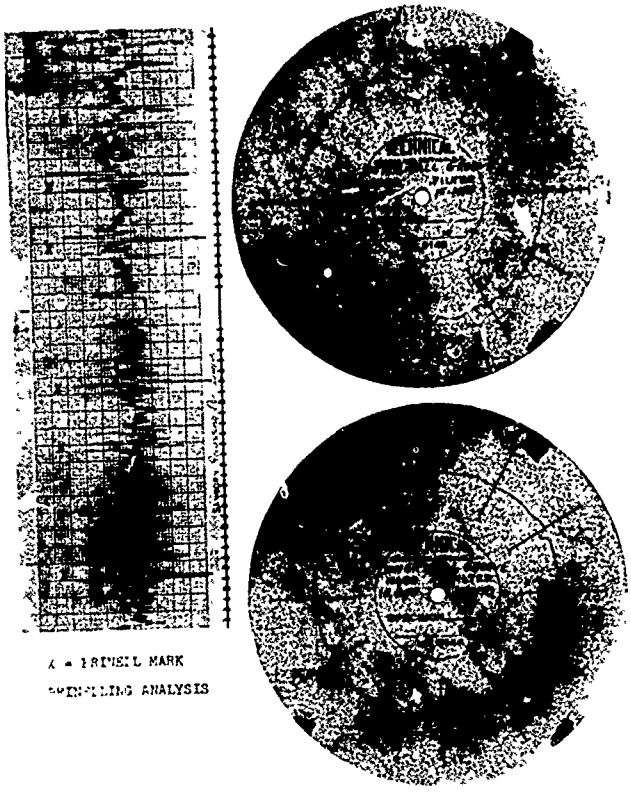

FIGURE 20

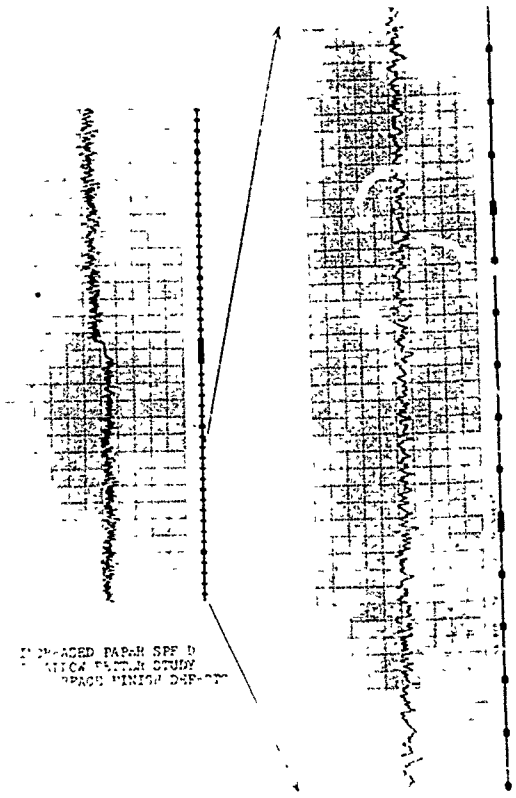

FIGURE 21

FIGURE 22

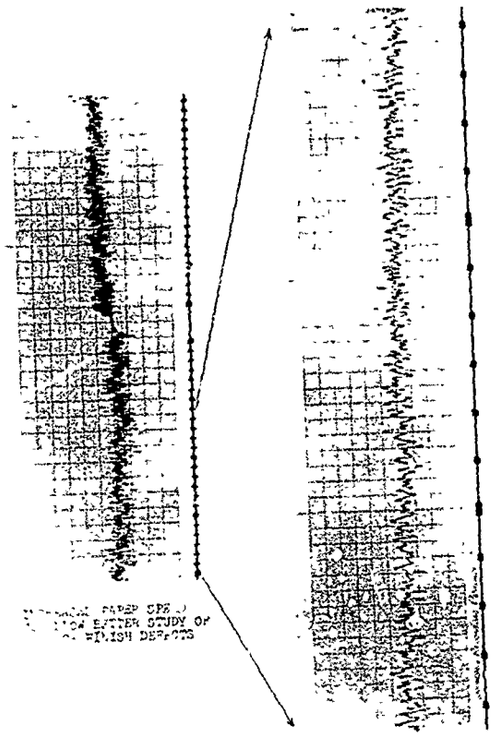

FIGURE 23

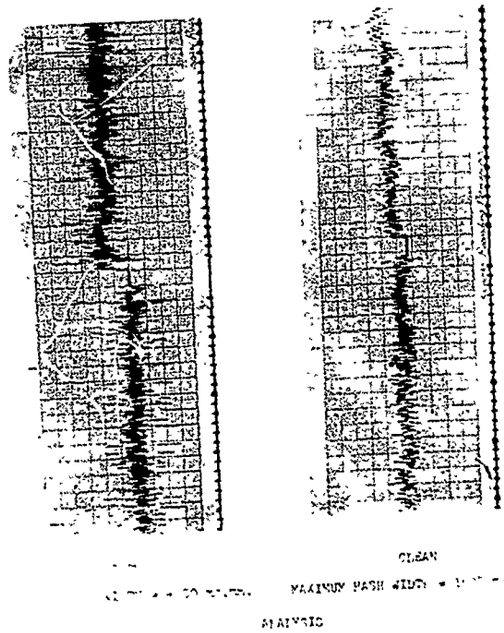

FIGURE 24

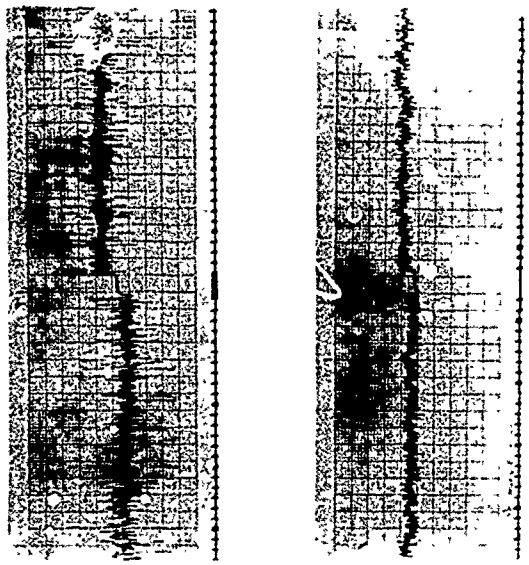

DIRTY

MAXIMUM PASH WIDTH = 5500 eg.cm.

CLEAN

MAXIMUM PASH WIDTH = [illegible]

DIRT ANALYSIS

FIGURE 25

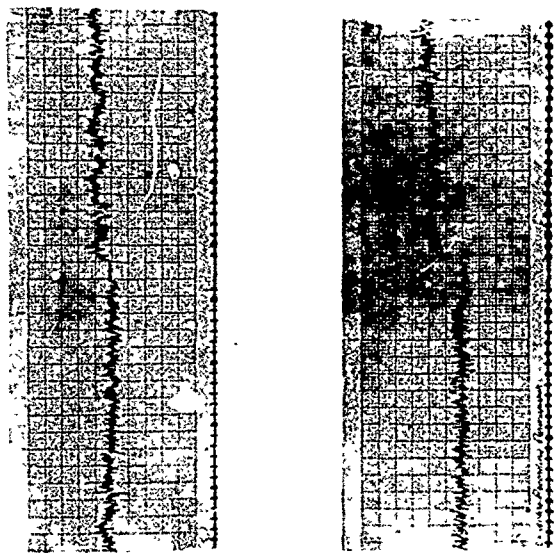

[illegible] eg.cm
850 eg.cm.

AVERAGE RUNNING TORQUE
PEAK RUNNING TORQUE

460 eg.cm.
1150 eg.cm.

LUBRICATION ANALYSIS

FIGURE 26

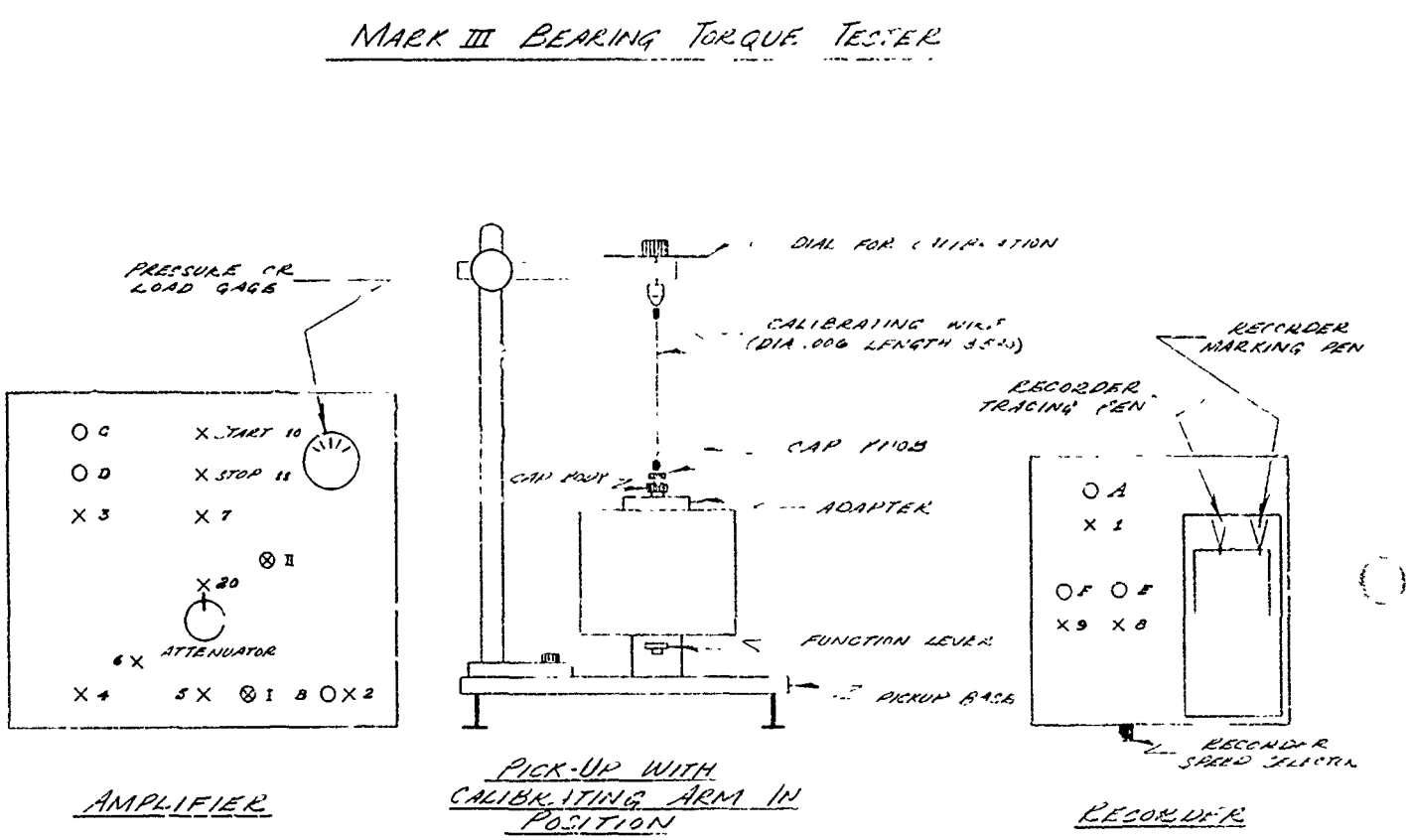

Amplifier, Pick-up with Calibrating Arm in Position, Recorder

FIGURE 27

Test Bearing - Adapter - Cap Detail

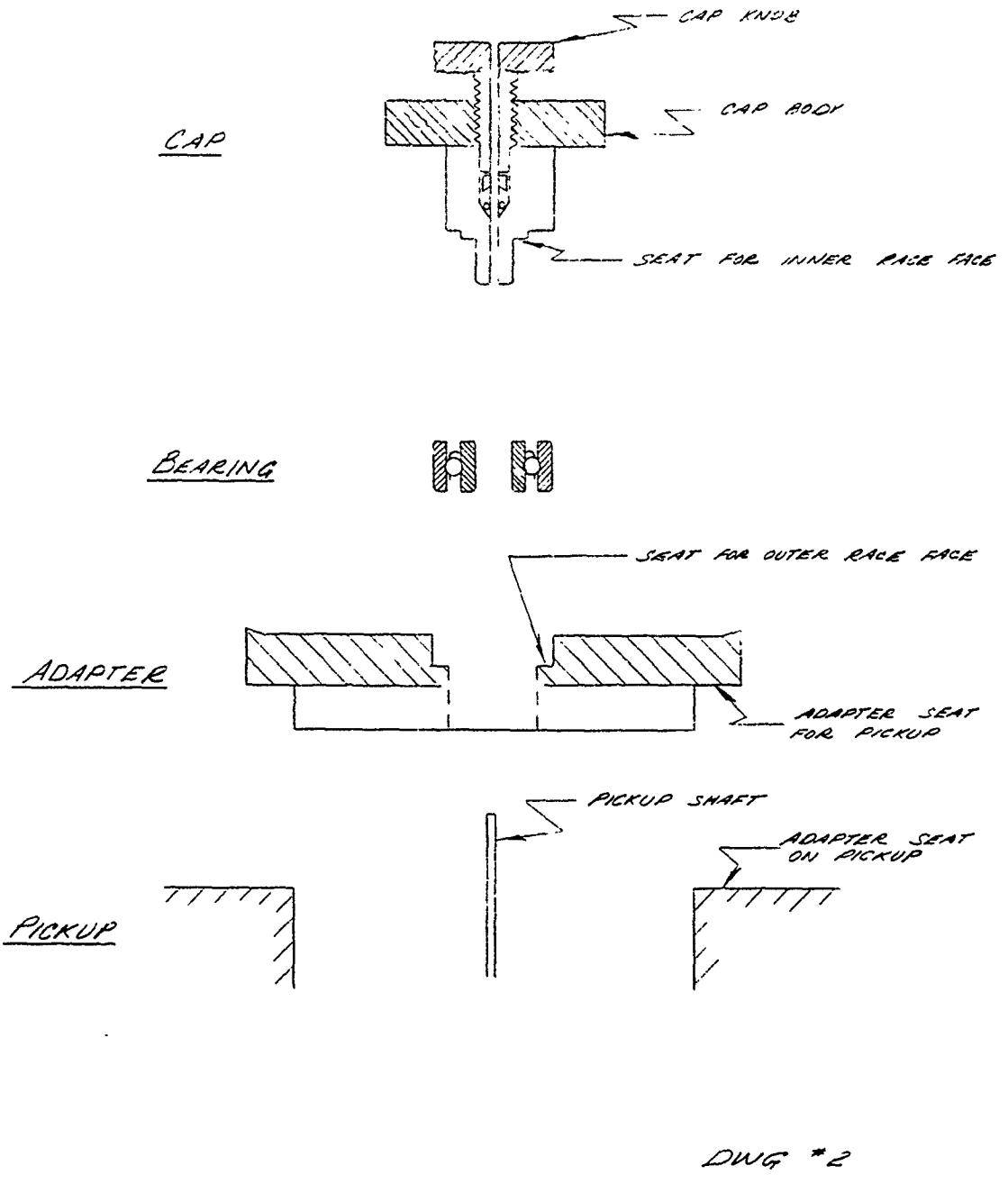

Test Bearing — Adapter — Cap Detail

FIGURE 28

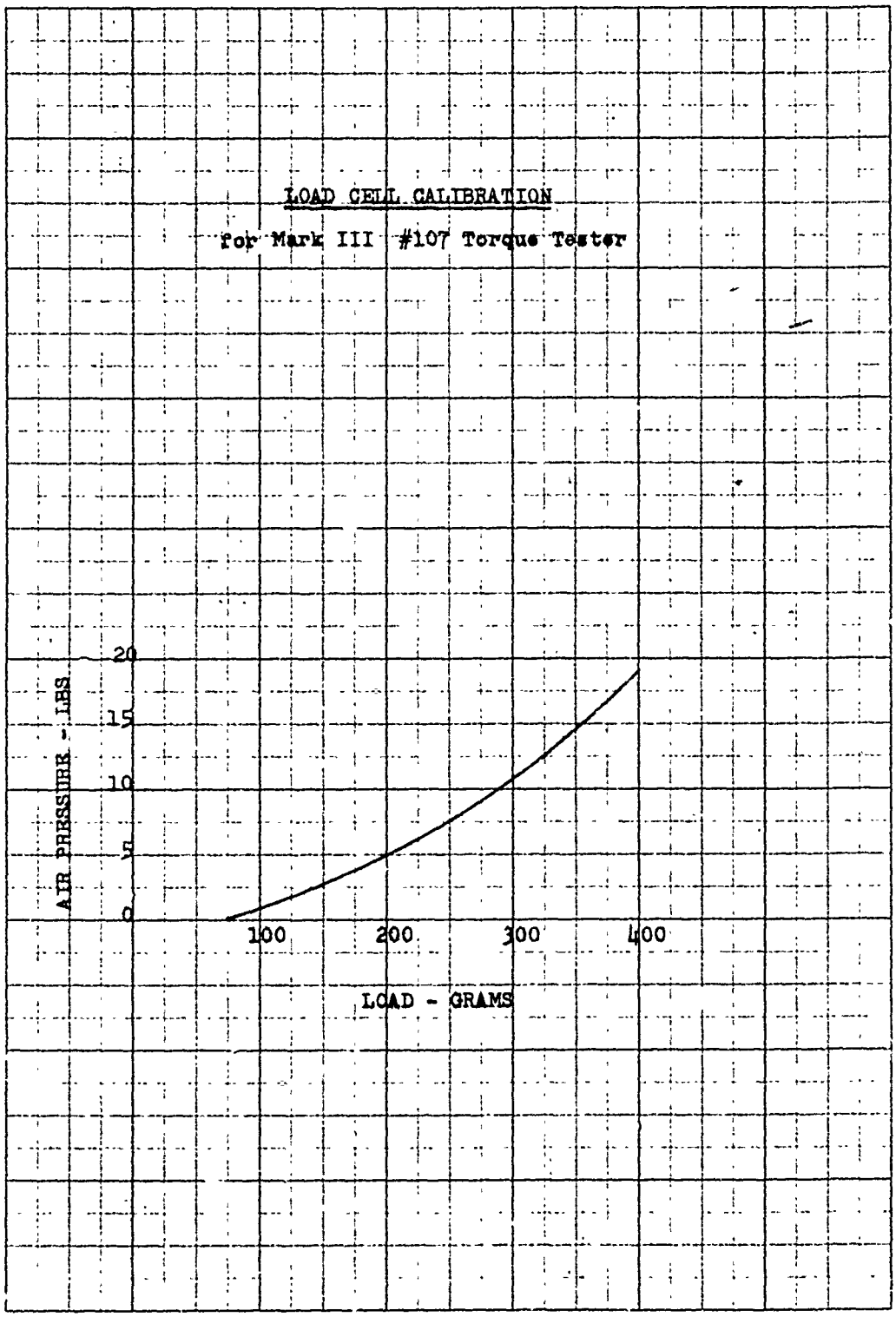

Load Cell Calibration Chart

FIGURE 29

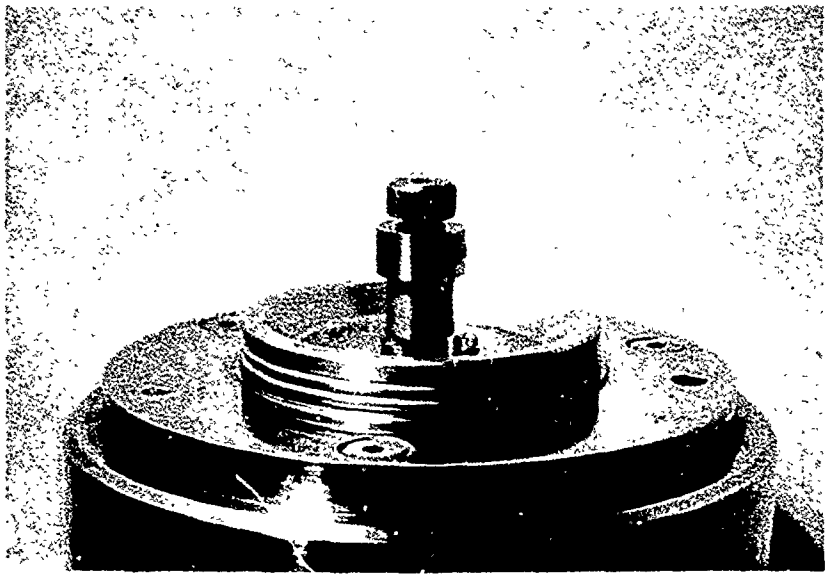

Fixturing for a DF Preloaded Pair

FIGURE 30

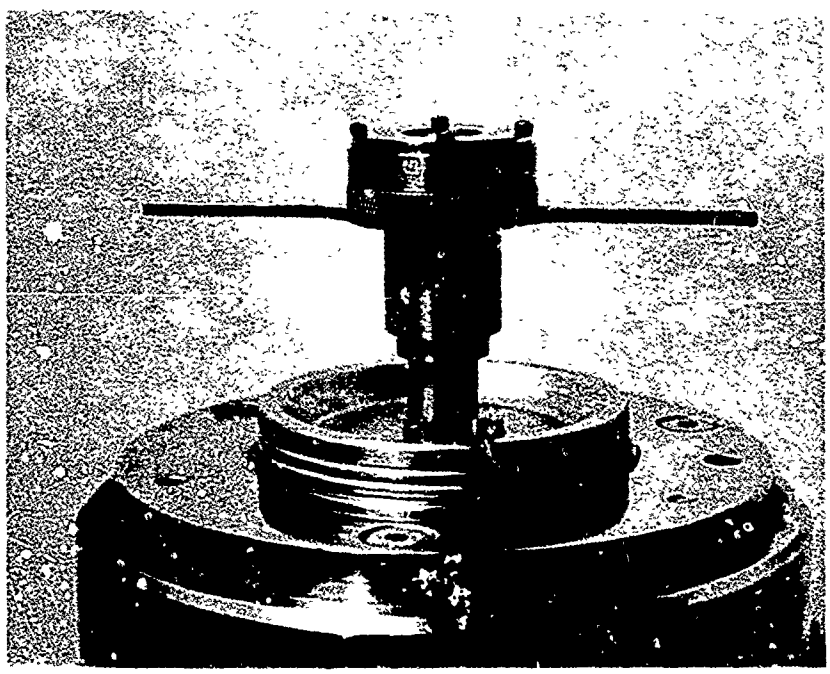

Fixturing for a DF Preloaded Pair

FIGURE 31

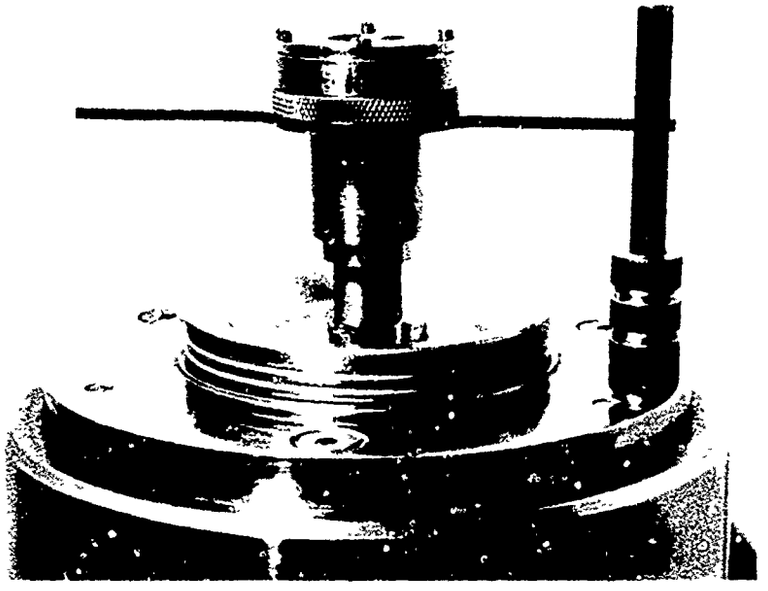

Fixturing for a DF Preloaded Pair

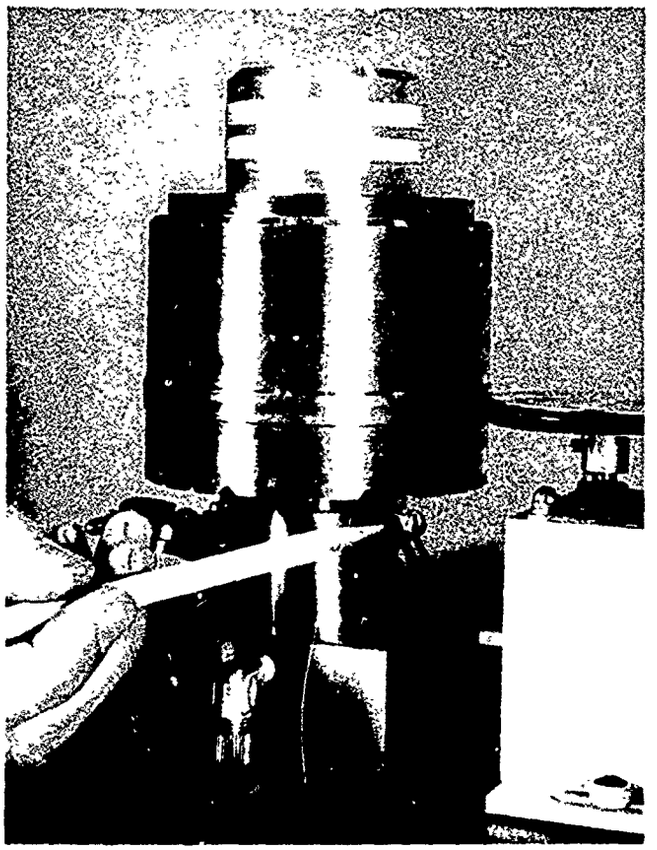

FIGURE 32

Null Adjustmen

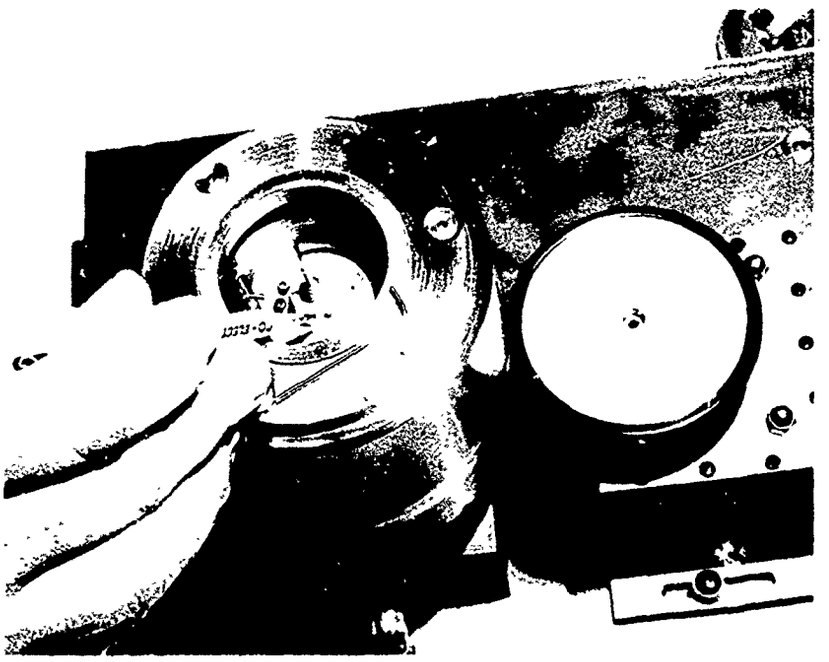

FIGURE 33

Damping cup installation

FIGURE 34

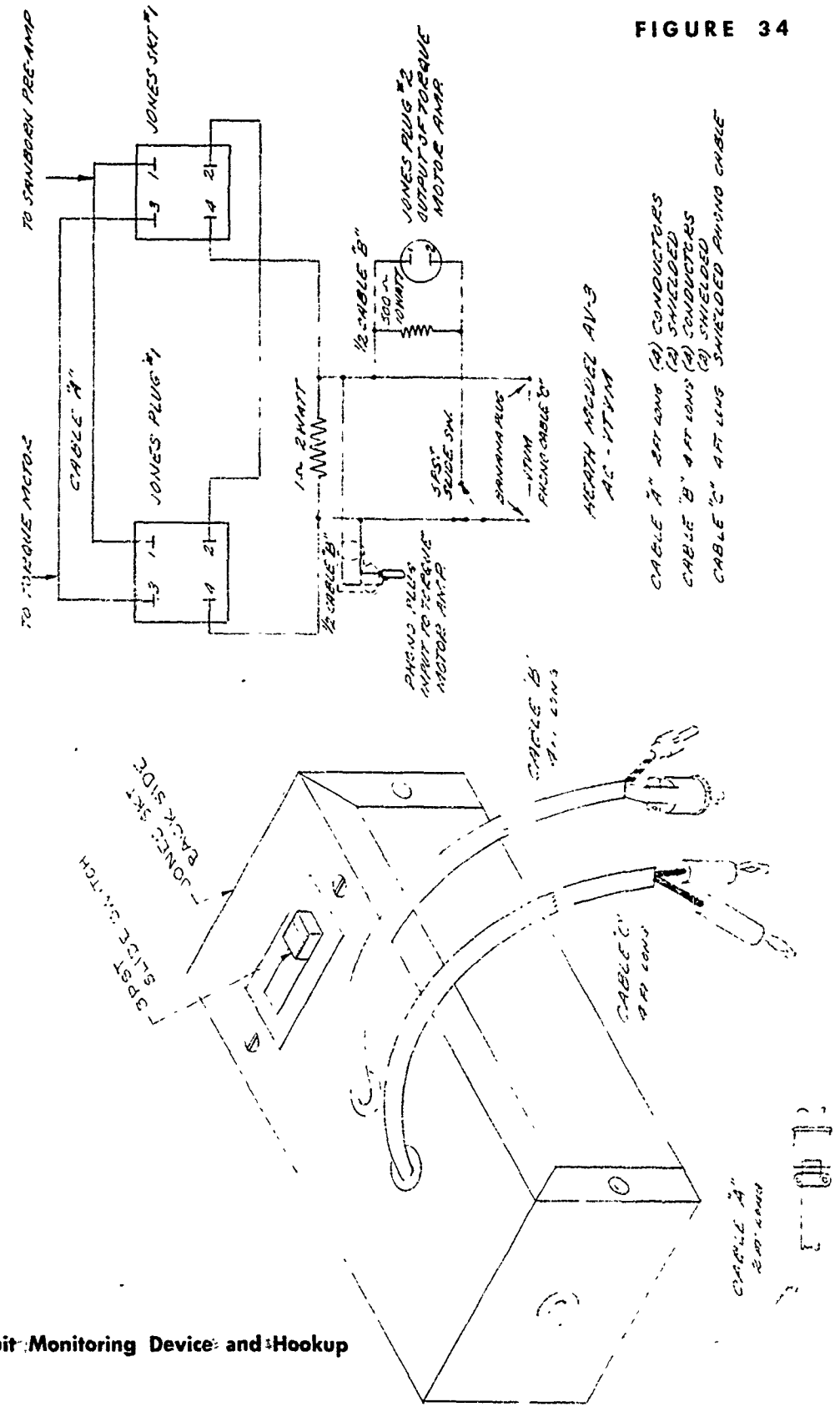

Circuit Monitoring Device and Hookup

APPENDIX B

ECLIPSE-PIONEER SERVICE TEST EQUIPMENT
- INSTRUMENT -
TESTER-BEARING TORQUE, TYPE 13716-1-A
(EXCERPTS FROM T. & T.E. PUBLICATION NO. 1-13716)

I. GENERAL -

A. Purpose

The subject test unit, with its accessories, has been designed to give a high degree of accuracy and convenience in the precision testing of instrument ball bearings. It can test bearings with outside diameters of 1/4" to 1 3/16" inclusive and whose starting friction may range from .02 to 1.5 gm.cm.

B. General Description

The 13716 - Tester is housed in a cast metal case. Its base is 6 5/16" x 5 1/4" and the overall height is 6 5/16". The visual components and their use are as follows:

1. Pressure Indicator - Graduated from 0 to 8; indicates the bearing reject point as determined by the Calibrator QB72217-1 or QB72218-2.

2. Level - The support platform is level when the bubble is centered.

3. Metering Valve - Adjustment of this valve will produce desired "Pressure Indicator" reading for any air jet force.

4. Metering Valve Lock - To lock the metering valve after the desired pressure indicator reading is set.

5. Power Cable - Connected to 110 volt, 60 cycle power source; used to energize circuit for the red light.

6. Red Light - Indicator of maximum torque point. Factory adjusted to light when indicator reads "4". (Normal reject point setting) used to speed up testing bearings.

7. Air Jet Assembly - May be turned 180° in order to reverse the direction of the rotor.

8. Control Valve - Regulates the air pressure.

9. Test Rotor Guide - To properly position a test rotor or calibrator against the air jet assembly, producing an accurate air gap between jet and outside diameter of rotor.

10. Leveling Screws

II. ACCESSORIES

The items listed below are available as accessories to be used with the basic unit.

A. Calibrators - QB72218-1 and QB72218-2

1. Used, when applying air pressure, to measure the generated torque which is registered as deflection of the rotor. The rotor is engraved with 2° graduations from 0° to 360°; each degree of deflection represents 20 mg.mm. of generated torque for the "-1" and 40 mg.mm. for the "-2" calibrator.

2. The calibrator is provided with two standard weights which, when added to the rotor, produce a deflection of 90° or 180° when the calibrator is placed in a horizontal position; used to check the torque of the calibrator. The four holes which receive the weights are located 15 mm. from the center of the rotor.

B. Test Rotor - QB72217-

The test rotor consists of a mandrel, rotor and knock-out in a plastic shipping container.

1. 75 gm. Test Rotor - Used for bearings whose outside diameters are 1/4" to 3/8" inclusive.

2. 400 gm. Test Rotor - Used for bearings whose outside diameters are greater than 3/8".

NOTE: Combinations of rotors and mandrels are available for standard and some special ball bearings. A list of the test rotors and respective bearing sizes is attached.

SETUP -

A. General

The Bearing Torque Tester should be used in a clean, dust free location, with a minimum of traffic in the area. It is also recommended that the room in which the tester is used be air conditioned or of low humidity, to keep bearings free from rust.

B. Connect the Bearing Torque Tester to a source of regulated dry clean air. If available, Eclipse-Pioneer Bearing Cleaner, Type 13638-1-B, will provide this requirement.

C. Level the Unit

D. Connect the power cable to a 110 volt, 60 cycle source of power.

OPERATION -

NOTE:: The following information concerns the subject test unit. For other detailed information on bearing testing, see Eclipse-Pioneer Publication #79-22A.

CAUTION: The air pressure into the tester should not exceed 12 PSI; more than 12 PSI may damage the diaphram within the test unit.

A. Calibrators - QB72217-1 and QB72218-2

Place the calibrator in position against the guides of the tester, bringing the rotor in line with the air jet. Open the control valve gradually; a stream of air, impinged upon rotor buckets, deflects the rotor which is being restrained by the

calibrated spring. This deflection in degrees, when multiplied by 20 for QB72218-1 or 40 for the QB72218-2, equals the milligram-millimeters the force generated.

i.e. If a bearing whose reject point was 1500 mg.mm. was under test, the calibrator QB72218-1 would be placed on the tester and the valve opened until the rotor deflected 75 degrees. The 75 degree reading of the indicator would thus represent 1500 mg.mm.

B. Metering Device

This device may be used in two distinct ways as follows:-

1. Testing bearings with the same "breakaway" allowances. Position the calibrator in the test unit. From the "maximum torque allowable" table find the generated torque allowed for the particular bearing; open the control valve until the desired deflection is indicated on the calibrator. Turn the metering valve until the pointer on the pressure indicator is at 4 and then lock the valve in this position. At this point (4) the red light should glow, indicating that the reject point of the bearing has been reached. Close the control valve and remove the calibrator from the tester.

Mount the bearing being tested in a suitable test rotor assembly and position the test rotor in the test unit. Open the control valve gradually, watching for rotation of the rotor. If the rotor does not begin to turn before the red light glows (the glow if seen by the operator without raising the eyes from the rotor) the bearing is a reject. (Provided the bearing is properly cleaned and oiled). Thus, by watching only the rotation and observing the glow of the red light, identical bearings may be tested rapidly and efficiently.

To reverse rotation of the rotor, turn the air jet assembly 180°.

2. Testing assorted bearings with different torque values.

NOTE: Small and medium sized bearings should be tested as a group separate from large bearings.

Position the calibrator in the test unit. From the "maximum torque allowable" table find the generated torque allowed for the different bearings A, B, C, D, etc. Open the metering valve slightly and lock it. Open the control valve and as the desired deflection for each bearing is indicated on the calibrator, note the reading on the pressure indicator and form a table of "maximum resistance points."

Example: (No true relationship is intended)

Bearing under Test	A	B	C	D	Etc.
Calibrator Readings (or generated torque allowed)	20	30	50	80	
Pressure Indicator (or maximum resistance points)	1	2.5	4	5.5	

The bearings under test may now be picked at random or grouped and matched with a test rotor which is positioned in the test unit. If bearing "B" is being tested, open the control valve until the pressure indicator reads "2.5" (refer to the prepared table). If the rotor does not begin to turn before this point, the bearing is a reject. All bearings on the prepared table may be tested in the same way. The red light is ignored in the above test procedure.

CAUTION: The metering valve must not be touched after the first bearings point of "maximum resistance" is noted. Any movement of the metering valve changes the friction range of the pressure indicator.

NOTE: If many bearings of the same type are in the assortment to be tested, it would be advisable to sort the bearings and use the first procedure outlined.

APPENDIX C

EXCERPTS FROM INSTRUCTION & MAINTENANCE MANUAL

FOR

MPB VANT
(VIBRATION & NOISE TESTER)

SECTION I

I. Introduction

The vibration level of a ball bearing is a good indication of the quality of the bearing. Excessive vibration dissipates energy and this energy loss in a bearing indicates an undesirable condition if allowed to exceed certain levels. Factors which can cause vibration within a ball bearing can be divided into two distinct groups.

The first group comprises those factors which are present due to bearing component design or manufacturing techniques. In this group the two major contributors are geometric variation and surface finish. The effects of these factors have been substantially reduced in recent years through the application of such instruments as the Wavometer and the Talyrond which are used to control manufacturing operations.

Other contributors to the vibration level are — rotating ring unbalance due to the minor eccentricity of ring sections, retainer unbalance, variations in ball spacing within the rotating bearing and possible ball skidding at high operating speeds.

The second group of factors contributing to vibration is the product of conditions to which the bearing may be exposed. Improper handling of bearings can produce brinells, rust, nicks, and scratches. It can completely destroy the super-fine finishes of the rolling contact surfaces. Dirt is the most important single source of random non-recurring bearing vibration. Operating a bearing in a dirty condition can destroy the bearing because of the permanent scratches made on the balls and races.

The importance of proper handling techniques, proper environmental conditions, and the need for cleaner lubricants cannot be overemphasized because of their direct affects on bearing vibration and performance.

II. Theory of the VANT

The MPB VANT (vibration and noise tester) is of the moving coil design with a velocity sensitive transducer.

A velocity sensitive pickup offers the best means of measuring instrument bearing vibration. It is of simple construction. Its flexibility of design helps reduce the effect of frequency variation and changes due to changes in the rotational speed of the bearing being tested. The moving coil design eliminates some of the shortcomings of a mechanically-driven-spindle tester. The VANT is a moving coil tester in which an induction coil is attached to the shaft which supports the inner ring of the bearing. An air-driven rotor is mounted on the outer ring of the bearing and is accelerated to the pre-set test speed. The rotor is then allowed to coast through a pre-set speed deceleration range during which time the bearing vibration is measured. The vibrations generated in the bearing cause the supporting shaft to move vertically, in an axial relation to the bearing. This motion is monitored by the transducer. The transducer signal is amplified and indicated on a meter, usually as an rms value of microns per second.

Fig. 1 is a block diagram of the circuit of the MPB VANT. The vibration meter circuit starts with a coil and magnetic field inside the pickup. Voltage in the coil is fed to an amplifier. The amplifier output signal operates the vibration meter and oscilloscope. The speaker amplifier branches off from the main amplifier and the speaker volume does not affect the vibration meter reading. The tachometer circuit starts from the 8 magnets found at the edge of the rotor. These magnets pass by the coil mounted next to the rotor generating voltage pulses. The voltage coil output is fed to a frequency meter amplifier and then to the tachometer. The tachometer with its high and low limit contacts controls the air drive circuit and the interval timer. It activates the vibration meter circuit to read the bearing vibration during coastdown through the pre-set speed range.

SECTION III

III. (A) General VANT Operation

Fig. 2 shows the pickup of the VANT disassembled. Notice the 75 gram rotor with the turbine buckets on its periphery The air drive is accomplished through the two air jets located inside the cylindrical housing.

The vertical shaft supports the bearing through the inner ring. When the rotor, outer ring and ball train turn, the vibration induced in the bearing causes the shaft to move up and down on its support of two very flexible diaphragms.

A coil of very fine wire is fastened to the lower end of the shaft. A strong magnetic field from a permanent magnet surrounds the wire coil. A voltage is induced in the coil as a result of axial motion. The amount of this voltage is proportional to the velocity of the shaft motion.

The entire assembly is mounted on a shock absorbing base which damps out external vibrations.

Fig. 3 is a picture of the VANT and pickup assembly. Fig. 4 is a sketch of the VANT with the various features labeled.

The voltage from the moving coil is displayed on the vibration meter in microns per second. The small 1" oscilloscope provides a picture of the form of the vibration. A speaker is mounted in the cabinet top to amplify the sound produced by the test bearing. There are phone plugs which may be used with earphones in place of the speaker.

The speed of the rotor is controlled by pre-setting the high limit hand on the tachometer. The elapsed time indicator, which measures in seconds, starts when the rotor reaches the pre-set speed limit at which time the driving air circuit is shut off. The timer runs until the speed drops to the low limit hand setting. The timer makes it possible to compare the spindown torques of a group of bearings. The speed-torque relationship is determined from the period of deceleration of a bearing supporting a rotor of known moment of inertia.

(B) Controls

Above the oscilloscope is a calibration button. When this button is pressed during spindown, the proper amplifier calibration level is checked. If the amplifier and line voltage are in calibration, the meter will read 47-53.

A switch to select the high or low rpm scale is located below the oscilloscope.

There is a volume control for the speaker or earphones. Above the tachometer is a switch which controls the main air supply. The cycle-start button is located below the tachometer.

The sensitivity range hi-low switch (Fig. 8) is the large knob on the back of the chassis. The switch is usually used in the hi position. The low position reduces the sensitivity of the VANT so that the vibration meter indicates only ½ of the actual vibration level.

(C) Test Cycle

The test cycle may be started after a bearing is mounted on the spindle and the rotor is placed on the bearing. When the cycle-start button is pushed, air enters through the jets impinging on the rotor. The speed of the rotor increases until the hand of the tachometer closes the high speed limit contacts.

At this point the air supply is closed, the timer is started and the vibration meter circuit is closed to read axial velocity in microns per second. Speed indication is continuous during deceleration. When the hand of the tachometer touches the low limit speed contact, the timer is stopped, having measured the period of deceleration of the rotor and bearing through the pre-set speed range.

A limit light circuit is closed should the vibration measurement exceed a predetermined maximum as set by the high limit hand on the vibration meter. Upon re-starting the cycle, the timer and the vibration meter are re-set automatically.

(D) Electrical and Mechanical Characteristics

The successful design of an instrument bearing vibration measuring gage is the marriage of good electronics amplifiers and an excellent pickup.

Of the two major components, the electronic amplifier with the required fidelity of frequency response is the easier to design and build. Fig. 5 is a curve which represents the frequency response of the VANT amplifier. With a 6-millivolt signal applied to the pickup input the frequency was varied from 0 to 100 kilocycles and the readings of the vibration meter were plotted. The frequency response of this amplifier is 200 cps to 10 k cps. Notice the slightly downward concave characteristic of the curve.

It is extremely difficult to induce an exact velocity and vibration level for purposes of analyzing the pickup. It is, however, relatively easy to induce a constant force when changing frequencies in order to determine the response of the pickup.

Fig. 6 shows that the response to force falls off as the frequency increases. By mathematically operating on this curve the response to velocity vs. frequency can be determined. The slight concave slope of this curve above 150 cycles per second results in a substantially flat velocity vs. frequency curve with a slightly upward concave characteristic.

Combining the amplifier response curve with the pickup response curve results in an overall response which is very nearly flat with constant peak velocity within the frequency range of 200 cps to 20,000 cps.

The frequencies at which most bearing vibrations occur lie somewhere in 500 to 2000 cps range. The specific fundamental frequency is determined by the bearing size and its spring rate or yield rate under a particular load. If the races are extremely rough, or there is excessive dirt in the bearing, then the vibration spectrum is disbursed over a wider frequency range with poor definition.

Fig. 7 shows a typical bearing vibration signal readout on a panoramic sonic analyzer. The location of the vibration spike at 600 cycles is determined by the mass of the supporting shaft and the yield rate of the bearing. As the heavy rotor or mass rotates on the bearing, the balls and races experience elastic deformation. Any dirt or imperfections at the points of contact will tend to make the deformation vary around the predominant frequency of 600 cps in this case.

IV. Operating Instructions — See Fig. 4

General

1. Insure cleanliness of instrument, particularly pickup diaphragm, adapter and rotor. The diaphragm must be cleaned with extreme care to prevent damage. Wipe it gently with lens tissue or similar lint-free material.

2. Level the pickup. (Pickup must at all times be in upright position to keep damping fluid from spilling.)

Operation

1. Check the following:

   Switch #5 — "up" position

   Switch #3 — on low or high, as desired

   Potentiometer 1 — turned fully counterclockwise

2. If desired, set vibration indicator limit needle to the required level.

3. Set the tachometer indicators to the desired test speed and lower cutoff speed respectively.

4. Turn master switch #1 "on". After a short period a light green trace will appear on the screen of the oscilloscope. Warm-up time should be 30 minutes The VANT should not be used to evaluate bearings for at least 30 minutes after having been turned on.

5. Select the right size adapter to match the bearing bore size, and screw this adapter into the pickup. Make sure the adapter is positioned correctly on the shoulder of the shaft. The adapter must be seated firmly. Do not tighten unnecessarily. If the adapter is over-tightened the diaphragm can be damaged.

6. Place the bearing on the adapter and make sure that the bearing seats correctly.

7. Select a rotor to fit the bearing O. D.

8. Place the rotor very lightly on the bearing and make sure that rotor seats squarely on the bearing outer ring face.

9. Push switch #2 to start the cycle. The automatic timer will clear and return to zero but will not start timing until the bearing reaches the pre-set test speed on the tachometer.

10. When the bearing reaches the pre-set test speed, the automatic timer engages and measures the run-down time. The timer stops when the bearing speed has decreased to the pre-set lower cutoff speed. The vibration meter circuit is closed when the timer starts. The test bearing vibration level is read directly on the meter in microns per second. If a vibration upper limit has been pre-set and the vibration level of the test bearing is greater than this pre-set limit, the limit light will go on, the vibration indicator will not advance further on the scale. The timer and tachometer remain activated until the speed reaches the pre-set lower cutoff speed limit.

11. After the tachometer indicates the pre-set lower cutoff speed limit, the bearing may be stopped by hand. Be careful — avoid any pressure on the diaphragm.

12. If it is necessary to stop the rotor after the test has been started and prior to the bearing having reached the pre-set test speed, the airflow can be shut off by momentarily putting switch #5 in the down position.

13. In addition to recording the vibration level on the meter, the VANT also has audio equipment. The volume can be increased by turning Potentiometer I clockwise. With experience the audible sound can be used to distinguish dirt (a random peening or crackling sound) or brinells (a constant rumble) from the general sound level. The audible sound should not be used to accept or reject bearings except for dirt or brinelling, and then only after thorough operator training.

V. (A) Calibration — See Figs. 8, 9, 10

The following calibration method is to be used as a convenient day-to-day check and is not to be confused with the more theoretical and complicated dynamic driving force method:

1. Press the calibration button during spindown of the bearing.
2. The vibration meter should read 50 ±3.

The pickup unit, having only 2 coils, is not checked in the normal calibration process. If the meter reads 47 — 53 the gain of the amplifier and the line voltage are as they should be. There is very little to go wrong with the pickup. This range of meter reading can be due to line voltage variation. This variation enters into the meter reading twice:

1. It affects the small signal which is fed into the amplifier when the calibration button is pressed.
2. It affects the gain of the amplifier .

If the meter variation from 50 is between ±3 and ±10 units the vibration amplifier gain control (Fig. 8) may be moved to bring the amplifier back to read 50 when the calibration button is pressed.

If the reading is below 40 on the meter when the calibration button is pressed during spindown, check and/or replace the 2 — 6SL7 tubes in the meter amplifier. Other tubes which should be checked are the 5Y3 and the 6K6 near the meter.

1. Pull out the phono plug connected into the vibration input of Fig. 8.
2. Measure the resistance with an ohm meter. The ohm meter should read 500 ohms.

(B) Calibration of the Micron — DB Meter

All MPB VANT pickups are calibrated by the driving force method and each is correlated to the MPB standard. The damping fluid in the pickup is important to this correlation. Should the pickup be tipped or displaced with loss of damping fluid, it can be brought in approximate calibration by putting 7 cc's of 100 centistokes Dow Corning silicone oil into the carefully disassembled, cleaned and reassembled pickup. Correlating checks should be made on a group of test bearings and the damping fluid in the refilled pickup should be varied in quantity until the same results are obtained on the test bearings as run on two or more testers.

(C) Calibration of the Speed Section — 1st Method

The tachometer on the VANT can be calibrated with an audio frequency standard which is furnished with the VANT.

The frequency standard is 200 cycles per second which is equivalent to 1500 rpm or full scale on the low setting of speed.

Connect the Frequency Standard to the speed input (Fig. 8). (A phono plug connected to the standard is convenient for this.)

Press the pushbutton on the Frequency Standard to turn it on. Make sure the low-high knob on the front of the VANT is in the low position. Turn the 1500 rpm — 200 cps Potentiometer (Fig. 8) until the speed meter reads full scale. The low speed scale is now calibrated.

Turn the low-high knob to the high position. The meter should read 1500 rpm on the high scale. If it doesn't, adjust the 7500 rpm 1000 cps knob until it does read 1500 rpm. This completes the calibration of the 0 — 7500 rpm scale.

The speed pickup coil can be checked in the following way:

The connections from this coil come out to a phono plug. Measure the resistance of the coil with an ohm meter. The resistance should be 20 ohms.

(D) 2nd Method of Speed Calibration

If a Frequency Standard is not available an audio oscillator may be used for calibration.

Any convenient voltage between .05 and 5 volts can be used. The value of the voltage is not critical, as the calibration depends on the frequency.

Set the oscillator to 200 cycles at some voltage value between .05 and 5 volts.

Follow the procedure as outlined for the Frequency Standard.

(E) 3rd Method of Speed Calibration

A Stroboscope can be used to calibrate the speed section of the VANT. The VANT rotor speed is measured directly with the Stroboscope and compared with the tachometer indication. The tachometer can then be adjusted with 1500 or the 7500 rpm Potentiometer (Fig. 8) as the case may be.

FIGURE 1

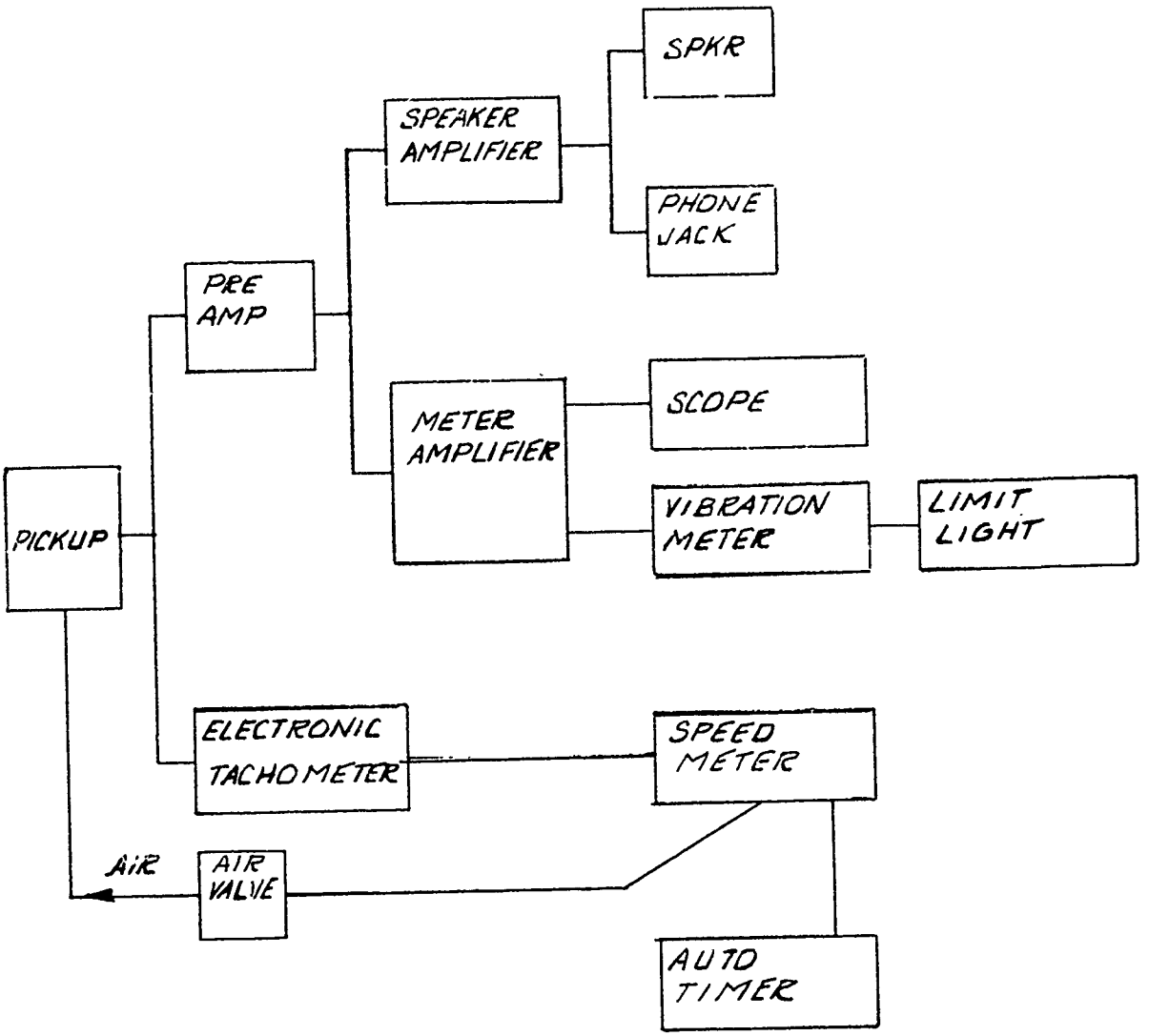

Block diagram of the circuit of the VANT

FIGURE 2

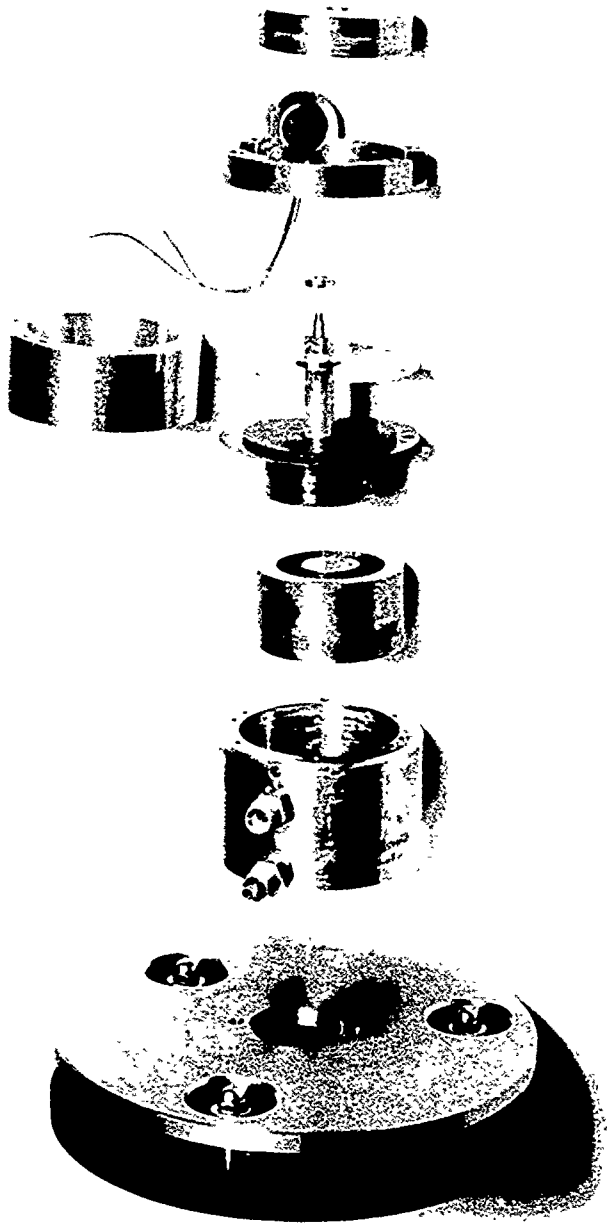

Pickup of VANT disassembled

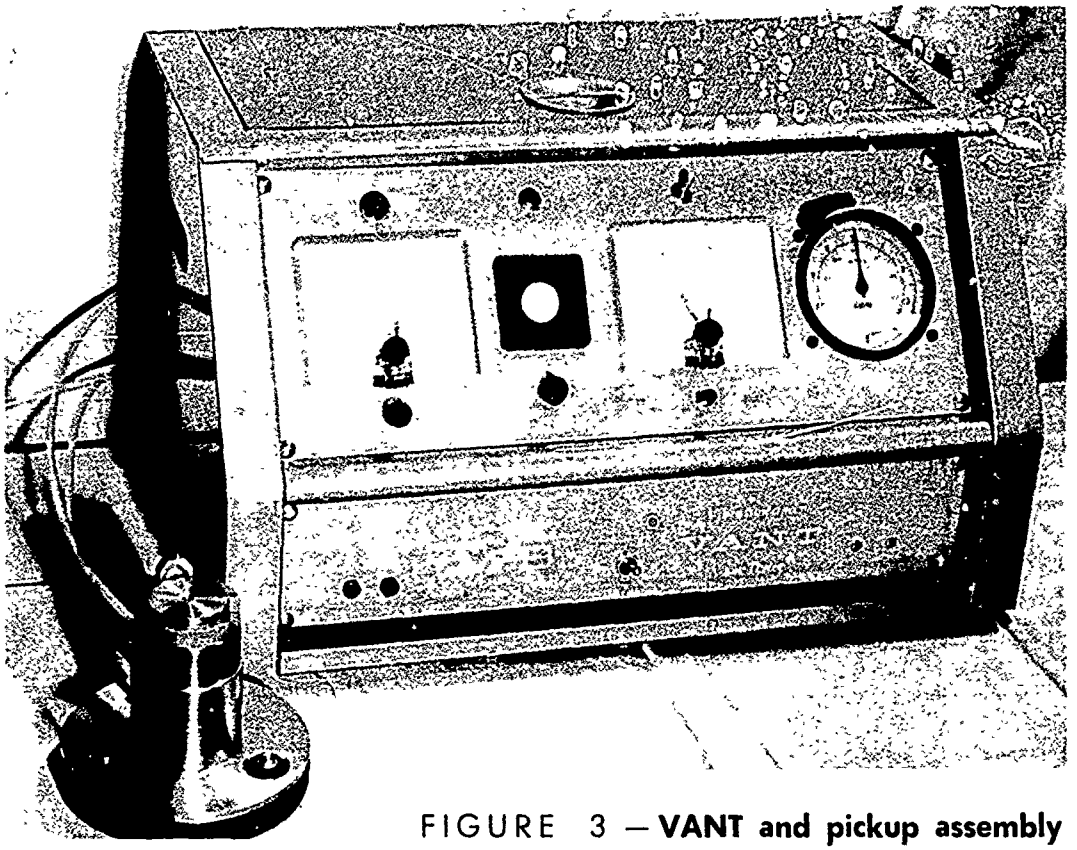

FIGURE 3 — **VANT and pickup assembly**

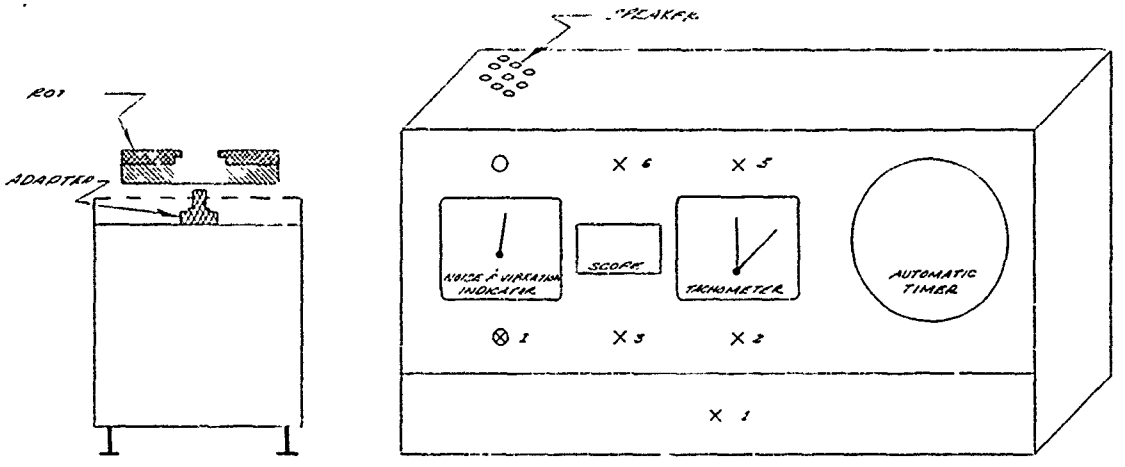

⇌ WARNING ⇌
DO NOT TILT THE PICKUP

× SWITCH
○ LIGHT
⊗ POTENTIOMETER

FIGURE 4 — **VANT**

FIGURE 5

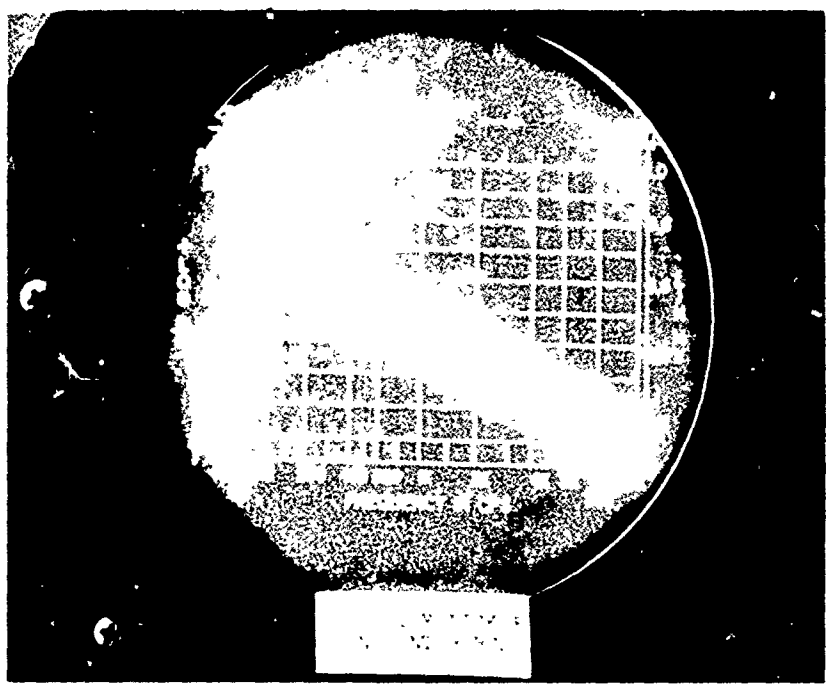

Frequency response of VANT amplifier — trace

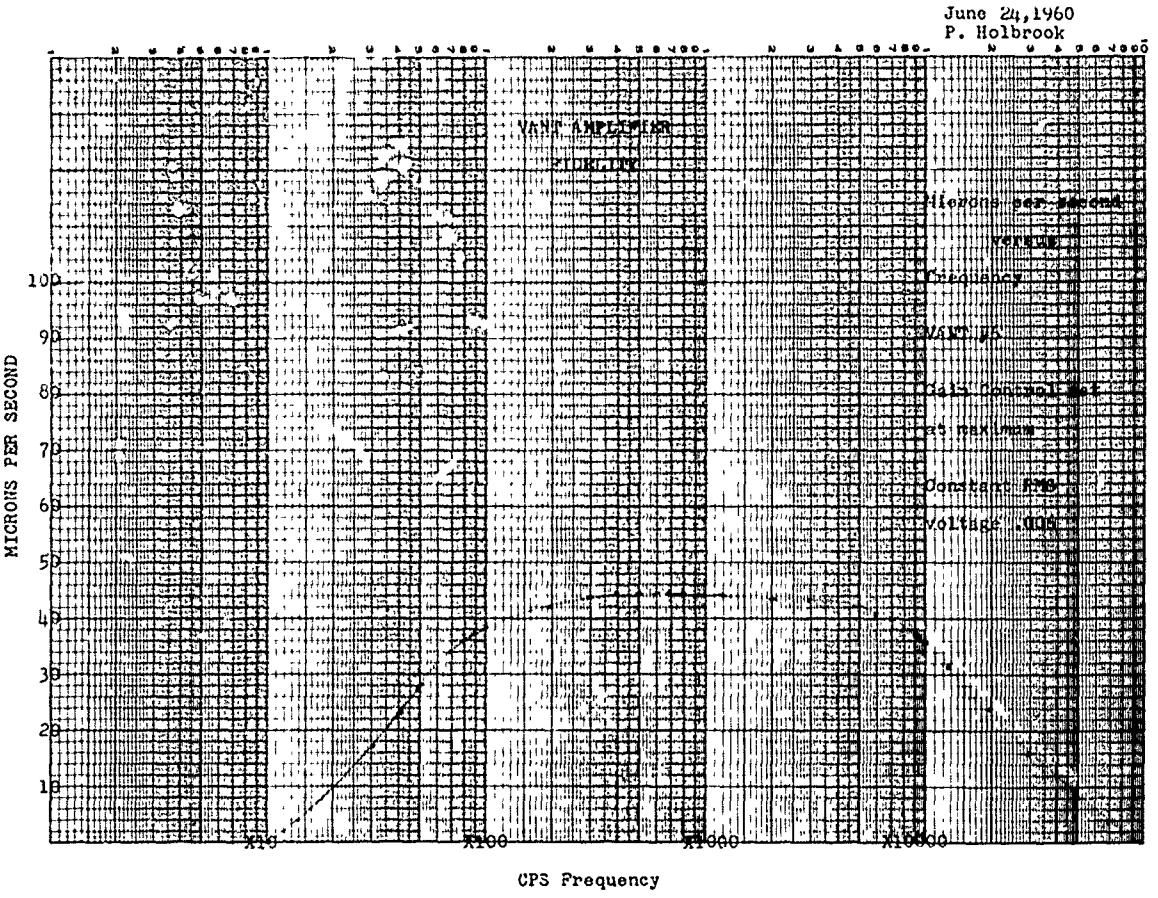

FIGURE 6 — **VANT amplifier fidelity**

FIGURE 7

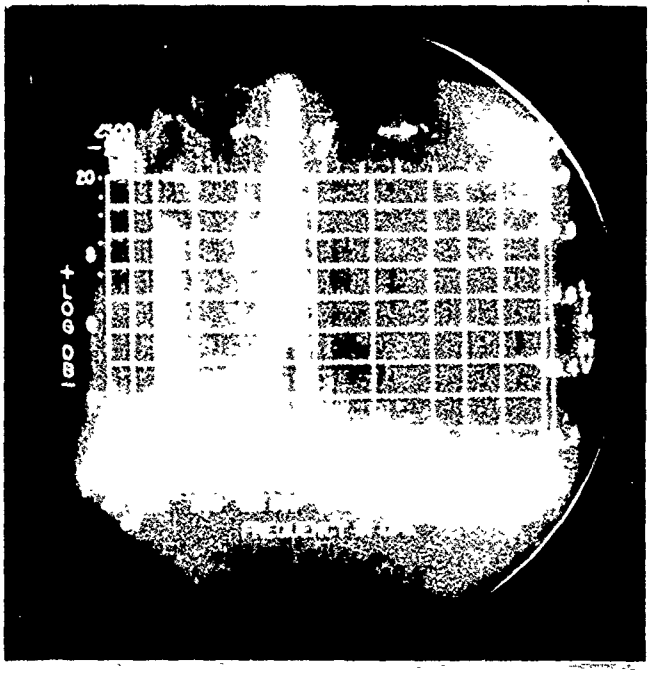

Vibration signal trace

FIGURE 8

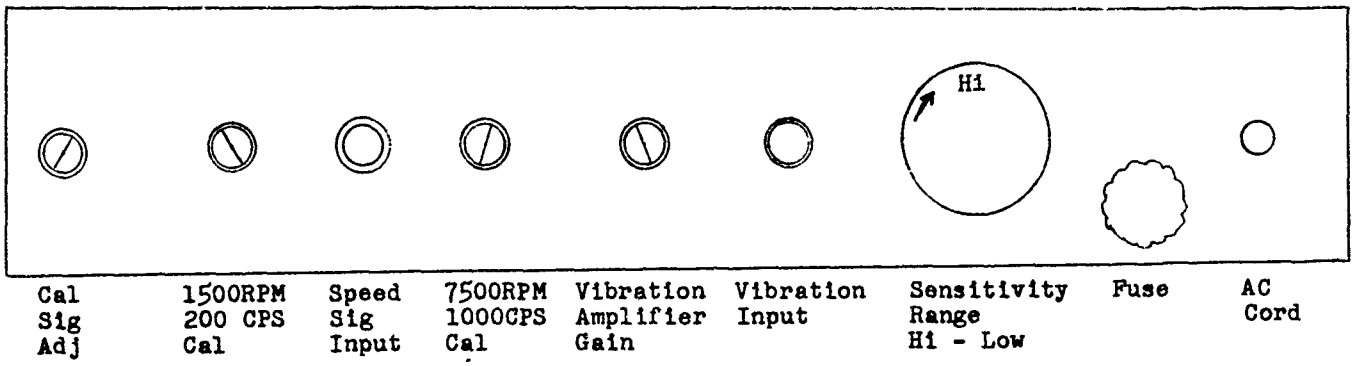

VANT chassis — back view

FIGURE 9

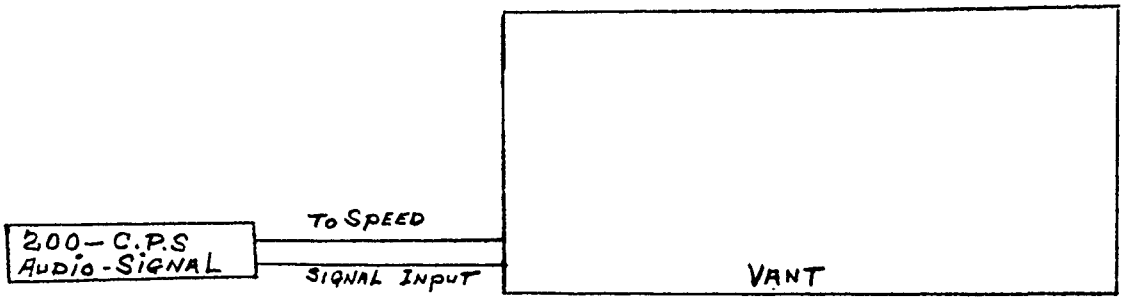

200- C.P.S. = FULL SCALE ON LOW (1500-R.P.M.
200- C.P.S = 1500 R.P.M. ON HIGH SCALE

Tachometer calibration

FIGURE 10

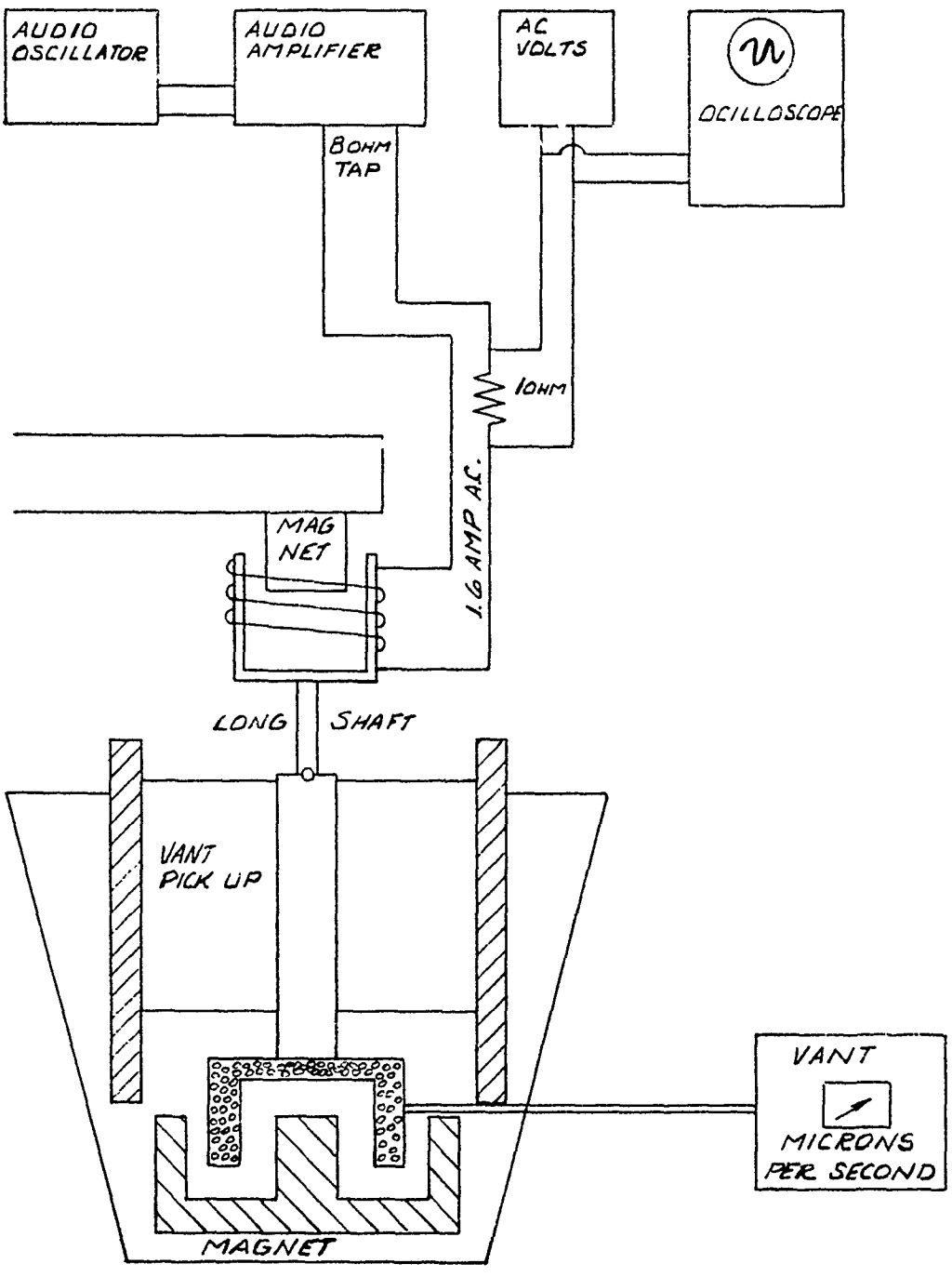

VANT calibration

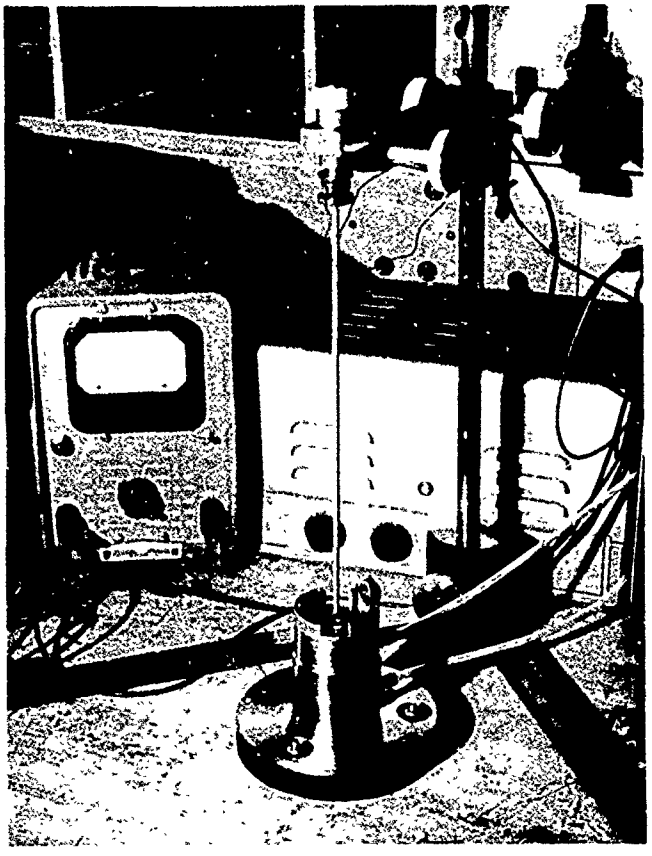

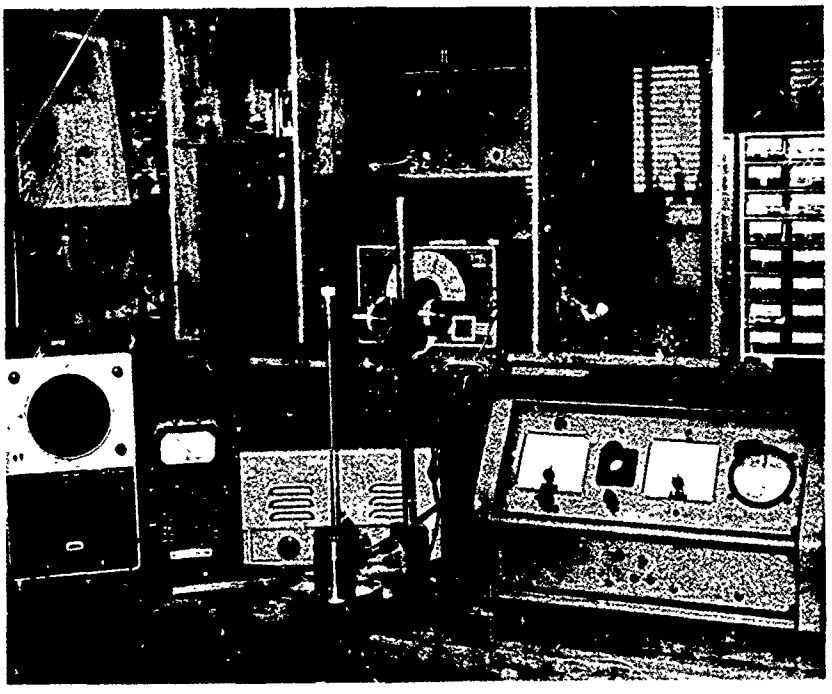

APPENDIX D

EXCERPTS FROM:

A PRELIMINARY STUDY OF THE CHARACTERISTICS OF BEARING TEST METHODS

By:

P. A. Pelton and C. L. Grant
Center for Industrial and Institutional Development
Kingsbury Hall
University of New Hampshire
Durham, New Hampshire 03824

SYNOPSIS

Two sets of "defect-free" bearings have been tested on the MARK III Torque Tester, the Bendix Starting Torque Tester, and VANT. Detailed statistical analyses of these test results have been conducted. A number of significant correlations between measurements were discovered. It was found that "set up" of the MARK III torque tester on different days had a large influence on the results for average hash width. It was shown that, for most of the measurements, the scatter of results is approximately described by a normal distribution.

Sample sizes necessary to detect differences in the average levels of each of the test measurements at specified probability levels were calculated. It was found that the number of bearings required in each group varied with the tests. In general, adequate sensitivity at a 99% probability level could be achieved with between 10 and 40 bearings.

I. ANALYSIS OF THE FIRST SET OF DATA

On 28 January 1972, results of tests on 33 good bearings were submitted for analysis. These tests were conducted on 24 January and 25 January 1972. All tests were done by the same technician.

The data are summarized in Table 1. Frequency histograms for average running torque, average hash width, average starting torque, and VANT are presented in Figures 10 and 11. The distribution of data for average running torque is strongly non-normal; and, therefore, a standard deviation could not be legitimately calculated. In the case of the average hash width, there is again a non-normal distribution although it more nearly approaches normality. A standard deviation was calculated, but it should be interpreted cautiously. The VANT data in Figure 11 suggest a rectangular distribution although there is some peaking in the area of central tendency; and, therefore, a standard deviation has again been calculated. The average starting torque values come the closest to forming a more or less normal distribution. The individual peak starting torques were not plotted separately.

Table 1. Summary of 24 & 25 January Data on Good Bearings

Bearing Number	Torque Values in mg. mm. Average Running	Average Hash	Average Starting	Peak Starting	VANT
1	100	400	1165	1750	12
2	100	400	1065	1400	8
3	250	300	925	1000	5
4	100	250	740	1000	4
5	75	250	955	1200	6
6	150	300	760	1000	6
7	125	600	1120	1500	9
8	250	700	1395	1750	14
9	250	300	1100	1300	8
10	175	300	685	850	4
11	250	450	1170	1400	12
12	100	300	1055	1300	-
13	200	425	1155	1550	10
14	250	200	1055	1250	10
15	100	300	1320	1600	15
16	150	500	1005	1300	14
17	100	300	1140	1500	8
18	125	300	1090	1300	6
19	75	500	945	1600	14
20	100	500	1155	1800	10
21	150	500	1025	1250	13
22	100	400	1140	1500	10
23	50	450	985	1250	10
24	100	500	995	1200	15
25	125	300	920	1100	7
26	175	300	940	1250	4
27	250	500	945	1150	8
28	250	500	960	1200	10
29	150	300	1015	1500	10
30	100	500	980	1300	9
31	200	500	1285	1800	13
32	75	400	915	1500	9
33	250	300	1030	1300	9
Mean, $\bar{y}$	150	400	1034	1350	9.3
Std. Deviation, S_y	---	116	150	240	4.0
Range	50-250	200-700	685-1395	850-1800	4-15

FREQUENCY HISTOGRAMS FOR AVERAGE RUNNING TORQUE & AVERAGE HASH WIDTH

AVERAGE RUNNING TORQUE

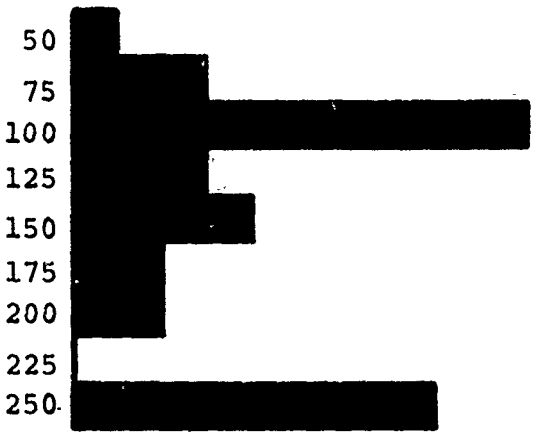

$\bar{Y}$ = 150 S_y - Not Valid

AVERAGE HASH WIDTH

$\bar{Y}$ = 400 S_y = 116

Figure 10D

FREQUENCY HISTOGRAMS FOR VANT & AVERAGE STARTING TORQUE

VANT

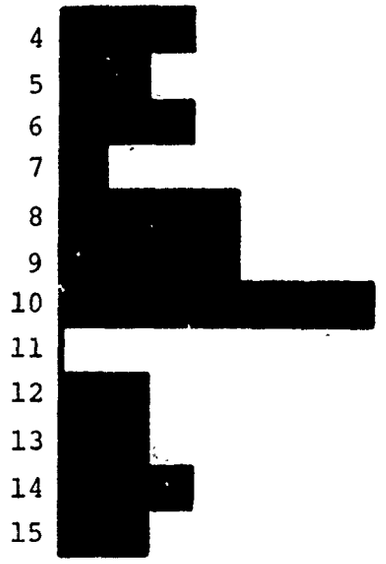

$\bar{Y}$ = 9.3

S_y = 3.3

AVERAGE STARTING TORQUE

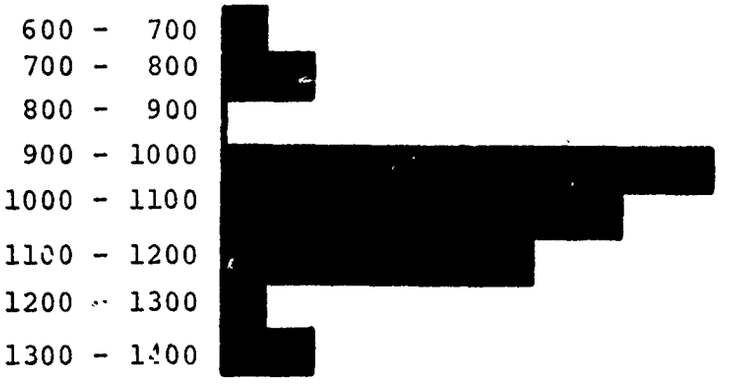

$\bar{Y}$ = 1034 mg.mm.

S_y = 150 mg.mm.

Figure 11D

The correlation of average hash width and VANT is shown in Figure 12. Statistical correlation analysis of these data indicate that the relationship is significant at well over the 99% probability level. A correlation coefficient of 0.61 was obtained. Stated another way, it appears that these two measurements are sufficiently precise to detect differences in surface quality even within this group of "homogeneous" good bearings.

In Figure 13, we have presented the relationship between the average starting torque and VANT. Again, statistical correlation analysis yields a correlation coefficient of 0.61, demonstrating a significant relationship between the variables at the 99% probability level.

In Figure 14, we have plotted the peak starting torque versus the average starting torque. The correlation coefficient of 0.975 proves that these two variables are highly correlated. This is not at all surprising although we were uncertain at the outset that the correlation would be strong since one can envision the presence of individual surface defects which could give a single very high starting torque with all the others quite low. With ten starts, a single high value would not elevate the mean sufficiently to explain the high degree of correlation. Similarly, one large value per

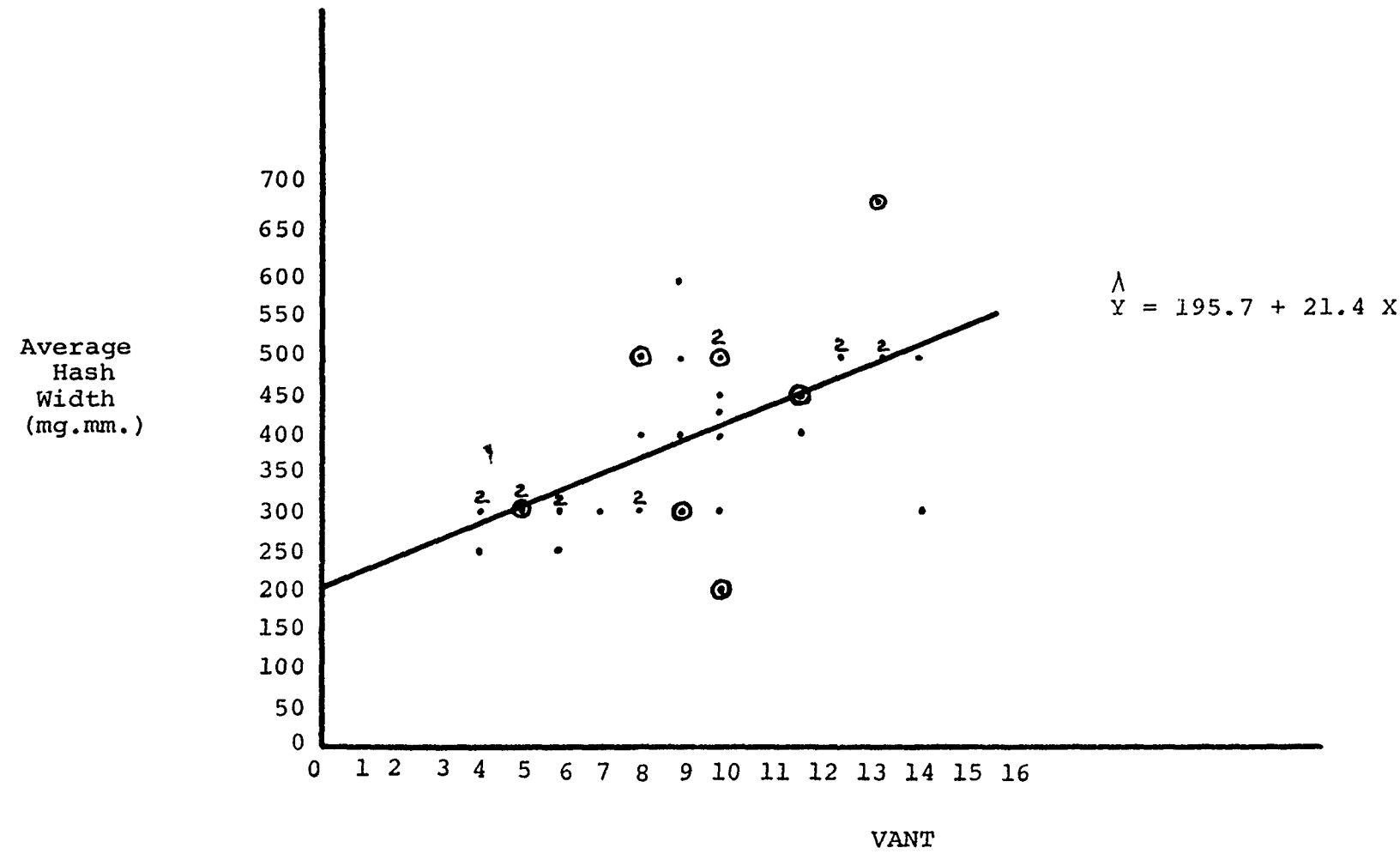

RELATIONSHIP BETWEEN AVERAGE HASH WIDTH & VANT FOR GOOD BEARINGS

Figure 12D

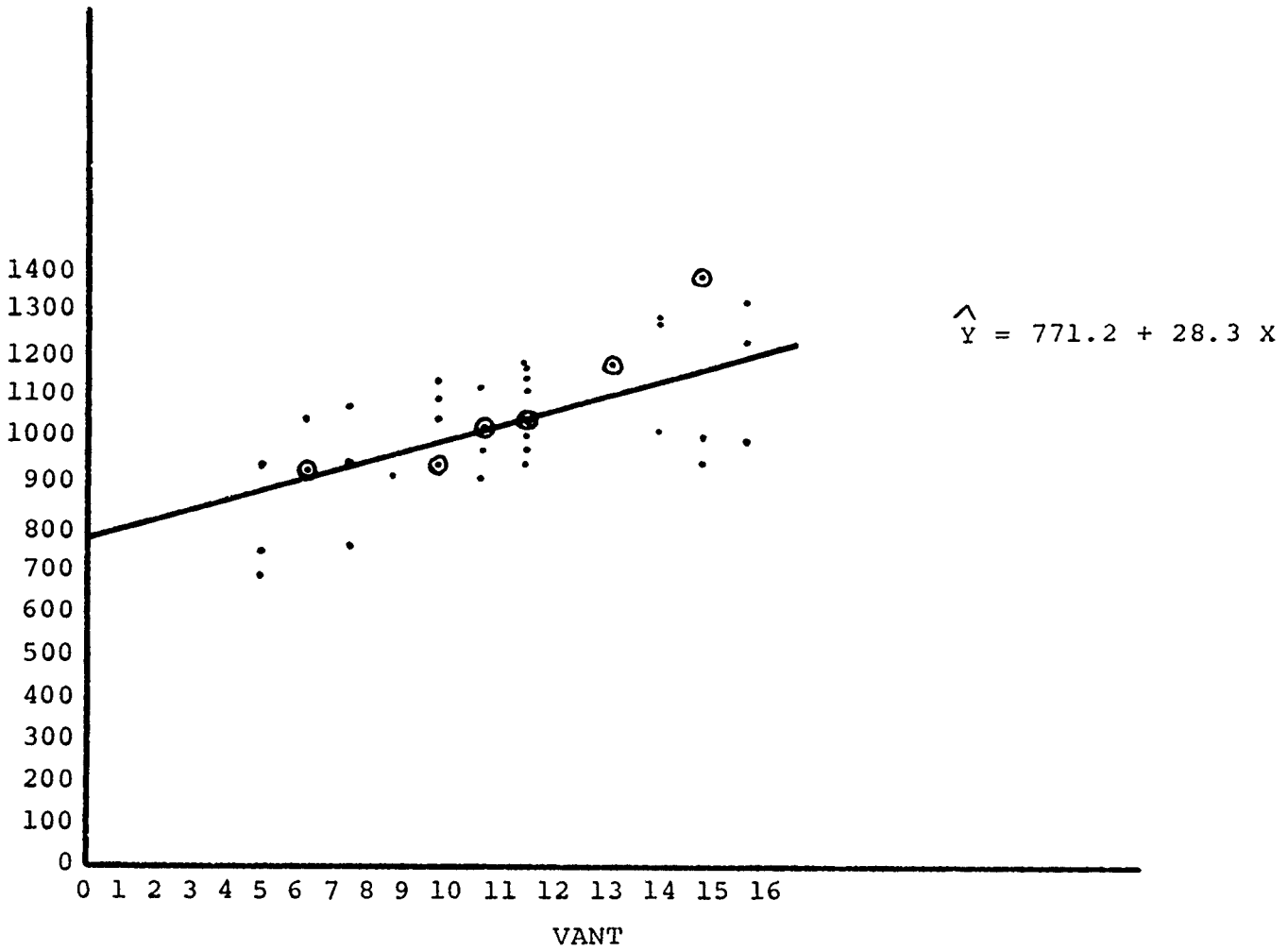

RELATIONSHIP BETWEEN AVERAGE STARTING TORQUE & VANT FOR GOOD BEARINGS

Figure 13D

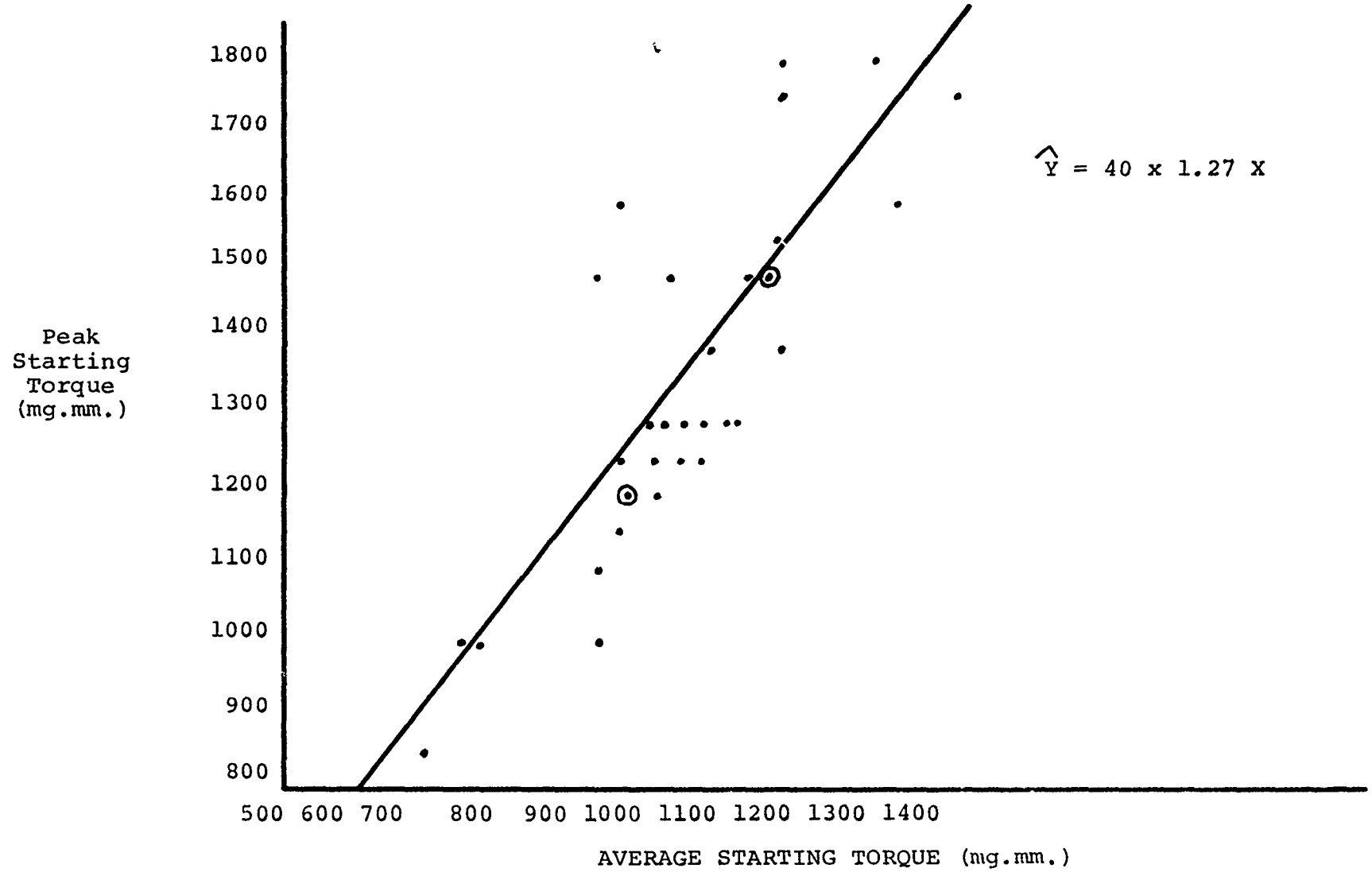

RELATIONSHIP BETWEEN PEAK STARTING TORQUE & AVERAGE STARTING TORQUE FOR GOOD BEARINGS

Figure 14D

set of ten would produce a slope of approximately 10 rather than the low value obtained (1.27). Apparently, bearing surfaces with a high probability of causing a high peak starting torque will tend to give a significantly higher average starting torque when ten starts are employed. Thus, both peak and average starting torques should provide useful information. Possibly, the ratio of peak to average starting torque will be related to the type of surface defect.

II. ANALYSIS OF THE SECOND SET OF BASELINE DATA

A. The Experimental Plan

Because of our dissatisfaction with the shapes of the frequency histograms from the first trials, it was agreed to generate a second set of baseline data for good bearings. In this case, the selected group of 44 bearings was spray cleaned due to the apparent presence of dirt particles after the initial cleaning. More will be said on this fact later in the discussion.

To generate additional information concerning the reliability of the measurement procedures, duplicate determinations were performed on each bearing for each of the tests. In the

case of starting torques, two sets of ten starts were employed. For VANT and average starting torque, one complete set of tests was done on each of two separate days (except that No. 77 was inadvertently omitted from the starting torque tests). For the running torque tests, the first set of measurements on Bearings 41 through 65 were done on one day. Testing of the balance of the bearings, 66 through 84, was conducted on the second day along with the repeat testing of the entire set of 44 bearings. This fact has an important influence on the data as will be shown later.

The data are summarized in Table 2. For each of the measurements, except peak starting torque, the duplicate values are recorded along with the difference value, i.e., the first minus the second. The difference values were not recorded for peak starting torque because the duplicates cannot legitimately be considered as pairs. In the case of the average hash width, the grand averages are not recorded because further statistical analysis indicated that a day-to-day effect was superimposed on the normal variability. This is analyzed in greater detail in a later section.

Table 2. Summary of February Tests on Good Bearings

Torque Values in mg. mm.

Bearing No.	Average Running			Average Hash			Average Starting			Peak Starting		VANT		
	1st	2nd	Δ	1st	2nd	Δ	1st	2nd	Δ	1st	2nd	1st	2nd	Δ
41	150	200	-50	400	300	100	545	590	-45	750	1250	5	4	1
42	200	200	0	500	300	200	485	540	-55	600	650	8	8	0
43	150	200	-50	500	300	200	555	535	20	650	650	5	4	1
44	250	150	100	400	350	50	545	685	-140	700	800	4	4	0
45	350	250	100	500	300	200	555	525	30	700	600	8	8	0
46	150	200	-50	500	350	150	605	630	-25	1500	1750	4	4	0
47	150	250	-100	300	250	50	510	525	-15	600	650	4	4	0
48	200	150	50	500	250	250	605	735	-130	950	1200	6	5	1
49	150	200	-50	400	200	200	610	570	40	750	650	5	6	-1
50	250	250	0	400	300	100	590	520	70	650	650	3	3	0
51	200	200	0	400	300	100	590	745	-155	750	1800	4	3	1
52	200	400	-200	450	400	50	625	835	-210	850	950	5	5	0
53	100	150	-50	400	200	200	585	555	30	650	750	6	4	2
54	150	150	0	500	300	200	500	485	15	600	650	6	7	1
55	250	150	100	400	250	150	585	555	30	700	750	4	4	0
56	350	150	200	450	300	150	605	585	20	750	1000	4	4	0
57	200	100	100	300	200	100	600	545	55	800	650	4	4	0
58	200	150	50	400	250	150	560	535	25	700	650	6	4	2
59	250	125	125	400	200	200	570	560	10	700	700	4	5	-1
60	200	350	-150	450	300	150	685	570	115	950	800	4	3	1
61	300	250	50	400	250	150	580	540	40	700	650	4	4	0
62	100	150	-50	400	250	150	625	580	45	1000	750	4	4	0
63	250	150	100	450	200	250	550	460	90	800	550	4	4	0
64	250	250	0	400	300	100	545	480	65	650	650	5	4	1
65	150	250	-100	400	200	200	585	565	20	700	700	4	4	0

Table 2. Summary of February Tests on Good Bearings (Cont.)

Torque Values in mg. mm.

Bearing No.	Average Running			Average Hash			Average Starting			Peak Starting		VANT		
	1st	2nd	Δ	1st	2nd	Δ	1st	2nd	Δ	1st	2nd	1st	2nd	Δ
66	100	250	-150	300	300	0	585	510	75	750	700	6	6	0
67	100	150	-50	300	300	0	530	505	25	600	600	5	4	0
68	100	250	-150	300	350	-50	615	585	40	750	750	7	7	0
69	100	200	-100	200	300	-100	565	565	0	750	650	5	5	0
70	150	150	0	300	250	50	540	660	-120	650	1500	5	4	1
71	300	150	150	250	250	0	605	535	70	750	650	5	4	1
72	150	150	0	200	300	-100	550	580	-30	750	700	3	4	-1
73	100	200	-100	300	250	50	530	540	-10	700	600	6	5	1
74	100	200	-100	300	300	0	640	630	10	850	1250	4	5	-1
75	200	150	50	250	200	50	555	570	-15	800	750	5	6	-1
76	200	100	100	200	200	0	540	620	-80	700	750	6	7	-1
77	150	100	50	250	200	50	Missing			Missing		4	5	-1
78	250	200	50	250	200	50	555	550	5	650	750	4	5	-1
79	100	200	-100	100	200	-100	530	595	-65	650	750	6	4	2
80	150	150	0	150	150	0	505	575	-70	600	750	4	7	-3
81	100	150	-50	100	150	-50	515	615	-100	750	1200	4	4	0
82	150	250	-100	150	250	-100	525	640	-115	800	750	4	5	-1
83	150	100	50	150	100	50	600	590	10	700	900	5	5	0
84	150	100	50	150	100	50	500	550	-50	600	750	5	4	1
Mean, $\bar{y}$	181	187	-6.25	*	*	*	567	578	-11.3	743	828	4.84	4.75	0.091

*See Table 4.

B. Paired "t" Tests

If there is any systematic difference between the duplicates, the average difference should deviate significantly from zero. This hypothesis is easily tested by calculating the "t" value according to the equation below.

$$t = \frac{\bar{Y}_1\text{-}2}{S_d \sqrt{n}} \quad \text{----------(1)}$$

where $\bar{Y}_1\text{-}2$ = the average difference between pairs of values

S_d = the standard deviation of the differences

n = the number of differences

If the calculated "t" value exceeds the tabular "t" value at a stated level of confidence and for the appropriate number of degrees of freedom (df), then the hypothesis that the average difference between pairs is zero can be rejected. A summary of the results of these calculations is presented in Table 3. It is clear that there is no systematic variation between pairs of values for average running torque, average starting torque, or VANT. It is also apparent that the pairs of values for average hash width differ systematically at greater than the 99% probability level.

The significant difference in pairs of values for average hash width is further examined in Table 4. In this analysis, Bearings 41 through 65 are grouped together since the first

Table 3. Summary of Paired "t" Tests on the February Data for Good Bearings

	Torque Values in mg. mm.			
	Ave. Running	Ave. Hash	Ave. Starting	VANT
$\bar{y}_{1-2}$ (Average Difference in Pairs)	-6.25	79.5	-11.3	0.091
S_d (Standard Deviation of Differences)	91.0	101.	72	0.984
df (Degrees of Freedom)	43	43	42	43
t_{calc} (Calculated t)	0.45	5.20	1.00	0.61
t_{tab} (Tabular t) 95%	2.02	2.02	2.02	2.02
99%	2.70	2.70	2.70	2.70
Conclusion	No Diff.	Diff. 99%	No Diff.	No Diff.

Table 4. Further Analysis of February Average Hash Width Data

Different Days				Same Day			
	Day				Run		
Bearing No.	1st	2nd	Diff.	Bearing No.	1st	2nd	Diff.
41	400	300	100	66	300	300	0
42	500	300	200	67	300	300	0
43	500	300	200	68	300	350	-50
44	400	350	50	69	200	300	-100
45	500	300	200	70	300	250	50
46	500	350	150	71	250	250	0
47	300	250	50	72	200	300	-100
48	500	250	250	73	300	250	50
49	400	200	200	74	300	300	0
50	400	300	100	75	250	200	50
51	400	300	100	76	200	200	0
52	450	400	50	77	250	200	50
53	400	200	200	78	200	250	-50
54	500	300	200	79	250	300	-50
55	400	250	150	80	250	300	-50
56	450	300	150	81	300	400	-100
57	300	200	100	82	300	300	0
58	400	250	150	83	300	250	50
59	400	200	200	84	200	250	-50
60	450	300	150				
61	400	250	150				
62	400	250	150				
63	450	200	250				
64	400	300	100				
65	400	200	200				

$\bar{y}_{1-2}$	152	-15.8
S_d	59	53
df	24	18
t_{calc}	12.7	1.32
t_{tab} 95%	2.10	2.10
t_{tab} 99%	2.80	2.80
Conclusion	Diff. 99%	No Diff.

set of values on these bearings was obtained on one day and the second on a different day. The average difference between pairs of values is 152 mg.mm. and the calculated value of "t" is 12.7 which greatly exceeds the tabular value at the 99% probability level. Obviously, there was a large difference between pairs of values run on different days. For Bearings 66 through 84, both runs were made on the second day of testing. In this case, the average difference was -15.8 mg.mm.; and the calculated "t" value is 1.32. This value does not exceed the tabular value at the 95% probability level; and, therefore, we cannot reject the hypothesis of no difference between pairs of values.

The above findings are worthy of somewhat more detailed interpretation. It is apparent that "set up" of the MARK III torque tester has an influence on the results that is significant when compared to the random variability for a set of good bearings. It is also interesting to note that similar differences were not observed for the average running torque even though this data was acquired from the same charts. Apparently, it will be necessary to employ some type of internal standardization for average hash measurements when studying the effect of various types of defects. Some internal standardization can be achieved by subtracting a blank value generated from a series of "standard" bearings which would be run each time tests are conducted.

C. Further Comparison of Pairs of Values

Graphs of first-run versus second-run values for each bearing and for each test were made. If the variation in the data is entirely random, we would expect to see a circular pattern of data points. If on the other hand there were no measurement error and all variation were due to real differences between individual bearings, we would expect to observe a straight-line array of points passing through the origin and having a slope of 1.0. Since we know that there will always be some random error superimposed on any systematic effects, what we will see if the measurements are reflecting real differences between bearings is an elongated ellipse with its long axis approximating a 45 degree line through the origin.

In Figure 15, we see a plot of the first versus second runs for the average running torque. It is apparent that the array of points approximates a circular scatter diagram; and, therefore, the variation in these values is a reflection of random error in the measurement system rather than real differences between bearings.

In Figure 16, a similar plot for the average hash width is presented. Here, it is noted that the data are segregated

PLOT OF FIRST VERSUS SECOND TRIALS FOR AVERAGE RUNNING TORQUE

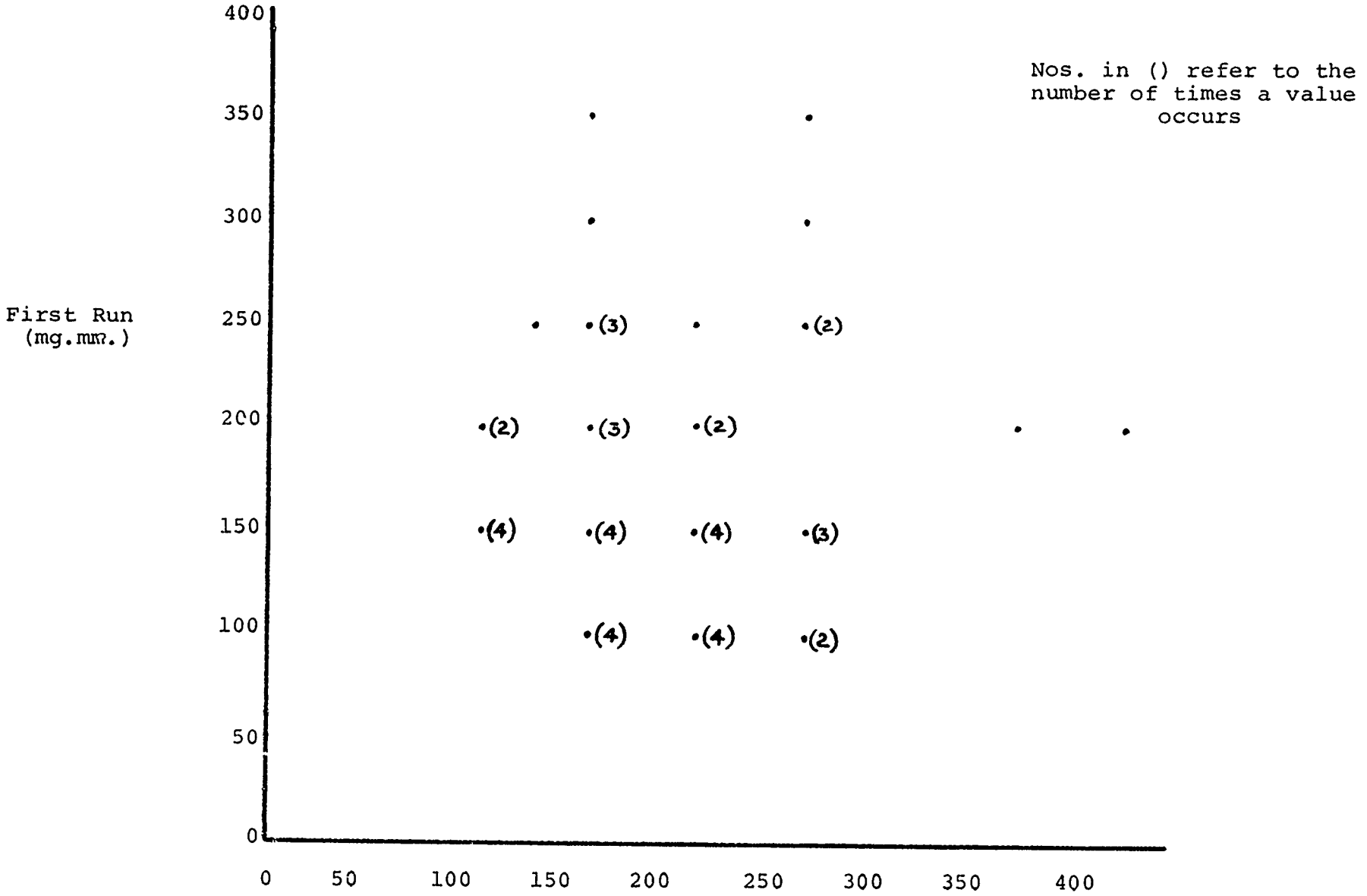

Figure 15D
Second Run (mg.mm.)

PLOT OF FIRST VERSUS SECOND TRIALS FOR AVERAGE HASH WIDTH

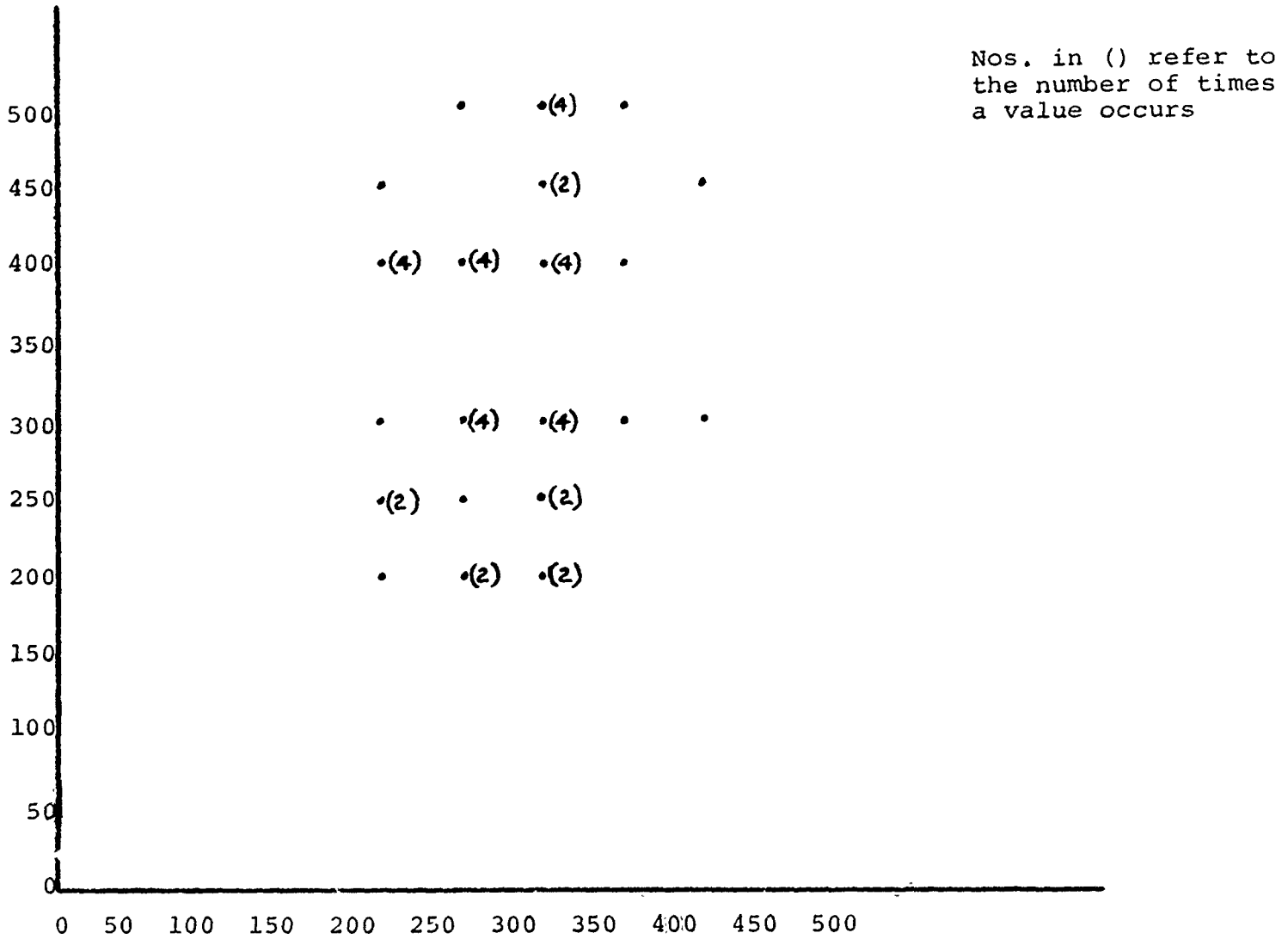

Figure 16D

in two groups. This separation is accounted for by the difference in days discussed earlier. Discounting this segregation of points, it is again clear that the array approaches a random circular pattern.

In Figure 17, the first versus the second trials for average starting torque are plotted. In this case, there is a hint of a functional relationship between the points; and the least squares line is drawn on the graph. However, a statistical regression analysis of the data provided an F ratio for the slope of 3.69 with a value of 4.07 required for significance at the 95% level. Therefore, the existence of a functional relationship has not been demonstrated. A closer inspection of the data suggests that there are three points at the high torque values which are the primary cause of suggesting a systematic relationship between the values. The balance of points form a fairly random array. In any case, it appears that, for these good bearings, the majority of variation is accounted for by random measurement error.

In Figure 18, the first versus the second run for VANT is plotted. In this case, there is a highly significant functional relationship between the values. A statistical analysis indicates that the relationship is significant at

PLOT OF FIRST VERSUS SECOND TRIALS FOR AVERAGE STARTING TORQUE

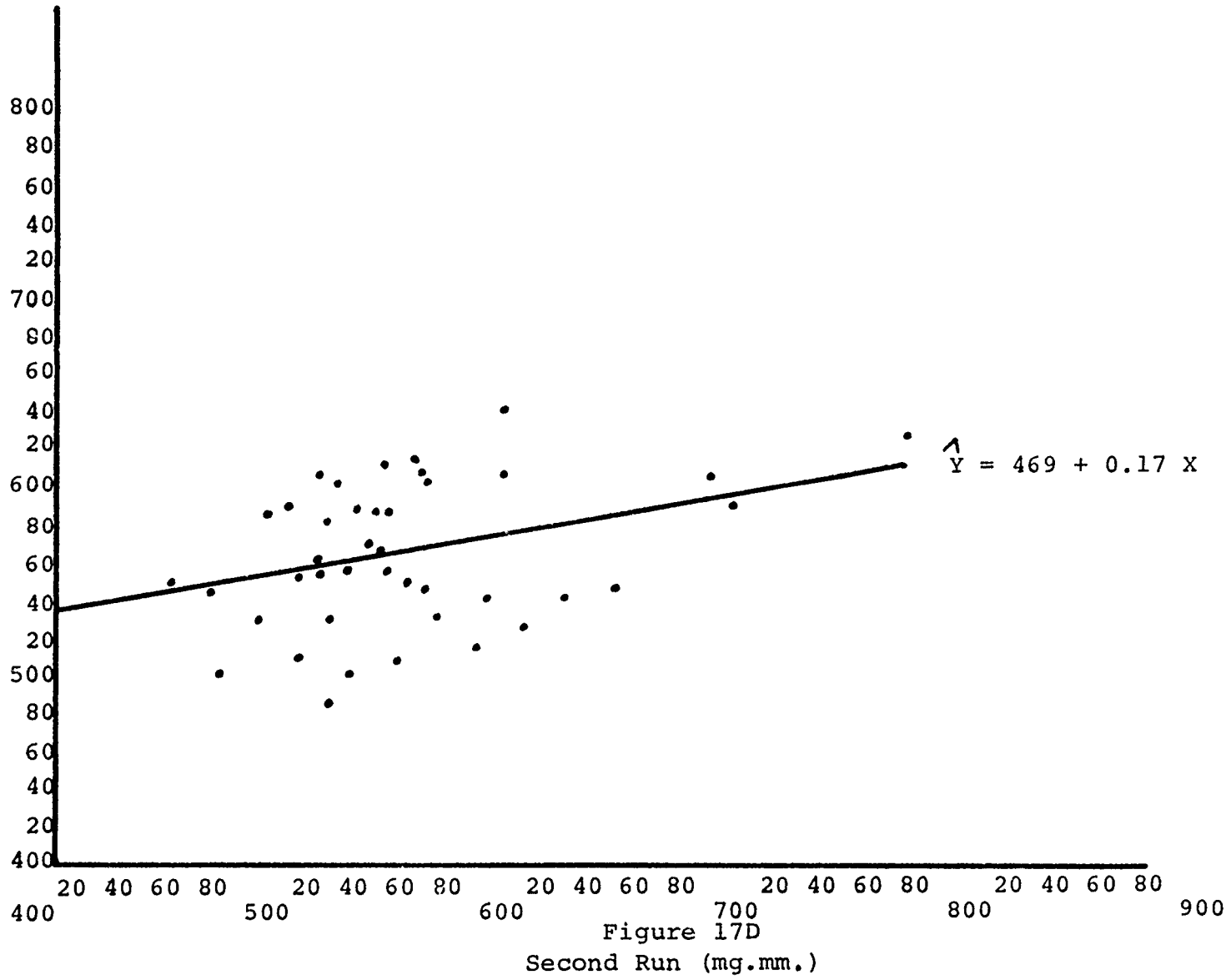

Figure 17D

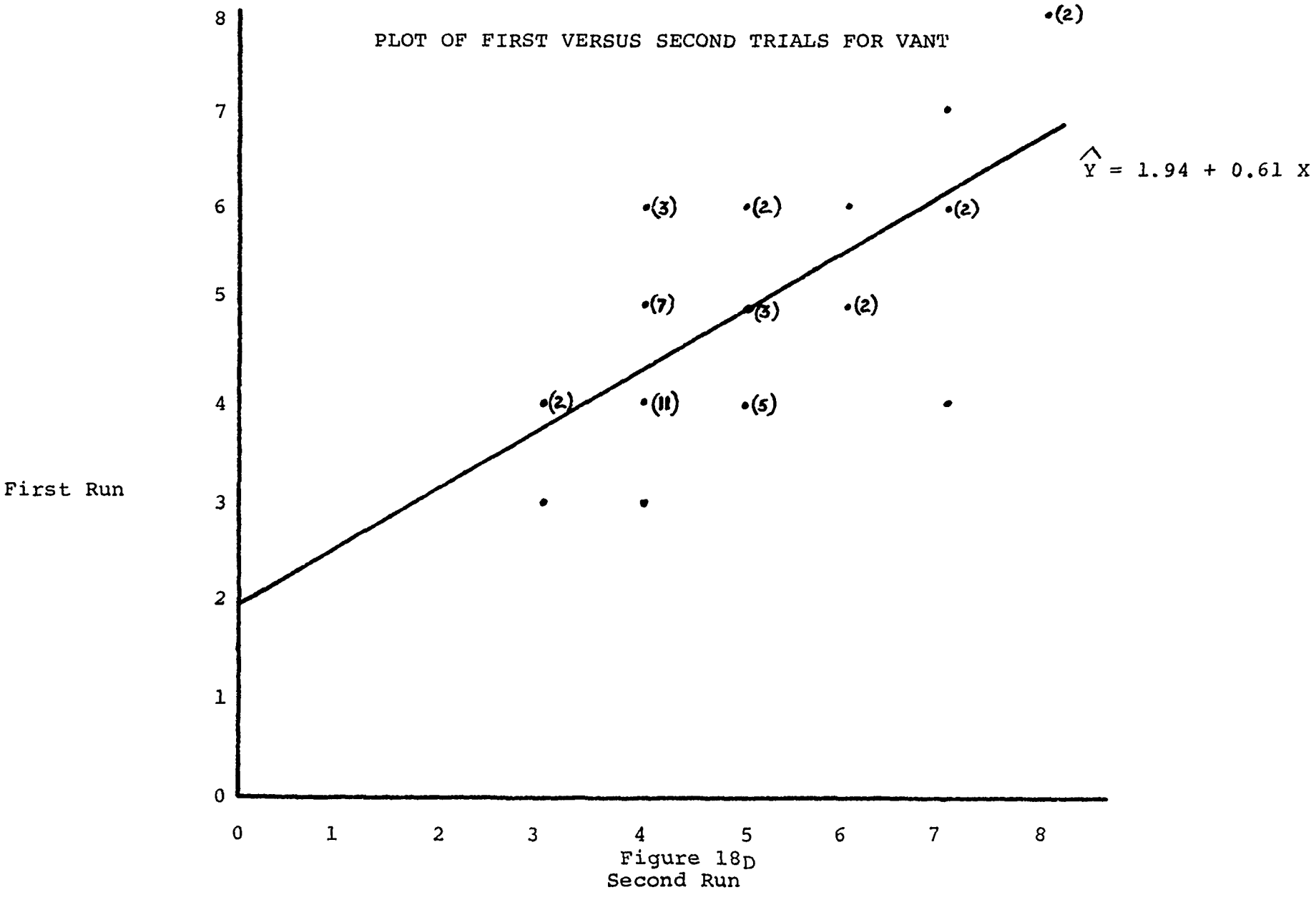
PLOT OF FIRST VERSUS SECOND TRIALS FOR VANT
$\hat{Y} = 1.94 + 0.61 X$
First Run
Second Run
0
1
2
3
4
5
6
7
8
(2)
(3)
(2)
(2)
(7)
(3)
(2)
(2)
(11)
(5)

Figure 18D

much greater than the 99% level. The correlation coefficient, r, is 0.67. It is usually assumed that 100 r^2 is a rough estimate of the percentage of the total variability that is explained by the functional relationship. Thus, we would say that approximately 45% of the variation is a reflection of real differences between bearings of this group. The balance of the variation is presumably due to random measurement error. Of course, ideally, we would expect the intercept to be zero and the slope to be 1.0. Departure from these ideal values as indicated by the least squares equation is probably most expecially meaningful for this limited set of data.

D. Frequency Histograms

In Figures 19 and 20, frequency histograms are plotted. In the case of average running torque, a reasonable approximation to a normal distribution is obtained. All 88 values were employed in this plot and in the calculation of the average and standard deviation since there was no indication of systematic differences between the first and second trials.

For average hash width, the data from the first day trials are plotted separately from the data from the second day trials. This separation is based on the findings reported in a previous section.

FREQUENCY HISTOGRAMS FOR AVERAGE RUNNING TORQUE
AND AVERAGE HASH WIDTH

AVERAGE RUNNING TORQUE

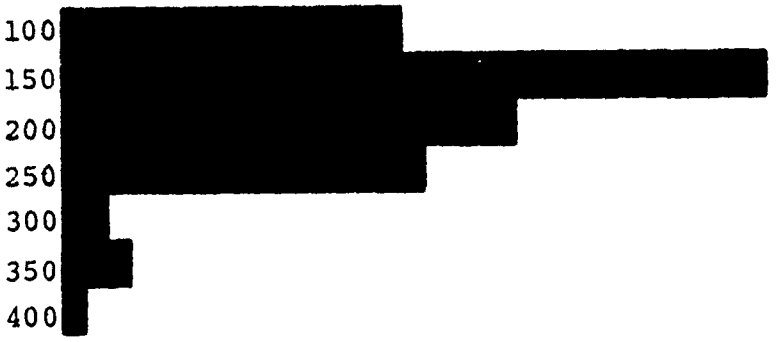

$\bar{Y} = 184$

$S_y = 65$

AVERAGE HASH WIDTH

First Day

$\bar{Y} = 424$

$S_y = 56$

Second Day

$\bar{Y} = 270$

$S_y = 50$

Figure 19D

FREQUENCY HISTOGRAMS FOR VANT & AVERAGE STARTING TORQUE

VANT

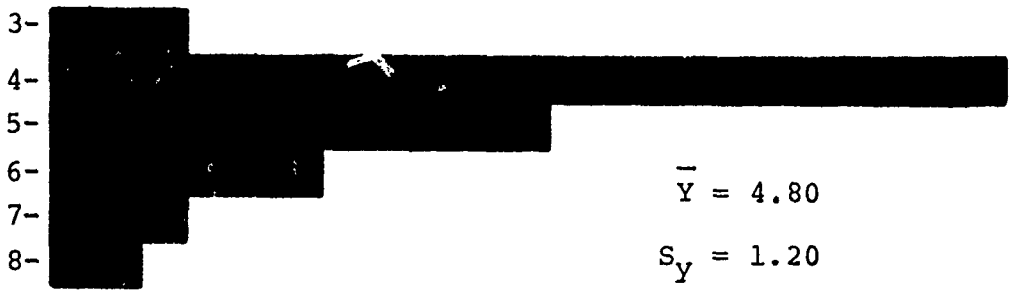

AVERAGE STARTING TORQUE

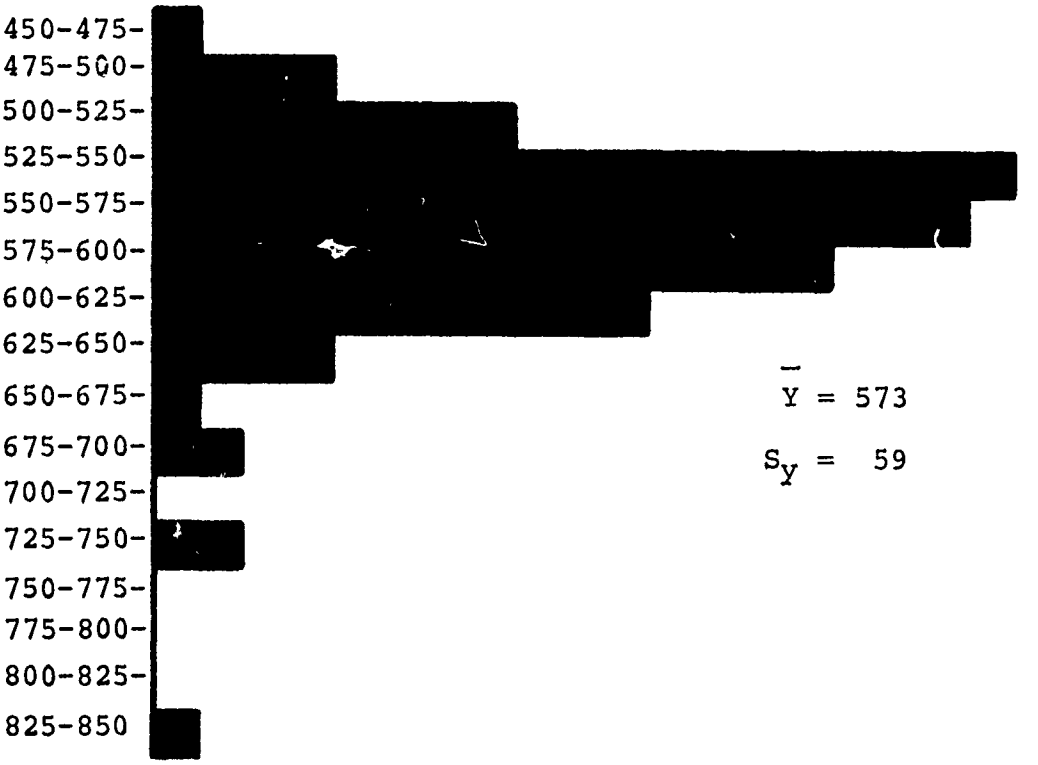

Figure 20D

For VANT, all 88 values have been plotted as a single frequency histogram; and a single mean and standard deviation were calculated, despite the fact that the plot of first versus second trials shows that there is a significant relationship between the values. When the two sets of data were considered individually, the mean and standard deviation for the first day were 4.84 and 1.14 respectively; while the corresponding values for the second day were 4.75 and 1.26. It is clear that the standard deviation estimate for the data considered as a single group of 88 values shows no meaningful departure from the values for the two sets of data individually. The frequency histogram indicates a reasonably normal distribution.

For average starting torque, a single frequency histogram has been plotted. The histogram shows an excellent approximation to a normal distribution.

E. Comparison of January and February Data Sets

We next compared the January and February sets of data with respect to reproducibility and means. The reproducibility was compared by the F test which is obtained by dividing the larger error variance by the smaller error variance. If the calculated ratio exceeds the tabular value for the appropriate number of degrees of freedom at a stated probability level,

the hypothesis of no difference in reproducibility can be rejected. Means for the two sets of test data were compared by the "t" statistic using the equation shown below.

$$t = \frac{\bar{Y}_1 - \bar{Y}_2}{S_{yp}\sqrt{\frac{1}{n_1} \quad \frac{1}{n_2}}} \qquad \text{----------(2)}$$

where $\bar{Y}_1 - \bar{Y}_2$ = the difference in the two means

S_{yp} = the pooled standard deviation

n_1 = the number of measurements in Set 1

n_2 = the number of measurements in Set 2

In applying the above equation, the pooled standard deviation can only be calculated if the previous F test has shown that the variances for the two sets of data do not differ significantly.

In Table 5, we have presented a summary of the calculations for average running torque, average starting torque, and VANT. The variances for average running torque show no difference for the January and February data. It should be remembered that the variance for the January data is slightly suspect because the frequency histogram indicated a non-normal distribution. In any case, it seemed reasonable to proceed with the comparison

Table 5. Comparison of January and February Results

	Torque Values in mg. mm.					
	Average Running		Average Starting		VANT	
	Jan	Feb	Jan	Feb	Jan	Feb
$\bar{y}_1-\bar{y}_2$ (Difference in Means)	152	184	1034	573	9.3	4.8
S_y^2 (Variance)	4373	4284	23,317	3421	10.7	1.43
S_y (Standard Deviation)	66	65	153	58.5	3.28	1.20
n (Number of Observations)	33	88	33	86	33	88
F_{calc} (Ratio of Variances)	1.02		6.81		7.48	
F_{tab} (Tabular F) 95%	1.59		1.59		1.59	
99%	1.92		1.92		1.92	
Conclusion on Variances	No Diff.		Diff. 99%		Diff. 99%	
t_{calc} (Calculated t for comparison of means)	2.4		14.8*		6.7*	
t_{tab} (Tabular t) 95%	1.98		2.04		2.04	
99%	2.61		2.75		2.75	
Conclusion on Means	Diff. 95%		Diff. 99%		Diff. 99%	

*Because variances were different and, therefore, not appropriate to be pooled, we used the standard deviation estimates from the January data to be very conservative.

of means for the two sets of data using the pooled standard deviation estimate from the combined January and February variances. The calculated "t" value of 2.4 exceeds the tabular value at the 95% probability but not at the 99% probability level. Therefore, we can reject the hypothesis of no difference in the means at the 95% probability level.

For the average starting torque, the variance for the January data is significantly larger than for the February data as shown by the F ratio of 6.81. This exceeds the tabular value at the 99% level. Consequently, it is not legitimate to calculate a pooled standard deviation estimate from these two variances. In order to permit a comparison of the means, we employed the conservative tactic of using the larger of the two standard deviation estimates, namely the value of 153 mg.mm. from the January data. Even with this large standard deviation estimate, the calculated "t" value was 14.8 and greatly exceeded the tabular value even at the 99% probability level. Clearly, the average starting torque for the January bearings was much larger than for the February bearings. This can be explained on the basis of the improved cleanliness for the February bearings as a result of spray cleaning. It is also noteworthy that the February bearings show a standard deviation estimate that is smaller by a factor

of three as a result of this improved cleanliness. We can likely expect larger standard deviations with defect-containing bearings which will have larger average starting torques.

For VANT, the situation is quite analogous to the average starting torque. The variance for the January data is significantly larger than for the February data; and we again employed the standard deviation for the January data in comparing the means. As in the previous case, the calculated "t" value of 6.7 far exceeds the required tabular value for the 99% confidence level, again showing that the average VANT level for the cleaner February bearings is significantly lower than for the January bearings. Here, also, the standard deviation estimate was approximately three times as large for the January as for the February bearings.

A direct comparison of the January and February average hash width values could not be made since it had been discovered that the values on two different days of the February data were significantly different. Consequently, the comparison was made as though three sets of data had been produced--one in January and two in February. These results are summarized in Table 6. By an analysis of variance, it was determined that the three means did not constitute a homogeneous group; and, specifically, it was determined that the

Table 6. Comparison of January and February Results

	Average Hash Width (mg. mm.)		
	Jan	Feb (1st day)	Feb (2nd day)
$\bar{y}$ (Means)	395	424	270
S_y^2 (Variances)	13,428	3150	2463
S_y (Standard Deviations)	116	56	50
n (Number of Values)	33	25	63

second day of the February testing produced a smaller mean hash width than for the other two days of testing. Homogeneity of the variances was not tested, but it is suspected that the variance for the January data is significantly larger than for the two sets of February data. It is apparent that care will be required in setting up the running torque tests in order to produce dependable data on average hash width.

F. Correlation of Different Measurements - February Data

In Figure 12, we showed a significant correlation between average hash width and VANT for the January data. A similar plot was made for the average hash width from the second run of the February bearings (Figure 21). The second run only was employed since this was all produced on the same day. Figure 21 fails to reveal a relationship similar to that for the January data. Apparently, the cleaner bearings employed in the February study obscure the correlation observed in the January results. In a similar fashion, a significant correlation was observed between average starting torque and VANT for the January data (Figure 13). In the case of the February bearings, no similar correlation was obtained (Figure 22).

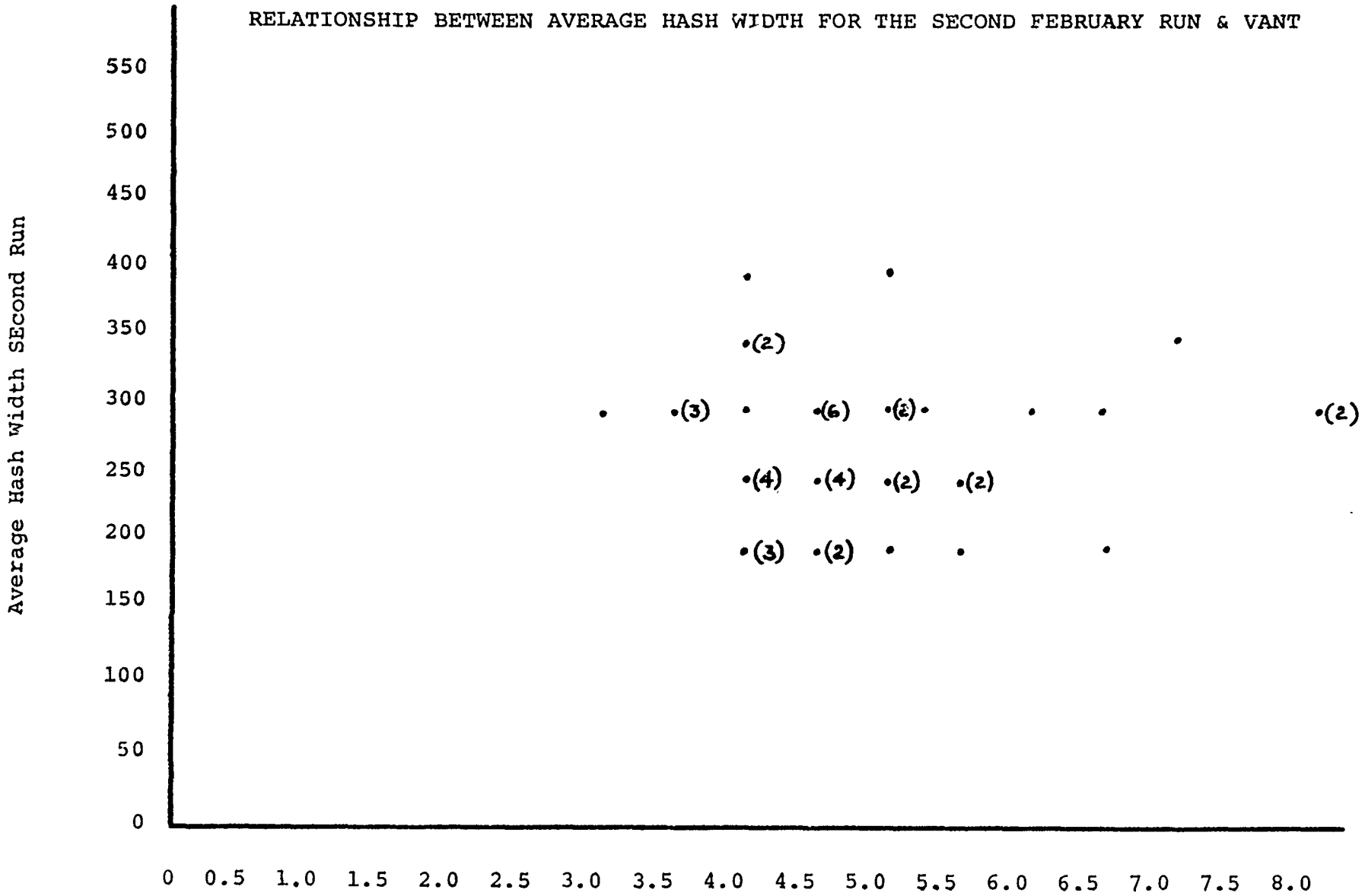
RELATIONSHIP BETWEEN AVERAGE HASH WIDTH FOR THE SECOND FEBRUARY RUN & VANT
Average Hash Width SEcond Run
550
500
450
400
350
300
250
200
150
100
50
0
(2)
(3)
(6)
(2)
(2)
(4)
(4)
(2)
(2)
(3)
(2)
0 0.5 1.0 1.5 2.0 2.5 3.0 3.5 4.0 4.5 5.0 5.5 6.0 6.5 7.0 7.5 8.0
AVERAGE VANT

Figure 21D

RELATIONSHIP BETWEEN AVERAGE STARTING TORQUE & VANT FOR THE FEBRUARY TESTS

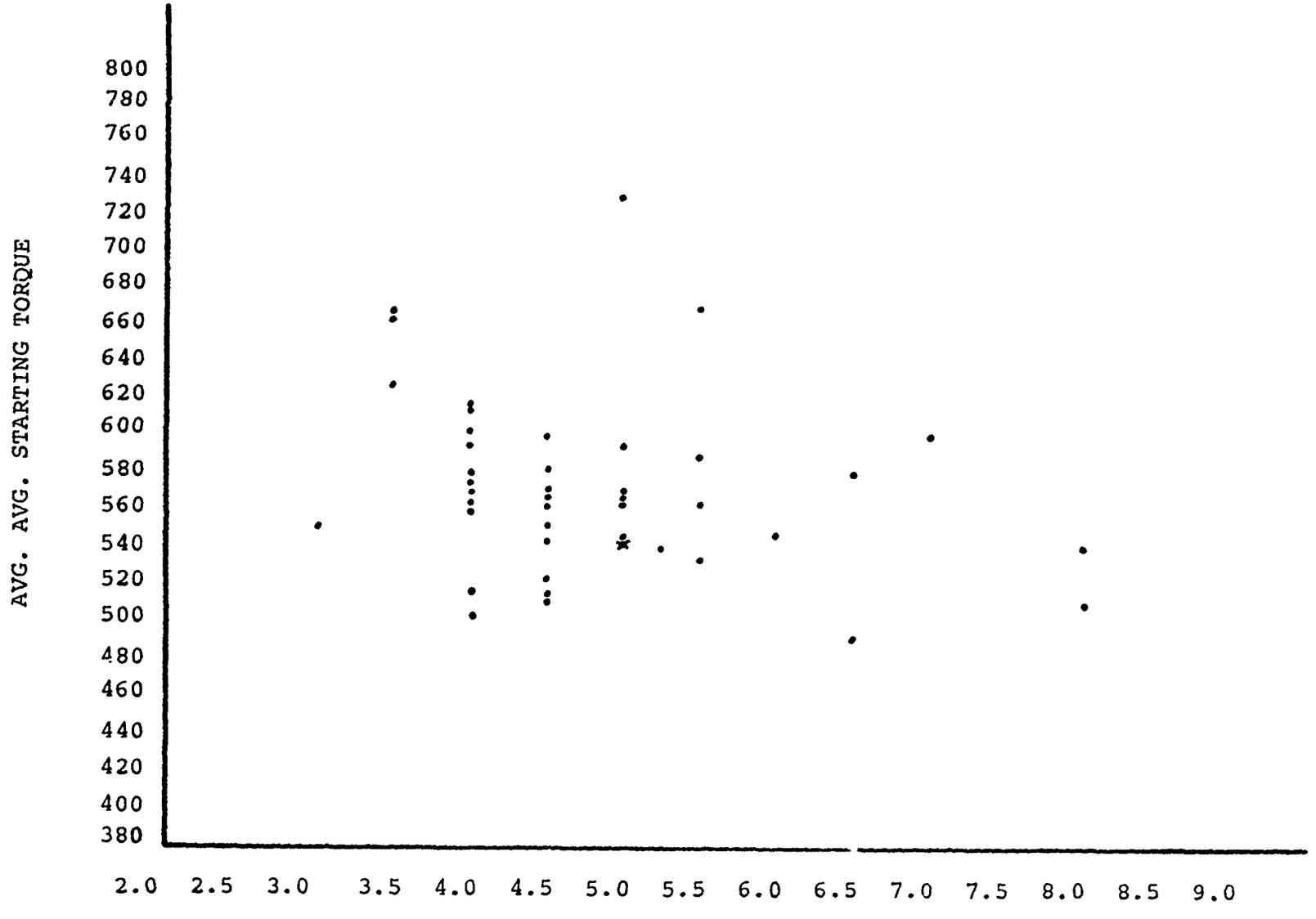

Figure 22D

For the January results, peak starting torque was strongly correlated with average starting torque (Figure 14). The low slope of 1.27 found for this relationship showed that the correlation did not depend on a single high value in a set. A similar plot (Figure 23) has been made for the February results. In this case, the slope is 2.32 indicating a greater dependency of the relationship on a single high value in a set. This is probably not too surprising for these cleaner bearings. The February results also show much more scatter with a correlation coefficient of only 0.58 compared to 0.975 for the January results.

III. DESIGN OF FUTURE EXPERIMENTS

A. Estimation of Sample Sizes for Future Test Work

In future test work, it is anticipated that groups of bearings with various types of defects will be tested. It is necessary to use a sufficient number of replicate bearings for each test to insure that differences can be detected. Equation 2 was employed earlier for the comparison of two means. If we designate the two means as $\bar{Y}_A$ and $\bar{Y}_B$ and if we assume that the sample size for each group is equal, Equation 2 can be rewritten in the form shown below.

RELATIONSHIP BETWEEN PEAK STARTING TORQUE & AVERAGE STARTING TORQUE
FOR FEBRUARY GOOD BEARINGS

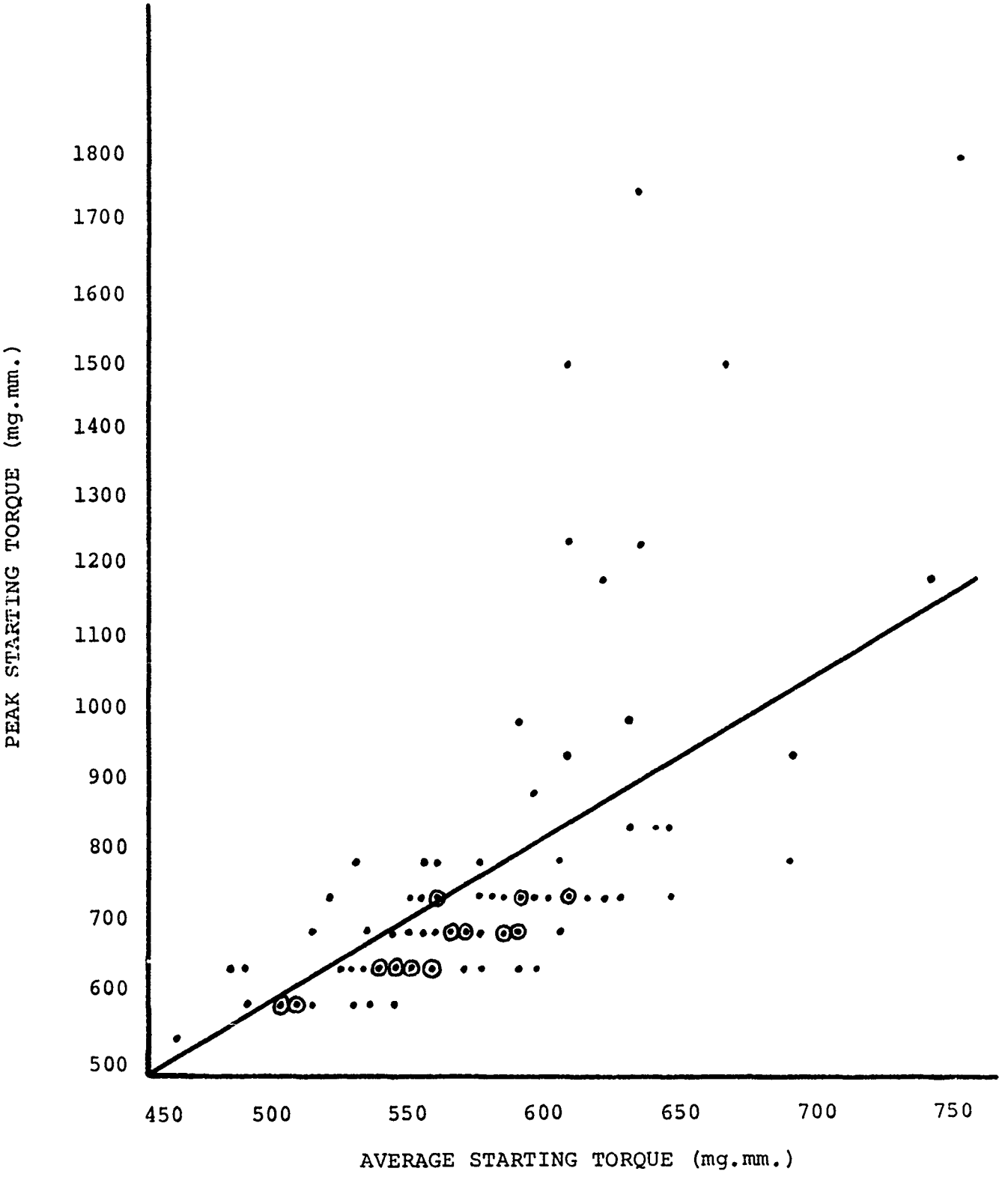

Figure 23D

$$t = \frac{\bar{Y}_A - \bar{Y}_B}{S_{yp}\frac{\sqrt{2}}{\sqrt{n}}} \quad \text{----------(3)}$$

where n = the number of measurements in each set

For calculation of sample size, it is convenient to rearrange the equation into the following form.

$$n = \frac{2t^2 S_{yp}^2}{(\bar{Y}_A - \bar{Y}_B)^2} \quad \text{----------(4)}$$

In order to calculate n, we must predict some value for S_{yp}. We have made the appropriate calculations by assuming three values of S_{yp}. As a starting point, we employed the value generated for the control bearings in the February test data. The calculations were repeated by assuming standard deviations two times and four times as large as those observed in the February data. This is an attempt to anticipate the expected increase in standard deviation for defect-containing bearings.

In addition to specifying S_{yp}, it is necessary to designate various minimum differences, $\bar{Y}_A - \bar{Y}_B$, which it is desired to detect. We used "t" values for both 95% (a = .05) and 99% (a = .01) probability levels. The results of these calculations are presented as a family of curves.

Figures 24 and 25, give the sample size relationships for average running torque determinations. Let us illustrate the use of these curves via some examples. It was agreed that there was a need to detect differences in means ranging from 150 mg.mm. to 3000 mg.mm. Referring to Figure 24 (95% probability level), let us use the curve for a standard deviation four times the value observed for the February data. To detect a difference of 150 mg.mm. in two means would require 25 bearings in each set. If the difference to be detected were 250 mg.mm., as few as ten bearings in each set would suffice. At the 99% probability level (Figure 25) still using a standard deviation four times the February value, approximately 42 bearings per set would be required to detect a difference as small as 150 mg.mm. For a difference of 250 mg.mm., only 16 bearings per set would be required. Of course, if the standard deviations are smaller than four times the February values, still fewer bearings per set would be adequate. As soon as the differences to be detected exceed 500 mg.mm. it makes little difference what standard deviation is employed since a small number of bearings is adequate.

Similar curves are presented for the average hash width in Figures 26 and 27. Since the standard deviation, S_y,

Figures 24 and 25, give the sample size relationships for average running torque determinations. Let us illustrate the use of these curves via some examples. It was agreed that there was a need to detect differences in means ranging from 150 mg.mm. to 3000 mg.mm. Referring to Figure 24 (95% probability level), let us use the curve for a standard deviation four times the value observed for the February data. To detect a difference of 150 mg.mm. in two means would require 25 bearings in each set. If the difference to be detected were 250 mg.mm., as few as ten bearings in each set would suffice. At the 99% probability level (Figure 25) still using a standard deviation four times the February value, approximately 42 bearings per set would be required to detect a difference as small as 150 mg.mm. For a difference of 250 mg.mm., only 16 bearings per set would be required. Of course, if the standard deviations are smaller than four times the February values, still fewer bearings per set would be adequate. As soon as the differences to be detected exceed 500 mg.mm. it makes little difference what standard deviation is employed since a small number of bearings is adequate.

Similar curves are presented for the average hash width in Figures 26 and 27. Since the standard deviation, S_y,

DETERMINATION OF SAMPLE SIZE FOR AVERAGE RUNNING TORQUE

$\alpha = 0.05$ $S_y = 1 \times S_y, 2 \times S_y, 4 \times S_y$ ($S_y = 65.3$)

N (vs) $(\bar{Y}_A - \bar{Y}_B)$

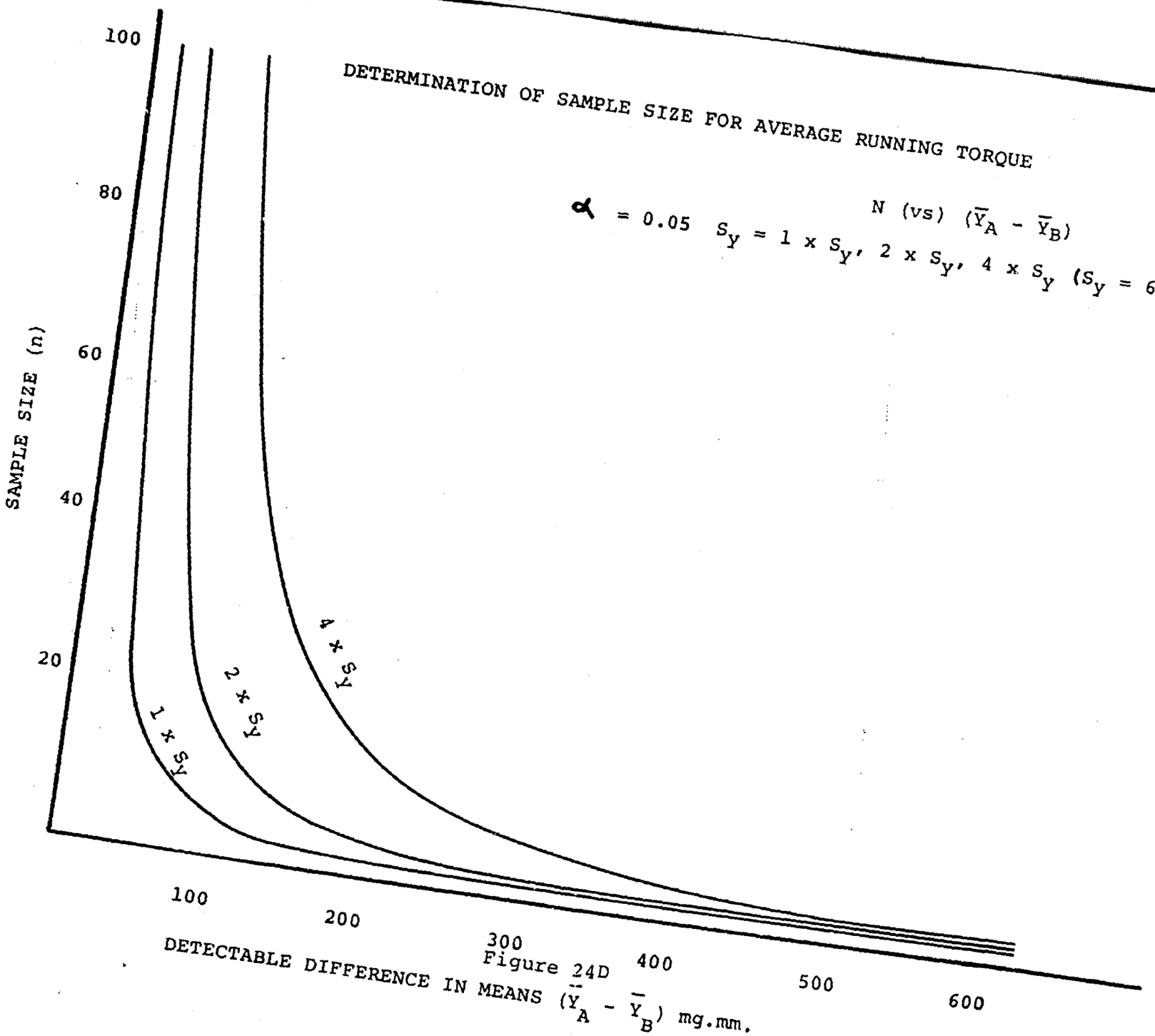

Figure 24D

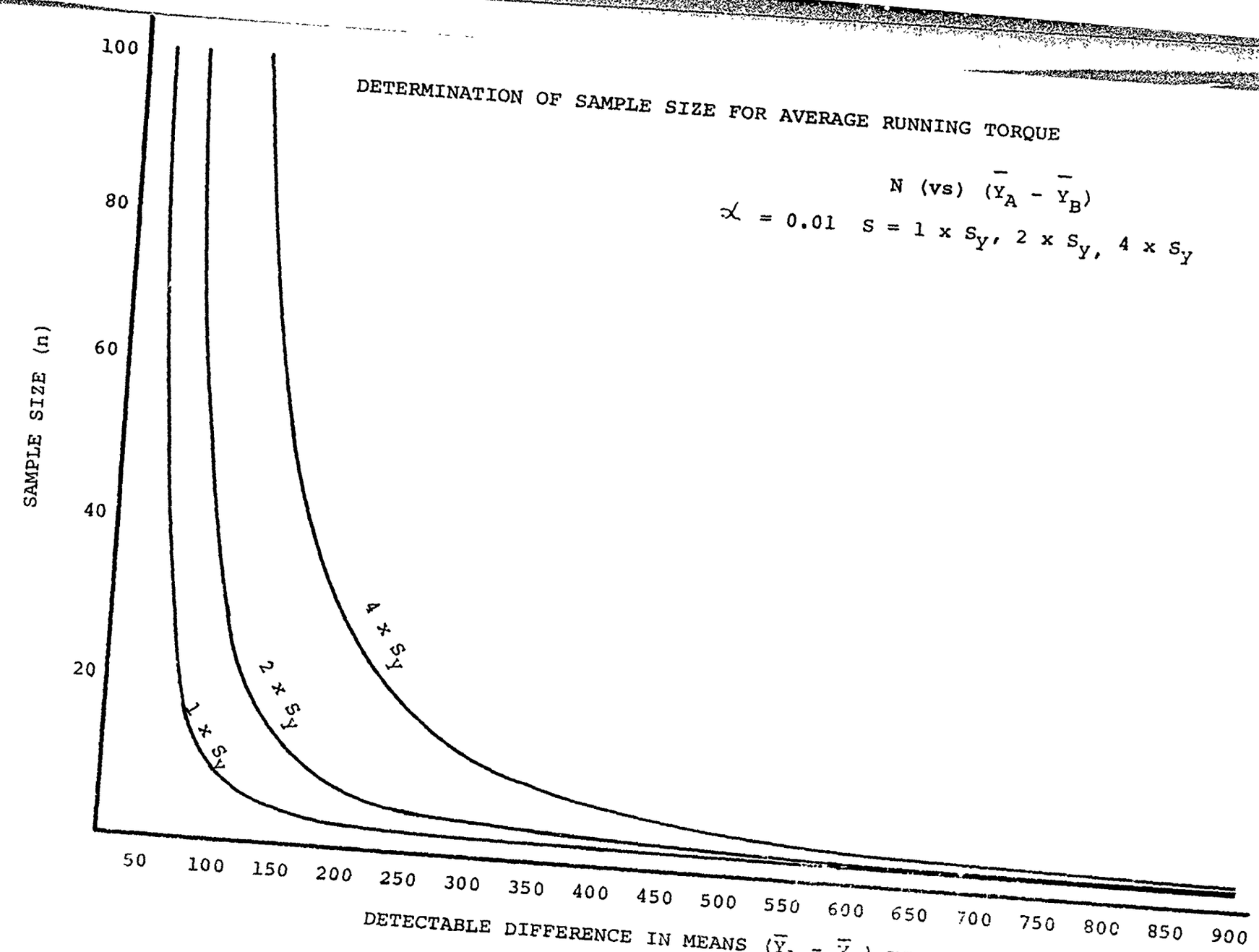
DETERMINATION OF SAMPLE SIZE FOR AVERAGE RUNNING TORQUE
N (vs) $(\bar{Y}_A - \bar{Y}_B)$
$\alpha = 0.01$ $S = 1 \times S_y, 2 \times S_y, 4 \times S_y$
SAMPLE SIZE (n)
100
80
60
40
20
1 x Sy
2 x Sy
4 x Sy
50 100 150 200 250 300 350 400 450 500 550 600 650 700 750 800 850 900
DETECTABLE DIFFERENCE IN MEANS $(\bar{Y}_A - \bar{Y}_B)$ mg.mm.

Figure 25D

DETERMINATION OF SAMPLE SIZE FOR AVERAGE HASH WIDTH

N (vs) $(\bar{Y}_A - \bar{Y}_B)$

$\alpha = 0.05$ $S = 1 \times S_y, 2 \times S_y, 4 \times S_y$ $(S_y = 50.)$

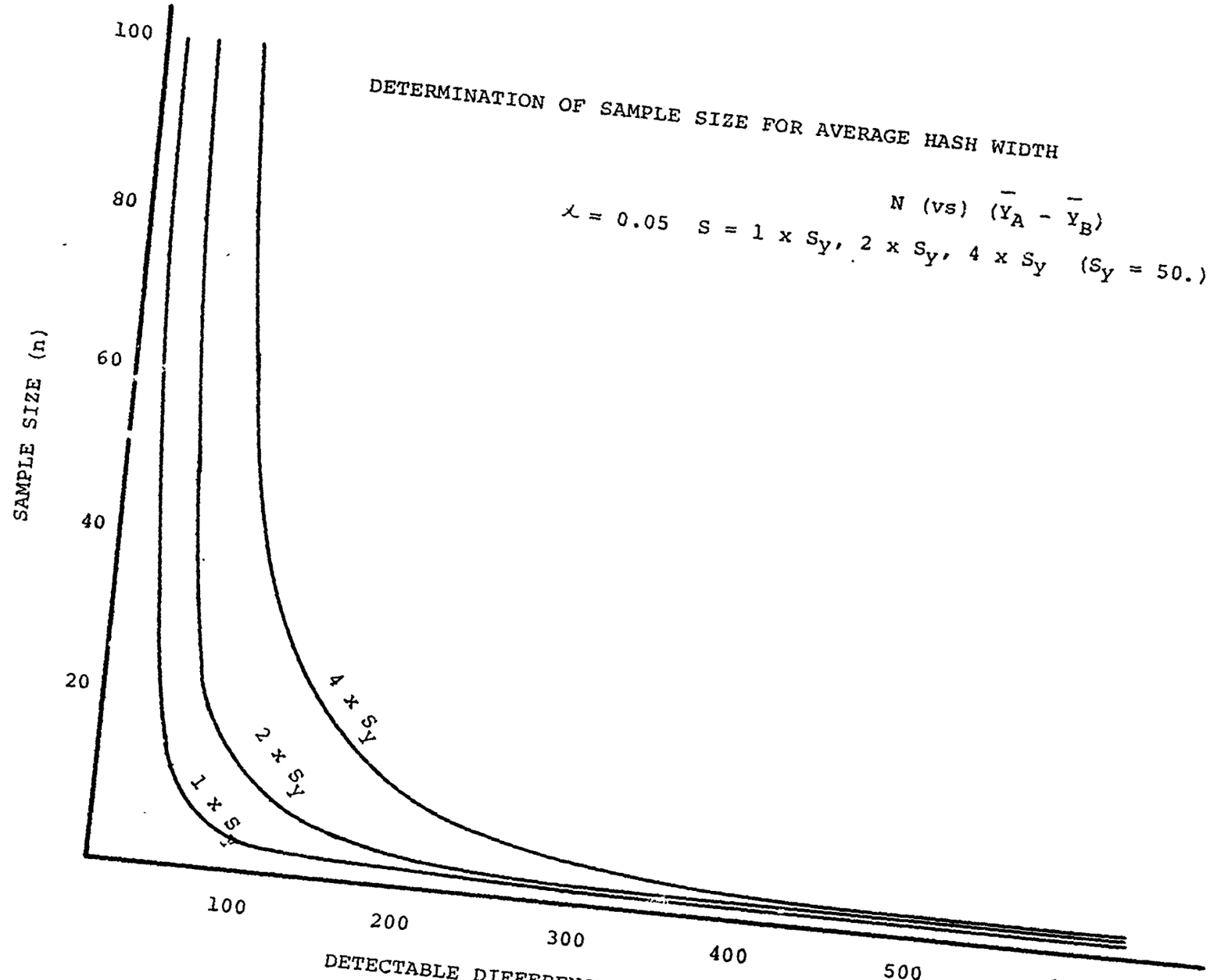

Figure 26D

DETERMINATION OF SAMPLE SIZE FOR AVERAGE HASH WIDTH

N (vs) $(\bar{Y}_A - \bar{Y}_B)$

$\alpha = 0.01$ $S = 1 \times S_y$, $2 \times S_y$, $4 \times S_y$ $(S_y = 50.)$

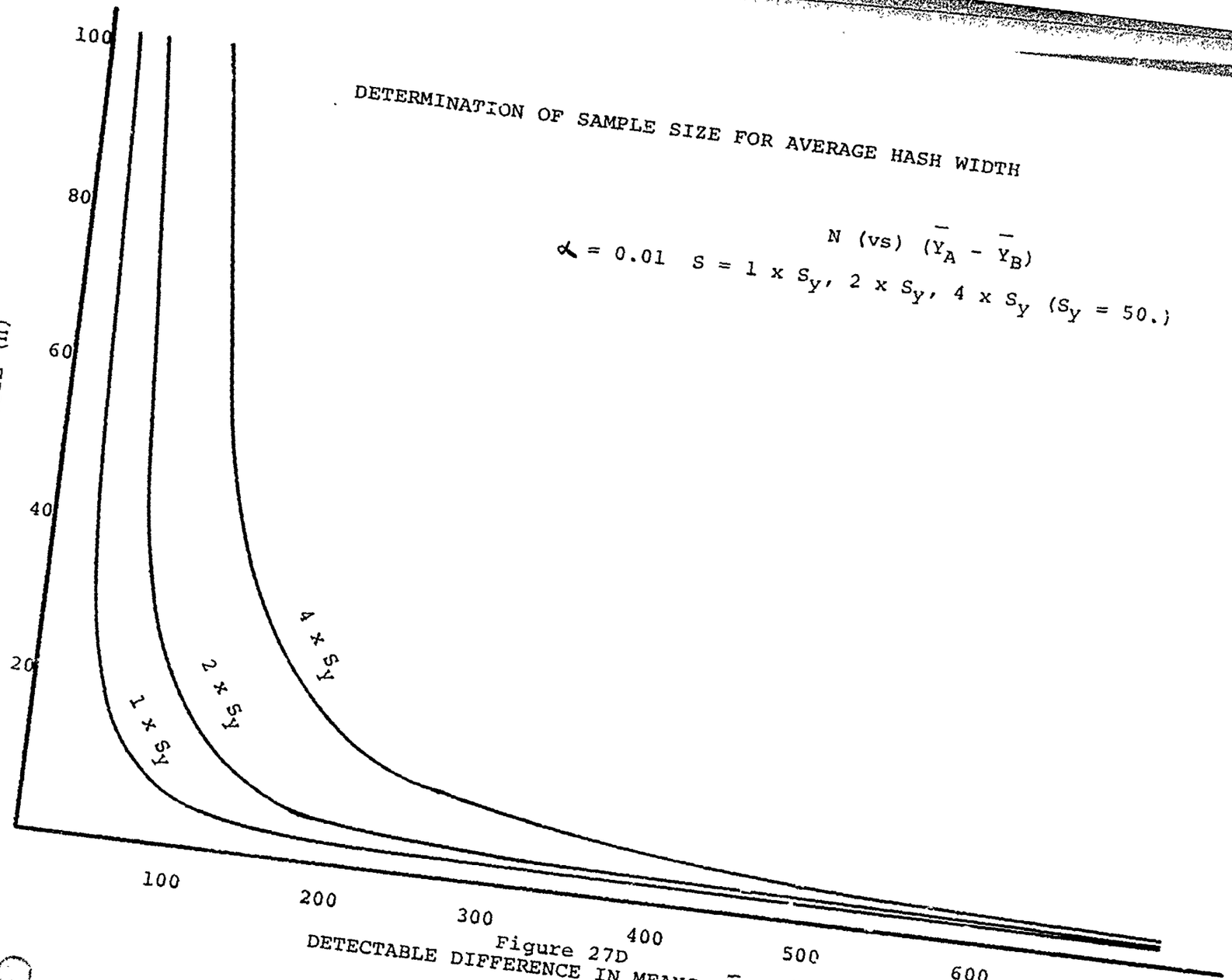

Figure 27D

employed for these calculations was smaller than for the average running torque values, the sample sizes required are smaller. This difference is further magnified by the assumption that the range of differences anticipated in defect-containing bearings is 300 to 3000 mg.mm. Thus, at the 99% probability level with a standard deviation four times the February results, a sample size of only 10 bearings per set would be adequate to detect a difference of 300 mg.mm.

Calculations for average starting torque were not performed because the standard deviation of 58.5 mg.mm. is intermediate between the values for the average running torque calculations and the average hash width calculations. Thus, sample sizes can be readily estimated for the range of differences of interest (300-6000 mg.mm.) by using the previously described curves.

Sample size determination curves for VANT measurements are presented in Figures 28 and 29. According to MPB personnel, the minimum difference in means that would be of interest is 5.0. If we again assume a standard deviation four times that observed for the February data, a difference of five could be detected at the 95% probability level for samples with 10 bearings per set. At the 99% level, 14 bearings per set would be required.

DETERMINATION OF SAMPLE SIZE FOR VANT

$\bar{N}$ (vs) $\bar{Y}_A - \bar{Y}_B$

$\alpha = 0.05$ $S_y = 1 \times S_y$, $2 \times S_y$, $4 \times S_y$ $(S_y = 1.2)$

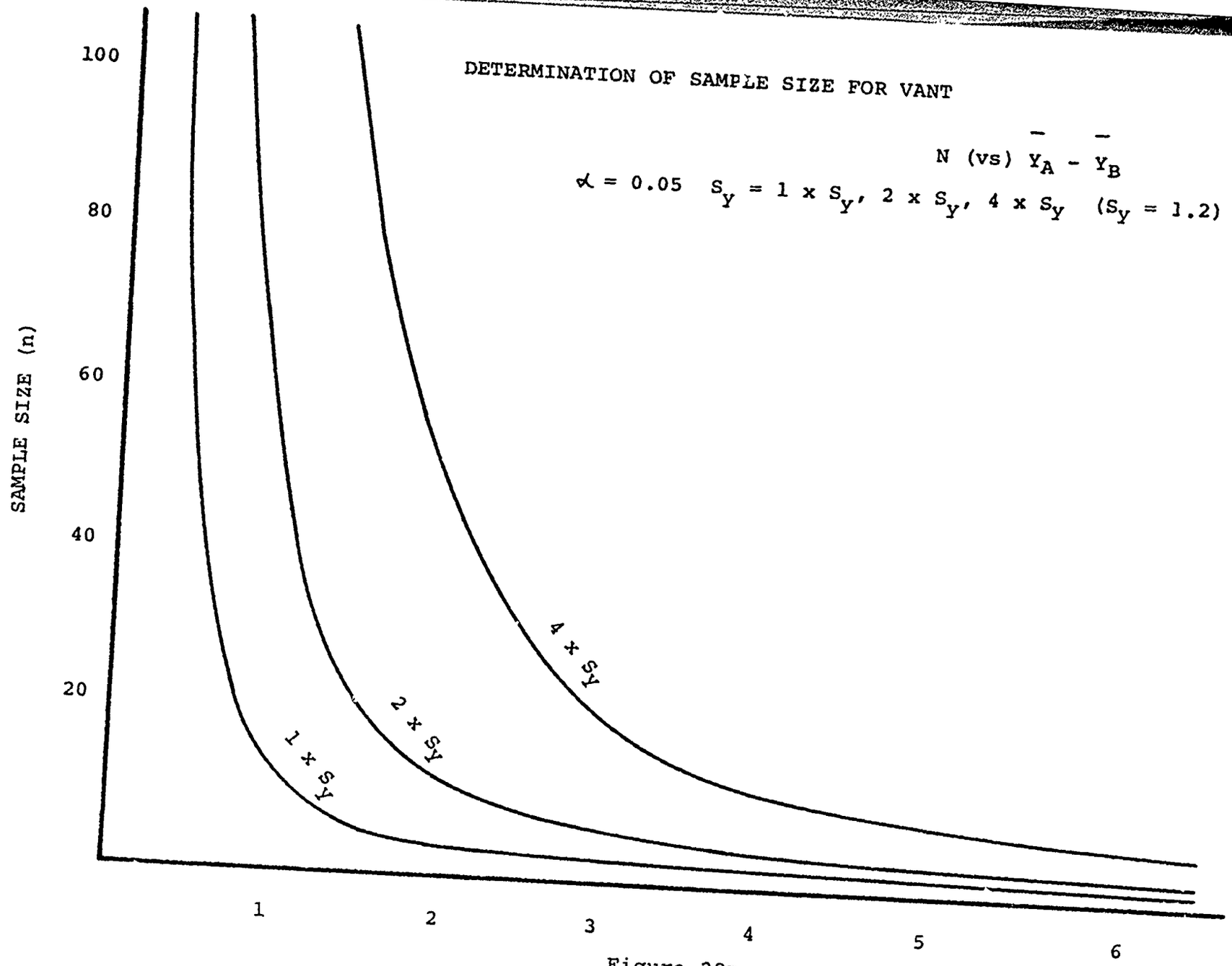

Figure 28D

DETERMINATION OF SAMPLE SIZE FOR VANT

$S_y = 1 \times S_y,\ 2 \times S_y,\ 4 \times S_y \quad (S_y = 1.2)$

$\alpha = 0.01$

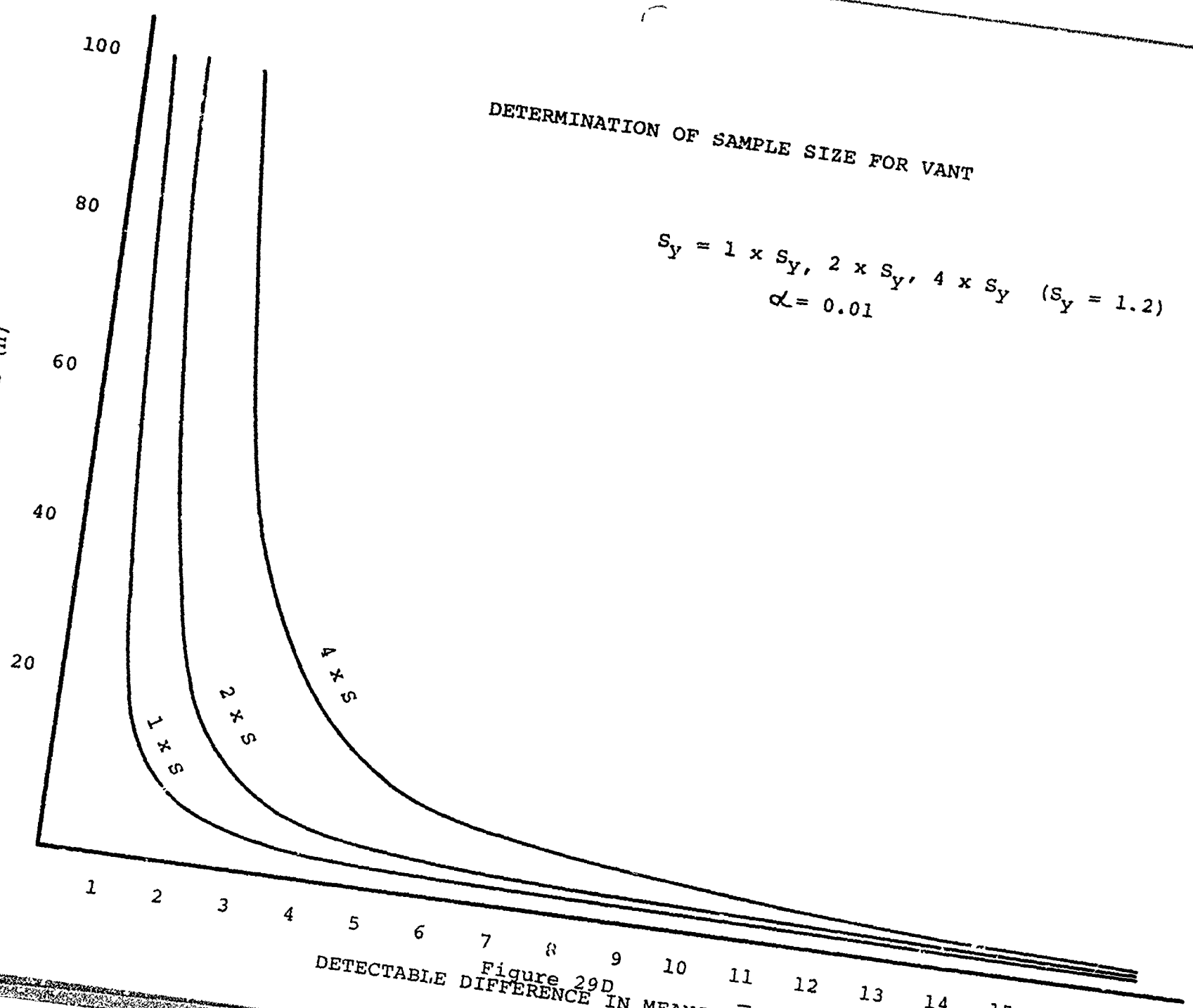

Figure 29D

B. Detection of Spikes Superimposed on Hash for the MARK III Torque Tests

A spike represents a very short-term response to a discrete defect. The spike is superimposed on a background of "normal" variability in the instantaneous running torque. Based on normal probability theory, we can assume that the total width of the hash in a running torque test represents six times the standard deviation. This is based on the fact that the mean ± three standard deviations includes 99.7% of the area under the normal curve. It further assumes that all of the hash represents random variation. The problem now becomes one of detecting a signal superimposed on this pattern of variation.

A number of schemes are available for specifying the minimum height of a signal above background which can be recognized as real. A very simple one which is probably appropriate for this application is the following. A signal which has a height above the top of the hash amplitude equal to three times the standard deviation of the hash is considered a real signal at the 99% probability level. Thus, if the average hash amplitude were 300 mg.mm., the estimated standard deviation would be one sixth this amount or 50 mg.mm. A signal

of 150 mg.mm. above the top of the hash would constitute a detectable signal at the 99% probability level. This is sketched below.

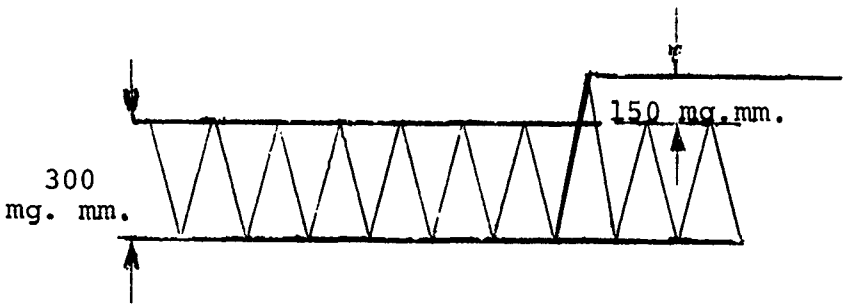

APPENDIX E

TURBINE TEST BANK

TURBINE TEST BANK

The general layout of the MPB designed turbine test bank is shown in Figures 1E and 2E.

The lower cabinet enclosed the 10 individual test turbine stations in a heated and acoustically insulated area.

A constant temperature is maintained by thermostatically controlled heating elements and circulating fans located in the cabinet.

The control panel, shown placed on top of the cabinet, automatically tests for turbine speed sequentially. That is, each turbine is monitored every 60 seconds and is automatically shut down if speed is outside a pre-set range.

The individual test turbine, shown in Figure 3E and depicted in cross section in Figure 4E, consists of a bearing supported air turbine rotor, with bearing preload obtained by a mechanically applied loading across the outer bearing rings. The test bearing is mounted adjacent to the turbine wheel.

A noncontacting, magnetic pick-up senses rotation of the turbine rotor.

Once speed stabilization has been attained for any given test by adjusting inlet air flow, turbine speed changes will be related to changes in bearing frictional torque. A sharp decrease in speed then signals a bearing torque increase or failure.

Wing nut clamping and quick-disconnect air lines allow rapid dismounting of the turbine for test bearing replacement.

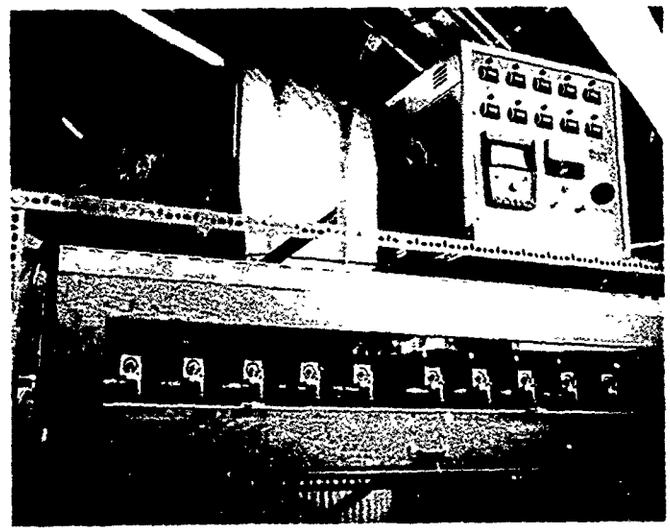

Control
Panel

Figure 9A - Turbine Test Bank

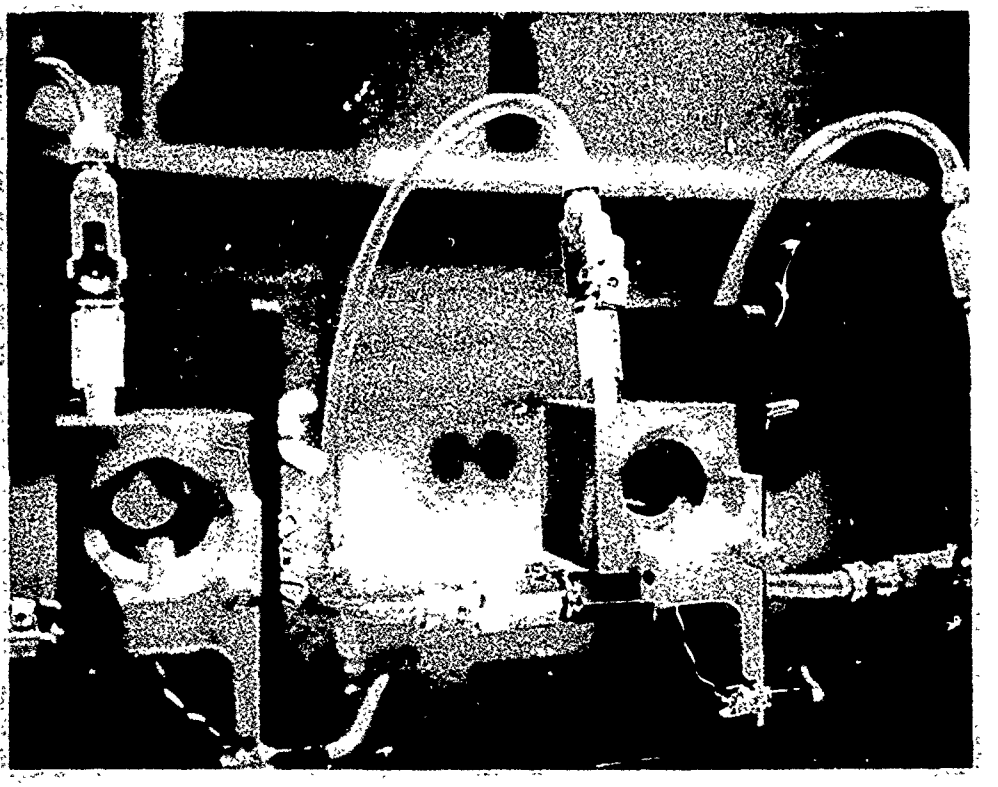

Figure 3E - Turbine Test Fixture

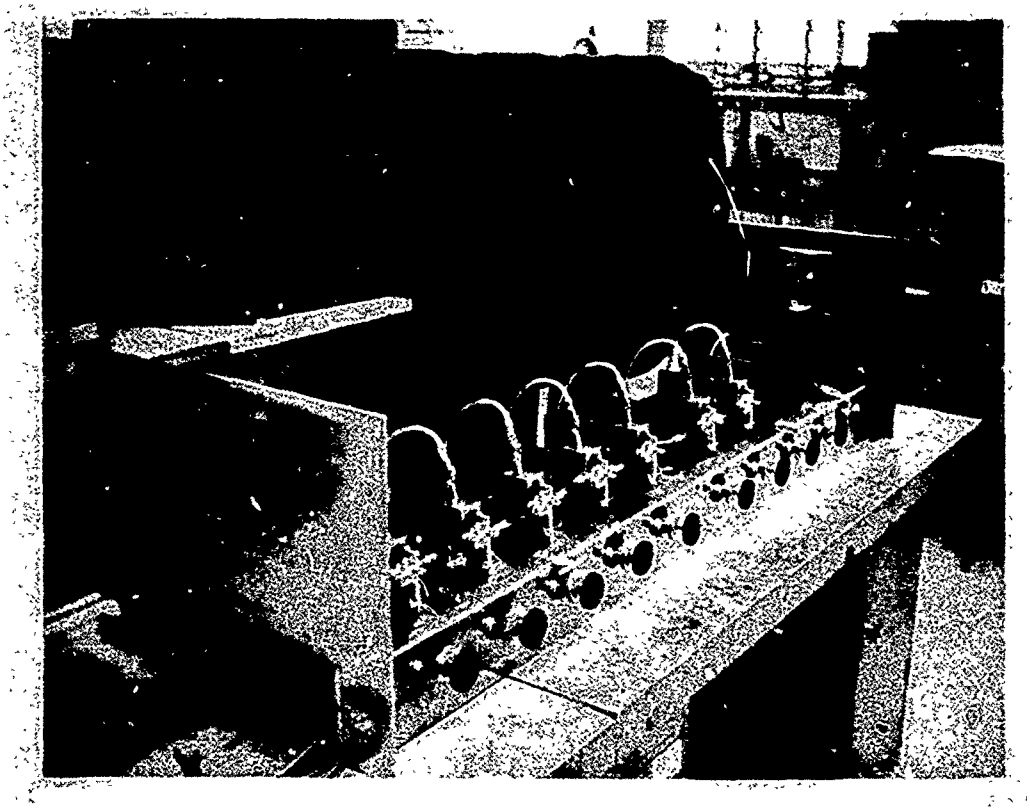

Figure 2E - Turbine Test Bank

Figure 4E

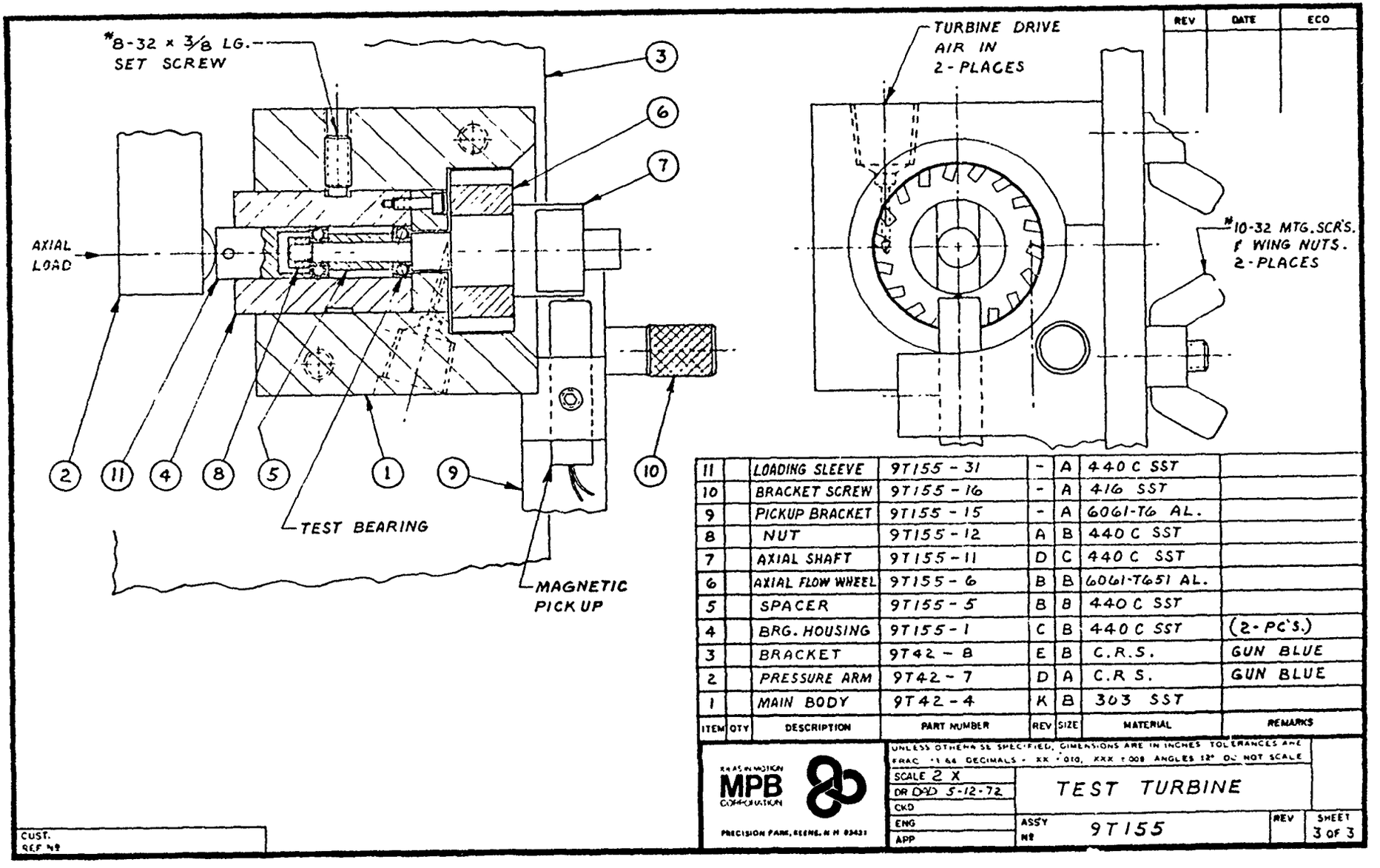

ITEM	QTY	DESCRIPTION	PART NUMBER	REV	SIZE	MATERIAL	REMARKS
11		LOADING SLEEVE	9T155 - 31	-	A	440 C SST	
10		BRACKET SCREW	9T155 - 16	-	A	416 SST	
9		PICKUP BRACKET	9T155 - 15	-	A	6061-T6 AL.	
8		NUT	9T155 - 12	A	B	440 C SST	
7		AXIAL SHAFT	9T155 - 11	D	C	440 C SST	
6		AXIAL FLOW WHEEL	9T155 - 6	B	B	6061-T651 AL.	
5		SPACER	9T155 - 5	B	B	440 C SST	
4		BRG. HOUSING	9T155 - 1	C	B	440 C SST	(2-PC'S.)
3		BRACKET	9T42 - 8	E	B	C.R.S.	GUN BLUE
2		PRESSURE ARM	9T42 - 7	D	A	C.R S.	GUN BLUE
1		MAIN BODY	9T42 - 4	K	B	303 SST	

MPB CORPORATION
PRECISION PARK, KEENE, N H 03431

UNLESS OTHERWISE SPECIFIED, DIMENSIONS ARE IN INCHES TOLERANCES ARE FRAC ±1/64 DECIMALS - XX ±.010, XXX ±.005 ANGLES 12° DO NOT SCALE

SCALE 2 X
DR DAD 5-12-72
CKD
ENG
APP

TEST TURBINE

ASSY NO 9T155

REV

SHEET 3 OF 3

CUST. REF NO

APPENDIX F

DEFECT-CONTAINING RING FABRICATION AND INSPECTION CRITERIA

Defect Type	Fabrication	Inspection
Scratch	Induced on inner raceways by hand-held, sharp tool, and traversing across raceway perpendicular to ball path	Three defect levels based on scratch width determined (<.0005", .0005" to .001", .001" to .005"). Five scratches induced on each raceway.
Dig-Nick	Induced on inner raceways by indenting surface with sharp tool mounted in arbor press	Three defect levels based on major dimension of defect inspected and grouped as for scratch, above
Dirt Brinell	Induced on assembled bearings by operating with typical contaminants, resulting in uniform multiple brinelled surfaces	Three defect levels based on approximate size of uniformly distributed individual brinells. (<.0008", .0008" to .001", .001" to .002")
Orange Peel	Induced on inner raceway by additional polishing, resulting in carbides standing in relief against matrix	Three defect levels determined by subjectively grading extent of relief under magnification (light, medium, heavy)
Pits	"Small" level obtained by selection of inclusions in steel. "Medium" and "Large" induced by chemical etch	Three defect levels based on max. dia. of pit. (<.0005", .0005" to .001", .001" to .005")
Impingement	Induced on inner raceway by indenting with a radiused tool mounted in arbor press	Three defect levels based on major dimension of defect. (<.005", .005" to .006", .006" to .008"). Three defects per raceway
Comet Tail	Induced on inner raceway by controlling race finishing process, producing varying densities of uniform width defects.	Three defect levels determined by number of defects in ball track. (2 to 6; 7 to 13; 14 to 64).
Grind-Skip Line	Produced on inner raceways by varying race finishing cycle. (The shorter cycle times allowed more of the original grind ridges to be exposed).	Three defect levels determined by subjectively grading the apparent density of residual grind lines. (Light, medium, heavy).
Liney Finish	Produced on inner raceways by varying polishing compound grit size, and cycle time.	Three defect levels determined by subjectively grading the apparent density. (Light, medium, heavy).

FABRICATION & INSPECTION CRITERIA

Figure 1F

Figure II

TYPICAL SCRATCHES
CLASS 7-3 200 X.MAG.

SMALL

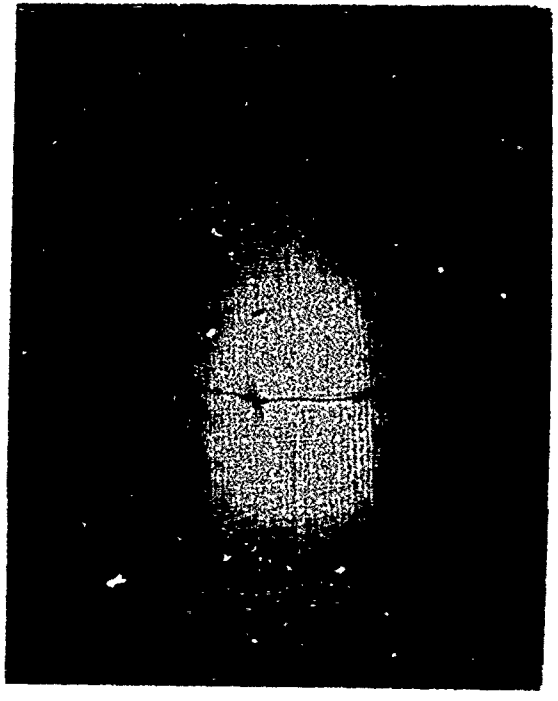

MEDIUM

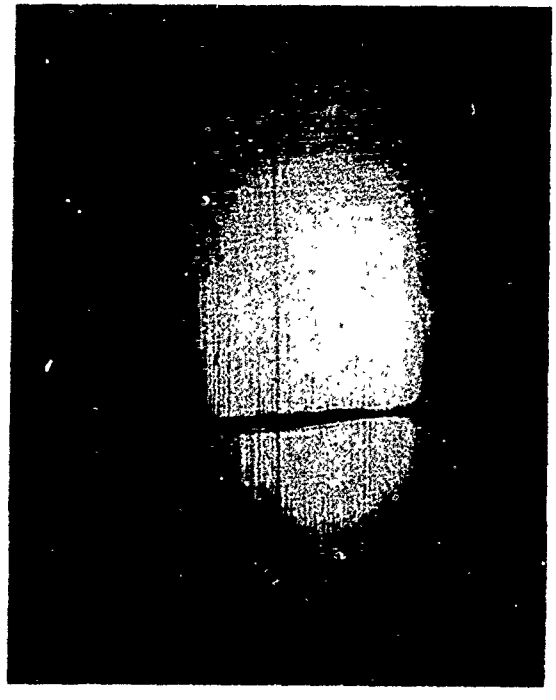

LARGE

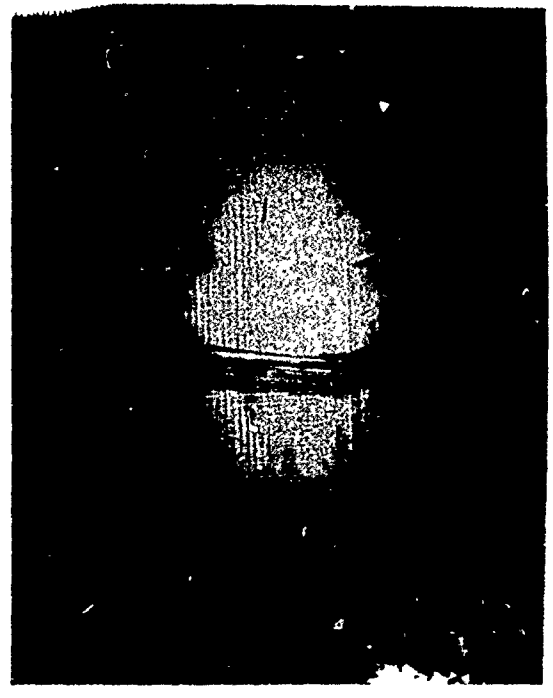

Figure III

TYPICAL DIG-NICK
CLASS 7-3-1 200 X MAG.

SMALL

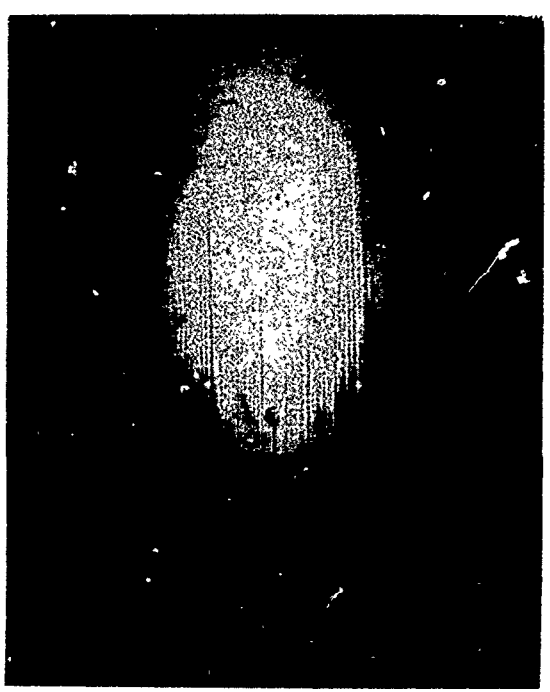

MEDIUM

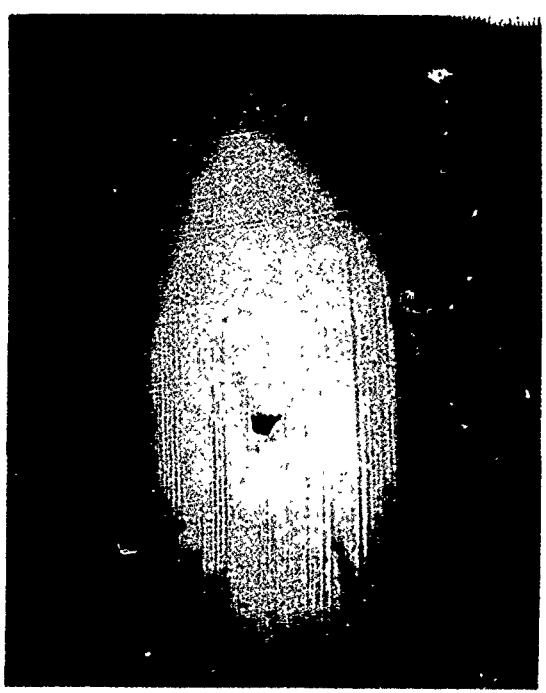

LARGE

Figure IV

TYPICAL DIRT BRINELL
CLASS 7 200 X MAG.

SMALL

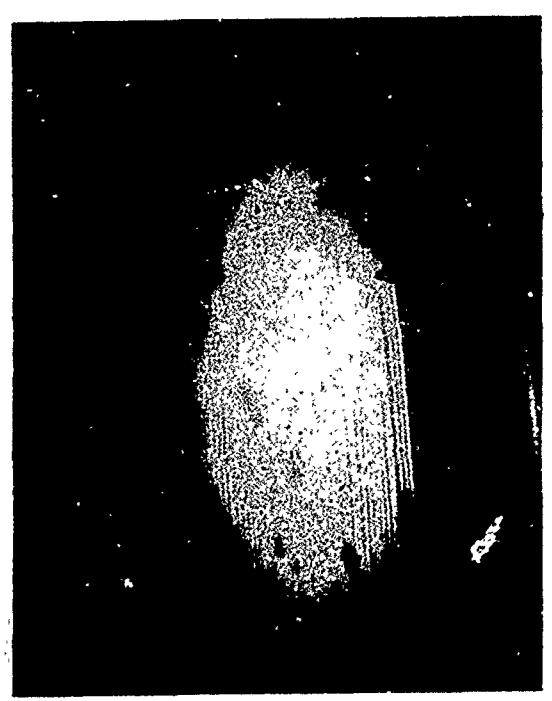

MEDIUM

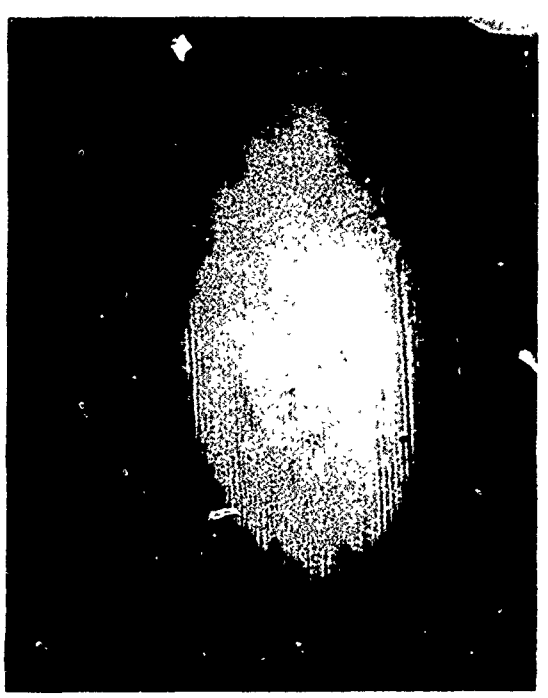

LARGE

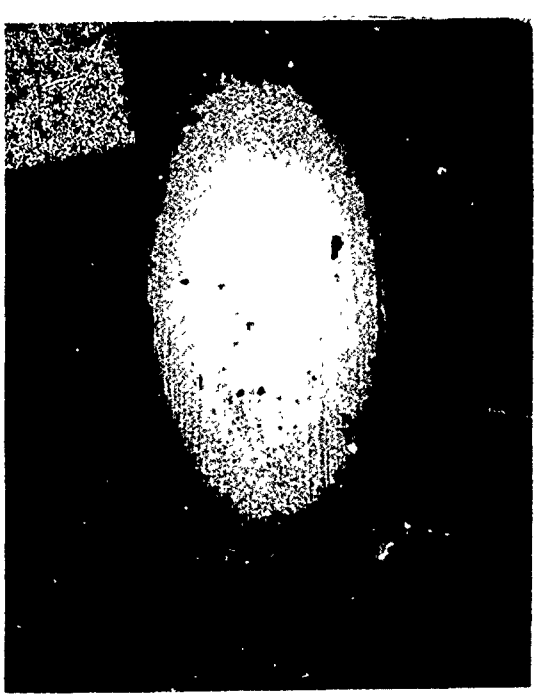

Figure V

TYPICAL ORANGE PEEL
CLASS 7 200 X MAG.

LIGHT

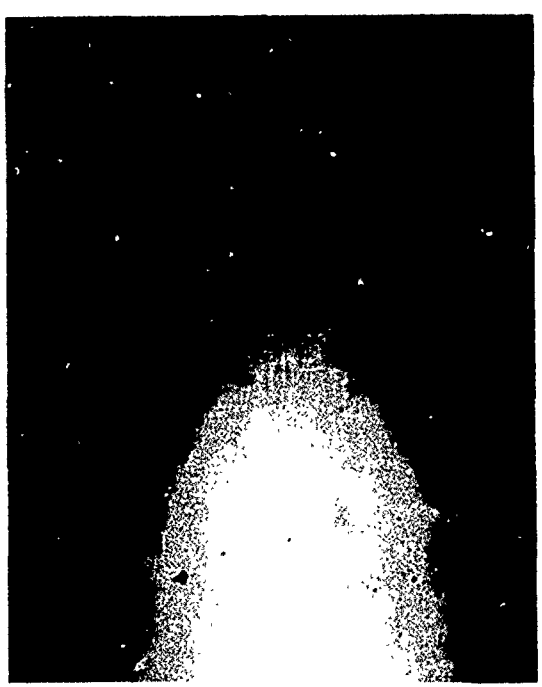

MEDIUM

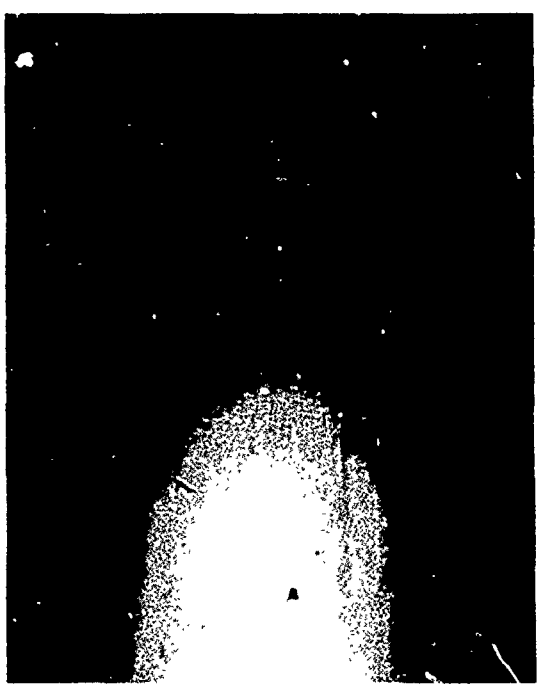

HEAVY

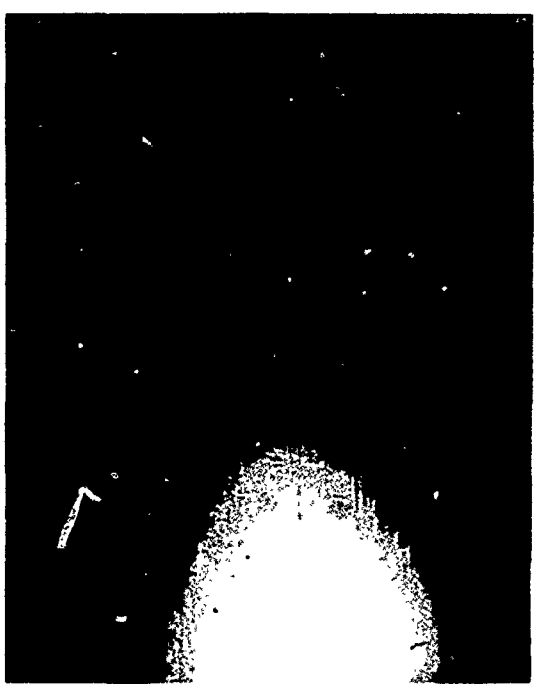

Figure VI

TYPICAL IMPINGEMENTS
CLASS 1 200 X MAG.

SMALL

MEDIUM

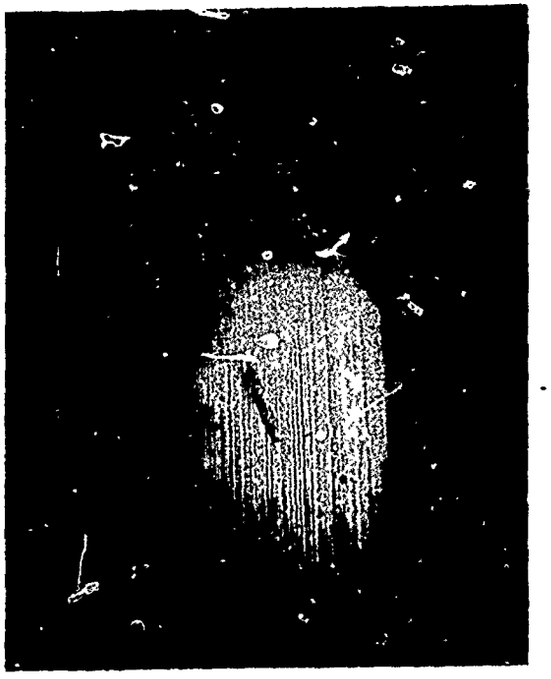

LARGE

Figure VII

TYPICAL COMET-TAILS
CLASS 7-1 100 X MAG.

LIGHT

MEDIUM

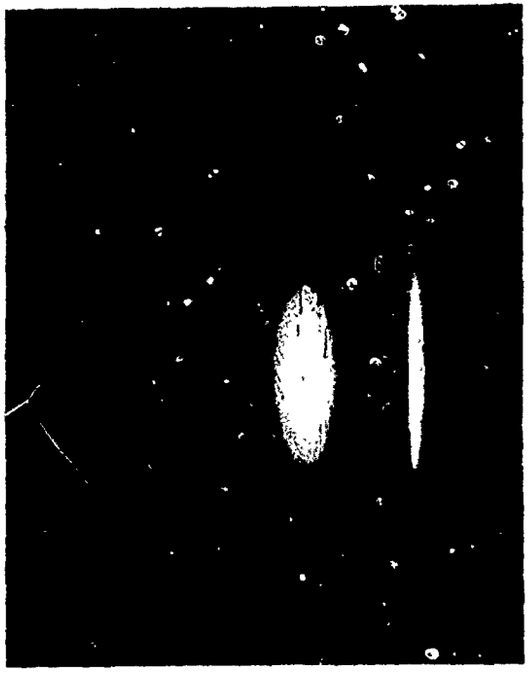

HEAVY

Figure VIII

TYPICAL GRIND-SKIP LINES
CLASS 1 & 7 100 X MAG.

LIGHT

MEDIUM

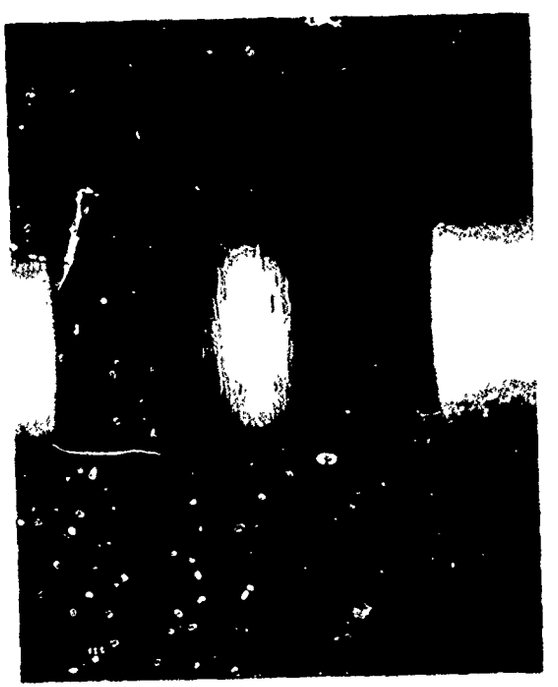

HEAVY

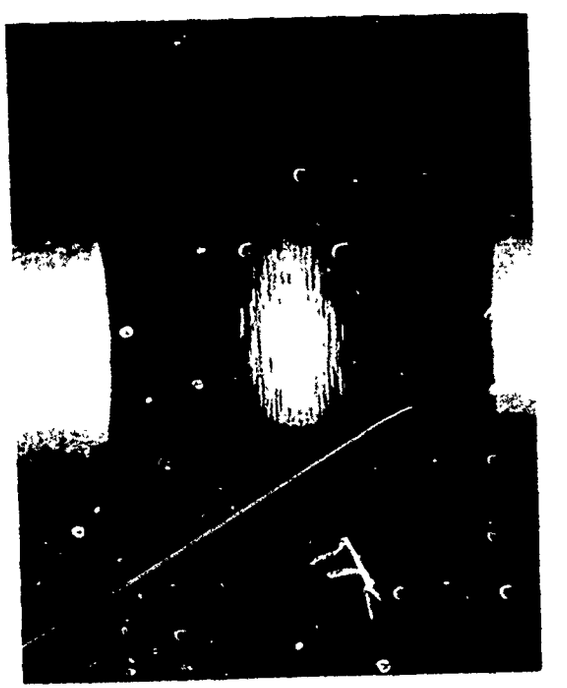

Figure IX

TYPICAL GRIND-SKIP LINES
CLASS 3 100 X MAG.

LIGHT

MEDIUM

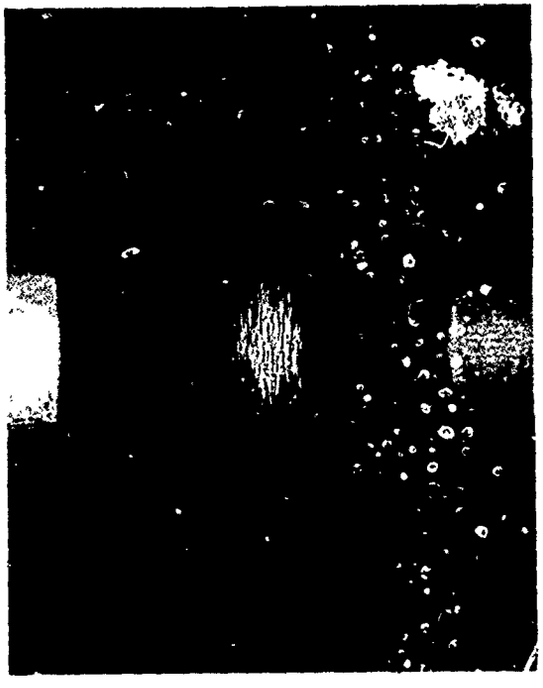

HEAVY

Figure X

TYPICAL PITS
CLASS 1-3-7 200 X MAG.

SMALL

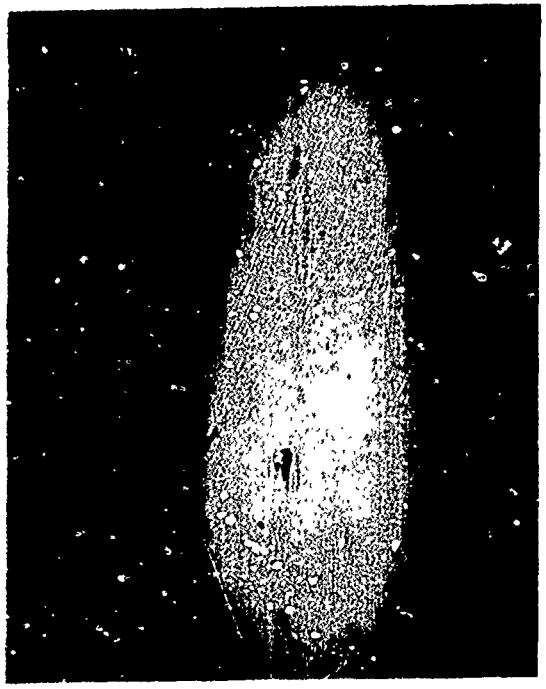

MEDIUM

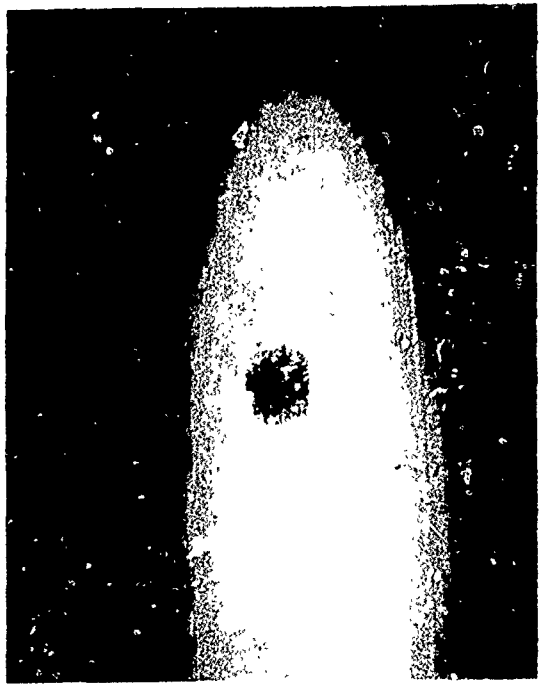

LARGE

Figure XI

TYPICAL LINEY FINISH
CLASS 1 & 7 200 X MAG.

LIGHT

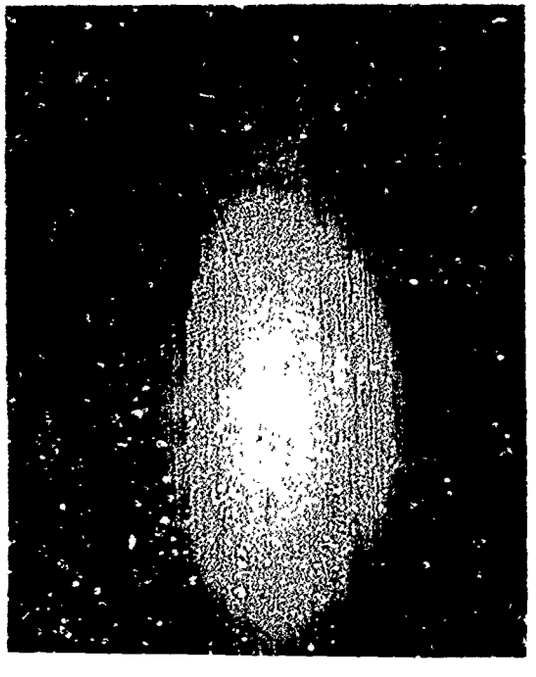

MEDIUM

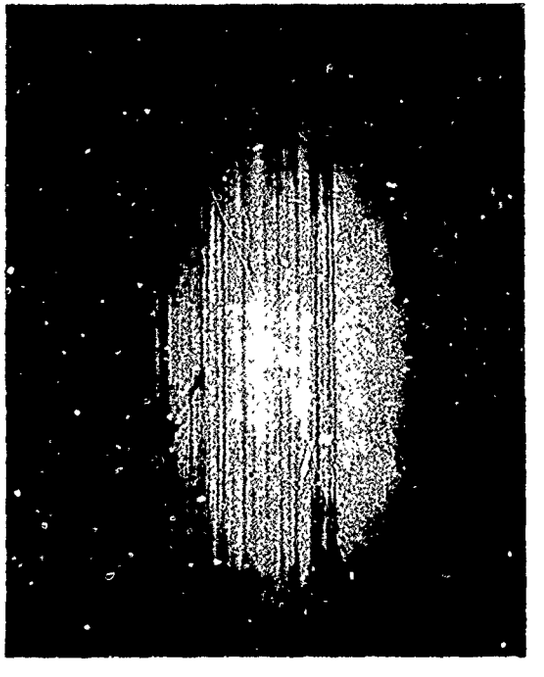

HEAVY

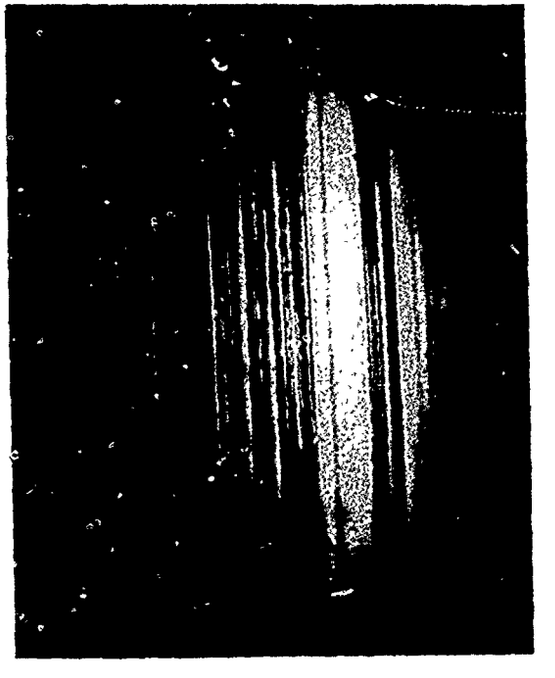

APPENDIX G

DEFECT CHARACTERIZATION - SEM VERSUS OPTICAL

FIGURE 1

TYPICAL SCRATCH

CLASS 3 (MEDIUM)

METALOGRAPH

200X

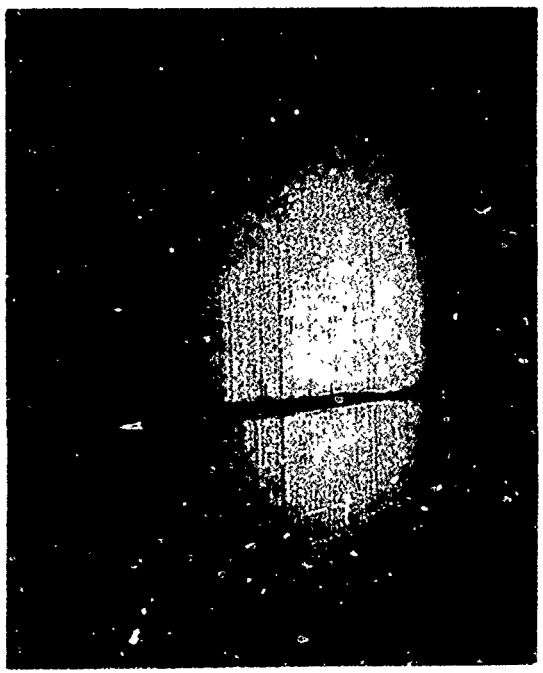

SCANNING ELECTRON MICROGRAPH

720X

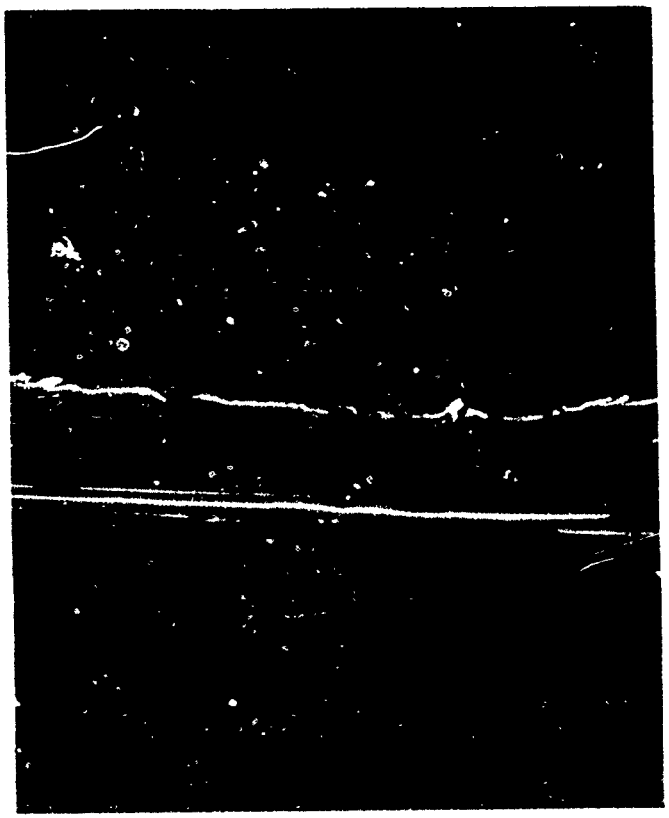

3600X

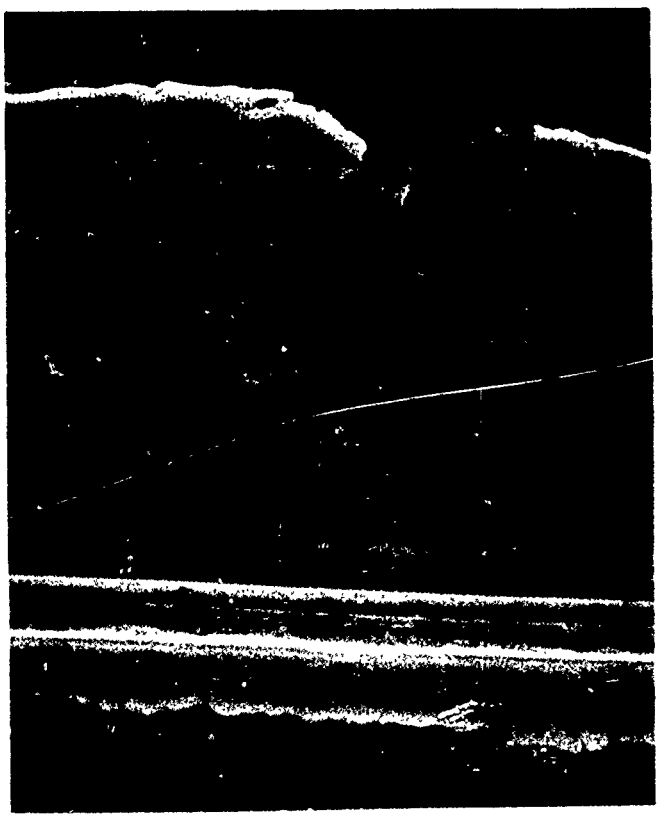

FIGURE 2

TYPICAL IMPINGEMENT

CLASS 1 (MEDIUM)

METALOGRAPH

200X

SCANNING ELECTRON MICROGRAPH

720X

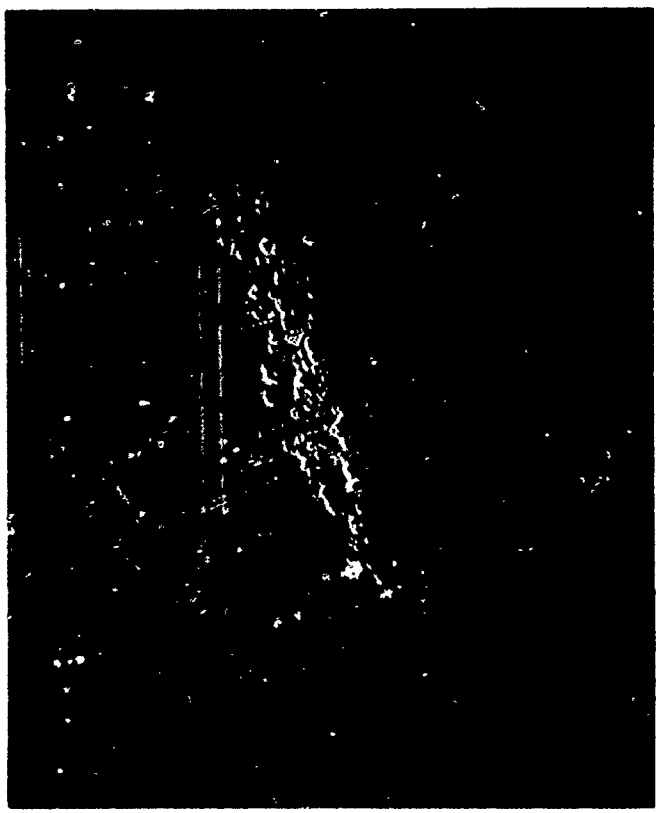

3600X

FIGURE 3

TYPICAL DIG-NICK

CLASS 7 (MEDIUM)

METALOGRAPH

200X

SCANNING ELECTRON MICROGRAPH

720X

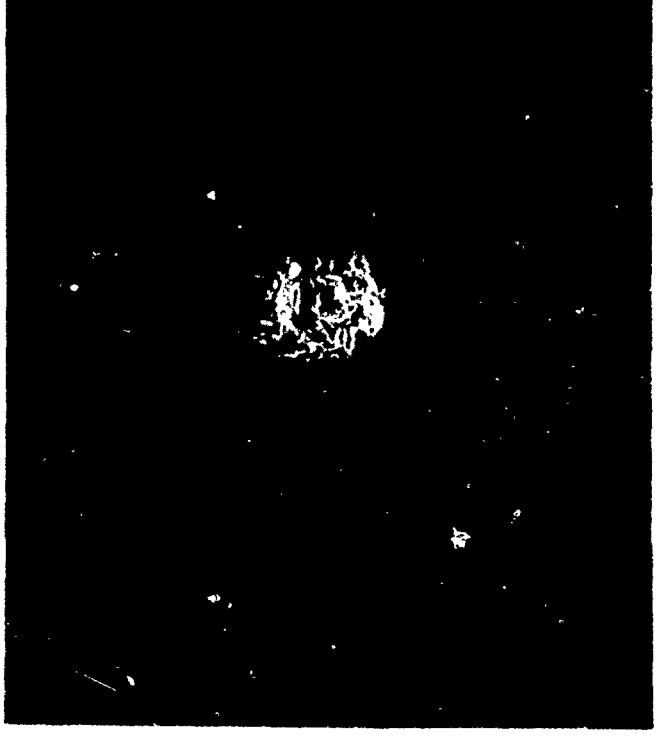

2400X

FIGURE 4

TYPICAL PIT

CLASS 7 (MEDIUM)

METALOGRAPH

200X

SCANNING ELECTRON MICROGRAPH

360X

1000X

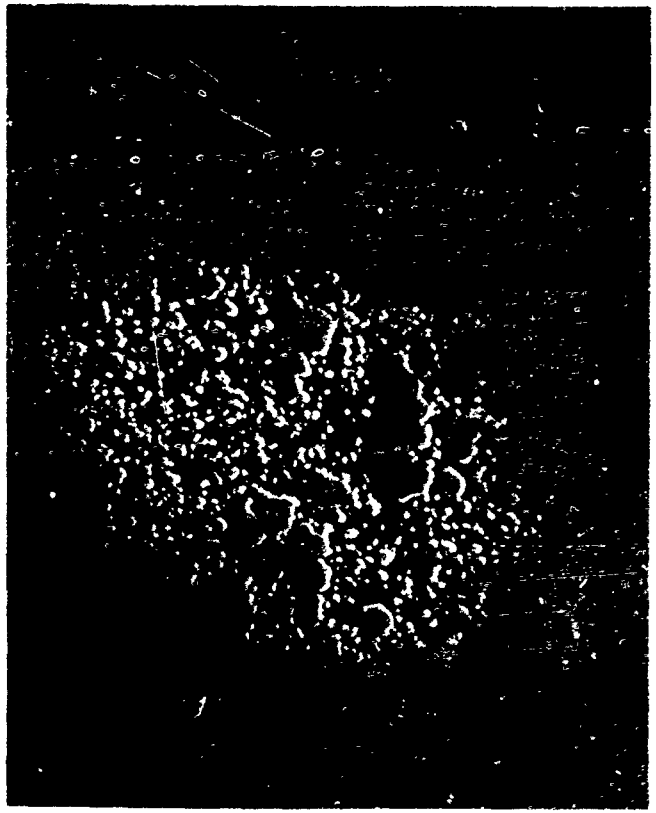

FIGURE 5

TYPICAL GRIND-SKIP LINES

CLASS 3 (LIGHT)

METALOGRAPH

200X

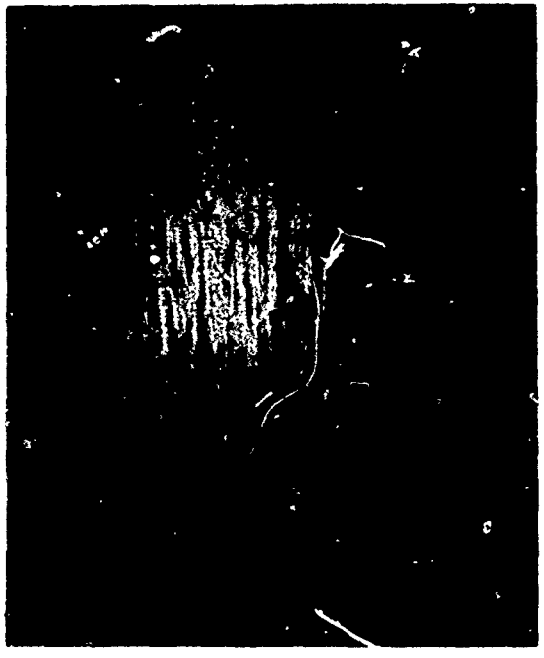

SCANNING ELECTRON MICRGORAPH

360X

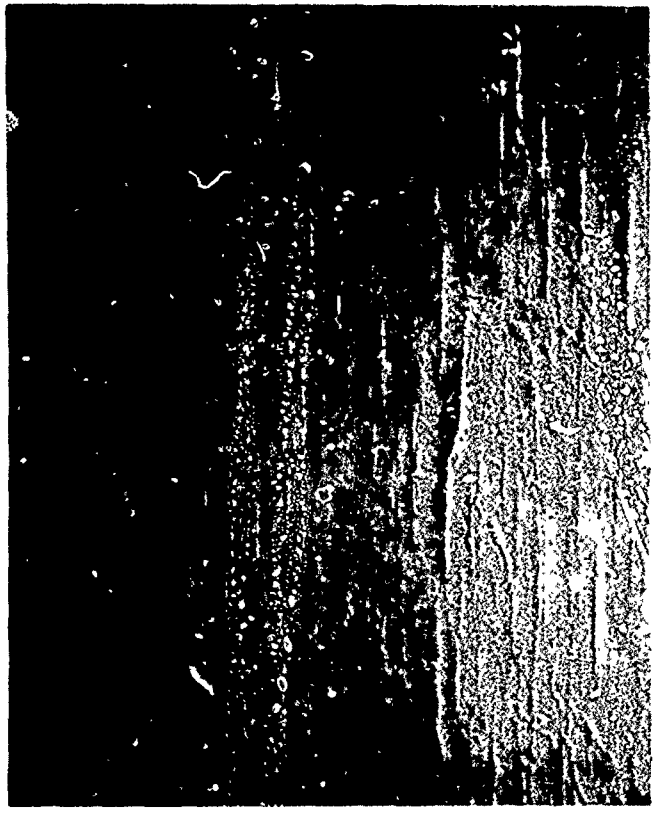

1000X

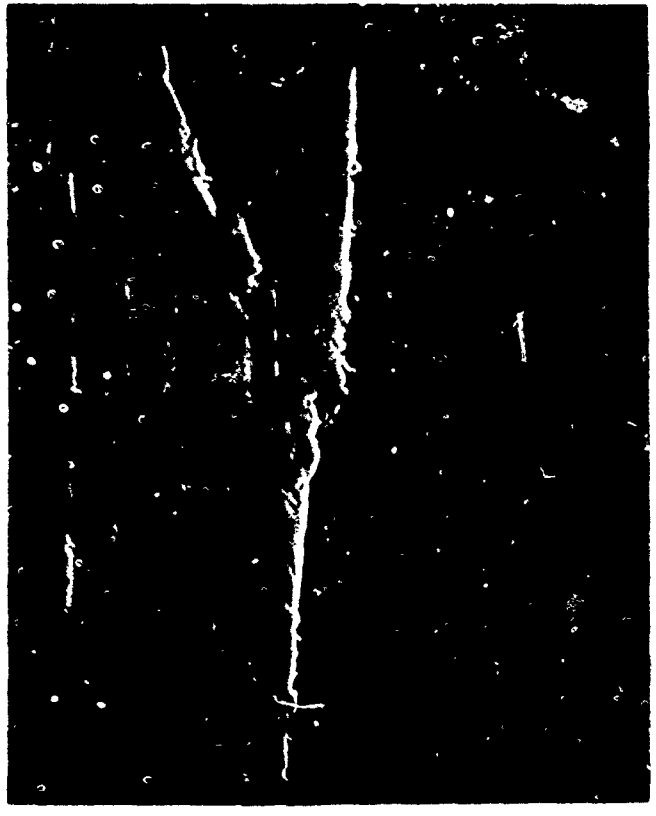

FIGURE 6

TYPICAL GRIND SKIP LINES

CLASS 7 (MEDIUM)

METALOGRAPH

200X

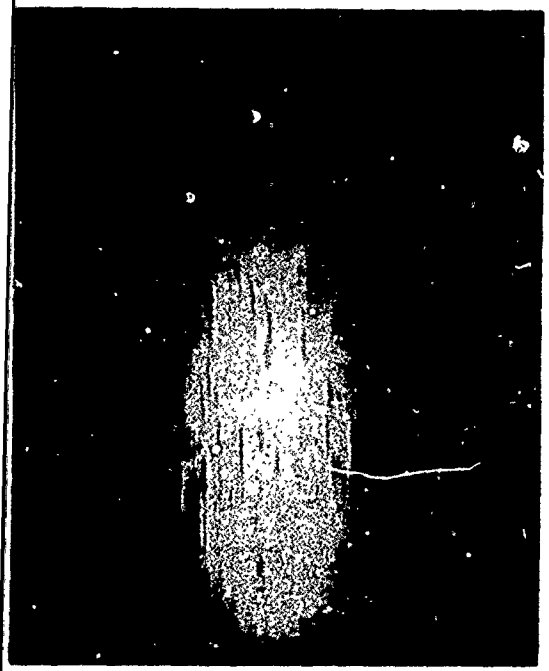

SCANNING ELECTRON MICROGRAPH

360X

1000X

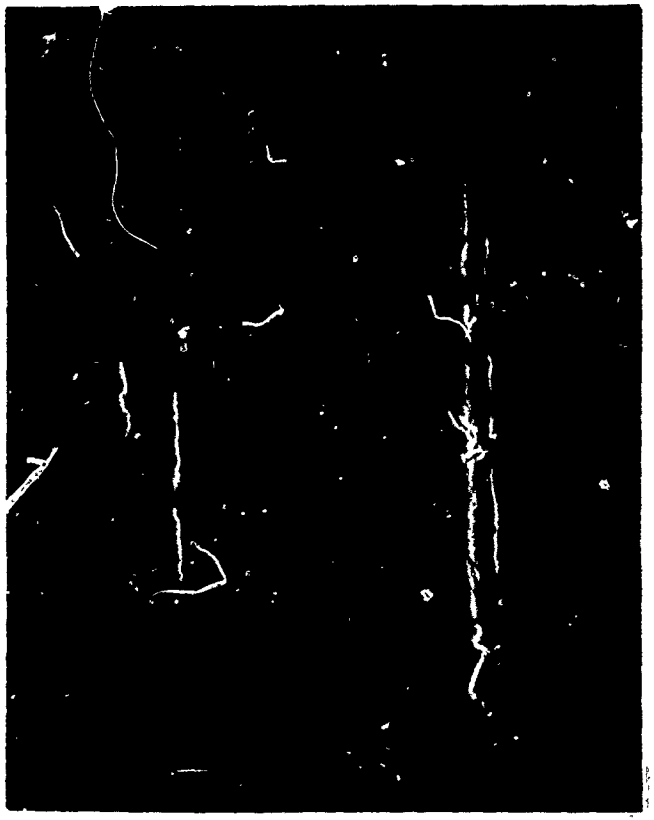

FIGURE 7

TYPICAL LINEY FINISH

CLASS 1 (HEAVY)

METALOGRAPH

200X

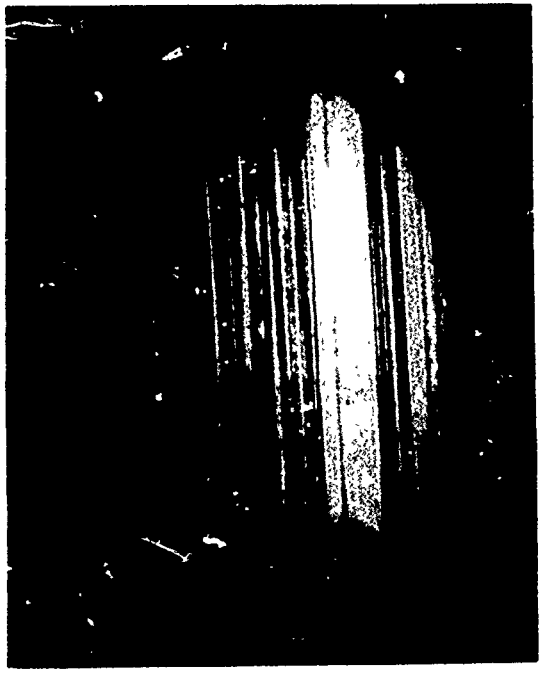

SCANNING ELECTRON MICROGRAPH

360X

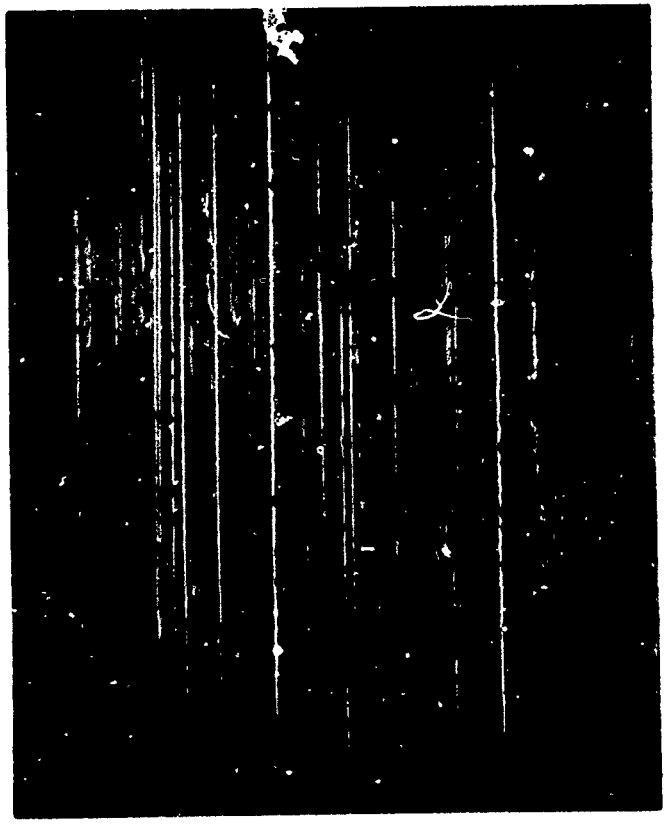

3600X

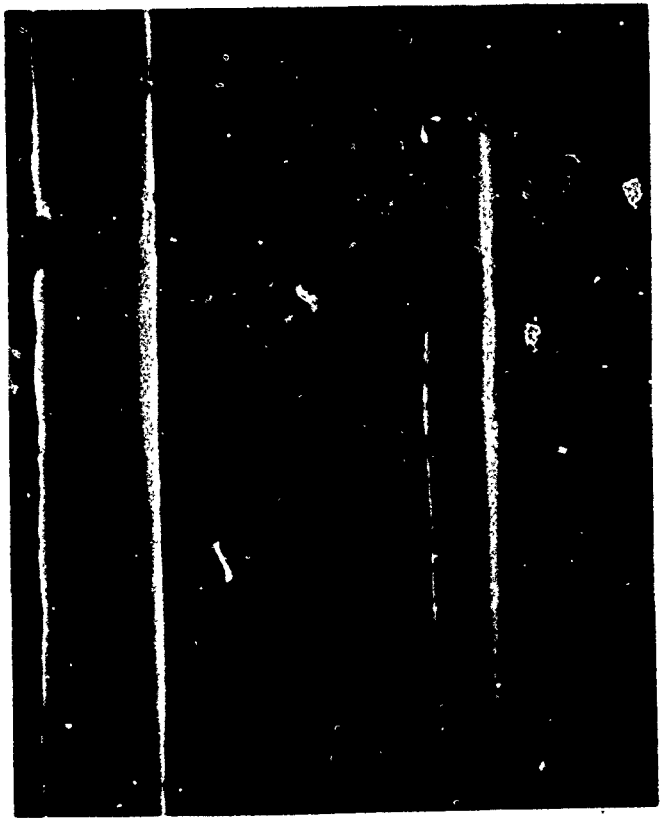

FIGURE 8

TYPICAL COMET TAIL

CLASS 7 (HEAVY)

METALOGRAPH

200X

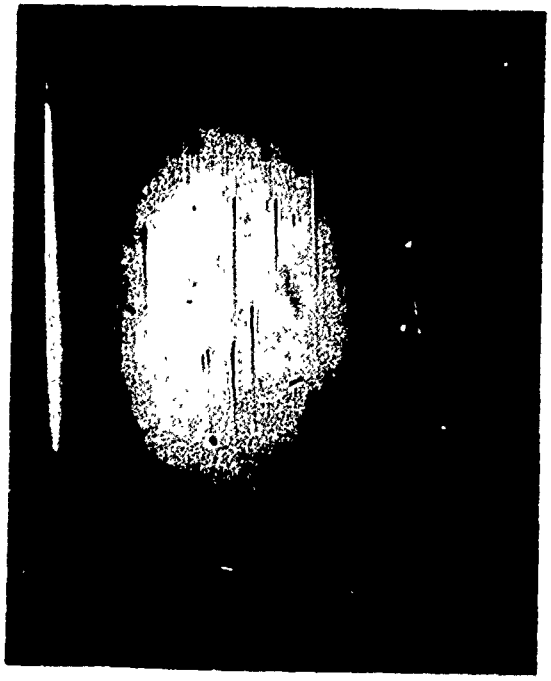

SCANNING ELECTRON MICROGRAPH

720X

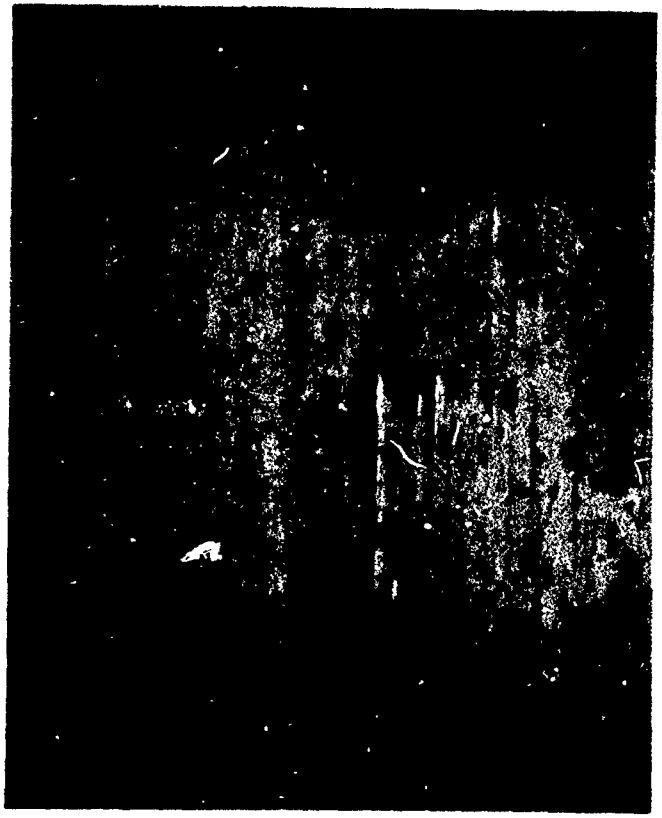

3600X

FIGURE 9

TYPICAL ORANGE PEEL

CLASS 7 (HEAVY)

METALOGRAPH

200X

SCANNING ELECTRON MICROGRAPH

720X

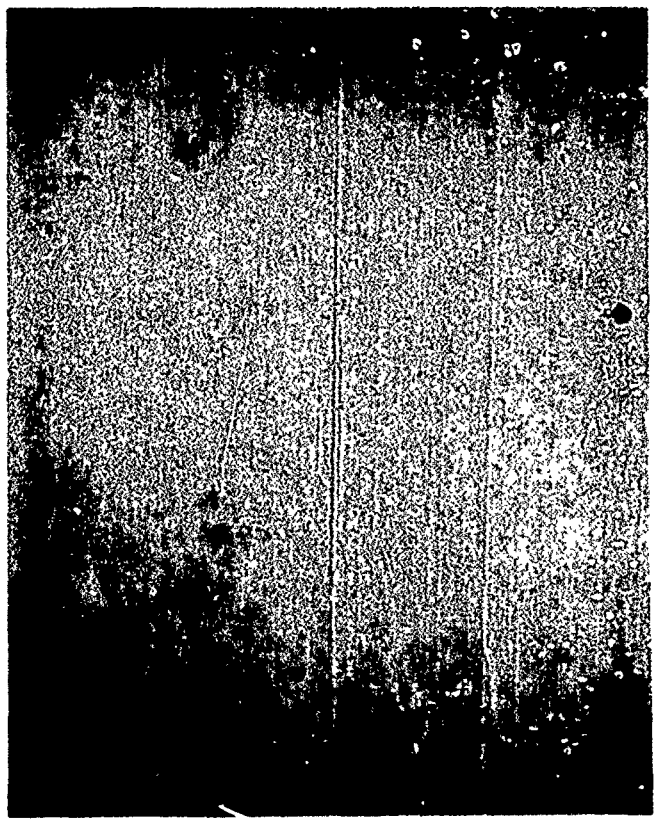

3600X

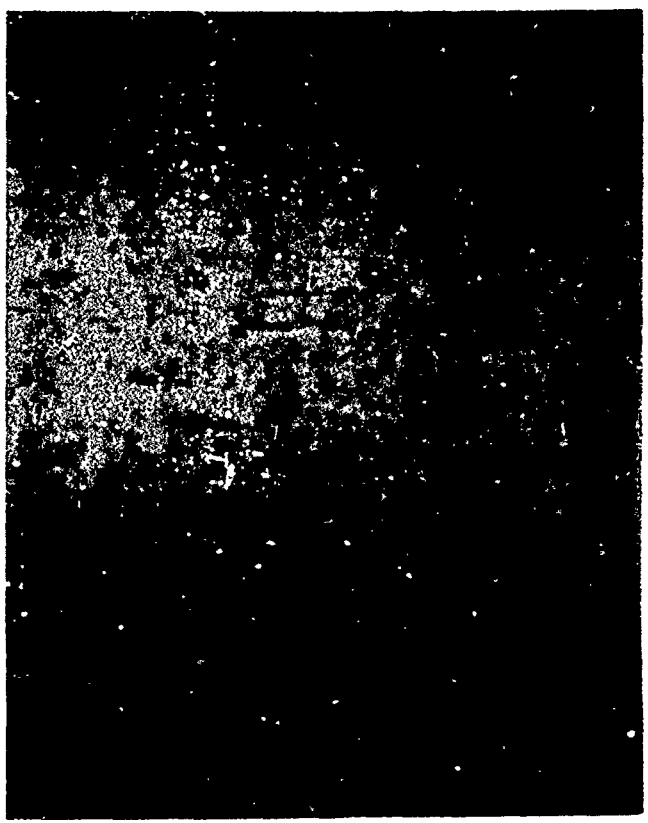

FIGURE 10

TYPICAL DIRT BRINELL

CLASS 7 (LIGHT)

METALOGRAPH

200X

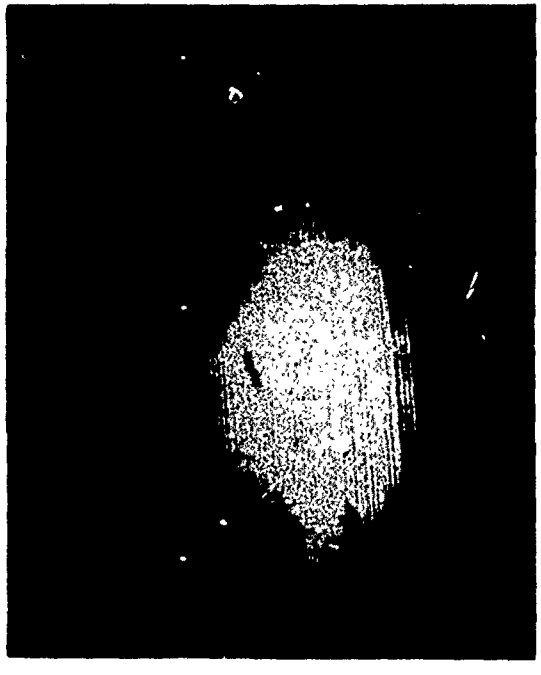

SCANNING ELECTRON MICROGRAPH

720x

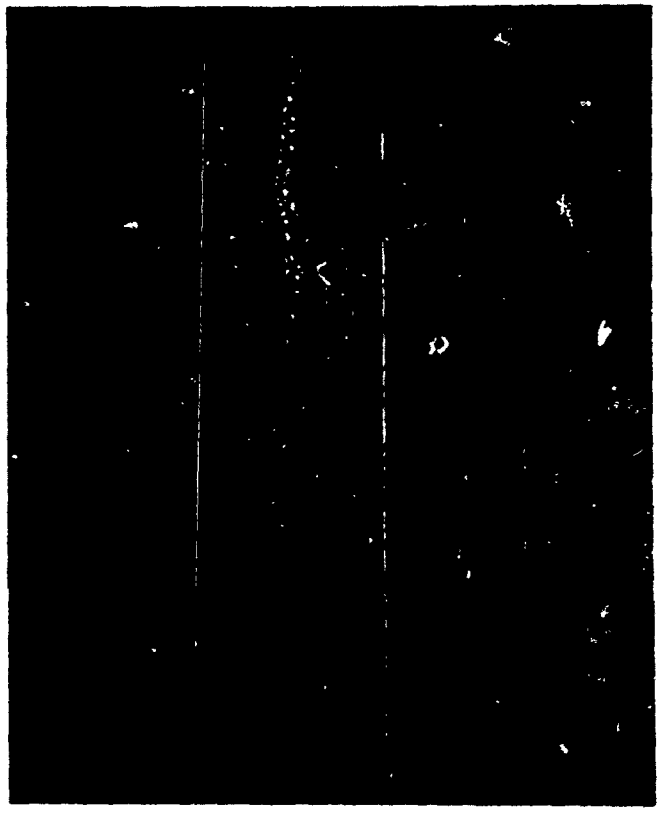

7200X

FIGURE 11

TYPICAL DIRT BRINELL

CLASS 7 (MEDIUM)

METALOGRAPH

200X

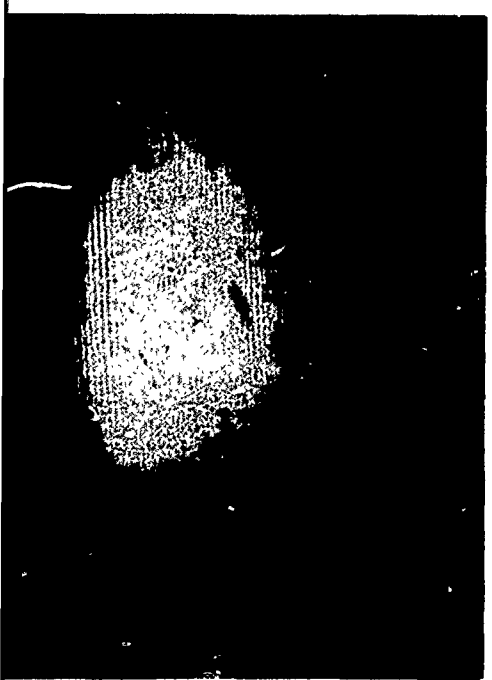

SCANNING ELECTRON MICROGRAPH

720X

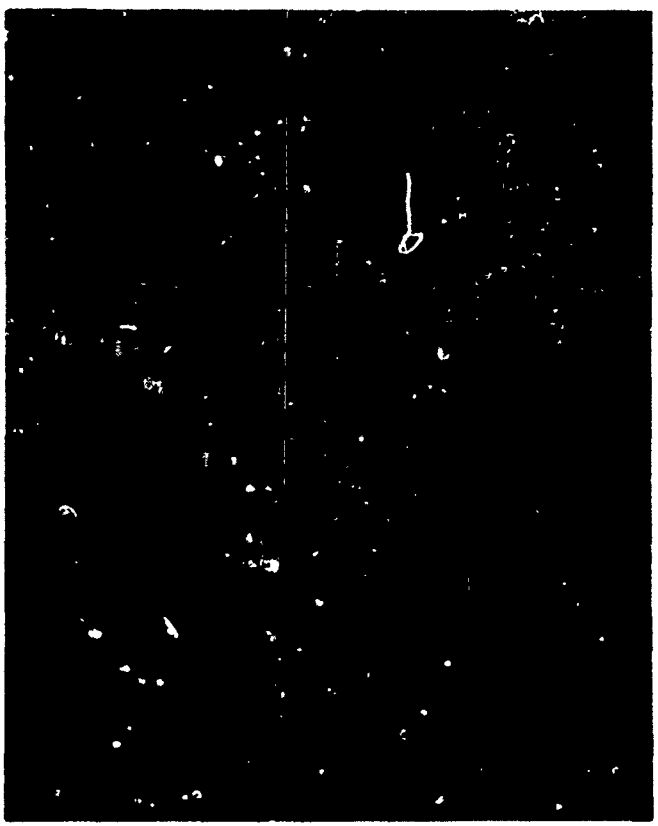

7200X

FIGURE 12

TYPICAL DIRT BRINELL

CLASS 7 (HEAVY)

METALOGRAPH

200X

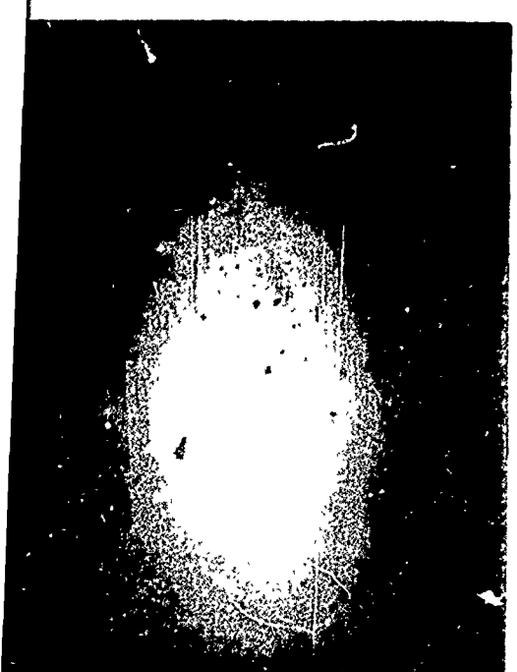

SCANNING ELECTRON MICROGRAPH

720X

3600X

APPENDIX H

PROGRESS REPORT ON INVESTIGATION OF FAILURE DATA

By

Paul A. Pelton and C. L. Grant
Center for Industrial and Institutional Development
Kingsbury Hall
University of New Hampshire
Durham, New Hampshire 03824

I. INTRODUCTION

In the previous report under date of 30 August 1972, a limited number of results on bearing life tests were submitted for analysis of the functional model which would best describe their behavior. It was found that a log-normal model appeared to be an adequate description of the data, but this conclusion was derived from "eyeball" considerations by plotting on log-normal probability paper rather than statistical considerations. In the following report, a more rigorous statistical test of the original plus additional data generated since the August report will be presented. Additionally, other forms of data presentation will be considered; and comparison will be made of the performance of several turbine banks using "good" bearings.

II. GOODNESS OF FIT TESTS

The chi-square goodness of fit test, simply described, consists of dividing a set of data into a series of cells with boundaries chosen depending upon the values for the data. A theoretical distribution of the same mean and standard deviation as the experimental data is then used to calculate the expected percentage or frequency of values which should lie in each of the cells. These theoretical or expected values are compared with the observed values in each cell. Using this information, the chi-square value is calculated according to the equation shown below

$$\chi^2 = \Sigma \left[\frac{(o_i - e_i)^2}{e_i} \right]$$

where o_i = observed frequency in a given cell

e_i = theoretical frequency in the same cell for the distribution under test

The calculated value can then be compared with tabular values at a stated probability level to determine whether or not an experimental distribution can be adequately explained by a given theoretical distribution.

This procedure was applied to the 40 data points studied in the August 1972 report by first testing a normal distribution model using cell intervals of 75 hours. The chi-square value obtained was 79. At the 95% probability level, a chi-square value of 22.4 or larger, permits rejection of the normal distribution model as an adequate fit to the data. This agrees with our earlier visual observations that the normal distribution did not describe this data. A chi-square calculation was conducted on the grouped logs of the times-to-failure; and a value of 16.9 was obtained. Here, at the 95% confidence level, a value of 23.7 or larger is required to reject the hypothesis that the model fits. Otherwise stated, we must accept the hypothesis that a log-normal model adequately describes the data because the calculated chi-square value is less than the tabular value at the stated confidence level.

Table 1 is a summary of the time-to-failure (hours) obtained for seven turbine banks designated A, B, C, D, E, F, and G. This data covers tests through 28 February 1973. For all but Turbine G, 20 good bearings were run to failure. In the case of Turbine G, only 17 bearings had failed at the time of submission of these data.

The complete set of 137 values shown in Table 1 were tested for conformance to a log-normal distribution. The calculated chi-square value for a log-normal distribution was 14.4, as shown in Table 2. In order to reject the hypothesis of a log-normal distribution, this value would have

to have exceeded 23.7. In other words, at the 95% confidence level, we accept the hypothesis that a log-normal distribution adequately describes the complete set of data obtained from the seven turbine banks.

III. ANALYSIS OF VARIANCE ON THE LOG-TRANSFORMED DATA

Analysis of variance assumes homogeneity of within group variances. Since we had found that the log transformation was acceptable for this data, the variance was calculated for the logs of the data from the seven different turbine banks. The variances are shown in Table 3 along with the equation for Bartlett's Test to determine if the variances are homogeneous, that is, if they come from the same population. The calculated value for Bartlett's Test, also shown in Table 3, was 4.74 while the required value for significance at the 95% confidence level is 12.6. Thus, we can accept the hypothesis of homogeneity of variances and analysis of variance of the logs of the data is appropriate.

In Table 4, the results of the analysis of variance of the log-transformed data are presented. The F ratio of 1.04 comparing the variance of the means to the random error variance, is not significant. As a matter of fact, the expected F ratio, if there is no difference in means of the logs of time-to-failure, would be 1.0. Therefore, we conclude that the seven different turbines are producing failure data which is homogeneous or, in other words, not different with respect to the geometric mean time-to-failure.

Table 1

Times-to-Failure For Bearing Test

Turbines (Data of 28 February 1973)

	Turbine Banks						
Number	A	B	C	D	E	F	G
1	132	66	91	90	171	59	111
2	155	67	92	95	174	107	158
3	162	81	121	119	247	129	205
4	178	129	159	122	289	144	240
5	263	180	167	204	313	203	316
6	266	184	288	274	342	217	329
7	268	202	331	307	374	421	330
8	349	238	356	366	410	453	406
9	357	239	409	438	461	484	501
10	400	258	444	509	592	508	546
11	433	279	544	635	613	533	592
12	477	362	544	654	655	560	627
13	491	377	567	685	698	586	706
14	612	529	616	685	934	890	975
15	758	534	909	751	1,002	894	1,207
16	804	558	1,064	1,088	1,364	1,373	1,935
17	961	642	1,108	1,681	1,416	1,395	2,323
18	978	1,141	1,354	1,843	1,521	1,567	
19	1,103	1,163	2,350	2,048	1,756	1,603	
20	1,180	1,771	2,555	2,557	2,452	1,986	
Total	10,327	9,000	14,069	15,151	15,784	14,112	11,507
Mean time-to-Failure	516	450	703	758	789	706	677
Grand Mean Time-to-Failure	657						

Table 2

Chi-Square Goodness of Fit Calculations of Log Times-to-Failure for Bearing Test Turbines
(Data of 28 February 1973)

Cell Boundaries Logs of Times-to-Failure, log y	$\left(\frac{\log y - \overline{\log y}}{S_{\log y}}\right)$*	Cumulative Normal Probability	Theoretical Relative Frequency	Theoretical Frequency, e_i	Observed Frequency, o_i	$\frac{(o_i - e_i)^2}{e_i}$
$-\infty$	$-\infty$	0				
			0.0105	1.4385		
1.7500	-2.3075	0.0105		}2.7537	3	0.5641
			0.0096	1.3152		
1.8500	-2.0519	0.0201				
			0.0160	2.1920	1	0.6482
1.9500	-1.7965	0.0361				
			0.0256	3.5072	6	1.7718
2.0500	-1.5411	0.0617				
			0.0375	5.1375	6	0.1448
2.1500	-1.2857	0.0992				
			0.0523	7.1651	8	0.0973
2.2500	-1.0303	0.1515				
			0.0677	9.2749	8	0.1752
2.3500	-0.7749	0.2192				
			0.0823	11.2751	10	0.1442
2.4500	-0.5195	0.3015				
			0.0944	12.9328	10	0.6651
2.5500	-0.2641	0.3959				
			0.1006	13.7822	14	0.0034
2.6500	-0.0087	0.4965				
			0.1010	13.8370	16	0.3381
2.7500	0.2467	0.5975				
			0.0947	12.9739	16	0.7058
2.8500	0.5021	0.6922				
			0.0836	11.4532	4	4.8502

Table 2 (Cont.)

Cell Boundaries Logs of Times-to-Failure, log y	$\left(\frac{\log y - \overline{\log y}}{S_{\log y}}\right)$*	Cumulative Normal Probability	Theoretical Relative Frequency	Theoretical Frequency, e_i	Observed Frequency, o_i	$\frac{(o_i - e_i)^2}{e_i}$
2.9500	0.7575	0.7758				
			0.0913	12.5081	11	0.1818
3.0500	1.0129	0.8671				
			0.0305	4.1785	8	3.4950
3.1500	1.2683	0.8976				
			0.0386	5.2882	7	0.5541
3.2500	1.5237	0.9362				
			0.0262	3.5894	4	0.0470
3.3500	1.7791	0.9624				
			0.0167	2.2879		
3.4500	2.0347	0.9791		}5.1512	5	0.0044
			0.0209	2.8633		
$+\infty$	$+\infty$	1				
			1.000	137.00	137	14.3504

*$\overline{\log y}$ is the arithmetic mean log

$S_{\log y}$ is the standard deviation of log values

Tabular chi-square value at 95% probability level, with 14 degrees of freedom = 23.7.

Table 3

Bartlett's Test of Variances of Log Times-to-Failure
For Bearing Test Turbines (Data of 28 February 1973)

TURBINE	A	B	C	D	E	F	G
Variance of Log Time-to-Failure	0.0896	0.1611	0.1832	0.2001	0.1142	0.1903	0.1312

BARTLETT'S EQUATION $\chi^2 = 2.306\{(\log s_p^2)\Sigma(k_i-1) - \Sigma[(k_i-1)\log s_i^2]\}$

where k_i = number of data points in each sample

s_i^2 = variance of each sample

s_p^2 = pooled variance

It is necessary to correct χ^2 by dividing by c

where $c = 1 + \frac{1}{3(n-1)}\left[\Sigma\frac{1}{k_i-1} - \frac{1}{\Sigma(k_i-1)}\right]$

and n = number of variances compared.

Results for data above $\chi^2/c = 4.74$

Tabular value at 95% probability level and 6 degrees of freedom = 12.6

Table 4

Analysis of Variances of Log Times-to-Failure for Bearing Test Turbine
(Data of 28 February 1973)

Run Number	A	B	C	D	E	F	G
1	2.1206	1.8195	1.9590	1.9542	2.2330	1.7709	2.0453
2	2.1903	1.8261	1.9638	1.9777	2.2405	2.0294	2.1987
3	2.2095	1.9085	2.0828	2.0755	2.3927	2.1106	2.3118
4	2.2504	2.1106	2.2014	2.0864	2.4609	2.1584	2.3802
5	2.4200	2.2553	2.2227	2.3096	2.4955	2.3075	2.4997
6	2.4249	2.2648	2.4594	2.4378	2.5340	2.3365	2.5172
7	2.4281	2.3054	2.5198	2.4871	2.5729	2.6243	2.5185
8	2.5428	2.3766	2.5514	2.5635	2.6128	2.6561	2.6085
9	2.5527	2.3784	2.6117	2.6415	2.6637	2.6848	2.6998
10	2.6021	2.4116	2.6474	2.7067	2.7723	2.7059	2.7372
11	2.6365	2.4456	2.7356	2.8028	2.7875	2.7267	2.7723
12	2.6785	2.5587	2.7356	2.8156	2.8162	2.7482	2.7973
13	2.6911	2.5763	2.7536	2.8357	2.8439	2.7679	2.8488
14	2.7868	2.7235	2.7896	2.8357	2.9703	2.9494	2.9890
15	2.8797	2.7275	2.9586	2.8756	3.0009	2.9513	3.0817
16	2.9053	2.7466	3.0269	3.0366	3.1348	3.1377	3.2867
17	2.9827	2.8075	3.0445	3.2256	3.1511	3.1446	3.3660
18	2.9903	3.0573	3.1316	3.2655	3.1821	3.1951	
19	3.0426	3.0656	3.3711	3.3113	3.2445	3.2049	
20	3.0719	3.2482	3.4074	3.4077	3.3895	3.2980	
Total	52.4063	49.6138	53.1739	53.6521	55.4991	53.5082	45.6587
Mean	2.6203	2.4807	2.6587	2.6826	2.7750	2.6754	2.6858
Variance	0.0896	0.1611	0.1832	0.2001	0.1142	0.1903	0.1312

Analysis of Variance Table

	Sum of Squares	Degrees of Freedom	Mean Square	F Ratio	Tabular F Ratio α(0.01) df(6.130)
Total	985.4241	137			
Correction Factor	964.5332	1			
Turbine Banks	.9591	6	0.1599	1.04 (N.S.)	2.76
Residual	19.9318	130	0.1533		

N.S. = Not significant

FIGURE I

COMPARISON OF EXPERIMENTAL SURVIVAL CURVE WITH THEORETICAL SURVIVAL CURVE FOR COMPOSITE OF ALL DATA OF 28 FEBRUARY 1973

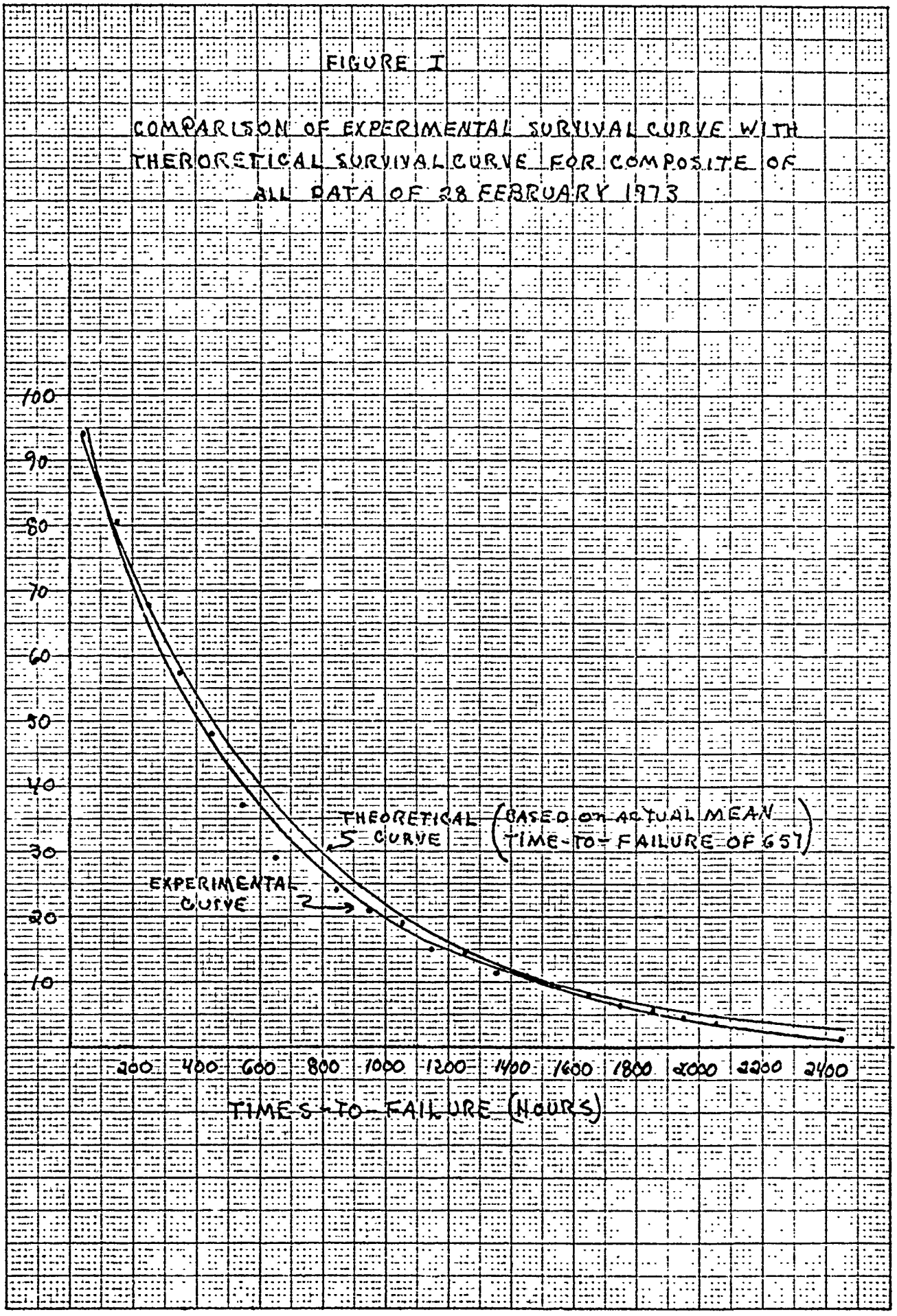

APPENDIX I

FINAL REPORT ON METHODS OF ANALYZING FAILURE DATA FOR MPB BEARING DEFECT STUDY

By

Paul A. Pelton and C. L. Grant
Center for Industrial and Institutional Development
Kingsbury Hall
University of New Hampshire
Durham, New Hampshire 03824

INTRODUCTION

The purpose of our involvement in the MPB study of the effect of bearing defects on bearing life has been to investigate methods of statistically determining (1) differences between test turbine banks using baseline (nondefect) bearings and (2) significance of the various defects compared to baseline bearings. The first step in this investigation was to determine which statistical distribution best described the failure data.

In the report of 30 March 1973 (previous report), we stated that a log-normal distribution adequately described the failure data for baseline bearings from the first seven turbine banks available for testing. At this point, MPB was involved in a program of building and qualifying 14 banks of 10 test turbines each; and the only data available were for baseline bearings. However, we felt that methods that could be used to test differences between turbine banks could also be used to test differences between types and levels of bearing defects. An analysis of variance was performed on the log-transformed data (see previous report), and we found no difference between the means indicating no difference between the turbine banks. However, we were not completely satisfied that analysis of variance was the best method to employ because (1) the means tested by the analysis are geometric not arithmetic and (2) a plot of the survival curve for each turbine bank

indicated a probable difference in the slope among some of the curves. This suggested the possibility that the arithmetic means could be statistically different even though the geometric means were not. Therefore, we continued to search for more sensitive statistical test procedures. The following report describes our continued effort and presents statistical procedures we feel are sufficient for the design and analysis of the bearing failure study.

LOG-NORMAL

Two additional tests were performed on the log-transformed data of the previous report. First, Duncan's multiple range analysis was applied to the mean log times to failure even though our previous analysis of variance had indicated no difference between them at the 95% confidence level. The multiple range test showed there was a difference between the geometric means for Turbine Banks B and E at the 95% confidence level. Next, a multiple comparison of the slopes of the failure curve for each turbine bank was made following the procedure outlined in Volk (1). Slopes of failure curves were compared rather than slopes of the survival curves because the x axis of the failure curves is in log time to failure and is, therefore, more easily compared to the analysis of variance data. The calculated

"between slopes" F ratio is 13.4 with 6 and 123 degrees of freedom. The corresponding tabular F ratio at the 99% confidence level is 2.95. Clearly, some, if not all, of the slopes differ from one another as we had previously suspected.

Both of these additional tests strengthened our belief in the inadequacy of simply applying a log transformation to future data and doing an analysis of variance to test for differences between sets of failure data.

TWO PARAMETER WEIBULL

Mean Life Ratio Analysis

After consulting numerous texts and journals, we found a method in Lipson and Sheth (2) for statistically comparing the mean lives of two sets of failure data. The ratio of the two mean lives is calculated and its significance determined at a given confidence level by comparing it with the statistically required "tabular" mean life ratio (MLR).

The graph from which the tabular MLR is determined is in terms of degrees of freedom and slope. However, the slope is for the Weibull least squares fit rather than log-normal. Therefore, we further investigated the Weibull distribution. Recall in the report of 30 August 1972, we had fit some of the first failure data available to both Weibull and log-normal probability paper and concluded that the fit was better with log-normal. The equation for the Weibull cumulative distribution

function is

$$F(x) = 1 - \exp\left[-\left(\frac{x - x_0}{\theta - x_0}\right)^b\right] \quad \text{----------(1)}$$

where x_0 is the expected minimum value of x

b is the Weibull slope

θ is the characteristic value (for our purposes, the characteristic life)

Generally, in life phenomena, it is reasonable to assume that the lower bound of life x_0 is equal to zero. This reduces Equation 1 to

$$F(x) = 1 - \exp\left[-\left(\frac{x}{\theta}\right)^b\right] \quad \text{----------(2)}$$

This equation is called the two parameter Weibull cumulative distribution function and can be natural log transformed to

$$\ln \ln \frac{1}{1 - F(x)} = b(\ln x) - (b \ln \theta) \quad \text{----------(3)}$$

which is the equation of a straight line of the form

$$Y = b_1 X + b_0 \quad \text{----------(4)}$$

where $Y = \ln \ln \frac{1}{1 - F(x)}$

$X = \ln x$

$b_1 = b$

$b_0 = -b \ln \theta$

The seven turbine bank data sets were linearly transformed using equation 3. The line parameters, correlation coefficients, and mean lives are listed in Table 1.

TABLE 1

Summary of Two Parameter Weibull Fit of Data
for Turbine Banks A-G

Turbine Bank	Weibull Slope, b	Characteristic Life, θ	Correlation Coefficient, r	Mean Life	No. Data Pts, n
A	1.65	581	0.969	516	20
B	1.22	472	0.965	450	20
C	1.15	731	0.970	703	20
D	1.10	789	0.970	758	20
E	1.45	867	0.964	789	20
F	1.15	761	0.984	706	20
G	1.35	725	0.968	677	17

The correlation coefficients are not as good for the two parameter Weibull fit as for the log-normal; but, even for Turbine Bank E (which has the lowest correlation coefficient), 93% of the variation within the data is explained by the Weibull line. This degree of fit was considered adequate to justify using the Weibull model for further testing.

A mean life ratio analysis was done for Turbine Banks B and E (the two showing the greatest mean life difference) with the following results.

$$MLR = \frac{789}{450} = 1.75$$

Tabular MLR at 95% probability level and 361 degrees of freedom is 1.47. (From Table A-21, Lipson & Sheth, the degrees of freedom are $(n_1-1)(n_2-1)$ where n_1 and n_2 are the number of data points in data sets 1 and 2.) Since the calculated MLR is greater than the tabular MLR, we can conclude that the mean lives differ for these data sets. It would be unfair to compare this result with the result of the analysis of variance for the entire set of turbine banks since the latter was a multiple comparison and this is a single comparison. We do not have a method for doing a multiple mean life ratio analysis, but we do not really need one since we are principally interested in comparing defect to baseline bearings and not defect to defect bearings. The results of the MLR analysis on Turbine Banks B and E encouraged us to apply this method to

other MPB data which will be discussed later in this section.

Simultaneously, we were also studying sequential analysis as applied to data described by the Weibull distribution. Basically, sequential analysis is a technique whereby bearings would be tested in sequence; and, after each failure, two tests of significance are applied. If neither test is satisfied, then testing continues.

In a meeting in mid November, the state of our progress was discussed with Jack Beecher, Keith Gordon, and Ed Jarvis of MPB. It was agreed that MPB would supply us with additional bearing failure test data to which we would apply MLR and sequential analyses. Tables 2 and 3 contain the data that we actually tested. Other data sets received were not tested because several bearings within each set had not failed.

Log-normal, exponential, and two parameter Weibull curve fits were applied to each set of data. The linear transformation for each of these curves is

Log-normal	$y = b_1 \ln x + b_0$
Exponential	$\ln \frac{1}{1-y} = b_1 X + b_0$
Two Parameter Weibull	$\ln \ln \frac{1}{1-y} = b_1 \ln x + b_0$

For these equations, the y values (probability of failure) were estimated using median ranking. A summary of this curve fitting is given in Table 4. Included are the correlation

TABLE 2

MPB Baseline and Defect Bearing Times to Failure
in Order Bearings Were Placed on Test

Bearing Class	Class 7									
Defect	Baseline		Small Scratch		Medium Scratch		Large Scratch		Small Dig-Nick	
	Hrs. to Failure		Hrs. to Failure		Hrs. to Failure		Hrs. to Failure		Hrs. to Failure	
Test Order Nos.	(1-20)	(21-40)	(1-20)	(21-40)	(1-22)	(23-43)	(1-23)	(24-46)	(1-20)	(21-27)
	379	560	2551	526	167	924	2260	557	718	1023
	717	553	1832	904	1060	1325	3202	1863	360	688
	367	1172	2025	799	852	3611	434	106	301	2648
	871	234	613	1206	1724	747	323	246	386	1100
	1428	4321	995	5010	2095	5499	2025	2829	3576	1293
	2143	4853*	454	535	1112	338	3836	1601	144	1758
	815	341	1251	939	406	2374	1100	1776	1993	1278
	3072	648	1064	860	938	3497	106	3074	120	
	259	428	1941	1657	1900	2067	295	1062	1171	
	1045	1647	1164	724	719	134	505	2123	1878	
	486	356	875	1233	635	823	2797	261	367	
	1706	1053	1761	852	1375	2289	1133	133	577	
	3991	3603*	1634	947	726	1219	915	496	2307	
	950	186	726	368	860	120	3853	222	1189	
	334	2774	690	801	561	3221	2256	3467	274	
	2088	293	396	908	1032	1051	383	1667	433	
	4103	555	557	250	1029	252	2438	652	2738	
	1619	1261	243	852	335	229	1910	222	4316*	
	2338	153	5657	427	1909	996	3695	436	280	
	188	1412	474	[illegible]	2667	1858	730	253	1808	
					495	915	925	1692		
					1822		1774	1525		
							2388	633		
Mean Life, Hrs.	1385		1183		1346		1439		1286	

*Bearings not failed.

TABLE 3

MPB Defect Bearing Times to Failure in Order Bearings Were Placed on Test

Bearing Class	Class 7		Class 3					
Defect	Large Dig-Nick		Small Scratch		Medium Scratch		Large Scratch	
	Hrs. to Failure		Hrs. to Failure		Hrs. to Failure		Hrs. to Failure	
Test Order Nos.	(1-23)	(24-46)	(1-25)	(26-49)	(1-25)	(26-49)	(1-24)	(25-48)
	360	834	128	334	969	1029	648	371
	598	503	638	951	825	477	602	251
	280	821	1664	495	883	985	2143	256
	1379	802	1154	3030	358	950	1975	188
	1097	518	2137	1012	260	282	569	1004
	676	1762	682	1506	942	466	841	221
	1098	422	1484	167	370	1218	801	196
	124	1395	1063	1033	1059	1595	140	131
	210	869	908	219	902	311	764	2338
	110	263	1502	1150	264	2220	1000	1225
	399	1175	634	1325	262	2833	693	4173
	383	288	671	135	1886	642	466	1663
	377	1722	523	844	661	1029	666	812
	161	2182	1037	1451	1465	3360	501	429
	263	1514	400	1265	612	2541	375	1876
	822	3292*	406	108	118	745	1521	225
	501	803	1294	590	949	3543	1043	151
	552	452	2215	167	682	2211	362	133
	2111	220	142	251	1155	1220	1118	2272*
	931	318	373	648	565	156	237	753
	597	595	2906	1933	264	3339	411	767
	137	149	532	2085	675	901	2498	110
	1710	372	1026	316	559	1099	1251	631
			293	2334	322	1219	541	731
			344		317			
Mean Life, Hrs.	786		969		1055		876	

*Bearings not failed.

TABLE 4

Summary of Curve Fitting Analysis for MPB Baseline and Defect Bearings**

Bearing Class	Defect	Correlation Coefficient			Weibull Slope	Characteristic Life, Hr.	Mean Life	Number of Bearings Failed
		Log-normal	Exponential	Weibull				
7	Baseline	.998	.985	.962	1.19	1426	1385	40
		.993	.987	.979	1.24	1562	1449	20*
7	Small Scratch	.951	.938	.941	1.67	1276	1183	40
		.975	.948	.965	1.51	1461	1345	20*
7	Medium Scratch	.965	.992	.989	1.35	1459	1346	43
		.954	.980	.992	1.73	1256	1105	20*
7	Large Scratch	.982	.960	.978	1.14	1535	1439	46
		.968	.942	.984	1.11	1878	1710	20*
3	Small Scratch	.984	.987	.983	1.35	1055	969	49
		.957	.973	.987	1.46	1083	953	20*
3	Medium Scratch	.977	.983	.974	1.47	1141	1055	49
		.953	.969	.985	1.67	867	759	20*
3	Large Scratch	.988	.989	.969	1.32	924	876	48
		.959	.985	.987	1.74	927	823	20*
7	Small Dig-Nick	.987	.994	.982	1.20	1371	1286	27
		.989	.990	.959	1.04	1269	1246	20*
7	Large Dig-Nick	.990	.995	.974	1.42	843	786	46
		.989	.994	.980	1.43	679	621	20*

*First 20 bearings placed on test.

**Two parameter Weibull curve fit was used.

coefficients for each curve, the two Weibull parameters, b and θ, the mean life, and the number of bearings in each set. Also included is the same information for the first 20 bearings placed on test for each set. These data will be analyzed to determine if 20 bearings run to failure are adequate for MPB's testing purposes.

Before going on to MLR and sequential testing, let's look further at Table 4. First, by comparing the correlation coefficients for the full data sets, it is clear that log-normal and/or exponential provides a better fit than does two parameter Weibull. This is not necessarily so for the data of the first 20 bearings from each set. Generally speaking, for these data, the two parameter Weibull fit is better. At any rate, the two parameter Weibull correlation coefficients are high enough to indicate adequate fit; and we can proceed with MLR and sequential analyses.

First, MLR analyses were done comparing the Class 7 baseline data with the five sets of Class 7 defect data (small, medium, and large scratch; small and large dig-nick). Next, the Class 7 baseline data were compared with the Class 7 defect data for the first 20 bearings placed on test. The results for these MLR analyses are presented in Table 5. The results are the same whether we compare the baseline mean life with the mean life for the entire data set or for the first 20 bearings placed on test. This is principally because the degrees of

TABLE 5

Mean Life Ratio Analysis

Class 7 Baseline Bearings (vs) Class 7 Defect Bearings

Entire Data Sets

Defect	Mean Life* Hrs.	Decision	Confidence Level
Small Scratch	1183	No Difference	90%
Medium Scratch	1346	No Difference	90%
Large Scratch	1439	No Difference	90%
Small Dig-Nick	1286	No Difference	90%
Large Dig-Nick	786	Different	99%

First 20 Bearings Placed on Test

Small Scratch	1345	No Difference	90%
Medium Scratch	1105	No Difference	90%
Large Scratch	1710	No Difference	90%
Small Dig-Nick	1246	No Difference	90%
Large Dig-Nick	621	Different	99%

*Comparative mean life for Class 7 baseline bearings = 1385 hrs.

freedom axis for the MLR curves is logarithmic; and, for certain combinations of degrees of freedom, there is little difference in the MLR. For instance, the approximate number of degrees of freedom for the comparison of baseline mean life with defect mean ljfe for the entire data set is 1600. The approximate number for the comparison using the first 20 bearings placed on test is 740. At the 95% confidence level and with a Weibull slope of one, the MLR for 1600 degrees of freedom is approximately 1.44 while MLR for 740 degrees of freedom is 1.53. This means that, for a baseline mean life of 1385 hours, the defect mean life must be 961 hours for a significant MLR with 1600 degrees of freedom (95% confidence level); but, for only a slight drop in the defect mean life to 905 hours, the MLR is still significant with 740 degrees of freedom for the same confidence level. The small gain in sensitivity does not justify the additional time and expense for testing more than 20 bearings.

Additionally, an MLR analysis was performed on the Class 3 medium scratch bearings. The mean life (1055 hours) for the entire data set was compared with the mean life (759 hours) for the first 20 bearings placed on test. The two means are different at the 95% confidence level. Apparently, a systematic change occurred during testing. The mean life of 1259 hours for the last 29 bearings of this data set magnifies this shift in mean life. For the other eight data sets, there is no

significant difference between the mean life for the entire set and the mean life for the first 20 bearings placed on test. We conclude that life testing 20 defect bearings should be sufficient for the MLR analysis in most cases.

Sequential Analysis

As mentioned previously, sequential analysis enables one to test for differences as failure data accumulate. First, decision conditions must be set. For our purposes, they would be

Decision 1 -- The defect bearings come from a Weibull distribution of slope b and $\theta > \theta_1$.

Decision 2 -- The defect bearings come from a Weibull distribution of slope b and $\theta < \theta_2$.

(Note: θ_2 is always greater than θ_1.)

Decision 3 -- There is insufficient evidence--continue testing.

Next, it is necessary to stipulate what risks we are willing to take that we may be making the wrong decision. These risks are

(1) α_1, the probability of rejecting the hypothesis that $\theta > \theta_1$ when it is true.

(2) α_2, the probability of rejecting the hypothesis that $\theta < \theta_2$ when it is true.

It should be noted that, when we reject the hypothesis that $\theta > \theta_1$, we are not accepting the hypothesis that $\theta = \theta_2$. We are

merely concluding at the $(1-\alpha_1)$ probability level that θ is significantly greater than θ_1. In the same manner, when we reject the hypothesis that $\theta<\theta_2$, we are concluding at the $(1-\alpha_2)$ probability level that θ is significantly smaller than θ_2, not that $\theta=\theta_1$.

In order to accept Decision 1 for failure data described by a Weibull distribution, the following inequality must be satisfied.

$$\sum_{i=1}^{r} x_i^b > \frac{\theta_1^b}{\left(\frac{\theta_2}{\theta_1}\right)^b - 1}\left[br \ln\left(\frac{\theta_2}{\theta_1}\right) + \ln\left(\frac{1-\alpha_2}{\alpha_1}\right)\right] \quad ---(5)$$

To accept Decision 2, the inequality to be satisfied is

$$\sum_{i=1}^{r} x_i^b < \frac{\theta_1^b}{\left(\frac{\theta_2}{\theta_1}\right)^b - 1}\left[br \ln\left(\frac{\theta_2}{\theta_1}\right) - \ln\left(\frac{1-\alpha_1}{\alpha_2}\right)\right] \quad ---(6)$$

where r = number of failures

b = Weibull slope

If neither inequality is satisfied, then Decision 3 is accepted.

To determine if the defect bearings characteristic lives are different from the baseline characteristic life, the following conditions were arbitrarily established. Let θ_2 equal the Class 7 baseline characteristic life (1426 hours) and θ_1 30% lower, or 1000 hours. Next, we set b equal to the

baseline Weibull slope (1.2) since, in practice, this is the only value we would have. Lastly, we chose $\alpha_1=\alpha_2=0.05$. These conditions will allow us to be 95% confident that we will not conclude that θ for the defect bearings is greater than 1000 hours when, in fact, θ=1000 hours. Also, we will be 95% certain that we will not conclude that θ is less than 1426 hours when, in fact, θ=1426 hours. By applying these conditions to the data for the Class 7 large dig-nick bearings, we found that after the 13th failure the Decision 2 inequality is satisfied, i.e., θ is less than 1426 hours (95% confidence level).

If we changed θ_1 to one half θ_2 or 713 hours with other conditions unchanged, the Decision 2 inequality is satisfied after the 10th failure. If we leave θ_1 at 713 hours and change α_2 to 0.01 (α_1 and b unchanged), the Decision 2 inequality is satisfied after the 12th failure. By calculation, θ is 624 hours and the mean life is 560 hours for these 12 failures. A mean life ratio analysis comparing this mean life (560 hours) to that for the Class 7 baseline bearings also established that there is a significant difference between the two mean lives at the 99% confidence level. It appears that sequential analysis can be helpful in determining when to stop testing defect bearings that have characteristic and mean lives appreciably smaller than the characteristic and mean life for baseline bearings.

Sudden Death Testing

Sudden death testing, as described in Lipson and Sheth (2)

and Johnson (3), was also studied. It is a method for accelerating experiments and, thereby, shortening test time. Statistical tests of significance are made using 10% failure (B_{10}) life or 8% failure (B_8) or some other similar low failure level rather than the mean life. The technique is to test k groups of n devices in each group. Testing is stopped for each group after the first failure occurs within that group. In this manner, k estimates of the B_x life are obtained (x=100(1-.3)/(n+.4). A Weibull fit is then made for these k estimates. The B_x life for the entire population of kn bearings is estimated at the 50% failure level of the Weibull line. This estimate is just as reliable as the one obtained if all kn bearings had been run to failure. B_x life ratio (B_xLR) analysis can then be done if appropriate tables are available. Table A-23 in Lipson and Sheth (2) is for B_{10} life ratio testing.

Unfortunately, the results of B_xLR testing cannot be correlated to the results of MLR testing, i.e., for a given confidence level, two B_x lives may not differ when the corresponding mean lives do differ. For example, the Class 7 baseline bearings B_{10} life is 214 hours. The Class 7 large dig-nick bearings B_{10} life is 173 hours. There is no significant difference between these two B_{10} lives, but we did find a difference at the 99% confidence level in the mean lives for these two sets of bearings. B_{10}LR testing does not appear to be the appropriate test method for the MPB bearing defect study.

THREE PARAMETER WEIBULL

The preceding sections of this report were presented to Jack Beecher, Keith Gordon, and Ed Jarvis at MPB on 26 December by Paul Pelton. At that meeting, it became apparent that we needed to look at the data in Tables 2 and 3 using a three parameter Weibull fit, i.e., the assumption that x_0 is zero may not be adequate for these data. Table 6 summarizes the data obtained for the three parameter Weibull curves. In comparing these data with the two parameter Weibull data in Table 4, we see that, in all cases, the three parameter correlation coefficient is as high and, in most cases, higher than the corresponding two parameter correlation coefficient. This means there is a better fit for the three parameter curve. In all but three cases, the three parameter slope is lower (it is the same in those three cases) than the corresponding two parameter slope. Similarly, in all but three cases, the three parameter characteristic life is lower (it is also the same in those three cases) than the corresponding two parameter characteristic life.

Mean Life Ratio Analysis

Since the mean lives remain unchanged, any effect on our previous MLR analysis would be due to the smaller slopes for the three parameter curves. The only changes that must be made in the conclusions drawn from the two parameter MLR analysis are

TABLE 6

Summary of Three Parameter Curve Fit for MPB Baseline and Defect Bearings

Bearing Class	Defect	Correlation Coefficient	Weibull Slope, b	x_0, Hours	Characteristic Life, Hrs.	Mean Life	Number of Bearings Failed
7	Baseline	0.996	0.855	143	1326	1385	40
		0.995	0.911	155	1487	1449	20*
7	Small Scratch	0.977	1.18	205	1214	1183	40
		0.987	1.12	188	1401	1345	20*
7	Medium Scratch	0.992	1.17	65	1444	1346	43
		0.992	1.73	0	1256	1105	20*
7	Large Scratch	0.988	0.921	80	1496	1439	46
		0.984	1.04	34	1868	1710	20*
3	Small Scratch	0.994	0.994	92	1023	969	49
		0.987	1.46	0	1083	953	20*
3	Medium Scratch	0.988	1.19	92	1114	1055	49
		0.985	1.67	0	867	759	20*
3	Large Scratch	0.996	0.917	102	872	876	48
		0.988	1.57	43	922	823	20*
7	Small Dig-Nick	0.992	0.954	90	1331	1286	27
		0.986	0.765	106	1183	1245	20*
7	Large Dig-Nick	0.997	1.01	98	804	786	46
		0.995	1.00	87	648	621	20*

*First 20 bearings placed on test.

that we can now only be 95% confident there is a difference between the Class 7 baseline mean life and the Class 7 large dig-nick mean life. This applies to the large dig-nick mean life for both the entire set of data and for the first 20 bearings placed on test.

Sequential Analysis

The previous conclusions drawn concerning sequential analysis are still valid. However, the analysis conditions to be set will have to be less restrictive because the three parameter slope and characteristic life for a given set of data are, in most cases, smaller than the two parameter slope and characteristic life.

REFERENCES

(1) William Volk, "Applied Statistics for Engineers," McGraw-Hill, New York, 1958.

(2) C. Lipson and N. J. Sheth, "Statistical Design and Analysis of Engineering Experiments," McGraw-Hill, New York, 1973.

(3) Leonard G. Johnson, "The Statistical Treatment of Fatigue Experiments," Elsevier Publishing Company, Amsterdam, 1964.

DISTRIBUTION LIST FOR FINAL REPORTS

Contract No. F33615-72-C-1243 PROJECT 743-1

DEPARTMENT OF THE AIR FORCE

AFML (LAE)
WPAFB, Ohio 45433

AFML (DO-Librarian)
WPAFB, Ohio 45433

AFML (LTM) 6 Copies
WPAFB, Ohio 45433

AFML (CC)
WPAFB, Ohio 45433

AIR LOGISTIC CENTERS (ALC)

Ogden Air Logistic Center
Technical Library
Hill AFB, Utah 84401

Oklahoma Air Logistic Center
Technical Library
Tinker AFB, Okla. 73145

Sacramento Air Logistic Center
Technical Library
McClellan AFB, CA 95652

San Antonio Air Logistic Center
Technical Library
Kelley AFB, Texas 78241

Warner Robins Air Logistic Center
Technical Library
Robins AFB, Ga. 31093

DEFENSE CONTRACTORS

The Barden Corporation
Danbury, Conn. 06813

KuBar Inc.
21 Erie Street
Cambridge, Mass. 02139

MPB Corporation
Precision Park
Keene, New Hampshire 03431

Mass. Institute of Technology
Charles Stark Draper Laboratory
68 Albany Street
Cambridge, Mass. 02139

Marlin-Rockwell
Attn: Arthur S. Irwin
402 Chandler Street
Jamestown, N. Y. 14701

Union Carbide Corporation
Carbon Products Division
P. O. Box 6116
Cleveland, Ohio 44101

SKF Industries
Research & Engineering
Attn: Dr. N. R. DesRuisseaux
King of Prussia, Pa.

AFML/LNL
Attn: Mr. George Morris
WPAFB, Ohio 45433

Delphi Corporation
2623 Marden Drive
Dayton, Ohio 45433

New Departure-Hyatt Bearing Division
General Motors Corporation
Attn: Mr. J. C. Spohr
2509 Hayes Avenue
Sandusky, Ohio 44870

Bearing Inspection Inc.
Santa Fe Springs
California 90670

Abex Bearing Company
86 Owen Brown Street
Hudson, Ohio 44236

The Fafnir Bearing Company
Attn: Mr. Richard J. Matt
New Britain, Connecticut 06050

New Hampshire Ball Bearings, Inc.
Attn: Mr. Robert Allen
Director of Engineering
Peterborough, New Hampshire 03458

GOVERNMENT AGENCIES

ASD/ENFI
Attn: Mr. J. Andres
WPAFB, Ohio 45433

ASD/ENFL
Attn: Mr. P. Smith
WPAFB, Ohio 45433

DEPARTMENT OF THE NAVY

Naval Air Ship Command
Attn: Dick Retta
Hdqrs. (AIR 520-22)
Washington, D. C. 20360

Naval Ammunition Depot
Attn: Mr. Ken Rush
Code 7051
Crane, Indiana 47522

AFAL/TSR
WPAFB, OH 45433

2750 AB Wg/SSL
WPAFB, OH 45433

AFSC/INA
Andrews AFB, MD 20334

Air University Library
Maxwell AFB, AL 36112

Defense Documentation Center (2 cys)
Cameron Station
Alexandria, VA 22314